TETHERING OF RUTHENIUM AND OSMIUM CLUSTERS TO INORGANIC SUPPORTS.

by

Benjamin P. Gracey

A Thesis submitted in partial fulfilment
for the Degree of Doctor of Philosophy
at the University of Southampton

University of Southampton July 1983

UNIVERSITY OF SOUTHAMPTON

ABSTRACT

FACULTY OF SCIENCE

CHEMISTRY

Doctor of Philosophy

TETHERING OF RUTHENIUM AND OSMIUM CLUSTERS TO INORGANIC SUPPORTS

by Benjamin Patrick Gracey

This thesis describes the synthesis, structure, reactivity and fluxionality of several platinum group metal clusters and the subsequent catalytic testing and tethering of some of these.

Anchored clusters of the types: $|M_3(CO)_{10}(H)\{S(CH_2)_2Si(OMe)_{3-x}(O\text{-}M'O_n)_x\}|$ (M = Ru, Os, and $M'O_n$ = SiO_2, TiO_2, MgO, γ-Al_2O_3, ZnO and SnO_2); $|Os_3(CO)_9(H)(Y)\{S(CH_2)_3Si(OMe)_{3-x}(O\text{-}M'O_n)_x\}|$ (Y = CH_3CN, C_2H_4, O-$M'O_n$, and PPh_3; $M'O_n$ = SiO_2, γ-Al_2O_3, TiO_2 and in some cases MgO, ZnO); $|Co_3(CO)_9\{\mu_3\text{-}CSi(Cl)_{3-x}(O\text{-}M'O_n)_x\}|$ ($M'O_n$ = SiO_2, γ-Al_2O_3, MgO, TiO_2, ZnO and SnO_2); $|Os_3(CO)_{10}(H)\{CN(H)(CH_2)_3Si(OMe)_{3-x}(O\text{-}M'O_n)_x\}|$ ($M'O_n$ = SiO_2, γ-Al_2O_3, TiO_2, MgO and ZnO); $|Ru_3(CO)_{11}L|$, $|H_4Ru_4(CO)_{11}L|$, $|Ru_5C(CO)_{14}L|$ and $|Ru_6C(CO)_{16}L|$ where L = $\{PPh_2(CH_2)_3Si(OEt)_{3-x}(O\text{-}M'O_n)_x\}$ and $M'O_n$ = SiO_2, γ-Al_2O_3, TiO_2 and MgO; and $|Ru_6C(CO)_{15}$(-)-Diop---γ-$Al_2O_3|$, have been prepared and characterised.

A catalysis study on the thiolate clusters is described. Flash chromatography has been shown to be a valuable technique for purifying silanated clusters and fast atom bombardment mass spectroscopy in characterising them.

The tailoring of polydentate phosphines to clusters was investigated and compounds of the general formulae; $|Ru_3(CO)_{10}(Z)|$, $|H_4Ru_4(CO)_{10}(Z)|$, $|Ru_5C(CO)_{13}(Z)|$, and $|Ru_6C(CO)_{15}(Z)|$ (where Z = DPPM, DPPE, DPPP, DPPB (and (-)-Diop in most cases) have been prepared and characterised. The results of a ^{31}P n.m.r. study on these is also reported.

ACKNOWLEDGEMENTS

I wish to thank Dr. J. Evans for constant guidance and encouragement during the supervision of this work, and for spending much time in helpful discussion.

I am grateful to Dr. W. Levason (for analyses and entertainment), Mrs. J.M. Street (for ^{13}C and ^{1}H n.m.r. spectra run on the Varian XL 100), Mr. A.G. Avent (for help in recording the ^{31}P n.m.r. spectra), Mr. R. Bedder (for the fast atom bombardment mass spectrum), Dr. P.F. Todd (for neutron activation analyses) and Dr. I.H. Sadler at the S.E.R.C. n.m.r. service at Edinburgh.

I am indebted to Dr. M. Webster, Mr. A.G. Jones, and Dr. L.R. Gray for the solutions of several complexes produced during this work, and Dr. M.B. Hursthouse for the use of the S.E.R.C./Q.M.C. CAD-4 diffractometer.

My thanks also go to my colleagues for their helpful contributions, to Mr. P. Jones for fatherly advice, to Mrs. B. Staves for typing this thesis, and to the technical staff of the Department of Chemistry for their services.

Finally, the award of a research studentship by the Science and Engineering Research Council is gratefully acknowledged.

ABBREVIATIONS

Me: methyl; Et: ethyl; Pr: n-Propyl; Bu: n-Butyl; ^{t}Bu: tertiary butyl; Ph: Phenyl; t.h.f.: tetrahydrofuran; DPPM: Bisdiphenylphosphino-methane; DPPE: 1,2-bisdiphenyl-phosphino-ethane; DPPP: 1,3-bisdiphenylphosphino-propane; DPPB: 1,4-bisdiphenylphosphino-butane; (-)-Diop: (-)-2,3,-o-isopropylidene-2,3,-dihydroxy-1,4,-bisdiphenylphosphinobutane; t.l.c,: thin layer chromatography; u.v.: ultraviolet; m.s.: mass spectrum.

With reference to the infrared data:
i.r.: infrared; ν_{CO}: carbonyl stretching frequency; s: strong; m: medium; w: weak; sh: shoulder; br: broad; v: very (e.g. vw: very weak).

With reference to the nuclear magnetic resonance data:
n.m.r.: nuclear magnetic resonance; Hz: Hertz; J: coupling constant; s: singlet; d: doublet; t: triplet; q: quartet; m: multiplet; br: broad; $\{^{1}H\}$: proton decoupled; t.m.s.: tetramethylsilane; p.p.m.: parts per million.

CONTENTS

CONTENTS (Continued) Page No.

CONTENTS (Continued) Page No.

Chapter 1

Introduction

This thesis describes the results of a study directed at producing a new class of metallic catalysts derived from tethered clusters. A cluster compound is defined, for the purpose of this thesis, as any compound in which there are three or more metal atoms with significant metal-metal bonding between them. It describes the synthesis, structure, reactivity and fluxionality of several platinum group metal clusters and the subsequent catalytic testing and anchoring of some of these.

As an introduction, a brief discussion of the supported metal cluster/dispersed metal catalyst analogy is presented, followed by an outline of the progress made so far in achieving this goal. A general review of cluster chemistry is not attempted because of the size and diversity of the topic though the reader is referred to several excellent reviews.[1-17]

(a) The supported metal cluster - dispersed metallic catalyst analogy.

Metallic catalysts used in industry are usually of the dispersed rather than the massive metal type,[18,19] primarily because of surface area considerations (e.g. to ensure maximum efficiency from an expensive catalyst) though other factors may be important (e.g. the nature of the catalytic activity is often particle size dependent). In dispersed metallic catalysts the metal particles are commonly separated from one another by a refractory oxide support, though other refractory materials such as carbon have been utilised.

The metal is usually introduced onto the support from aqueous solution or suspension by processes such as impregnation, adsorption or, ion exchange, co-precipitation or deposition and this is followed by a calcination or hydrogen reduction stage to activate the catalysts. A summary of the most widely used of these techniques is given below as these are applicable to the preparation of supported metal clusters and metal cluster derived dispersed metallic catalysts (when no anchoring ligand is employed).

(i) Impregnation

This involves the filling of the pores of a support with a solution of the metal salt, from which the solvent is subsequently evaporated and the salt decomposed by either reduction or thermal decomposition. A disadvantage of this technique is that the metal salt tends to form microcrystals on the surface and when reduced to the active catalyst these limit the degree of dispersion obtained.

(ii) Adsorption or ion exchange

This is achieved by the selective removal of either metal salts or metal ion species from their solution by either physisorption or chemical bonding with active sites on the support. The loading achieved is controlled by the strength of adsorption and the concentration of the active species. This technique is often used as it permits a greater degree of control over the dispersion of catalyst (compared to impregnation).

(iii) Co-precipitation or deposition

This method involves the co-precipitation of metal ions and the support ions. The advantage of this is that it produces an intimate mixing of the catalyst and support (which is important in oxide promoted catalysis), but a disadvantage is that not all the expensive catalyst is on the particle surface.

(iv) Chemical vapour deposition

This involves vapour plating the support with a volatile inorganic or organometallic compound. This has the advantage of producing a catalyst with a purely surface deposition.

These empirical approaches to the preparation of supported metallic catalysts have resulted in the existence of "cookery books" on how to prepare successful catalysts.[20,21] There is, however, some control over the nature of the catalyst which is determined mainly by the support, metal and particle size. The average particle size can be controlled by varying the concentration on the support of the catalyst precursor (higher concentrations favour larger metal particles), the temperature and time of reduction (higher temperatures and longer times favour less dispersion and larger particles) and the salt employed. However, the influence of these factors is heavily dependent on other variables, such as the atmosphere in contact with catalyst on reduction and the nature of the support. As a result, attempts to rationalise the preparation of metal catalysts have met with limited success. Metal

clusters by virtue of being preformed metal particles, usually in zero oxidation state, offer a means of achieving a specific metal particle synthesis.

This analogy between small metal particles used in catalysis and clusters has been reviewed in depth by several workers,[22-29] in particular Muetterties.[30-33] Similarities found to date include; (i) structures - the cluster frameworks are fragments of cubic and hexagonal close packed or body centred cubic metal bulk structures; (ii) ligand stereochemistry ; where the geometric features of ligands bound to clusters and to metal surfaces are similar; (iii) thermodynamic parameters - where the average bond energies for ligand metal and metal-metal bonds are comparable for a specific metal/cluster; (iv) the mobility of ligands bonded to metal cluster frameworks and to metal surfaces.

(b) The potential importance of cluster based catalysts

Recently, solutions of clusters such as $|Ru_3(CO)_{12}|$,[34] $|Os_3(CO)_{12}|$,[35] $|Ir_4(CO)_{12}|$,[36] and $|Rh_6(CO)_{16}|$,[37] have been shown to catalyse the formation of hydrocarbons from a mixture of carbon monoxide and hydrogen, thus mimicking metal surfaces. In addition, $|HRu_3(CO)_{11}|^-$ and $|H_4Ru_4(CO)_{12}|$ have been implicated in a synthesis gas preparation of ethylene glycol using a highly active ruthenium "melt" catalyst derived from ruthenium(IV) oxide or ruthenium(III) acetylacetonate dispersed in a molten quaternary phosphonium or ammonium salt.[38] Results such as these suggest the possibility of a cluster based Fischer-Tropsch catalyst.

The Fischer-Tropsch synthesis was first reported[39] in 1923, when it was found that a high pressure reaction of carbon monoxide and hydrogen over alkanised iron fillings yielded a liquid product containing a range of organic functionalities, e.g. alkanes, alkenes, alcohols, aldehydes, ketones, and carboxylic acids. The reduction of carbon monoxide was reported earlier by Sabatier and Senderens[40] in 1902. It is a synthesis distinguished by a lack of selectivity, which is a reflection of there being a myriad of competing reactions present.

A selective Fischer-Tropsch synthesis is a desirable technological achievement, as it would save both raw materials and expenditure incurred in refining. This is particularly important as the price of raw materials in the petroleum industry has increased considerably in the past decade.[41] Cluster catalysts, by virtue of their discrete structures, unlike the currently used dispersed metal catalysts, offer the possibility of realising this.

Cluster catalysts occupy an intermediate position between the classical conventional metallic and mononuclear homogeneous catalysts.[42] Some important and contrasting features are summarised in Table 1.1. The principle drawbacks of mononuclear homogeneous catalysts are their low activity, particularly for the energetically more demanding transformations, such as the activation of C — C and C — H bonds in saturated hydrocarbons and the hydrogenation of triple bonds in compounds such as CO and N_2. A possible reason for this is that

TABLE 1.1

	Catalyst type	
	mononuclear homogeneous	metallic
state	usually in solution	usually supported on oxides
phase	liquid	gas/solid
selectivity	high	low
activity	low	high
temperature of operation	low (< 200 ^{o}C)	high (typically 250 - 550 ^{o}C)
reaction types	hydrogenation isomerisation carbonylation polymerisation oxidation	all those observed for homogeneous catalysts but in addition; C — C and C — H bond activation in saturated hydrocarbons, and hydrogenation of multiple bonds in CO and N_2.
understanding	well understood due to the applicability of molecular techniques.	poorly understood

multiple bonding is required in these cases to activate the reactants. These conversions are currently only commercially achievable with dispersed metal catalysts, where the neighbouring metal centres allow this multiple bonding of the reactants. Clusters, because they possess more than one metal centre, also offer this opportunity. In addition, because of their discrete structures, like mononuclear metal complexes, they also offer the prospect of a high selectivity in the products, which is not currently attainable with dispersed metal catalysts (with the possible exceptions of the polymethylene, methanol[41] and methane[43] synthesis reactions).

A series of clusters exist which demonstrate how the reduction of carbon monoxide on metal surfaces, involving multicentre bonding, could come about. Initially CO is thought to absorb as a terminal ligand on metal surfaces and the synergic nature of the bonding weakens the C --O bond. This weakening, which can be conveniently monitored by ν_{CO}, is thought to be important if C --O bond scission is to occur. For example, the stretching frequency of unco-ordinated CO is 2 143 cm^{-1} whereas the stretching frequency of terminally bound CO in neutral complexes is typically in the range 2 150 - 1 900 cm^{-1}. Further bond weakening is observed when the ligand binds to more than one metal atom. For example, when this ligand assumes a μ_2-bridging mode the ν_{CO} is observed usually between 1 900 - 1 700 cm^{-1} (e.g. $|Ru_6C(CO)_{17}|$ $\nu\mu_2$-CO = 1 835 cm^{-1}) and when it occurs as a cap (i.e. μ_3-CO) it is further reduced to a value resembling that observed for a C --O

single bond when compared to aldehydes and ketones (e.g. $|Ru_4Cp(\mu_3\text{-}CO)_4|$, ν_{CO} = 1 633 cm^{-1}, acetone ν_{CO} = 1 712 cm^{-1})

Further C —O bond weakening is observed when the oxygen atom becomes co-ordinated. For example, in $|Fe_4(CO)_{13}H|^-$ the oxygen atom is co-ordinated to the metal (see Diagram 1.1) and the CO bond order is approximately unity.[44] This compound is thought to represent a model compound for the dissociation of a carbon monoxide molecule at a step in a metal surface to yield a carbide and a chemisorbed oxygen atom. An alternative way of cleaving a C —O bond is represented by the compounds $|(\mu_3\text{-}HOC)Co_3(CO)_9|$[45] and $|(\mu_2\text{-}HOC)Fe_3(CO)_{10}(H)|$[46] in which the oxygen atom becomes hydrogenated and should eventually give rise to a carbide atom and a molecule of water.

Evidence exists to suggest that it is the hydrogenation of these carbides which is responsible for the occurrence of alkanes and alkenes in the Fischer-Tropsch synthesis. For example, the compounds $|Ru_5C(CO)_{15}|$,[47] $|Fe_4(CO)_{12}C|^{2-}$, $|Fe_4(H)(CO)_{12}(\mu_4\text{-}CH)|$,[49] $|Os_3(CO)_9(H)_3(\mu_3\text{-}CH)|$[50] and "$|H_2Os_3(CO)_{10}(CH_2)|$"[51] represent possible steps in the hydrogenation of a carbide (see Diagram 1.2, carbonyls omitted for clarity). Possible mechanisms to account for the other observed Fischer-Tropsch products have been advanced which involve similar intermediates to those seen on clusters in CO reduction and carbide hydrogenation. These have been reviewed in detail and, therefore, are not discussed further here.[52-59, 27]

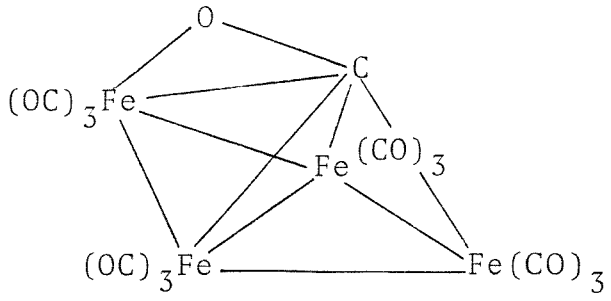

$|Fe_4(CO)_{13}H|^-$

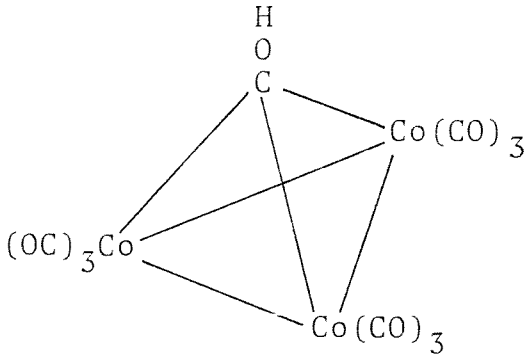

$|(\mu_3\text{-HOC})Co_3(CO)_9|$

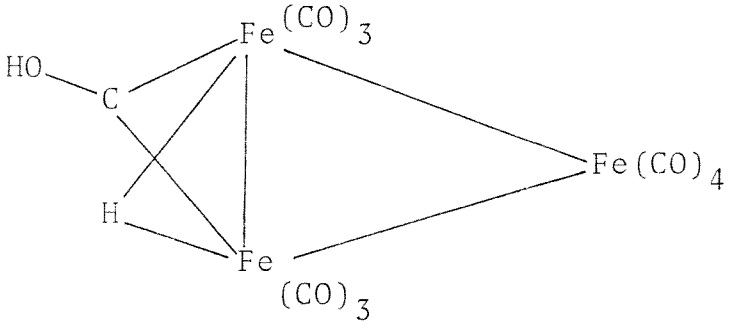

$|(\mu_2\text{-HOC})Fe_3(CO)_{10}(H)|$

Diagram 1.1

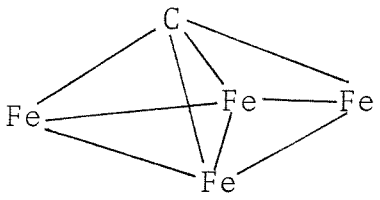

$|Fe_4C(CO)_{12}|^{2-}$

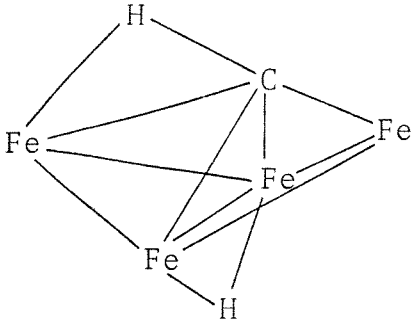

$|H_2Fe_4C(CO)_{12}|$

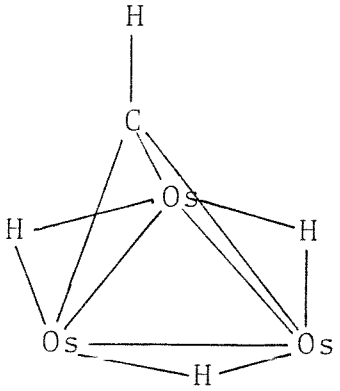

$|Os_3(CO)_9(H)_3(\mu_3\text{-}CH)|$

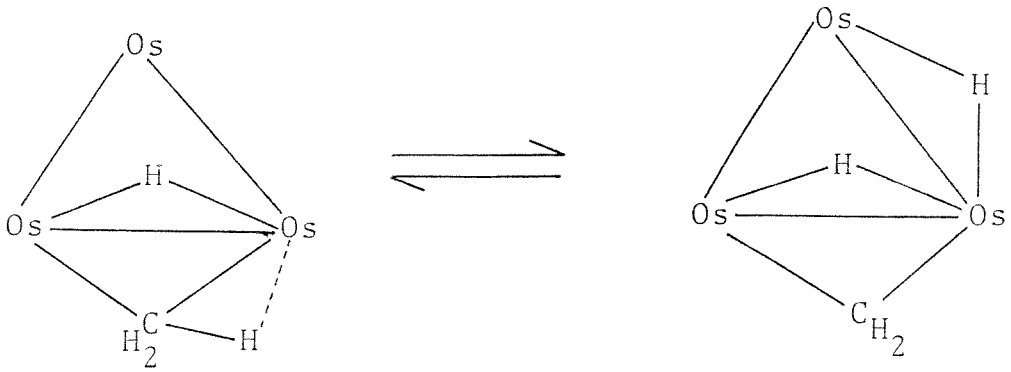

"$|Os_3(CO)_{10}(H)_2(CH_2)|$"

Diagram 1.2.

(c) Homogeneous cluster catalysis?

In recent years the literature has contained many examples of homogeneously catalysed reactions using small metal cluster compounds as catalyst precursors. These have spanned many diverse classes of reaction such as hydrogenation,[60] isomerisation,[61] polymerisation,[62] oxidation,[63] hydroformylation,[64] and the water-gas shift[65] reaction. An important point that has to be made at this point is that there is no conclusive proof of catalysis by clusters: indeed, in several cases the reverse is specifically thought to apply with the cluster breaking down and acting as a source of highly reactive mononuclear entities (e.g. the hydroformylation of olefins with $|Rh_4(CO)_{12}|$[66] and $|Rh_6(CO)_{16}|$[67]).

As suggested by Norton[68] the only conclusive way to demonstrate catalysis by clusters is to detect an asymmetric preference in the reaction products obtained in catalytic runs with inherently chiral clusters. Asymmetric clusters such as $|H_4Ru_4(CO)_8\{(-)\text{-Diop}\}_2|$[69] would be unsuitable for this, as any fragmentation products could still remain in contact with a chiral centre and induce asymmetry in the catalysis products. For this reason the asymmetry has to occur in the metal skeleton of the cluster, so that none of the fragmentation products will be chiral. There are three main ways to achieve this. These are, (i) to have four different metal atoms in a tetrahedral cluster, (ii) to have four different metal atom environments in a tetrahedral cluster, and (iii) to have a chiral cluster by virtue of the clusters' shape or substitution by a ligand.

The former has been realised by Vahrenkamp and co-workers;[70-72] they synthesised clusters of the general formulae $|SFeCoM(CO)_8Cp|$ (M = Cr, Mo, W) and resolved them by means of an optically active ligand, (-)-(R)-PMePrPh, which gave on reaction pairs of diasteroisomers, $|SFeCoM(CO)_7Cp$-(PMePrPh)|, which could be separated by fractional crystallisation. Their reconversion to the pure optically active clusters was achieved by the scavenging of the phosphine ligand by methyl iodide under carbon monoxide pressure. The resultant clusters showed a rather high $|\alpha|$ value and their absolute configuration (for the molybdenum and tungsten compounds) was determined by X-ray analysis (see Diagram 1.3). The enantiomers were found to be relatively stable against thermal but not against photochemical racemisation.

It was found that these clusters were probably active for photoinitiated hydrosilation of acetophenone but unfortunately, photoracemisation of the clusters proceeded faster than the hydrosilation. So doubt still exists as to what the active catalyst is, despite the clusters being recovered in high yields (over 95 %). Hopefully, a non-fluxional capping ligand such as $HC(PPh_2)_3$ instead of sulphur may overcome this, and allow catalysis by clusters to be proven.

The second way to obtain a chiral cluster is to substitute the metal atoms with different ligands. This has been achieved by Bruce and co-workers whose radical anion catalysed reaction allowed these to be prepared in moderate to high

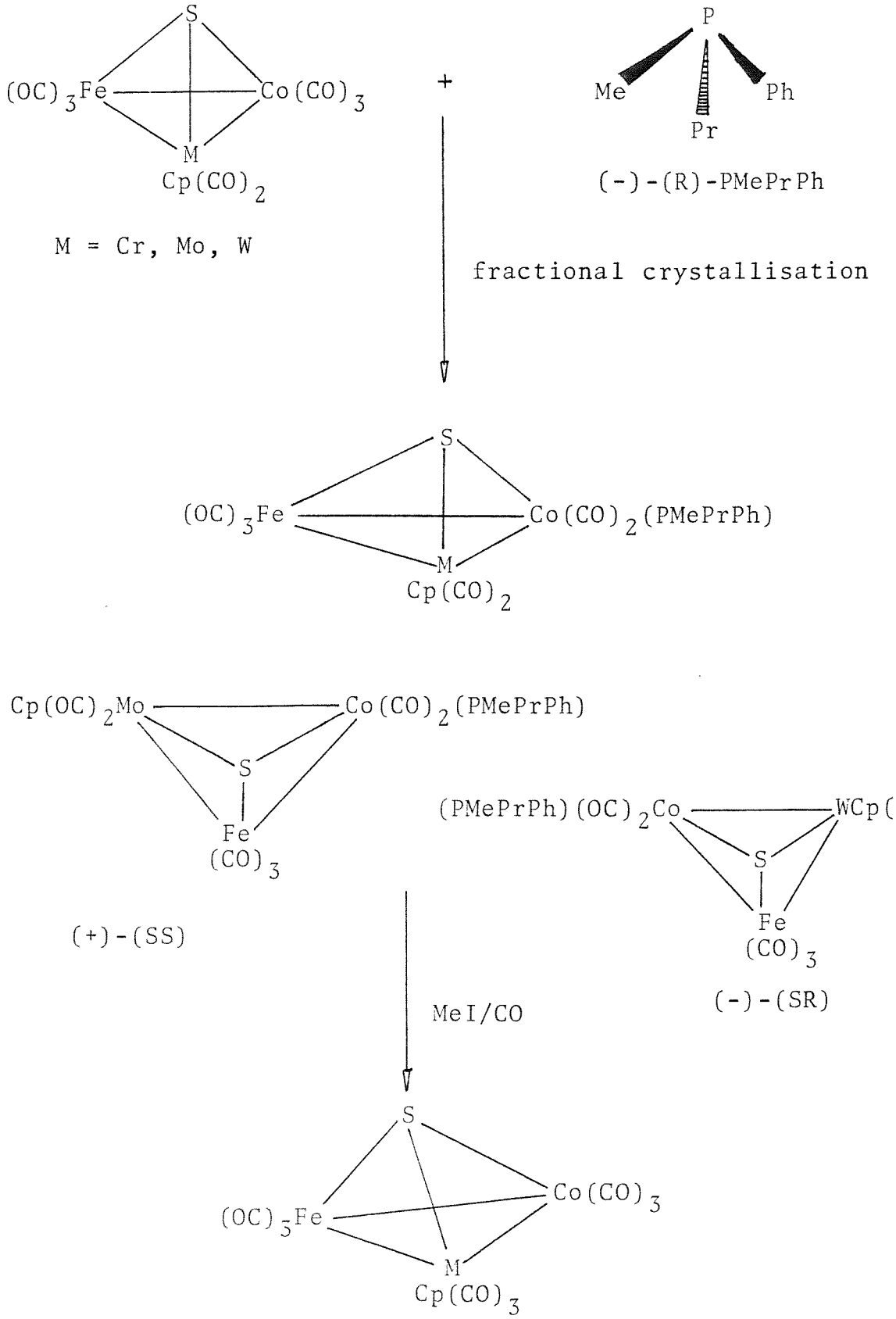
S
(OC)3Fe
Co(CO)3
M
Cp(CO)2
M = Cr, Mo, W
+
P
Me
Ph
Pr
(-)-(R)-PMePrPh
fractional crystallisation
S
(OC)3Fe
Co(CO)2(PMePrPh)
M
Cp(CO)2
Cp(OC)2Mo
Co(CO)2(PMePrPh)
S
Fe
(CO)3
(+)-(SS)
(PMePrPh)(OC)2Co
WCp(CO)2
S
Fe
(CO)3
(-)-(SR)
MeI/CO
S
Co(CO)3
(OC)3Fe
M
Cp(CO)3

Diagram 1.3.

yields.[73] For example, by using sequential radical-anion initiated reactions with the cluster carbonyl complexes $|Ru_3(CO)_{12}|$, $|H_4Ru_4(CO)_{12}|$ and $|Co_3(CO)_9(\mu_3\text{-}CR)|$ and isocyanides or group V donor ligands, they have been able to prepare a range of derivatives containing two or more different ligands attached to the cluster, such as $|Ru_3(CO)_{10}(CNBu^t)(PMe_2Ph)|$, $|Co_3(CO)_7(\mu_3\text{-}CCl)\{P(OMe)_2Ph\}\{P(OC_6H_4Me\text{-}P)_3\}|$ and $|H_4Ru_4(CO)_9(PMe_2Ph)(P(OMe)_2Ph)(P(OMe)_3)|$ (see Diagram 1.4). Potentially all these are chiral but it is unlikely that the Ru_3 cluster would be resolvable because of fluxionality. The resolution of the Ru_4 and Co_3 clusters should be possible, using a method similar to Vahremkamp's, with a weakly co-ordinated ligand such as a chiral amine or cyanide instead of a chiral phosphine.

Another possible advantage of generating clusters with differing metal sites by varying the ligand environment is that the individual metal atoms may be tailored to promote a particular aspect of the catalytic reaction. For example, one metal atom may be specifically modified to bond one reactant and the other metal atoms modified to bind another, in much the same way as enzymes. A class of clusters which should also offer this advantage are the bimetallic clusters such as $|RuPt(CO)_5PPh_3|$ in which the different metals should promote different aspects of the catalytic reaction. The chemistry of such clusters has been recently reviewed by Geoffroy[6,7] and as a result is not discussed here.

Other methods of obtaining a chiral cluster suitable for

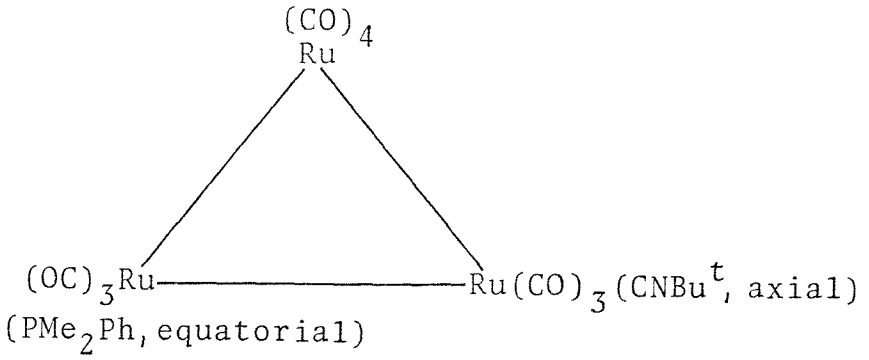
(CO)4
Ru
(OC)3Ru
Ru(CO)3(CNBut, axial)
(PMe2Ph, equatorial)

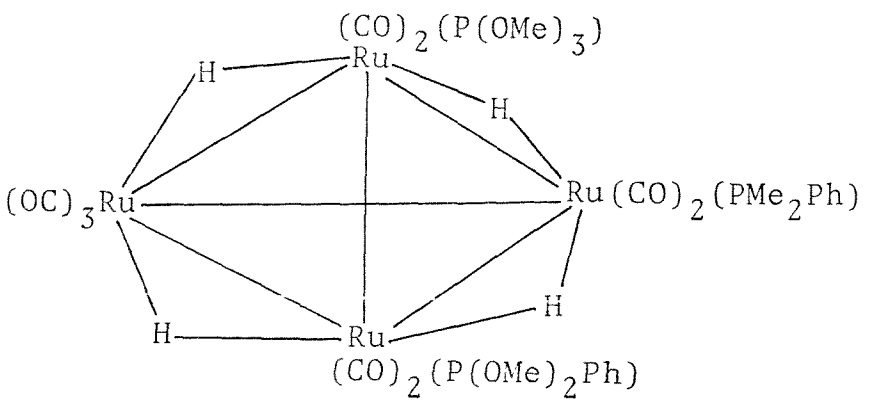
(CO)2(P(OMe)3)
Ru
H
H
(OC)3Ru
Ru(CO)2(PMe2Ph)
H
H
Ru
(CO)2(P(OMe)2Ph)

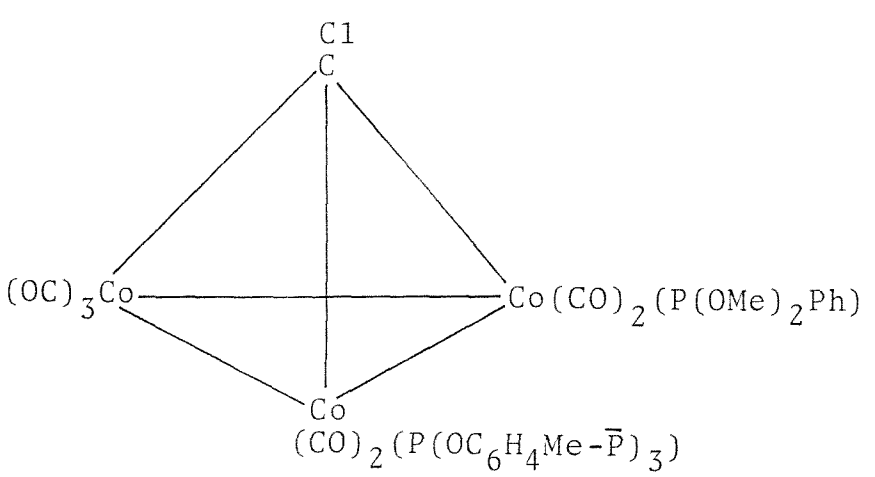
Cl
C
(OC)3Co
Co(CO)2(P(OMe)2Ph)
Co
(CO)2(P(OC6H4Me-p)3)

Diagram 1.4.

testing the theorem of cluster catalysis involve the cluster chirality being caused by either the metal framework or ligand envelope. For example, $|Ru_3(CO)_{10}(PPh_3)(CNMe)|$ should potentially be chiral by virtue of the phosphine and isocyanide ligands occupying equatorial and axial environments, respectively. However, because of fluxionality this compound would easily autoracimise. That is, the rotation of the $Ru(CO)_3(PPh_3)$ and $Ru(CO)_3(CNMe)$ units is likely to be facile, as it has been observed for osmium analogues such as $|Os_3(CO)_{10}(PEt_3)_2|$ and $|Os_3(CO)_{10}(CNR)_2|$. The use of bridging, polydentate or bulky ligands with a strong site preference could overcome this problem. $|Ru_6(CO)_{15}(HSEt)_3C|$[74] provides an example of a compound potentially chiral in both the ligand envelope and metal framework.

The potential importance of cluster catalysis as previously mentioned, lies not in the reactions currently catalysed adequately by mononuclear catalysts, but in those currently catalysed only by metallic catalysts and where an increased selectivity or activity would be advantageous (e.g. the hydrogenation of CO, N_2 and cyanides, and the C --C and C --H bond activation in alkanes). Muetterties[75] has demonstrated that $|Ni_4\{CNC(CH_3)_3\}_7|$ is a catalyst for the specific hydrogenation of isonitriles to secondary amines and of acetonitrile to ethylamine under mild conditions. This is the first example of a homogeneous catalytic hydrogenation of an isonitrile and presumably requires a polynuclear catalyst for multiple bonding. However, catalysis by a fragmentation product cannot be ruled out.

The reduction of carbon monoxide by clusters has been reported by Pittman.[76,77] This is particuarly important since the metal clusters involved were bonded by stable non-fluxional bridging groups which should hinder cluster fragmentation (see Diagram 1.5). These clusters were found to hydroformylate both 1- and 2-pentenes to hexanols and 2-methyl-pentanol under mild conditions. The clusters were recovered

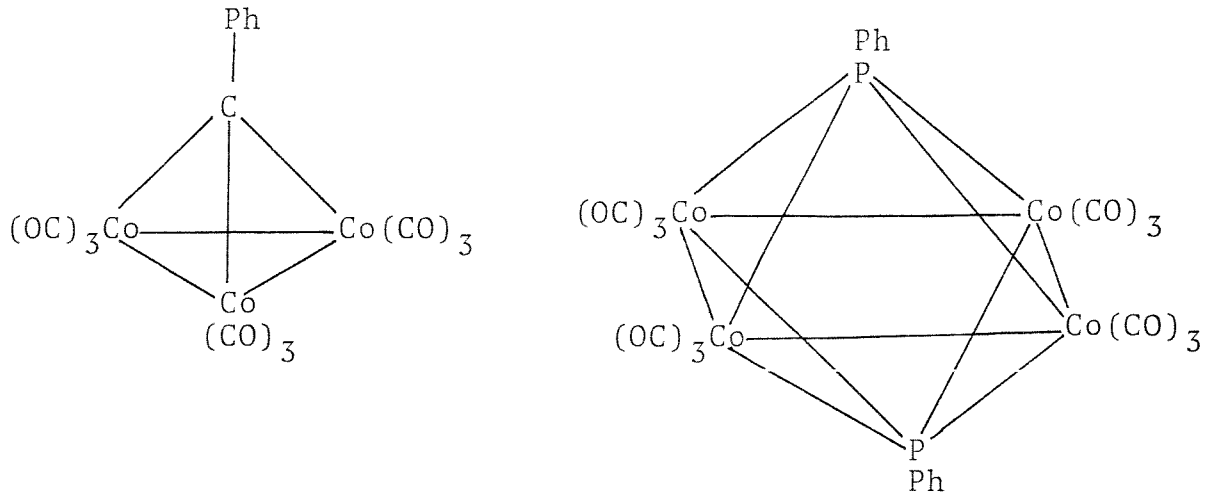

Diagram 1.5.

unchanged in very high yield at the end of the catalysis runs (no other organometallic species were detected) and because of the structure of the clusters it seems unlikely that the catalysis is due to fragmentation products which reform at the end of the catalysis run.

The mechanistic details of these reactions is unclear but it is likely that it involves the reversible opening of cobalt-cobalt bonds. A precedent for this is provided by the reversible reaction of $|(\eta^5\text{-}C_5H_5)MnFe_2(CO)_8(\mu_3\text{-}PPh)|$ with triphenyl phosphine and carbon monoxide which is accompanied

by the reversible breaking of a manganese-iron bond.[78] This illustrates the possibility of a catalytic reaction occurring by the addition of reactants to the cluster with concurrent breaking of a M --M bond, followed by the elimination of the products with the reformation of the M --M bond. If this is the case, the incorporation of bridging or capping ligands in clusters could be important in stabilising particularly small clusters under catalysis conditions.

Another good candidate for a cluster catalyst is $|Fe_4(\eta^5\text{-}C_5H_5)_4(\mu_3\text{-}CO)_4|$[79] which catalyses the selective hydrogenation of terminal alkynes to alkenes in the presence of internal alkynes and alkenes. The cluster was recovered unchanged and no other iron containing species were detected. The major possible fragmentation products appear not to be active as the dimer, $|Fe_2(\eta^5\text{-}C_5H_5)_2(CO)_4|$, under comparable conditions is inactive. In addition to this, the cluster contains face capping carbonyl ligands which should serve to protect it from fragmentation; thus, catalysis by the intact cluster seems likely.

(d) Catalysis by clusters physically or chemically adsorbed onto supports.

Production of dispersed metal catalysts by conventional impregnation techniques generally affords a wide particle size distribution peaking in the 30 - 50 Å region for second row transition metals. By carefully controlling the experimental conditions (e.g. support pretreatment, temperature of reduction, reducing atmosphere etc), narrower size distributions

can be obtained with smaller particles (20 - 30 Å). However, no method permits the reproducible preparation of very small particles (< 10 Å). Metal cluster compounds provide a possible way to realise this, if particle aggregation can be prevented.

Catalysts prepared in this way should offer the following advantages over conventional dispersed metal catalysts:

(i) non-aqueous methods of catalyst preparation can be used since metal clusters are usually soluble in organic solvents. It is possible that metal particle aggregation during reduction is facilitated by the presence of surface hydroxyl groups, so surface pretreatment with compounds which bind to hydroxyl groups may overcome this problem. Unfortunately, most compounds employed for this cause the support to become hydrophobic (e.g. $SiMe_3Cl$ and $(SiMe_3)_2NH$) and so prevent the subsequent application of water soluble metal salts.

(ii) clusters are usually halide free so the catalysts prepared will also be halide free and this is advantageous as residual halide can act as a catalytic poison and halide is thought also to assist the aggregation of metal particles.

(iii) Since the oxidation state of the metal atoms in clusters is usually zero, a high temperature hydrogen reduction should be unnecessary. A low temperature activation is desirable as this would minimise the problems of aggregation and cluster dissolution on the support.

(iv) Mixed metal clusters should offer a route to preparing alloy catalysts with a uniform and precise composition.

(v) If the cluster framework can be retained during activation, the catalysts should be more specific.

The main method utilised for introducing clusters onto supports is impregnation. A major disadvantage of this route is that the clusters tend to be deposited from solution not as a monolayer on the support but as microcrystals and as a result tend to produce larger metal crystallites than would otherwise occur. The first detailed report of preparing dispersed metallic catalysts was by Robertson and Webb in 1974.[80] They prepared silica supported ruthenium catalysts by depositing $|Ru_3(CO)_{12}|$ from solution onto silica and pyrolysing the product under varying conditions. The partially decarbonylated product was found to have a markedly different catalytic behaviour from that obtained with dispersed metallic catalysts. The nature of the active catalytic species is unknown, but $|Ru_3(CO)_{12}|$ is known to fragment on oxides before producing metal, so the active catalyst may be a mononuclear species.

The nature of the interaction of clusters with oxides is currently receiving a large amount of attention mainly because of the relevance of this to conventional metallic catalysts. In general, when a cluster is added to an oxide (see Chapter 2 for further details), it is at first physisorbed and then the hydroxyl groups add oxidatively to the cluster eventually forming mononuclear or binuclear species, which under more forcing conditions (reducing) yield the metallic catalyst. An implication of this is that unless the cluster is held together during the activation step, the cluster metal

framework is likely to lose its integrity and the potential advantages (IV) and (V) will be lost.

Basset et al. have characterised an intermediate cluster in the breakdown of $|Os_3(CO)_{12}|$ on oxides, namely $|HOs_3(CO)_{10}(O_{M'O_n})|$ and have found that when $M'O_n = SiO_2$ it is an ethylene hydrogenation catalyst.[81] The fact that reversibly formed ethylene and hydrogen adducts have both been observed on the surface by i.r. spectroscopy, together with the observation that no catalyst ageing or cluster decomposition was found, suggests it is the grafted cluster and not some minor decomposition or side product which is the active catalyst. The addition of both the ethylene and the hydrogen are reversible with this complex and this demonstrates that they are formed without CO loss. To account for this the reversible opening of the oxide bridge to accommodate the incoming ligand (see Diagram 1.6) has been proposed. Both additions appear to be related as the ethylene derivative is easily converted to the hydrogen derivative by treatment with hydrogen at room temperature whereas $|HOs_3(CO)_{10}(O_{SiO_2})|$ requires heating to 373 K to react.

$|Fe_3(CO)_{12}|$ interacts with basic oxides,[32] such as γ-alumina and magnesia, to give "anchored" $|HFe_3(CO)_{11}|^-$. This "anchoring" reaction resembles the ion exchange or adsorption method of preparing dispersed metallic catalysts, which characteristically produces samples with a high degree of dispersion. Electron microscopy[83] on thermally activated samples of anchored $|HFe_3(CO)_{11}|^-$ (heated to 270 ^oC under CO

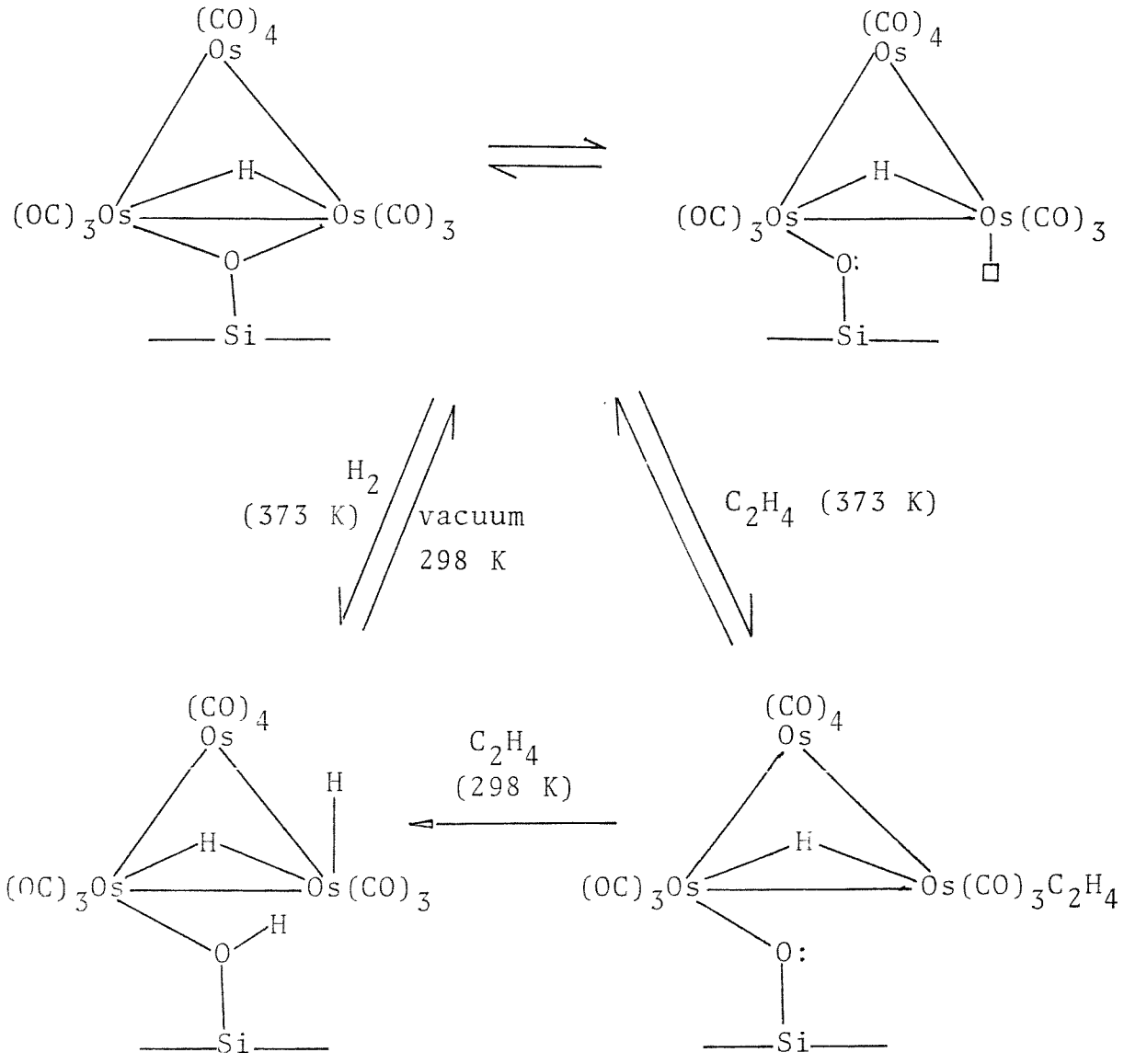
(CO)4
Os
H
(OC)3Os
Os(CO)3
O
Si
H2
(373 K)
vacuum
298 K
C2H4 (373 K)
C2H4
(298 K)
O:

Diagram 1.6.

), has shown that the iron particles formed do possess a high degree of dispersion (average particle size < 20 Å). This has been confirmed by electron spin resonance and low temperature ferromagnetic resonance measurements.

The catalysts prepared by this pyrolysis on alumina exhibit a higher selectivity towards propylene formation (from CO and H_2) than catalysts prepared by impregnation of alumina[84,85] with $|Fe_3(CO)_{12}|$ or $|Fe(NO_3)_3|$, followed by a hydrogen reduction. These latter catalysts exhibit a markedly different product distribution, with a minimum selectivity for C_2 --C_3 hydrocarbons and a maximum for C_5 --C_{12} hydrocarbons. It was concluded that this difference is because of the smaller iron particle size in the former catalyst. This is supported by the observations that as the $|Fe_3(CO)_{11}|^-$ catalyst aged, its selectivity changed to that of the other two and at the end of the run electron microscopy detected large iron particles (diameters 200 - 500 Å).

A similar high selectivity for low molecular weight hydrocarbons has been observed for catalysts prepared from $|Rh_4(CO)_{12}|$, $|Rh_6(CO)_{16}|$, $|Ir_4(CO)_{12}|$, $|Ru_3(CO)_{12}|$, and $|Os_3(CO)_{12}|$ supported on silica and alumina.[86] So, despite the complex nature of the interaction of clusters with supports, clusters can be used to prepare more highly dispersed metal catalysts.

Another example of the different properties of cluster derived catalysts from conventional catalysts is provided by the work of Anderson and Mainwaring on pyrolysed $|Co_2Rh_2(CO)_{12}|$ supported on silica.[87] This catalyst displays a significantly

different catalytic activity from conventional Co/Rh catalysts.[88] That is, the cluster based catalyst catalyses the hydrogenolysis of methylcyclopentane into monocyclic C_6 compounds whereas the conventional catalysts produce methane.

The activity of dispersed metallic catalysts derived from clusters, like conventionally prepared catalysts, is dependent on the support. This dependence can arise from either an electronic or a spacial interaction with the support. The Zeolites are a class of alumino-silicate supports with a controllable pore structure and because of this offer the prospect of greater catalytic selectivity. The Fischer-Tropsch products obtained from catalysts prepared from $|Fe_3(CO)_{12}|$ deposited in HY and NaY Zeolites display a chain length limitation not encountered with conventional catalysts[89,90] which is presumably due to a pore size effect.

$|Rh_6(CO)_{16}|$ supported on NaY Zeolite[91] by sublimation and treated with carbon monoxide at 100 ^{o}C has been found to possess an i.r. spectrum virtually identical to those obtained during hydroformylation experiments involving $|Rh(NH_3)_6Cl_3|$ exchanged into a NaY Zeolite, which suggests the presence of an entrapped cluster. The activity of this cluster prepared <u>in situ</u> is similar to that of the homogeneous catalysts derived from $|Rh(NH_3)_6Cl_3|$. That is, 1,5-hexadiene is hydroformylated to a mixture of monoaldehydes and dialdehydes in both cases. A notable difference, however, is that the Zeolite based catalyst produces predominantly dialdehydes whereas the major product for the homogeneous catalyst is monoaldehydes.

These results indicate that the pore structure causes the reactants to be retained longer with the catalyst.

Bard and co-workers[92] have used $|Ru_3(CO)_{12}|$, $|H_2Ru_4(CO)_{13}|$, and $|(PPh_3)_2N|^+|CoRu_3(CO)_{13}|^-$ as catalytic precursors on dried γ-alumina, silica gel and NaY Zeolite. These materials were prepared by impregnating the support with a solution of the cluster and after drying in vacuo, the catalysts were activated by heating in a stream of hydrogen. These materials all proved to be active in the hydrogenation of carbon monoxide to methane. It was found that in addition to this, the activity varied with the precursor and support. This illustrates the importance of the metal/support interaction on catalytic activity.

(e) Tethered cluster catalysts on supports.

The anchoring of clusters to supports by tethered ligands offers a way to heterogenise solution catalysts and hopefully combine the advantages of both solution and dispersed metallic catalysts.[93] For example, the following advantages may be attainable:

(i) Separation of the catalyst.

The major disadvantage of homogeneous catalysts is the problem of separating the very expensive catalyst from the products at the end of the reaction. With heterogeneous catalysts this can be achieved by filtration whereas with homogeneous catalysts, a distillation or ion exchange process is often required and unless these are efficient, catalyst

losses may occur and render the process uneconomic. Also, separation by distillation is not possible in the case of reactions giving high boiling side products.

(ii) Efficiency

In a heterogeneous catalytic reaction the reaction must necessarily take place on the catalyst surface and so all the metal atoms not present on the surface must remain unused. By contrast, all the molecules in a homogeneous catalyst are available for catalysis, so these catalysts should be the more efficient (if they possess the same activity). A heterogenised solution catalyst should still retain this advantage.

(iii) Reproducibility, specificity and controlability

These closely related aspects are all potentially obtainable with cluster catalysts because of their discrete structures and stoichiometry which could be modified in order to control a reaction. This controlability has been demonstrated with mononuclear complex catalysts,[93] such as $|Rh(acac)(CO)_2|$ and $|Rh(acac)(CO)(PPh_3)|$ in which the ratio of normal to branched aldehydes obtained by 1-hexene hydroformylation is controlable by phosphine substitution.

(iv) Solvent and phase

The range of suitable solvents for a homogeneous catalyst is often limited by the solubility of the catalyst and substrates, whereas for heterogenised catalysts mixed phase reactions and varying solvents present few problems.

A number of materials have been evaluated as supports for homogeneous mononuclear complex[93-97] and cluster catalysts (see Table 1.2). These supports can generally be divided into inorganic or organic supports, although there is some overlap, particularly in the cases of polysiloxanes and carbon. The most important of these materials at present are polystyrene and silica and many of the tethering reactions used for these are typical of those required for organic and inorganic supports respectively.

Table 1.2.

Some materials used to support metal complexes.

Inorganic	Organic
silica	polystyrene
alumina	polyamines
zincite	polyvinyls
magnesia	urethanes
clay	acrylic polymers
other metal oxides	polybutadiene
carbon	polysiloxanes

Taking polystyrene as an example of a typical organic polymer, organometallic compounds are anchored to polystyrene by means of pendant ligands, which can be introduced into the polymer in several ways. For example, one of the most important anchoring ligands is the phosphine. These can be introduced

into the polymer by reacting; i) lithium diphenylphosphide with a halogenated polymer, ii) lithiated polymer with chlorodiphenylphosphine, or iii) introducing the phosphine as part of one of the monomers (see Diagram 1.7). Other ligands introduced into supports include (-)-Diop, amines, cyanides, cyclopentadienyl, thiolate ligands and counter ions (e.g. sulphonate and quaternary ammonium groups).

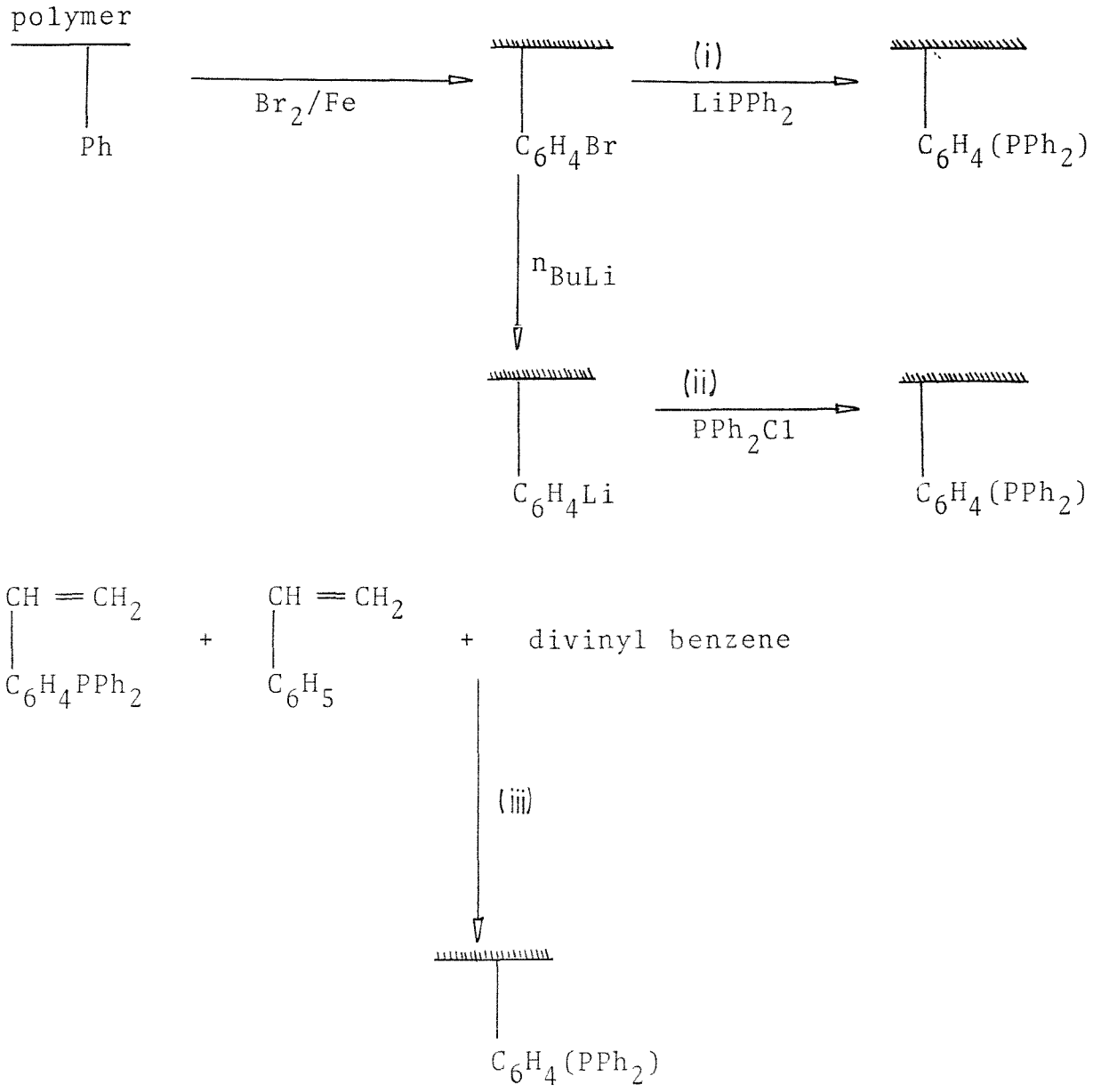

Diagram 1.7

Gates and co-workers have explored the catalytic applications of cluster compounds anchored on phosphine-functionalised poly(styrene-divinyl benzene)polymers.[98-102] In addition to the conventional particulate supports, use has been made of polymer membranes which allow the characterisation of the working catalyst by i.r. spectroscopy. The clusters anchored to date by this method include, $|Ir_4(CO)_{12-x}(P)_x|$ (x = 1 or 2), $|Fe_2Pt(CO)_8(P)_2|$, $|RuPt(CO)_5(P)_3|$, $|HAuOs_3(CO)_{10}(P)|$, $|H_4Ru_4(CO)_{12-x}(P)_x|$ (x = 1, 3 or 4), $|H_2Os_3(CO)_9(P)|$ and $|Rh_6(CO)_{13}(P)_3|$ where P = phosphinated poly(styrene-divinyl benzene)polymer.

For the tetraruthenium clusters,[101] two types of polymer membrane supports were synthesised. The first was prepared by the co-polymerisation of styrene, divinyl benzene and p-styryldiphenyl phosphine . The second by co-polymerisation of styrene, divinyl benzene and p-bromostyrene. The bromide groups in the latter were partially converted into phosphines by reaction with $LiPPh_2$ (see Diagram 1.7). The first kind of support was a block co-polymer having high local concentrations of the $-PPh_2$ groups in a polymer matrix and the second kind was a nearly random co-polymer having almost uniformly distributed $-PPh_2$ groups.

$|H_4Ru_4(CO)_{12}|$ was incorporated by phosphine substitution. Variations of the conditions used in preparing the polymers could be used to control the degree of substitution. The uniform polymer, when the phosphine loading was low, gave $|H_4Ru_4(CO)_{11}(P)|$. The structure of the block co-polymer was

varied to yield $|H_4Ru_4(CO)_9(P)_3|$ and $|H_4Ru_4(CO)_8(P)_4|$. The catalytic activity of the samples increased as the degree of phosphine substitution increased (i.e. hydrogenation of ethylene). This activity mirrors that of the homogeneous systems, studied by Frediani et al.,[103] for cyclohexanone hydrogenation catalysed in solution by tetrahydridotetra-ruthenium clusters substituted with phosphine groups.

The possibility that the catalysis was due to side products not observed in the i.r. spectra could not be ruled out. Though it was found that: (i) the i.r. spectra showed that the only detectable metal species was the attached cluster, (ii) the catalytic activity varied systematically with the clusters' ligand environment, (iii) the clusters were stable for long periods under the reaction conditions, (iv) the kinetics of the reactions differed markedly from those seen for the hydrogenation on metal surfaces, and (v) the activity was reproducible for separately synthesised membranes. These results suggest that the clusters are the active catalysts. The kinetics and mechanism of ethylene hydrogenation in solution by $|H_4Ru_4(CO)_{12}|$ has been studied[104] and appears to involve an $|H_3Ru_4(CO)_{12}(C_2H_5)|$ intermediate.

One problem encountered in determining the catalytic activity of tethered clusters is active side products. For example, when $Rh_6(CO)_{16}$ was anchored onto phosphinated-poly-(styrene-divinyl)benzene polymer membranes,[99] it initially formed $|Rh_6(CO)_{13}(P)_3|$ which is thought to be an active hydrogenation catalyst for cyclohexene and ethylene under mild

conditions (80 ^{o}C, 1 atm H_2). However, an ageing process produces supported metal (ca 15 Å particle size) which is also active.

A possible additional advantage of tethering catalysts is that the anchored catalyst once on the surface, unless it fragments, is effectively "matrix isolated" and cannot become deactivated by aggregation reactions. For example,[105] $|Rh_4(CO)_{12}|$ anchored by amines (amberlyst resin) onto a polymeric support proved to be a more active catalyst for the hydrogenation of α-β unsaturated carbonyl compounds using H_2O than a similar solution system (100 atm of CO was employed to stabilise the cluster). This is thought to be because the polymer prevents the formation of Rh aggregates, as $|Rh_5(CO)_{15}|^-$ predominates in solution.[106]

One drawback of polymers as supports is their relatively low chemical and physical stability compared to oxide supports. For example, the solvent polarity is known to affect the pore size and structure of polymers (due to solvent swelling) and hence the activity of anchored catalysts. Oxides in comparison have rigid structures and so are not affected by the nature of the solvent. Dispersed metallic catalysts typically require high operating temperatures (200 - 500 ^{o}C) and under these conditions denaturing of polymers occurs.

The most common oxide support for anchored clusters is silica. The tethering procedures used for silica are generally applicable to other oxides, as they depend on the

presence of the ubiquitous surface hydroxyl groups. The silanol groups on silica have been used to bind clusters either directly (e.g. $|Os_3(CO)_{10}(\mu\text{-}H)(\mu\text{-}O_{SiO_2})|$[81]) or through a tethered ligand (e.g. $|Os_3(CO)_{11}PPh_2(CH_2)_2Si(OEt)_{3-x}(O_{SiO_2})_x|$[107]).

A problem commonly encountered with deposited or chemisorbed clusters is aggregation. For example, when $|Rh_4(CO)_{12}|$ interacts with silica, $|Rh_6(CO)_{16}|$ is formed initially, and this interacts with molecular oxygen to give chemisorbed $Rh^I(CO)_2$ species.[108] These interact with carbon monoxide to regenerate the Rh_4 and Rh_6 clusters. This work illustrated how the mobility of mononuclear species on supports is important in the process of metal particle aggregation. A way to prevent this could be to tether the metal particles or fragments by anchored ligands. The work of Gates et al,[99] on $|Rh_6(CO)_{16}|$ interacted with amine and phosphine modified silicas, supports this suggestion. Initially in both cases Rh octahedron fragmentation occurs to give mononuclear species, $L_nRh(CO)_2$ (L = ligand, n is unknown), which on heating decarbonylate to give monocarbonyl species, $L_nRh(CO)$. These species when reduced by hydrogen yield Rh crystallites. Electron microscopy on these shows that the average crystallite size is smaller on the phosphinated than aminated silica samples (12 - 15 Å compared to 15 - 20 Å). So despite initial cluster fragmentation, the ligands do effect the amount of metal particle aggregation, though ideally the anchoring ligand should not cause fragmentation of the cluster during anchoring.

There are two main ways used to attach intact clusters

onto silica by ligands. These are to interact (i) the cluster with the liganded silica, and (ii) the liganded cluster with silica (see Diagram 1.8).[107,109] The potential advantages of route (i) are that some control over the degree of substitution may be achieved by varying the loading of the surface and that harsh ligand anchoring conditions (to anchor the ligand firmly) can be employed without any fear of damaging a tethered cluster. Route (ii), however, allows the cluster to be purified and characterised by molecular techniques before anchoring. In practice, however, clusters containing a hydrolysable silyl group are hard to purify as chromatography techniques, such as t.l.c., using hydroxylic phases cannot be employed. In addition to this they also tend to be reluctant to crystallise, though this can be partially overcome by changing the hydrolysable grouping. Other hydrolysable groups that can be used to anchor ligand silanes are: silyl halide, silyl ester, and silyl amides, but these suffer from the disadvantage of producing side products during anchoring which can react with the clusters, e.g.

$$R_3Si\text{--}Cl + \text{—}\overset{|}{\underset{|}{Si}}\text{—}OH \rightarrow R_3Si\text{—}O\text{—}\overset{|}{\underset{|}{Si}}\text{—} + HCl$$

The first report of the use of silanated tethering ligands to anchor clusters was by Brown and Evans,[107] though the anchoring of $|Co_3(CO)_9C(CH_2)_nX|$ had been reported[94] previously (using surface Si —H groups to interact with —X). Brown and Evans have anchored clusters of the formulae

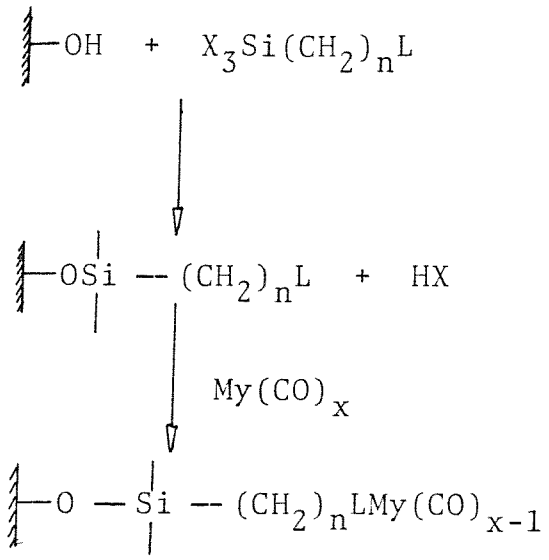

Route (i)

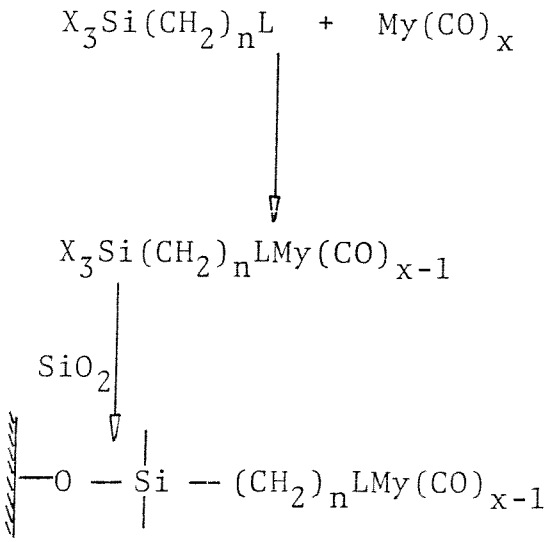

Route (ii)

For mononuclear species:

X = RO-, R --C(O)O-, Cl-, and R_2N-; and L = PPh_2, NRH_2-, NHR-, NR_2-, NC-, CN-, and HS-.

Diagram 1.8.

$|H_2Os_3(CO)_{10-9}\{PPh_2(CH_2)_2Si(OEt)_3\}|$ and $|Os_3(CO)_{11}\{PPh_2(CH_2)_2Si(OEt)_3\}|$ by both routes (i) and (ii) (shown in Diagram 1.8) and $|HOs_3(CO)_9CCSi(OEt)_3|$ by route (ii), onto silica. These were characterised by comparative i.r. spectroscopy and the ethylene hydrogenation activity of the phosphine anchored species was compared to the homogeneous analogues (i.e. $|H_2Os_3(CO)_9PPh_2Et|$ and $|Os_3(CO)_{11}PPh_2Et|$. The anchored materials were found to be less active than the dissolved model compounds under the same conditions.[110,111] Deactivation was observed to accompany the formation of $|(H)_3Os_3(CO)_8(\mu_3\text{-}CCH_3)(PPh_2R)|$ in both sets of compounds, but in addition to this the anchored species also showed deactivation by oxide induced decomposition.

Brown and Evans have also reported the anchoring of $|Ru_6C(CO)_{17}|$ onto silica by pendant phosphine ligands.[112] This under mild conditions yielded $|Ru_6C(CO)_{16}\{PPh_2(CH_2)_2Si(OEt)_{3-x}(O_{SiO_2})_x\}|$, which on warming reacted with residual free neighbouring phosphine ligands to give the disubstituted cluster, $|Ru_6C(CO)_{15}\{PPh_2(CH_2)_2Si(OEt)_{3-x}(O_{SiO_2})_x\}_2|$. On warming further (80 - 100 ^oC) oxide induced cluster decomposition occurred (despite the presence of the carbide atom) to give mononuclear species like those observed for $|Ru_3(CO)_{12}|$ on silica.

These last two examples illustrate two common problems encountered in the tethering of clusters to oxide supports - the problem of polysubstitution by neighbouring ligands and the problem of oxide induced cluster breakdown. The problem of polysubstitution has also been reported by Gates,[102] for

$|H_4Ru_4(CO)_{12}|$ anchored thermally onto phosphinated silica (i.r. spectroscopy demonstrated the presence of $|H_4Ru_4(CO)_{12-n}\{PPh_2(CH_2)_2Si(OEt)_{3-x}(O_{SiO_2})_x\}_n|$ where n = 1, 2 and 3). This problem can be overcome by choosing systems which only give one product with the anchoring ligand. For example, $|Os_3(CO)_{11}CH_3CN|$ gives specifically, even in the presence of a large excess of phosphine, $|Os_3(CO)_{11}PR_3|$. Obviously the number of reactions which display this required specificity for anchoring is limited. This has provided the impetus to investigate the use of new anchoring ligands (other than the monodentate phosphine ligands currently employed) and in particular, bridging and capping ligands which offer the prospect of stabilising the cluster framework on the oxide surface.

Recently oxides have been found to have a promotional effect on cluster substitution.[48] This should also apply to cluster catalysis. For example, PtO and PdO have been found to catalyse the substitution of $|Ru_3(CO)_{12}|$ and $|Os_3(CO)_{12}|$ with isocyanide ligands and this in addition to the already well established oxide promotion of dispersed metallic catalysts has shown the need to expand the tethering of clusters to oxides other than silica.

(f) General experimental details.

All operations were performed under a nitrogen atmosphere unless otherwise indicated. The solvents were distilled from an appropriate drying agent and purged with nitrogen before use. The infra-red, n.m.r. and mass spectra were

obtained on a Perkin-Elmer PE-580 with a model 3500 data station, Varian XL-100 and A.E.I. M.S.12 spectrometer, respectively, unless otherwise indicated.

The characterisation of the oxide supported clusters was usually achieved by transmission i.r. spectroscopy of mulls and pressed discs. A major problem encountered was the partial opacity of the oxides in the i.r. spectrum. Fortunately, most oxides have a window in the carbonyl stretching region which allowed characterisation by a fingerprint technique. The model 3500 data station greatly assisted the handling of data, allowing easy comparison of spectra, accumulation of weak spectra, subtraction of backgrounds and the routine monitoring of subtle changes in spectral intensity during reactions.

The starting materials $|Ru_3(CO)_{12}|$,[113] $|Os_3(CO)_{12}|$,[114] $|H_4Ru_4(CO)_{12}|$,[115] $|Ru_5C(CO)_{15}|$,[47] and $|Ru_6C(CO)_{17}|$,[112] were prepared by the literature methods and where necessary were ^{13}CO enriched by heating under a partial pressure of ^{13}CO in a suitable solvent ($|Ru_3(CO)_{12}|$, toluene, 125 ^{o}C; $|H_4Ru_4(CO)_{12}|$, cyclohexane, 60 ^{o}C; $|Ru_5C(CO)_{15}|$,CH_2Cl_2, 40 ^{o}C). ^{13}CO enriched $|Ru_6C(CO)_{17}|$ was prepared from ^{13}CO enriched $|Ru_3(CO)_{12}|$. The level of enrichment was kept below 45 % in order to avoid line broadening in the ^{13}C n.m.r. due to ^{13}C - ^{13}C coupling. All the ^{13}C n.m.r. were recorded with the aid of $Cr(acac)_3$ as a spin relaxant except where mentioned otherwise.

The chromatographic separations using normal column, flash

column and thin layer chromatography used silica gel 60 - 120 mesh (B.D.H., No. = 15049), Nagel silica gel 60, and silica 60G (Merck, No. = 7731, 1 mm thickness on 20 x 20 plates) respectively.

References to Chapter 1.

Review articles.

(i) General aspects of cluster chemistry.

1. "Transition metal clusters", ed. B.F.G. Johnson, Wiley, Chichester (1980).
2. B.F.G. Johnson and J. Lewis; Adv.Inorg.Chem.Radiochem., (1981), 24, 255.
3. B.F.G. Johnson and J. Lewis, Pure and Appl.Chem., (1982), 54, 97.
4. E.L. Muetterties; J.Organomet.Chem., (1980), 200, 177.
5. "Comprehensive Organometallic Chemistry", Ed. Sir G. Wilkinson, Pergamon Press, Oxford (1982).

(ii) Specific aspects of cluster chemistry.

(a) Mixed metal clusters.

6. W.L. Gladfelter and G.L. Geoffroy; Adv.Organomet.Chem., (1980), 18, 207.
7. G.L. Geoffroy; Acc.Chem.Res., (1980), 13, 469.

(b) Tetrahedral clusters.

8. P. Chini and T. Heaton; Top.Curr.Chem., (1977), 17, 1.

(c) High nuclearity in clusters.

9. P. Chini, G. Longoni, and V.G. Albano; Adv.Organomet.Chem., (1976), 14, 285.
10. P. Chini, J.Organomet.Chem., (1980), 200, 37.

(d) Carbide clusters.

11. M. Tachikawa and E.L. Muetterties; Prog.Inorg.Chem., (1981), 28, 203.

(e) Theoretical studies.

12. D.M.P. Mingos; Pure and Appl.Chem., (1980), 52, 705.

13. K. Wade; Adv.Inorg.Chem.Radiochem., (1976), 18, 1.

14. M.C. Manning and W.C. Tragler; Coord.Chem.Rev., (1981), 39, 89.

(f) Mechanistic studies.

15. E. Bond and E.L. Muetterties; Chem.Rev., (1978), 78, 639.

(g) Stereochemical considerations

16. B.F.G. Johnson and R.E. Benfield; Top.Stereochem., (1981), 12, 253.

(h) Nonrigidity.

17. J. Evans; Adv.Organomet.Chem., (1977), 16, 319.

18. J.H. Sinfelt; Progress in solid state chemistry, (1975), 10, 55.

19. "Structure of Metallic Catalysts", J.R. Anderson, Academic Press, (1975).

20. "Catalysis", P.H. Emmett, ed. Vol. 1, Reinhold, New York (1954), article by W.B. Innes, p.245.

21. E.I. Gil'debrand Int.Chem.Eng., (1966), 6, 449.

22. M. Moskovits; Acc.Chem.Res., (1979), 12, 229.

23. H.F. Schaefer; Acc.Chem.Res., (1977), 10, 287.

24. H. Vahrenkamp; Angew.Chem.,Int.Ed.Engl., (1978), 17, 379.

25. G.A. Ozin; Catal.Rev., (1977), 16, 191.

26. R. Ugo; Catal.Rev., (1975), 11, 225.

27. J. Evans; Chem.Soc.Rev., (1981), 10, 159.

28. F.C. Gault; Adv.Catal., (1981), 30, 1.

29. "Aspects of homogeneous catalysis", Ed. R. Ugo, Reidel, Dordrecht, (1977), Vol. 3.

30. E.L. Muetterties; Angew.Chem.,Int.Ed.Engl., (1978), 17 545.

31. E.L. Muetterties, T.N. Rhodin, E. Band, C.F. Brucker, and W.R. Pretzer, Chem.Rev., (1979), 79, 91.

32. E.L. Muetterties; Pure Appl.Chem., (1980), 52, 2061.

33. E.L. Muetterties, Pure Appl.Chem., (1982), 54, 83.

34. Shell Chem.Abstr., (1977), 87, 41656h.

35. M.G. Thomas, B.F. Beier, and E.L. Muetterties, J.Am.Chem. Soc., (1976), 98, 1296.

36. G.C. Demitras and E.L. Muetterties, J.Am.Chem.Soc., (1977), 99, 2796.

37. R.L. Pruett; Ann.N.Y.Acad.Sci., (1977), 295, 239.

38. J.F. Knifton; J.Am.Chem.Soc., (1981), 103, 3959.

39. F. Fischer and H. Tropsch, Brennst Chem., (1923), 4, 276.

40. P. Sabatier and J.B. Senderens; Hebd.Seances.Acad.Sci., (1902), 134, 514.

41. I. Wender, Catal.Rev., (1976), 14, 97.

42. B.C. Gates and J. Lieto; Chem.Tech., (1980), 195.

43. M.A. Vannice; Catal.Rev., (1976), 14, 153.

44. M. Manassero, M. Sansoni, and G. Longoni, J.Chem.Soc., Chem.Commun., (1976), 919.

45. G. Fachinetti, J.Chem.Soc.,Chem.Commun., (1979), 396.

46. H.A. Hodali and D.F. Shriver; Inorg.Chem., (1979), 18, 1236.

47. D.H. Farrar, R.F. Jackson, B.F.G. Johnson, J. Lewis, J.N. Nicholls, and M. McPartlin; J.Chem.Soc.,Chem.Commun., (1981), 415.

48. B.L. Moroz, V.A. Semikolenov, V.A. Kilholobov, and Y.I. Yermakov; J.Chem.Soc.,Chem.Commun., (1982), 1286.

49. M. Tachikawa and E.L. Muetterties; J.Am.Chem.Soc., (1980), 102, 4541.

50. R.B. Calvert and J.R. Shapley; J.Am.Chem.Soc., (1978), 100, 7726.

51. R.B. Calvert and J.R. Shapley; J.Am.Chem.Soc., (1977), 99, 5225.

52. C. Masters; Adv.Organomet.Chem., (1979), 17, 61.

53. B.R. James; Adv.Organomet.Chem., (1979), 17, 319.

54. E.L. Muetterties; Catal.Rev., (1981), 23, 69.

55. E.L. Muetterties and J. Stein; Chem.Rev., (1979), 79, 479.

56. C.P. Casey et al., Pure Appl.Chem., (1980), 52, 625.

57. P. Biloen and W.M.H. Sachtler; Adv.Catal., (1981), 30, 165.

58. W.A. Herrmann, Angew.Chem.,Int.Ed.Engl., (1982), 21, 117.

59. C.K. Rofer-De Poorter; Chem.Rev., (1981), 81, 447.

60. M. Bianchi, F. Piacenti, G. Menchi, P. Frediani, U. Matteoli, C. Botteghi, S. Gladiali, and E. Benedetti; Chim.Ind.(Milan), (1978), 60, 588.

61. M. Valle, D. Osella, and G.A. Vaglio; Inorg.Chim.Acta, (1976), 20, 213.

62. P. Pino, G. Braca, G. Sbrana, and A. Cuccuru, Chem.Ind., (1968), 1732.

63. C.S. Chin, M.S. Sennett, and L. Vaska; J.Mol.Catal., (1978), 4, 375.

64. R.M. Laine; J.Am.Chem.Soc., (1978), 100, 6451.

65. H. Kang, C.H. Maudlin, T. Cole, W. Slegeir, K. Cann, and P. Pettit; J.Am.Chem.Soc., (1977), 99, 8823.

66. B. Heil and L. Markó; Chem.Ber., (1968), 101, 2209; ibid, (1969), 102, 2238.

67. N.S. Imyanitov and D.M. Rudkowskii; Zh.Prikl.Khim., (1967), 39, 2020 and 2029.

68. J.R. Norton, Preprint, Petroleum chemistry Division, 172nd National ACS Meeting, (1976), 343.

69. M. Bianchi, F. Piacenti, G. Menchi, P. Frediani, U. Matteoli, C. Botteghi, S. Gladiali, and E. Benedetti; Chim.Ind.(Milan), (1978), 60, 588.

70. F. Richter and H. Vahrenkamp, Chem.Ber., (1982), 115, 3224.

71. F. Richter and H. Vahrenkamp, Chem.Ber., (1982), 115, 3243.

72. C.U. Pittman Jr., M.C. Richmond, M. Absi-Halobi, H. Beurich, F. Richter, and H. Vahrenkamp, Angew.Chem., Int.Ed.Engl., (1982), 21, 786.

73. M.I. Bruce, J.G. Matisons, B.K. Nicholson, and M.I. Williams, J.Organomet.Chem., (1982), 236, C57.

74. B.F.G. Johnson, J. Lewis, K. Wang, and M. McPartlin, J.Organomet.Chem., (1980), 185, C17.

75. E. Band, W.R. Pretzer, M.G. Thomas, and E.L. Muetterites; J.Am.Chem.Soc., (1977), 99, 7380.

76. R.C. Ryan, C.U. Pittman, and J.P. O'Connor; J.Am.Chem. Soc., (1977), 99, 1986.

77. C.U. Pittman and R.C. Ryan; Chem.Technol., (1978), 8, 170.

78. G. Huttner, J. Schneider, H.D. Muller, G. Mohr, J.von Seyerl, and L. Wohlfahrt; Angew.Chem.,Int.Ed.Engl., (1979), 18, 76.

79. C.U. Pittman, R.C. Ryan, and J. McGee; J.Organomet.Chem., (1979), 178, C43.

80. J. Robertson and G. Webb; Proc.Roy.Soc.London A, (1974), 341, 383.

81. B. Besson, A. Choplin, L.D. Ornelas, and J.M. Basset; J.Chem.Soc.,Chem.Commun., (1982), 843.

82. F. Hugues, A.K. Smith, Y.Ben Taarit, J.M. Basset, D. Commereuc, and Y. Chauvin; J.Chem.Soc.,Chem.Commun., (1980), 68.

83. D. Commereuc, Y. Chauvin, F. Hugues, J.M. Basset, and D. Olivier; J.Chem.Soc.,Chem.Commun., (1980) 154.

84. A. Brenner; J.Chem.Soc.,Chem.Commun., (1979), 251.

85. A. Brenner and D.A. Hucul; Inorg.Chem., (1979), 18, 2836.

86. A.K. Smith, A. Theolier, J.M. Basset, R. Ugo, D. Commereuc, and Y. Chauvin; J.Am.Chem.Soc., (1978), 100, 2590.

87. J.R. Anderson and D.E. Mainwaring; J.Catal., (1974), 35, 164.

88. J.R. Anderson and B.G. Baker, Proc.Roy.Soc.London A, (1963), 271, 402.

89. P. Gallezat, Catal.Rev., (1979), 20, 121.

90(a) H.H. Nijs, P.A. Jacobs, and J.B. Uytterhoeven, J.Chem.Soc.,Chem.Commun., (1979), 180 and 1095.

90(b) D. Ballivet-Tratchenko, G. Coudunier, H. Mozzanega, I. Tratchenko, and A. Kiennemann, J.Mol.Catal., (1979), 6, 293.

91. P. Gelin, Y. Ben Taarit, and C. Naccoche, J.Catal., (1979), 59, 357.

92. H.E. Ferkul, D.J. Stanton, J.D. McCowan, and M.C. Bard, J.Chem.Soc.,Chem.Commun., (1982), 955.

93. B.R. James, Adv.Organomet.Chem., (1979), 17, 319.

94. J.C. Bailar, Catal.Rev., (1974), 10, 17.

95. Yu.I. Yermankov, Catal.Rev., (1976), 13, 77.

96. Yu.I. Yermankov, Pure Appl.Chem., (1980), 52, 2075.

97. D.C. Bradley and S.H. Longer, Chem.Rev., (1981), 81, 109.

98. B.C. Gates and J. Leito, Chem.Technol., (1980), 10, 248.

99. E.W. Thornton, H. Knözinger, B. Tesche, J.J. Rafalko, and B.C. Gates, J.Catal., (1980), 62, 117.

100. J. Leito, J.J. Rafalko, and B.C. Gates, J.Catal., (1980), 62, 149.

101. Z. Otero-Schipper, J. Leito, and B.C. Gates, J.Catal., (1980), 63, 175.

102. R. Pierantozzi, K.J. McQuade, B.C. Gates, M. Wolf, H. Knozinger, and W. Ruhmann, J.Am.Chem.Soc., (1979), 101, 5436.

103. M. Bianchi, G. Menchi, F. Francalanci, F. Piancenti, U. Matteoli, P. Frediani, and C. Batteghi, J.Organomet. Chem., (1980), 188, 109.

104. Y. Doi, K. Kashizuka, and T. Keli, Inorg.Chem., (1982), 21, 2732.

105. T. Kitamura, T. Joh, and N. Hagihara, Chem.Lett., (1975), 203.

106. T. Kitamura, N. Sakamoto, and T. Joh, Chem.Lett., (1973), 379.

107. S.C. Brown and J. Evans, J.Chem.Soc.,Chem.Commun., (1978), 1063.

108. A. Theolier, A.K. Smith, M. Lecante, J.M. Basset, G.M. Zanderighi, P. Psaro, and R. Ugo, J.Organomet.Chem., (1980), 191, 415.

109. F.R. Hartley, and R.N. Vezey, Adv.Organomet.Chem., (1976), 15, 189.

110. S.C. Brown and J. Evans, J.Mol.Catal., (1981), 11, 143.

111. S.C. Brown and J. Evans, J.Organomet.Chem., (1980), 194, C53.

112. S.C. Brown, J. Evans, and M. Webster, J.Chem.Soc., Dalton Trans., (1981), 2263.

113. C.R. Eady, P.F. Jackson, B.F.G. Johnson, J. Lewis, M.C. Malatesta, M. McPartlin, and W.J.H. Nelson, J.Chem.Soc.,Dalton Trans., (1980), 383.

114. B.F.G. Johnson, J. Lewis, and P.A. Kilty, J.Chem.Soc.A, (1968), 2859.

115. F. Piacenti, M. Biakchi, P. Frediani, and E. Benedetti, Inorg.Chem., (1971), 10, 2759.

CHAPTER TWO

Generalised Cluster Anchoring and Chemisorption on Oxide Supports

At the commencement of this investigation the work concerned with the tethering of clusters had largely been restricted to diphenylalkylphosphine ligands on polymers (iridium,[1,2] ruthenium, mixed metal[3] and osmium clusters[4]) and amorphous silica (iridium, ruthenium, osmium and mixed metal clusters[3]). Although polymers offer the advantages of ease of functionalisation, precise synthesis, and characterisation, they suffer from the disadvantage of poor thermal and mechanical stability which makes them less suitable than inorganic supports for industrial catalysts. As a result this work was limited to oxide supports.

Some of the first tethered clusters were reported by Brown and Evans.[6] They characterised clusters of the types $|Os_3(CO)_{11}PPh_2R|$, $|H_2Os_3(CO)_{10}PPh_2R|$ and $|H_2Os_3(CO)_9PPh_2R|$ where R = ethyl, or $-(CH_2)_2Si(OEt)_{3-x}(O\text{-silica})_x$ by comparative i.r. It was found that while these monodentate ligands tethered the clusters well they did not stabilise them effectively towards fragmentation. For example,[7,8] it was found $|H_2Os_3(CO)_9|PPh_2(CH_2)_2Si(OEt)_{3-x}(O_{SiO_2})_x||$ decomposed under mild hydrogenation conditions (110 °C, 20 hr) to give mononuclear species which were loosely proposed to be $|Os(CO)_{2or3}|PPh_2(CH_2)_2Si(OEt)_{3-x}(O_{SiO_2})_x||$. This problem has also been reported by other workers.[9,10]

A possible way around this could be to hold the cluster together by means of bridging (e.g. CNR_2, $|M_3(\mu\text{-}H)_2(CO)_{10}(\mu\text{-}CNMe_2)|$, M = Fe,[11] Ru,[12] and Os[13]) or capping ligands (e.g. $PPh|_2$, $M_3(\mu\text{-}H)_2(CO)_9PPh|$, M = Fe,[14] Ru,[15] and Os[16]).

This approach was adopted for the present work, the thiolate ligands used react with $|M_3(CO)_{12}|$ (M = Ru and Os) to give a high yield of bridged clusters, $|M_3(\mu\text{-H})(CO)_{10}(\mu\text{-SR})|$,[18] in which both bridging groups occupy the same edge of the metal triangle.[19] The work of Osborne demonstrates this stabilising effect.[17] He found that the capping ligand $HC(PPh_2)_3$ can stabilise clusters towards fragmentation (relative to the parent or trimonodentate substituted cluster). For example, it was demonstrated that $|Rh_4(CO)_9(\mu_3\text{-tripod})|$ is stable at 100 ^{o}C for 18 hours under 30 bar of carbon monoxide, whereas $|Rh_4(CO)_{12}|$ and $|Rh_4(CO)_9(PPh_2R)_3|$ are not.

Another breakdown route for tethered clusters is by oxide interaction. This occurs with the free surface hydroxyl groups left over from the liganding of the oxide. Oxide interaction is also a problem common to gas liquid chromatography.[20] In this case oxide interaction causes tailing of chromatographic peaks and , in extreme cases, peaks due to breakdown of the eluted compounds. This difficulty is commonly overcome by acid washing the support to remove trace metals and by covering the support with a protective layer of alkylsilane. Two of the most frequently used protective silanes are $SiMe_3Cl$ and $NH(SiMe_3)_2$. They react with the hydroxyl groups to produce hydrogen chloride and ammonia, respectively, whilst silanating them. These side products affect the reactivity of the surfaces, so evaluation experiments on both agents were carried out.

The tethering of clusters to oxides offers a new route

to conventional supported "bare" metal industrial catalysts. The properties of these catalysts vary with the supporting oxide.[21] For example, in the case of chemisorbed $|Co_2(CO)_8|$,[22] the hydrogenation activity of the catalyst formed varies with the oxide (SiO_2, TiO_2, ZrO_2 > MgO, γ-Al_2O_3). This has provided the impetus in the present work to generalise the tethering of clusters to oxides other than just silica.

Reactions between metal carbonyls and functionalised oxides involve competition between the pendant ligand and the oxide itself. Consequently blank reactions were carried out by interacting ruthenium and osmium carbonyls with plain oxides under the same conditions as used for the thiolated oxide. This initiated my entry into a rapidly expanding field of investigation and as a result there has been a large amount of overlap with other work.

As the main breakdown pathway of tethered clusters appears to be by oxide interaction, this was investigated in a series of pyrolysis experiments. These were also used to evaluate the effectiveness of protective silanes. Preliminary[23] and full accounts[24] of this work have been published and another report of anchoring triosmium clusters to silica *via* a pendant thiol is also in the literature.[25]

RESULTS AND DISCUSSION

(a) The tethering of ruthenium and osmium carbonyl to thiolate oxides.

Thiolate ligands were employed to anchor triruthenium and osmium clusters since single products are formed from the reactions of $|M_3(CO)_{12}|$ and RSH.[18] This avoids the problem of separating several complexes each having a silyl group. There are two main problems in purification of compounds with hydrolysable silyl groups. That is, they are hard to crystallise and cannot be purified by thin layer chromatography (as they react with oxides). Thus, $|M_3(CO)_{10}(H)\{S(CH_2)_3Si(OMe)_3\}|$, M = Ru (1) and Os (2), were synthesised under the same conditions as required to form $|M_3(H)(CO)_{10}(SPr^n)|$, M = Ru (3) and Os (4), without any problems of separating several complexes each having the silyl group.

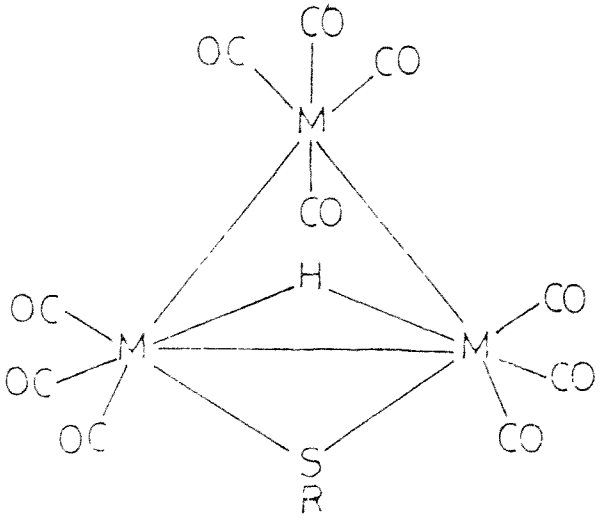

	M	R
(1)	Ru	$-(CH_2)_3Si(OMe)_3$
(2)	Os	$-(CH_2)_3Si(OMe)_3$
(3)	Ru	$-Pr^n$
(4)	Os	$-Pr^n$

Two tethering procedures were attempted (see Scheme 2.1). Both routes have inherent advantages. The main advantage of Route 1 is that the cluster can be purified and characterised before being anchored. However, its main disadvantage is that the forcing conditions used in Route 2 for anchoring the ligand cannot be applied without some risk of cluster degradation. Thus although Route 1 provides a well characterised tethered cluster, it does not produce a sample with a high resistance to leaching. For example, this was observed when the material produced by reacting the more robust cluster (2) (see Figure 2.1) with oxides was Soxhlet extracted with Et_2O and methanol (identified by its i.r. spectrum). There was some doubt as to how these clusters are tethered under these milder conditions. The silane was implicated by the trial reaction under the same conditions of (4) with oxides during which no cluster became attached. This leaves two main possibilities for the mode of attachment; either by hydrogen bonding, or by nucleophilic substitution at the $Si(OMe_3)$ group by the surface hydroxyl groups. The latter case was shown to occur by the detection of methanol in the filtrate (vacuum distilled from the remaining unabsorbed cluster) by g.l.c. The amount of methanol detected was unfortunately low, only 0.25 - 1.4 equivalents per cluster, when one would expect values of 2 - 3 but this may be due to physisorption or chemisorption of some of the methanol on the support.

From the intensities of the recorded i.r. spectra it is evident that anchoring *via* nucleophilic substitution had

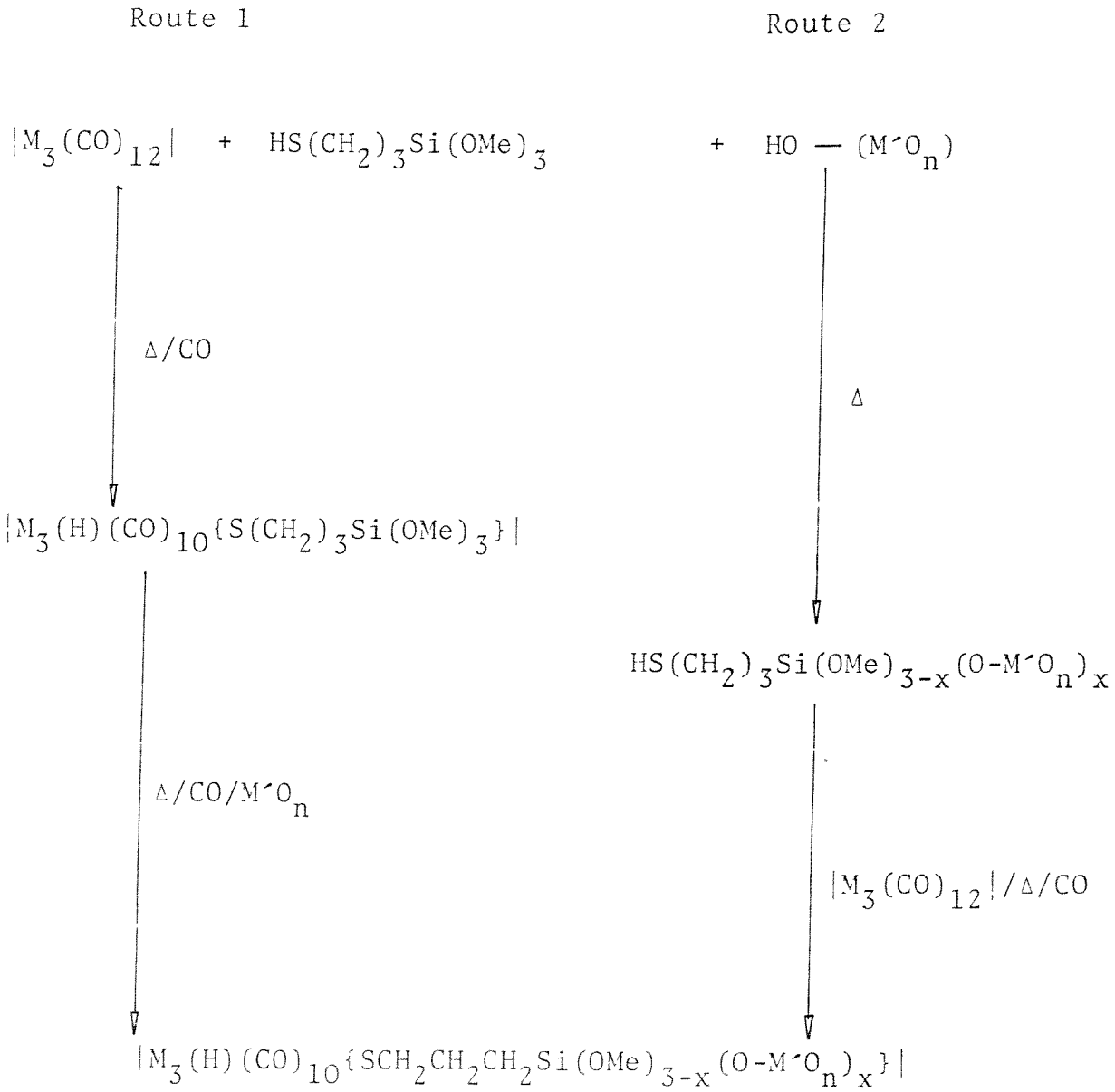
Route 1
Route 2
|M3(CO)12| + HS(CH2)3Si(OMe)3
+ HO — (M'On)
Δ/CO
Δ
|M3(H)(CO)10{S(CH2)3Si(OMe)3}|
HS(CH2)3Si(OMe)3-x(O-M'On)x
Δ/CO/M'On
|M3(CO)12|/Δ/CO
|M3(H)(CO)10{SCH2CH2CH2Si(OMe)3-x(O-M'On)x}|

Scheme 2.1.

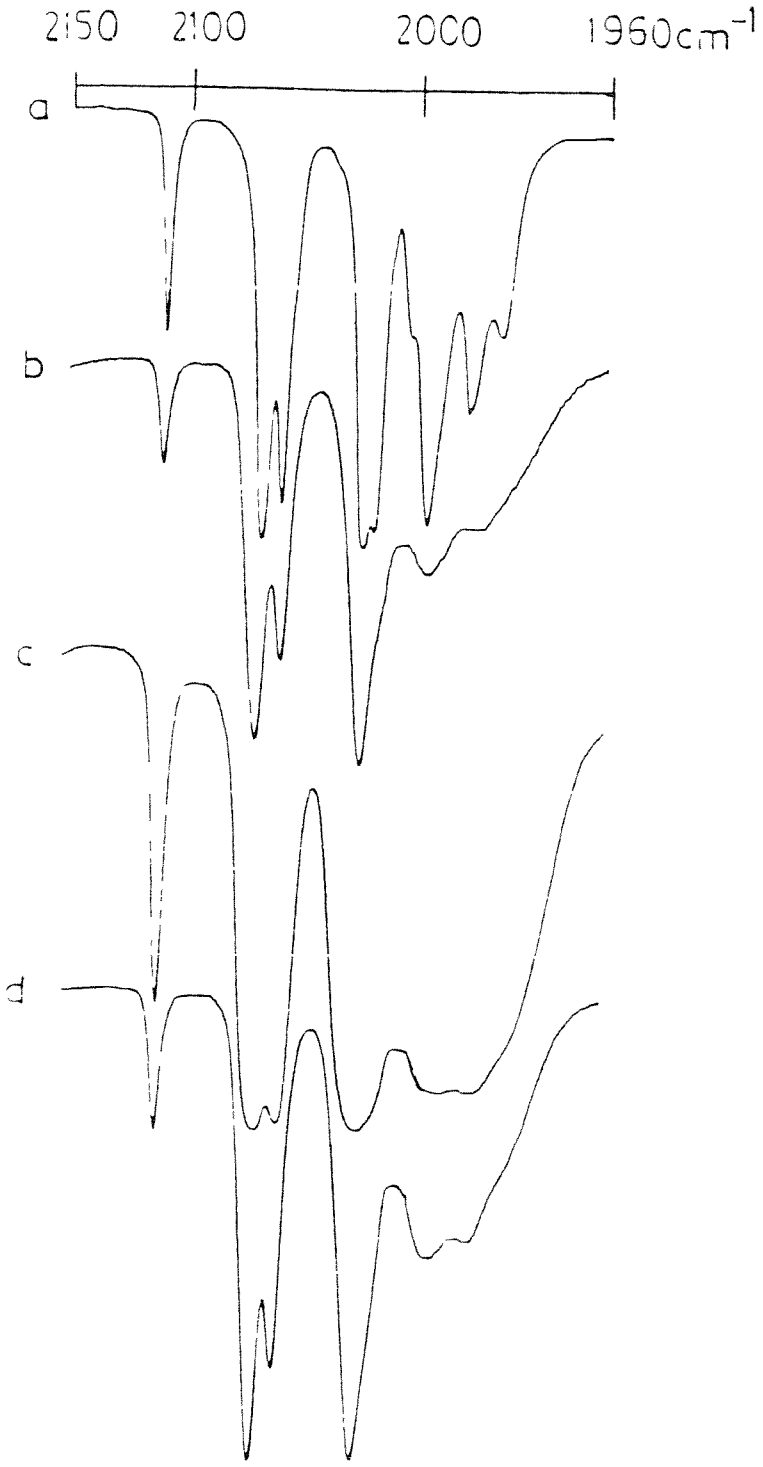

Figure 2.1. I.r. spectra (2 150 - 1 960 cm^{-1}) of (a) (2) in hexane, (b) (2) on γ-Al_2O_3, (c) the product of $|Os_3(CO)_{12}|$ with thiolated alumina, and (d) the product of $|Os_3(CO)_{12}|$ with $SiMe_3Cl$ pretreated thiolated alumina.

occurred to a much smaller extent on silica than on alumina or titania. In spite of the larger surface area of the Aerosil 380 (380 m^2/g) the osmium loading was only about one tenth of that on γ-Al_2O_3 (100 m^2/g) and TiO_2 (50 m^2/g). The reason for this is not immediately apparent as the mechanism for attachment is thought to involve the ionisation of the hydroxyl groups.[26] So, one might expect this difference in reactivity to be connected with differences in the pH of the oxides (γ-Al_2O_3 4 - 5, TiO_2 3 - 4, SiO_2 3.6 - 4.3, 4 % aqueous dispersion) but this is evidently not the case and the differences in reactivity must be due to differences in structure. In all cases the carbonyl absorptions agreed very closely with those of the two isolable analogues (2) and (4). Spectra obtained on alumina are shown in Figure 2.1.

The second route was to interact $|Os_3(CO)_{12}|$ with thiolated oxide in refluxing toluene. Again this afforded satisfactory results and the loading on silica gel was increased. Extraction experiments similar to those used for (2) on oxides (Route 1) in this case caused negligible leaching (exception ZnO when about 5 - 10 % was removed), illustrating the advantage of anchoring the ligand first (see Figure 2.1).

Using samples of functionalised oxides which had been treated with the protecting agent $SiMe_3Cl$ caused slight improvements in spectral quality, *viz*, narrower linewidths in some cases and resolution of weaker bands between 2 000 and 1 970 cm^{-1} (see Figure 2.1). It is interesting to note that the spectra on a surface resemble closely those obtained in

polar solvents like methylene chloride , i.e. the top bands remain sharp while the lower bands at around 2 000 cm^{-1} are broadened. This broadening could have three causes: it could be due to site effects (like in matrix isolation), it could be due to minor impurities, and lastly it could be caused by the polar environment of the surface of the oxide.[28] The i.r. spectra of the products of $|Os_3(CO)_{12}|$ with unprotected functionalised surfaces show no signs of side products. So the sharpening of the spectra on $SiMe_3Cl$ treated surfaces must be due to either a decrease in the variation between sites or a decrease in the effective polarity of the surface interface as a result of being coated with alkyl groups. Two pieces of evidence add support to the idea that it is the polarity of the surface which causes the broadening rather than site effects. First, when the cluster is made into a disc in KBr it shows similar broadening but to an even greater extent as, KBr is fully ionic and, therefore, provides a more polar environment than the oxides. Also, when a sample of (2) on SiO_2 is made into a disc and cooled to liquid nitrogen temperatures, the spectrum shows no changes; whereas, one would expect sharpening and splitting of peaks if the broadening was due to site effects. Little change in metal uptake was noted (exception ZnO) with the $SiMe_3Cl$ treated functionalised oxides indicating the silane reacted with surface hydroxyls in preference to the thiolate groups. This is as expected because of the greater stability of the Si-O bond.[27]

Further confirmation of the identity of $|Os_3(H)(CO)_{10}\text{-}\{S(CH_2)_3Si(OMe)_{3-x}(O_{SiO_2})_x\}|$ was obtained by diffuse reflectance u.v.-visible measurements which showed bands ≈ 30,000 and 25,270 cm^{-1}. These can be correlated with the two lower energy bands in the solution spectrum of $|Os_3(H)(CO)_{10}(SPr^n)|$ (45,600 ,39,500, 30,700 and 25,500 cm^{-1}, see Figure 2.2).

Similar experiments were carried out on the ruthenium analogues. Interaction of (1) with oxides at r.t. again afforded solids which exhibited ν_{CO} spectra similar to (1) and (3) as illustrated for alumina in Figure 2.3. The bonding on silica again was small but could be increased by raising the temperature to 40 ^{o}C under a stabilising CO atmosphere. It was found subsequently that all manipulations with these ruthenium clusters gave better results when carried out under CO rather than nitrogen. However, these materials are less stable than their osmium analogues and the extraction procedure could not be employed so doubt remains as to the effectiveness of the oxide binding (methanol was detected in the filtrates by g.l.c.). Again interaction of $|Ru_3(H)(CO)_{10}(SPr^n)|$ (3) with oxides under similar conditions did demonstrate the importance of the $Si(OMe)_3$ grouping in the chemisorption of the cluster. I.r. spectra obtained on these solids were very weak and were recorded on a 10 or 20 fold transmittance expansion indicating only a slight uptake of (3). The ν_{CO} bands which were observed for the species derived from (3) were oxide dependent.

Interacting $|Ru_3(CO)_{12}|$ with thiolate oxides afforded

Electronic Spectra of $HOs_3(CO)_{10}\{SC_3H_6Si(OMe)_3\}$

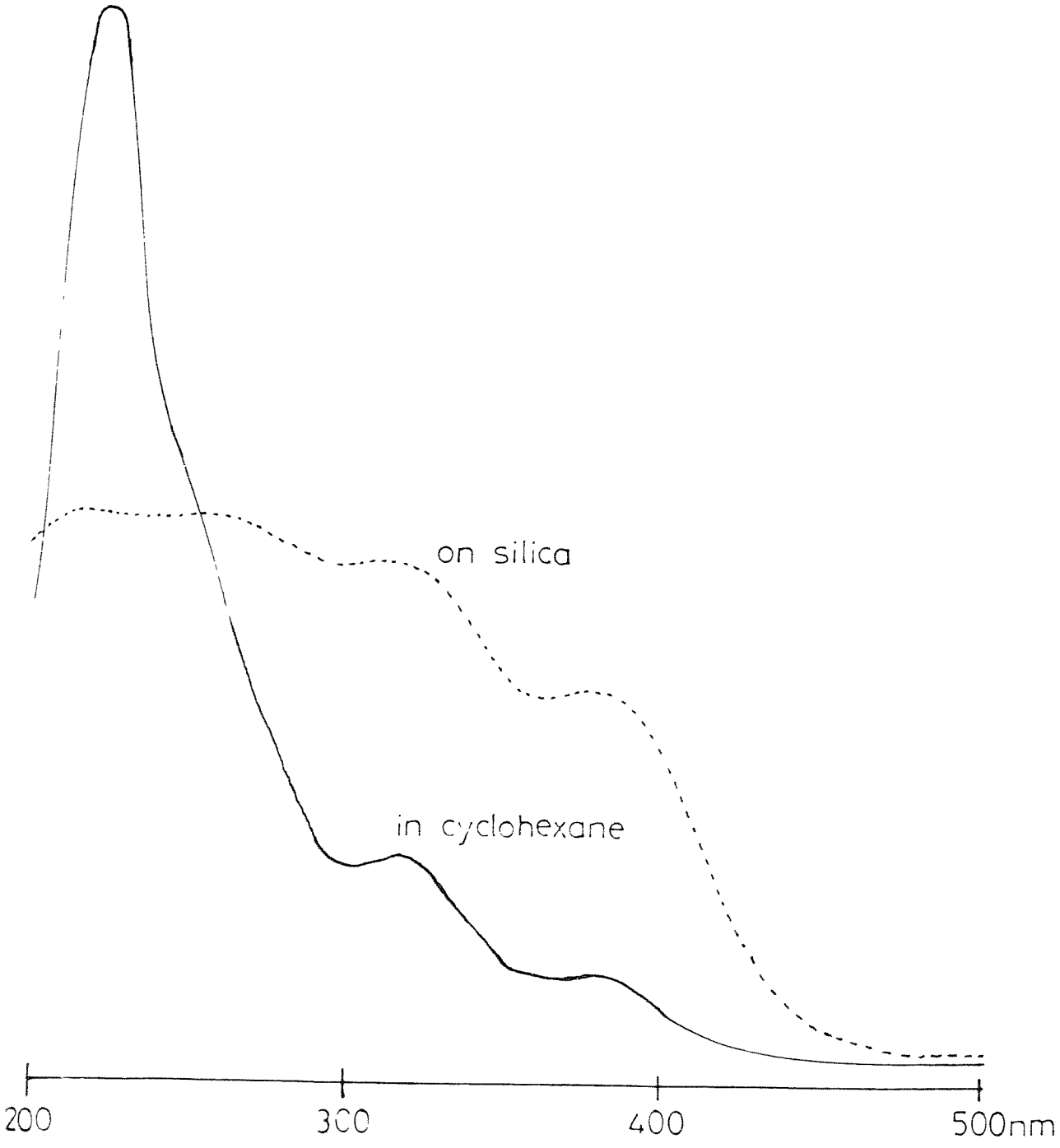

Figure 2.2.

$|Ru_3(H)(CO)_{10}\{S(CH_2)_3Si(OMe)_{3-x}(O\text{-}M'O_n)_x\}|$ species. On silica this appeared to be specific but on γ-Al_2O_3 (see Figure 2.3), TiO_2, ZnO and MgO, an additional broad ν_{CO} absorption near 2 000 cm^{-1} was also seen. The i.r. spectrum obtained on thiolated SnO_2 was of very poor quality arising from darkening and increased capacity of the oxide caused by the ligand anchoring reaction. The use of $SiMe_3Cl$ treated ligand-oxide caused only small improvements in the specificity of the anchoring reaction but did prolong the lifetime of the tri-nuclear complex (by a factor of 2). Shelf-lifes before total decomposition as monitored by the carbonyl absorptions at 2 105 and 2 066 cm^{-1} were of the order of weeks at -20 ^oC or 6 months under carbon monoxide. Both (1) and (2) were more stable than the anchored complexes and among the latter the stability on SiO_2 was greater than on γ-Al_2O_3 and this was in turn more than on TiO_2 and ZnO.

(B) The reactions between $|M_3(CO)_{12}|$ and tethered clusters with oxides.

The interaction of $|Os_3(CO)_{12}|$ with oxides has been reported under different conditions to those employed in the thiolate functionalised oxide experiments but the results are still relevant to the interpretation of these blank experiments. The reaction of $|Os_3(CO)_{12}|$ with oxides initially after physisorption is to produce species $|Os_3(H)(CO)_{10}(OM'O_n)|$ (5) (see Figure 2.4) on SiO_2,[29,30] γ-Al_2O_3,[29-31] ZnO,[31] TiO_2,[31] and MgO. The evidence for this includes i.r.

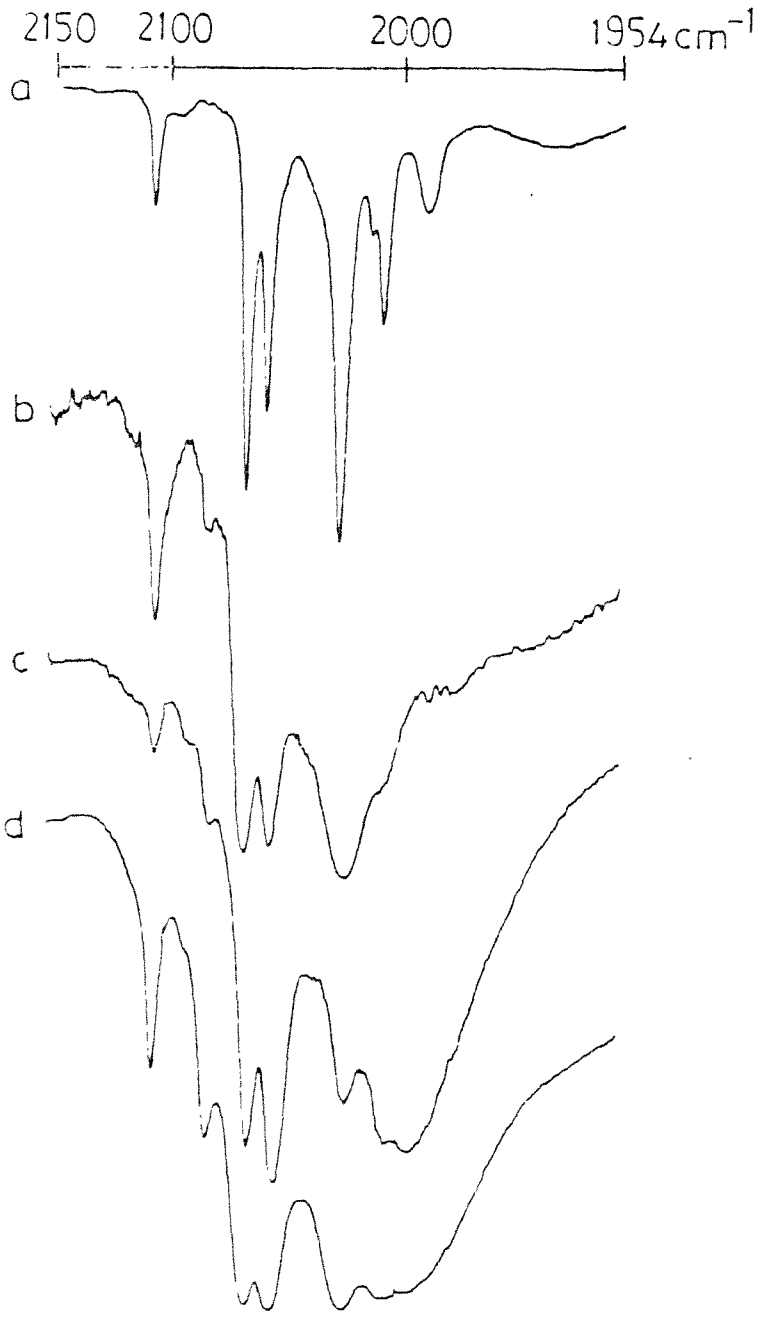

Figure 2.3. I.r. spectra (2 150 - 1 960 cm^{-1}) of (a) (1) in hexane, (b) (1) on γ-Al_2O_3, (c) the product of $|Ru_3(CO)_{12}|$ with thiolated alumina, and (d) the product of $|Ru_3(CO)_{12}|$ with $SiMe_3Cl$ pretreated thiolated alumina.

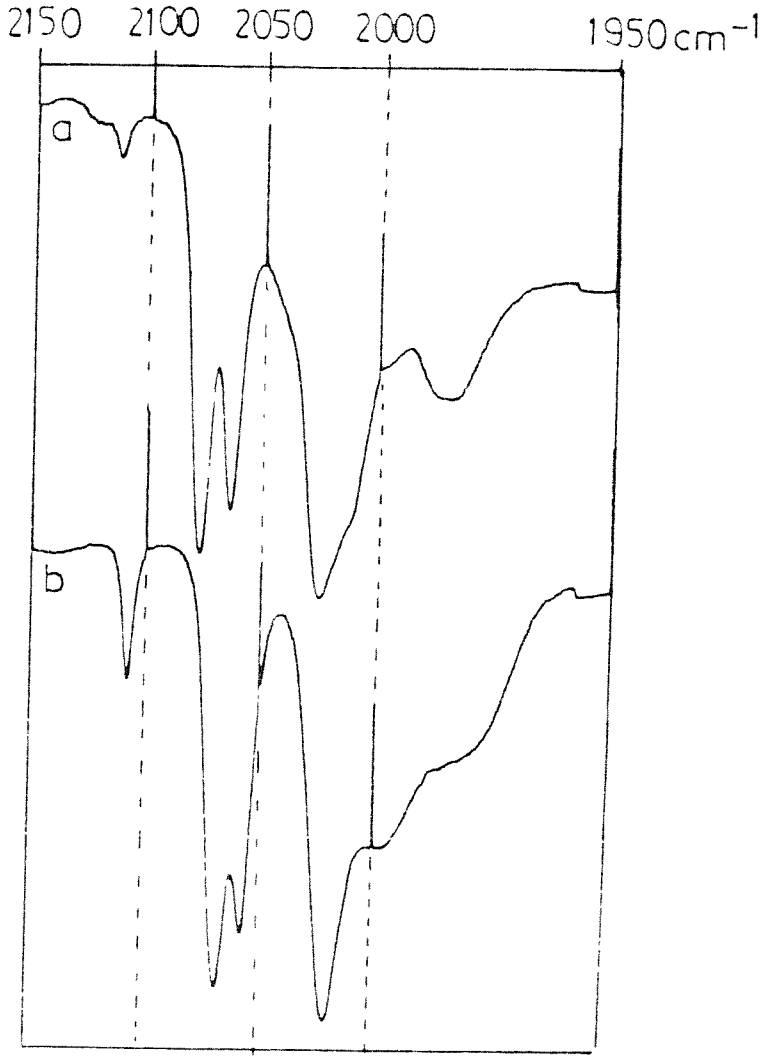

Figure 2.4. I.r. spectra (2 150 - 1 950 cm^{-1}) of (a) (5) on silica, and (b) $|Os_3(H)(CO)_{10}\{S(CH_2)_3Si(OMe)_{3-x}(OSiO_2)_x\}|$.

comparisons with $|Os_3(H)(CO)_{10}OSiPh_3|$[30] (6), extended X-ray absorption fine structure (EXAFS),[30] electronic absorption,[32] ^{13}C magic angle spinning n.m.r. and low frequency Raman spectra.[32]

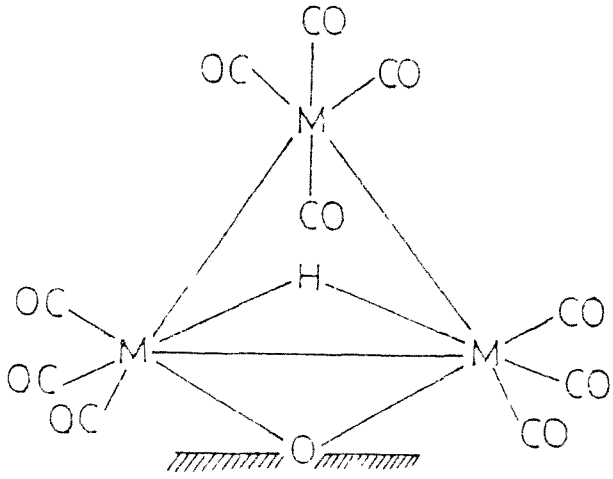

(5)

Under more vigorous conditions mononuclear species are thought to occur[29-31] but the systems, $|Os_3(CO)_{12}|/M'O_n$, are complex (involving two or more species) and as a result are not fully understood at present. One of the most highly studied is the $|Os_3(CO)_{12}|/SiO_2$ system.[29] Initially, after physisorption, (5) is formed by oxidative addition of a surface M-OH group to a Os-Os bond. Under more forcing conditions there is a breakdown of the cluster triangle with simultaneous oxidation of the osmium, to yield two osmium(II) complexes, by the surface proton and with the immediate release of hydrogen. These two species are thought to be $|Os^{II}(CO)_3(O_{SiO_2})_2|_2$ and $|Os^{II}(CO)_2(O_{SiO_2})_2|_n$. They can be interconverted by a reversible carbonylation-decarbonylation process at elevated temperatures. The evidence for these two species involves comparative i.r. with $|Os(CO)_3(OSiPh_3)_2|_2$,[30] $|Os(CO)_2X_2|_n$ and $|Os(CO)_3X_2|_2$[33] (where X =

Cl, Br) and the reaction of the latter with surfaces, e.g.

$$\tfrac{1}{2}|Os(CO)_3Cl_2|_2 \;+\; 2HO\text{-}Si \;\longrightarrow\; |Os(CO)_3(O_{SiO_2})_2| \;+\; 2HCl$$

However, a ^{13}CO enrichment/peak fitting study has been unsuccessful in obtaining a good fit[34] and an E.X.A.F.S. study on the silica system indicates the existence of osmium atoms at a M-M distance and two other non-bonding distances. In addition to this, exposure to CO regenerates some $|Os_3(CO)_{12}|$ (but not in the case of γ-Al_2O_3). These results suggest that the "mononuclear" Os/SiO_2 system is not as simple as was originally thought and the metal skeleton is partially preserved in one of the species.

The reaction of $|Os_3(CO)_{12}|$ with other oxides is similar to the silica system. Initially after physisorption a bridged species (5) (see Figure 2.5) is formed which, under more forcing conditions, breaksdown to "mononuclear" species. Unlike the situation with the functionalised oxides; where there is negligible transmission of any oxide electronic effects through the anchoring ligand to the cluster carbonyl ligands, the frequencies of (5) are oxide dependent (silica > (6) > alumina > zincite). It follows that silica is a more electron withdrawing ligand than Al_2O_3 or zincite. One also sees a similar trend in their stabilities which must be due

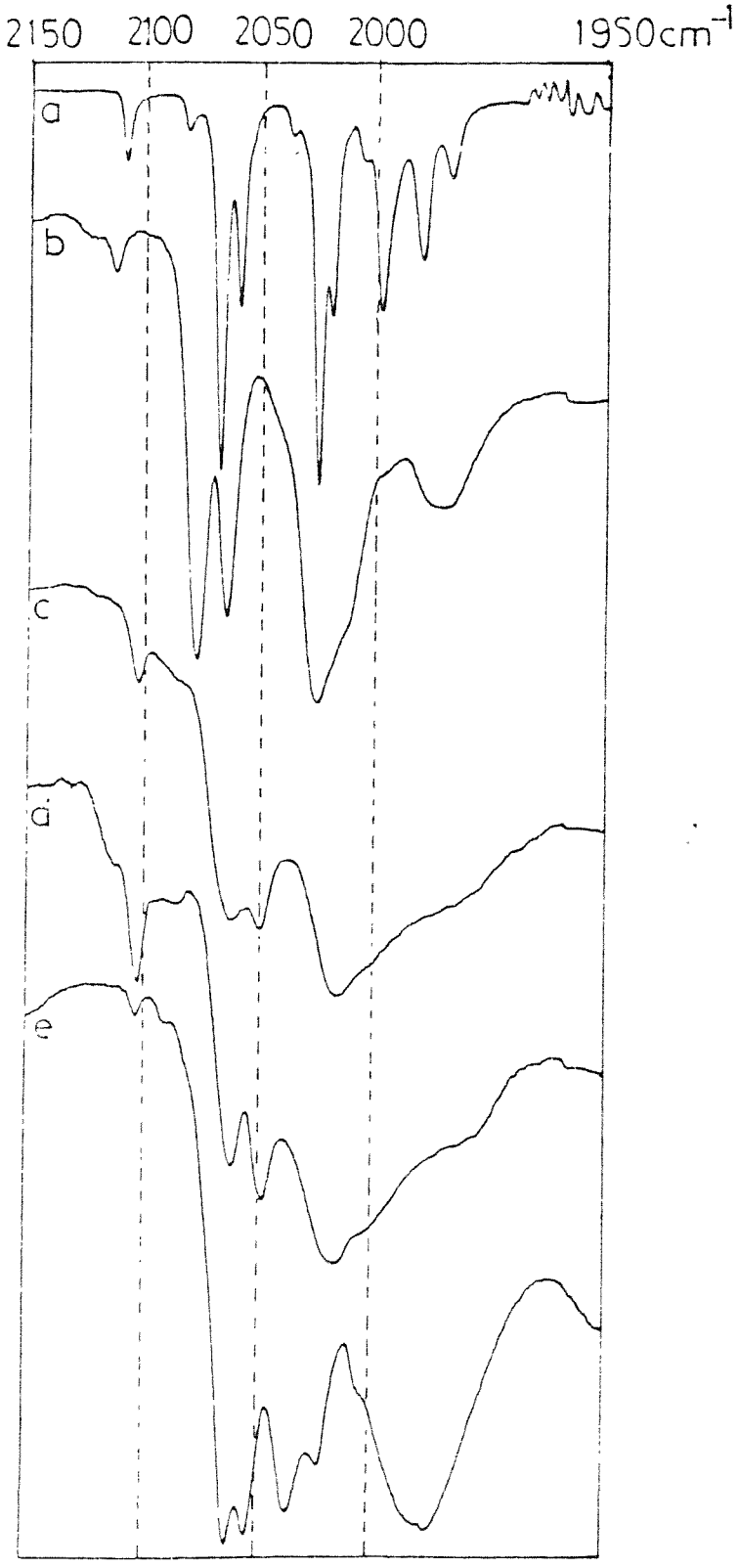

Figure 2.5. I.r. spectra (2 150 - 1 950 cm^{-1}) of (a) (6) in hexane, (b) (5) on silica, (c) (5) on γ-Al_2O_3, (d) (5) on ZnO, and (e) the ruthenium analogue of (5) on γ-Al_2O_3.

to oxide effects ((5) on SiO_2 > (6) > other oxides).

The $|Ru_3(CO)_{12}|/M'O_n$ systems mirror the $|Os_3(CO)_{12}|/M'O_n$ systems. First physisorption occurs, for example the interaction of $|Ru_3(CO)_{12}|$ with silica in refluxing benzene (15 minutes) afforded a material which exhibited the same i.r. spectrum as obtained by Robertson and Webb[45] on a sample prepared by depositing $|Ru_3(CO)_{12}|$ from CH_2Cl_2 onto silica at r.t.. It's i.r. is very similar to that of $|Ru_3(CO)_{12}|$ in solution and also it is yellow. Chemisorption follows and a species like (5) is formed, i.e. $|Ru_3(H)(CO)_{10}(O\text{-}M'O_n)|$. However, in the case of ruthenium these are much more unstable and in this work it has only been observed on γ-alumina (see Figure 2.5), though it has also been observed on silica.[34] Both of these rapidly decompose at r.t. to give "mononuclear" carbonylic complexes. The $|Ru_3(CO)_{12}|/\gamma\text{-}Al_2O_3$[35] system has been characterised by ^{13}CO isotopic substitution[36] and this has shown that there are 3 main mononuclear carbonylic complexes present, each having two coupled CO oscillators per ruthenium centre. They are thought also to have oxidation states of (III) (tetrahedral local environment), II and 0 (octahedral environments). The situation on the other oxides[37] seems to mirror these two systems but as yet there are no definitive studies in the literature.

The fragmentation of clusters on oxides is not restricted to this triad and has also been observed for the Rh triad. It has been particularly highly studied for the Rh/silica[41] and $Rh/\gamma\text{-}Al_2O_3$[40] systems because of their catalytic importance.[38,39] These studies[42,43] show that Rh clusters

like Ru and Os clusters after initial physisorption undergo chemisorption and then fragmentation to give various mononuclear species.

The loading obtained by reacting the parent $|M_3(CO)_{12}|$ carbonyls with plain oxides under the conditions used for the tethering of clusters to thiolated oxides were surprisingly high. In the case of osmium these were of the same order of magnitude as obtained for the thiolated surfaces. Evidently in the competition between the two possible ligands (-OH or -SH) the thiol is successful (see Figure 2.4). In the case of $|Ru_3(CO)_{12}|$ the situation is not so clear cut as the spectra show additional peaks. Besides, the peaks assigned to $|Ru_3(H)(CO)_{10}\{S(CH_2)_3Si(OMe)_{3-x}(O\text{-}M'O_n)_x\}|$ and $|Ru_3(H)(CO)_9\text{-}\{S(CH_2)_3Si(OMe)_{3-x}(O\text{-}M\ O_n)_x\}|$, the spectra often show additional weak broad features (usually 2 or more broad bands), e.g. SiO_2 2 120(br,w), and 2 030(br,w); $\gamma\text{-}Al_2O_2$ 2 100(br,w), 2 040(br,s), and 1 995(br,m); TiO_2 2 070(br,m) and 2 000(br,w) cm^{-1}. They could be formed as a result of the direct interaction of $Ru_3(CO)_{12}$ with oxide, or by excess thiolate ligand reacting with the tethered cluster or finally by oxide interaction with the tethered cluster. All these possibilities probably occur but the latter case is the one that predominates. The evidence for this comes in several pieces, the most important of which is that the observed i.r. positions for these bands vary with the oxide and do not correlate well with those obtained by direct interaction of $|Ru_3(CO)_{12}|$ with plain oxides under similar conditions. This,

incidentally, also rules out the possibility of species like $|Ru(CO)_2(SR)_2|_2$ and $|Ru(CO)_3(SR)_2|_n$[44] being responsible as the peaks in this case would not vary from surface to surface. A possible structure for these species involves mixed oxide and sulphide ligands, viz. $|Ru(CO)_{2or3}(SR)_x(O\text{-}M'O_n)_y|_{2or n}$ where $x + y = 2$, but confirmation of this will have to wait until a technique is available which can tell oxide and sulphide apart (Ru E.X.A.F.S. would probably be suitable).

Further evidence for oxide participation in the breakdown of tethered clusters comes from vacuum pyrolysis experiments. The most obvious result being that the homogeneous analogues are much more stable than the heterogeneous ones. For example, (1) in KBr disc is recovered virtually unchanged, by i.r., after being heated to 50 °C for 6 hours under vacuum whereas (1) on silica (pressed into a disc) decomposes within two hours under the same conditions. The time taken for pyrolysis (as measured by the disappearance of the peaks at 2 108 and 2 069 cm^{-1}) also varies from surface to surface (e.g. (1) on; SiO_2, 2 hours; γ-Al_2O_3, 1.5 hours, and TiO_2, 1.25 hours) and this interestingly mirrors the stability of (5) on various oxides.

The decomposition of (1) on surfaces is not a one step process. During pyrolysis peaks occur due to temporary species, the most notable being $|Ru_3(H)(CO)_9(SR)|$. For example, (1) on TiO_2 after 23 minutes at 50 °C and 5×10^{-2} mm Hg displays in addition to the remaining peaks of the parent cluster, weak peaks assignable to the nonacarbonyl

species at 2 090, 2 040, 2 015 and 2 000 cm^{-1}. The final apparently simple spectra obtained from these pyrolysis runs unfortunately do not correlate well with those obtained by either direct interaction of $|Ru_3(CO)_{12}|$ with oxides or as side products from the anchoring reaction (e.g. final pyrolysis spectra of (1) on: SiO_2 2 058(vs), and 2 008(vs); TiO_2 2 070(vs) and 2 010(m); γ-Al_2O_3 2 070(vs) and 1 999(s) cm^{-1}). However, this is not too surprising as each system probably contains quite a few different species and the distribution of these species in a sample will be history dependent.

Pyrolysis runs on $SiMe_3Cl$ treated thiolated oxides showed the trimethylsilyl group did indeed protect the clusters from oxide interaction. This was seen in the longer lifetimes of these tethered clusters when compared with those produced by the reaction of (1) with oxide, or $|Ru_3(CO)_{12}|$ with plain liganded oxide (these two have the same stabilities). For example, the analogue of (1) on $SiMe_3Cl$ pretreated liganded oxide took 4 hours for total decomposition compared with 2 hours for (1) on SiO_2 under the same conditions.

Further evaluation of the protecting agents $SiMe_3Cl$ and $(SiMe_3)_2NH$ was done on the $|Ru_3(CO)_{12}|/M\ O_x$ systems. In both cases the reagents essentially prevented the uptake by silica and greatly reduced it on other oxides. The former agent $SiMe_3Cl$ turned out to be the more effective probably because of its higher reactivity and smaller steric size compared with $(SiMe_3)_2NH$. The $SiMe_3Cl$ pretreatment of the

surface besides reducing the cluster uptake also served to protect from decomposition intermediates formed by oxide interaction. For example, $|Os_3(H)(CO)_{10}(O_{TiO_2})|$ was seen on $SiMe_3Cl$ pretreated oxide under conditions (toluene 6 hours reflux) during which it would have otherwise have gone to mononuclear species (on the plain oxide). Magnesia pretreated with $(SiMe_3)_2NH$ afforded a very complex i.r. pattern when treated with $|Ru_3(CO)_{12}|$ which included ν_{CO} bands at 1 817 and 1 788 cm^{-1} probably due to unknown cluster anion/s. This sample on standing overnight converted to that obtained normally with plain oxide. This silanation of the oxide also effects the mononuclear species present as can be seen by comparison of the i.r. spectra with those obtained on plain oxides. The difference probably occurs because the silanes preferentially block certain sites and so affect the distribution of the different types of mononuclear complexes present.

The pyrolysis results on the osmium thiolated samples were similar to those obtained for the ruthenium samples. That is, the homogeneous sample was more stable than the tethered one, and $SiMe_3Cl$ pretreatment of thiolate oxides afforded more stable heterogeneous clusters. However, they were different in that no trace of a $|Os_3(H)(CO)_9SR|$ intermediate was seen. An explanation for this is that the parent decacarbonyl cluster is much more stable than the ruthenium one (e.g. (1) in a KBr disc decomposed at 60 °C, whereas (2) also in a KBr disc required temperatures above 130 °C for decomposition). However, the corresponding nona-

carbonyl species is only slightly more stable and as it is only formed under the more forcing conditions its lifetime will be too short for it to build up to a detectable concentration. Indeed this is seen homogeneously; heating (4) in nonane produces only decomposition whereas (3) in refluxing hexane produces a detectable concentration of the nonacarbonyl species.

The products produced initially by the pyrolysis of (2) on SiO_2 appear, because of the sharpness and distribution of the peaks, to be a complex mixture of clusters or dinuclear species. These in turn decompose under the pyrolysis conditions to give decarbonylated species which readily take up carbon monoxide irreversibly (cannot be removed completely again under the pyrolysis conditions). This is shown by the growth of two strong broad peaks (SiO_2,2 120 and 2 030 cm^{-1}). The situation for (2) on γ-Al_2O_3 is similar but complete decarbonylation does not occur (see Figure 2.6, residual peaks at 2 123(br,w), 2 048(br,s) and 1 973(alumina background) cm^{-1}). Again a strong two peak pattern in generated when the sample is exposed to CO (see Figure 2.6, 2 120 and 2 030 cm^{-1}). An attempt to stabilise these fleeting intermediates was made by repeating the pyrolysis experiments under carbon monoxide. This failed for γ-Al_2O_3 but in the case of SiO_2 it succeeded in producing what appears to be a new cluster (see Figure 2.6, 2 125(w), 2 086(m), 2 059(vs), and 2 011(br,s) cm^{-1}). The spectrum shown is a result of two difference spectra. First the spectrum of the remaining parent cluster

Figure 2.6. I.r. spectra (2 200 - 1 900 cm^{-1}) of (a) the product from vacuum pyrolysis of (2) on γ-Al_2O_3 (disc), (b) the previous sample exposed for 20 minutes to 35 mm Hg of carbon monoxide, and (c) the intermediate seen from the pyrolysis of (2) on SiO_2 under carbon monoxide.

was subtracted out and then the SiO_2 background was removed. The fairly high frequency of the top peak suggests it is probably a cationic species. Such a species $[H_2Os_3(CO)_{10}SR^+]$[46] is known but the i.r. spectrum has not been reported. Unfortunately, this compound is only stable in concentrated sulphuric acid and an attempted i.r. was unsuccessful due to solvent broadening.

When comparing the stabilities of clusters in discs one has to be careful to consider a possible matrix effect. That is, the cluster may decompose by CO ejection but the disc may physically keep the CO molecule in close proximity to the cluster and stop it from decomposing. Interestingly, CO has been seen during these experiments to be taken up by both samples in oxide and KBr discs showing that this effect may be negligible. However, this may not be the case with discs produced at higher pressures than were used here.

Conclusion

It is apparent that the ligand anchoring procedures principally developed on silica gel can be applied to other oxides of varying acidities. In spite of fairly complex reactions between oxide surfaces and the metal carbonyl clusters studied, the pendant thiol ligands, nevertheless, specifically bind the carbonyls. No electronic effects are apparently transmitted from the oxides through the pendant ligands to the carbonyl ligands, as any oxide dependent reactivity stems from the surface environment and is not

intrinsic to the cluster. However, trinuclear species of the type $|M_3(H)(CO)_{10}(O\text{-}M'O_n)|$ (M = Ru and Os) do show oxide derived electronic effects and in their relative stabilities do show reactivity differences which correlate roughly with these electronic effects. Complexes of the type $|M_3(H)(CO)_{10}SR|$ (M = Ru and Os) have been decomposed under controlled conditions. All the osmium thiolate clusters are more stable than the ruthenium ones but within each metal series similar trends occur. For example, the stabilities are free cluster >> $|M_3(H)(CO)_{10}\{S(CH_2)_3Si(OMe)_{3-x}(O_{SiO_2})_x\}(Me_3Si)_y|$ > $|M_3(H)(CO)_{10}\{S(CH_2)_3Si(OMe)_{3-x}(O_{SiO_2})_x\}|$ > $|M_3(H)(CO)_{10}\{S(CH_2)_3Si(OMe)_{3-x}(O_{\gamma\text{-}Al_2O_3})_x\}|$ > $|M_3(H)(CO)_{10}\{S(CH_2)_3Si(OMe)_{3-x}(O_{TiO_2})_x\}|$. These trends demonstrate that oxide interaction is important in cluster breakdown and can be controlled by the use of protective silanes, e.g. $SiMe_3Cl$. Two of these were evaluated and were found to work well on SiO_2 and passibly on other oxides. The $SiMe_3Cl$ being better than the $(SiMe_3)_2NH$ in marginal cases. A cursory investigation was made on the decomposition products of $|M_3(H)(CO)_{10}SR|$ (heterogeneous analogues) but the systems were found to be too complex for confident assignment of the products except in one case; $|Ru_3(H)(CO)_9SR|$.

Experimental

Preparation of $|M_3(\mu\text{-H})(CO)_{10}(\mu\text{-SPr}^n)|$, M = Ru(3) and Os(4).

These were carried out according to the literature[18] but it was found that in both cases a stabilising carbon monoxide atmosphere enhanced the yields. For example, in the case of (3) the yield was increased from 60 - 70 % to 80 - 90 %.

$|Ru_3(H)(CO)_{10}(SPr^n)|$ (3)

I.r./hexane: 2 105(m), 2 082(vw), 2 065(vs), 2 058(s), 2 042(w), 2 026(s), 2 014(w), 2 008(m), and 1 996(m) cm^{-1}.

^1H n.m.r./$CDCl_3$, 31 °C: δ (p.p.m.) 2.55 (t, 2 H, S-$\underline{C}H_2$-), 1.6 (m, 2 H, S-CH_2-$\underline{C}H_2$), 0.9 (t, 3 H, $\underline{C}H_3$) and -15.36 (s, 1 H, Ru-H-Ru).

Mass spectra: The sample volatalised under vacuum at 50 °C to give a mass spectrum which exhibited a weak parent ion at 626 a.m.u. (for ^{102}Ru) followed by a relatively strong peak corresponding to the loss of one carbon monoxide (assigned to $|Ru_3(H)(CO)_9SPr^n|^+$). This correlates well with the solution chemistry of (3) which in refluxing hexane rapidly loses one carbon monoxide to give $|Ru_3(\mu\text{-H})(CO)_9(\mu_3\text{-SPr}^n)|$. The rest of the fragmentation pattern is complex but it can be interpreted in terms of a series of peaks, caused by successive carbonyl losses, with superimposed extra peaks due to fragmentation of the alkyl chain and doubly charged ions. Interestingly, the last fragmentation before dissolution of the ruthenium triangle is assignable to the loss of the sulphur atom. A successful elemetal analysis on this compound was unobtainable because of decomposition during handling.

$|Os_3(H)(CO)_{10}(SPr^n)|$ (4)

I.r./cyclohexane: 2 110(m), 2 068(vs), 2 060(vs), 2 020(s), 2 006(s), 1 999(m), 1 991(m), and 1 957(w) cm^{-1}.

^1H n.m.r./$CDCl_3$, 31 °C: δ (p.p.m.) 2.5 (t, 2 H, $S-CH_2$), 1.6 (m, 2 H, $S-CH_2\underline{C}H_2-$), 0.9 (t, 3 H, $\underline{C}H_3$), and -17.39 (s, 1 H, Os-H-Os).

Mass spectra: The mass spectrum obtained at 100 °C gave a strong parent at 896 a.m.u. (for ^{192}Os) followed by ten bands corresponding to ten successive carbonyl losses. This pattern has also in addition, extra bonds caused by fragmentation of the alkyl chain. This time, however, the sulphur does not appear to be lost before cluster fragmentation.

Raman/solid, ν_{CO}: 2 125(m), 2 106(s), 2 053(w), 2 028(m), 2 024(m), 2 013(vs), 2 010(sh), 2 006(vs), 2 001(sh), 1 992(sh), 1 988(w), and 1 978(vs) cm^{-1}.

ν_{M-H-M} 1 434(w) cm^{-1}

ν_{CO} (deformation) 480 - 510(br,s) cm^{-1}

ν_{M-M} 40(w), 110(vs), 145(sh), and 160(w) cm^{-1}.

u.v./cyclohexane: 45 600, 39 500, 30 700 and 25 500 cm^{-1}.

Analysis: calculated C, 16.4 %; H, 0.8 %.

found C, 16.6 %; H, 1.0 %.

Preparation of $|Ru_3(H)(CO)_9(\mu_3\text{-}SPr^n)|$

A sample of (3) was refluxed in pure n-hexane for twenty minutes, cooled, filtered and the i.r. taken. This showed mainly (3) but also additional peaks assignable to the product.

However, the inherent instability of the product prevented its purification. The ^1H n.m.r. spectrum was obtained by heating a sample of (3) in situ (70 ^oC, d^8-toluene). Again a pure spectrum was unattainable.
I.r./hexane: 2 090(m), 2 062(s), 2 039(s), 2 016(s), 2 008(sh), 2 005(m), and 1 975(m) cm^{-1}.
^1H n.m.r./d^8-toluene, 70 ^oC: δ (p.p.m.) -18.9 (s, 1 H, Ru-H-Ru), the signals in the alkyl region were swamped by residual (3).

Preparation of $|Ru_3(H)(CO)_{10}|S(CH_2)_3Si(OMe)_3|$ (1).

This reaction was initially carried out under nitrogen but an improved yield was obtained when it was repeated under carbon monoxide (60 % compared to 40 %). Typically $|Ru_3(CO)_{12}|$ (0.294 g) and $HS(CH_2)_3Si(OMe)_3$ (1.1 equivalents) were refluxed in dry benzene (100 cm^3) for 15 minutes, during which time the solution changed from a deep orange to a lemon yellow. After cooling and filtering, the solvent was removed in vacuo and the residue taken up in cold hexane (10 cm^3). This extract on drying afforded the product as an orange oil (60 %). The i.r. spectrum of this oil shows an extra weak band at 2 093 cm^{-1} indicative of a species like $|Ru_3(H)(CO)_9(SPr^n)|$. Upon exposure to carbon monoxide the oil becomes more yellow and this peak disappears together with a sharpening of the other peaks. This product is a slightly heat and air sensitive oil which is frozen at 0 ^oC.
I.r./hexane: 2 106(w), 2 093(vw), 2 064(s), 2 056(s), 2 025(vs), 2 012(m), 2 007(m), 1 994(w), and 1 966(w) cm^{-1}.

^{1}H n.m.r./$CDCl_3$, 0 °C: δ (p.p.m.) 3.5 (s, 9 H, $OC\underline{H}_3$), 2.5 (t, 2 H, $S\text{-}C\underline{H}_2$), 2 - 0.5 (m, 4 H, $Si\text{-}\underline{CH}_2\text{-}\underline{CH}_2$-) and -15.4 (s, 1 H, Ru-H-Ru).

Preparation of $|Os_3(H)(CO)_{10}|S(CH_2)_3Si(OMe)_3||$

$|Os_3(CO)_{12}|$ (0.054 g) and $HS(CH_2)_3Si(OMe)_3$ (1.1 equivalents) were refluxed in toluene (60 cm^3) for 6 hours, cooled, filtered, the solvent removed in vacuo, the residue extracted with hexane (10 cm^3) and the extract pumped to dryness. This afforded the product as a yellow crystalline solid (0.046 mg, 75 % yield based on $|Os_3(CO)_{12}|$ consumed).

I.r./hexane: 2 108(m), 2 067(s), 2 058(s), 2 024(s), 2 018(s), 2 005(w), 1 998(s), 1 989(s), 1 983(sh), and 1 955(br,w) cm^{-1}.

^{1}H n.m.r./$CDCl_3$, 31 °C: δ (p.p.m.) 3.5 (s, 9 H, $O\underline{Me}$), 2.5 (t, 2 H, $S\text{-}C\underline{H}_2$), 2 - 0.5 (m, 4 H, $Si\underline{CH}_2\underline{CH}_2$-) and -16.9 (s, 1 H, Os-H-Os).

Raman/solid: ν_{CO} 2 110(s), 2 060(br,w), and 1 999(br,s) cm^{-1}.

Mass spectra: This was unobtainable due to involatility.

Analysis: calculated C, 18.3 %; H, 1.5 %.

found C, 19.1 %; H, 1.9 %.

Reactions with oxides

The oxides were predried to remove physisorbed water. Most of the oxides were dried by heating to 120 °C in vacuo for 48 hours (ZnO was dried similarly at 50 °C).

Preparation of ligand functionalised oxide

$HS(CH_2)_3Si(OMe)_3$ (0.6 g) and oxide (5 g) were refluxed in xylene (50 cm^3) for 6 hours and then stirred at r.t. for a further 15 hours. The solid was filtered off, extracted with Et_2O for 4 hours in a Soxhlet apparatus and dried in vacuo for 16 hours to give a white powder. An i.r. spectrum was run on disc of thiolated aerosil 380 and the silica background subtracted out.

I.r. (4 000 - 1 300 cm^{-1}, aerosil 380 window Region)

$HS(CH_2)_3Si(OMe)_3$ (film, KBr discs)	$HS(CH_2)_3Si(OMe)_{3-x}(O_{SiO_2})_x$
2 942(s)	2 938
2 841(s)	2 845
2 557(w)	2 557
1 457(m)	1 459
1 444(m)	1 445
1 413(sh,w)	1 409
1 344(w)	1 345
1 309(w)	1 310

Silylation of the oxides

(a) By $SiMe_3Cl$: a suspension of the oxide (0.2 g) in a benzene (5 cm^3) solution of $SiMe_3Cl$ (0.04 g) was stirred for 16 hours at 30 ^oC, refluxed for one hour, filtered and washed witn CH_2Cl_2 (3 times) and dried in vacuo.

(b) By $NH(SiMe_3)_2$: the amine (1 cm^3) was added to a slurry of the oxide in CCl_4 and shaken overnight, refluxed for one hour, filtered, washed with CH_2Cl_2 (3 times) and dried in vacuo.

Reaction of $|Ru_3(H)(CO)_{10}\{S(CH_2)_3Si(OMe)_3\}|$ with oxides.

A suspension of the oxide (0.2 g) was stirred in hexane (40 cm^3) solution of $|Ru_3(H)(CO)_{10}\{S(CH_2)_3Si(OMe)_3\}|$ (0.01 g) for two hours. The pale yellow powders were collected by filtration, washed with CH_2Cl_2 (3 x 30 cm^3) and dried in vacuo.

I.r./Nujol mull: oxide = SiO_2, 2 106(w), 2 083(w), 2 065(w), 2 055(w), and 2 026(w); γ-Al_2O_3, 2 105(w), 2 082(vw), 2 066(s), 2 056(s), 2 023(vs), and 2 009(sh); TiO_2, 2 103(m), 2 080(w), 2 065(vs), 2 054(s), 2 023(vs), 2 006(m) and 1 994(w); ZnO, 2 105(w), 2 067(vs), 2 055(s), 2 036(w), 2 022(s), and 1 993(w); SnO_2, 2 104(m), 2 080(w), 2 064(vs), 2 054(s), 2 022(s), 2 006(m), and 1 933(w); MgO, 2 106(w), 2 080(w), 2 060(sh), 2 051(s), 2 040(s), and 2 000(m) cm^{-1}.

After some weeks at r.t. these samples became cream with new i.r. spectra (recorded after 12 weeks).

I.r./Nujol mull: $|Ru_3(H)(CO)_{10}\{S(CH_2)_3Si(OMe)_3\}|$ (decomposed) 2 111(w), 2 026(br,m), and 1 970(br,m); oxide = SiO_2, 2 120(br,w), 2 030(br,m), and 1 995(br,m); γ-Al_2O_3, 2 100(br,w), 2 040 (br,s), and 1 985(br,s); TiO_2, 2 070(br,m), and 2 000(br,w); ZnO, 2 055(br,m), and 1 975(br,w); SnO_2, 2 035(br,m), and 1 985(br,s) cm^{-1}.

It was found subsequently that if the manipulations were carried out under carbon monoxide improved spectra were obtainable. Most significantly the band at 2 083 - 2 080 cm^{-1} was absent and the remaining peaks were sharper. The

samples, when stored under carbon monoxide, were found to be stable almost indefinitely at -20 °C.

Interactions of $|Ru_3(H)(CO)_{10}(SPr^n)|$ with oxides.

This was carried out as above. I.r./Nujol: oxide = SiO_2, 2 104(w), 2 064(w), 2 055(w), and 2 024(m); γ-Al_2O_3, 2 028(m), and 1 980(br,m); TiO_2, 2 060(br,vw), 1 995(sh,vw), and 1 950(sh,vw); ZnO, 2 030(br,w), ans 1 975(br,w); MgO, 2 040(br,m), and 1 968(br,m) cm^{-1}; and SnO_2 no ν_{CO} peaks observed. When the reactions were repeated under carbon monoxide it was found that the amount of interaction was reduced to almost negligible levels (not detectable in the i.r.).

Reaction of $|Ru_3(CO)_{12}|$ with $HS(CH_2)_3Si(OMe)_{3-x}(OM'O_n)_x$.

A suspension of the oxide (0.1 g) was refluxed in a benzene solution (30 cm^3) of excess of $|Ru_3(CO)_{12}|$ (0.05 g) and allowed to cool. The bright yellow solids were collected by filtration, washed with CH_2Cl_2 (2 x 25 cm^3) and MeOH (2 x 25 cm^3), and dried in vacuo. I.r. (Nujol): $M'O_n$ = SiO_2, 2 104(w), 2 090(sh), 2 064(vs), 2 054(s), 2 038(m), 2 023(s) and 2 008; γ-Al_2O_3, 2 108(w), 2 094(w), 2 084(m), 2 067(s), 2 056(vs), 2 026(s), 2 010(s), and 2 000(br,s); TiO_2, 2 104(w), 2 091(w), 2 081(w), 2 064(vs), 2 053(vs), 2 023(vs), and 2 006(vs); ZnO, 2 104(w), 2 082(m), 2 063(vs), 2 054(s), 2 036(s), 2 021(vs), 2 006(vs), and 1 999(br,s); SnO_2. 2 104(w), 2 064(w), 2 053(w), 2 020(w), and 2 000(m); MgO,

2 104(w), 2 094(vw), 2 082(w), 2 063(m), 2 052(s), 2 038(m), 2 024(m), and 2 000(br,s) cm^{-1}.

The preparations were repeated on a sample of the thiolated oxides which had been treated with $SiMe_3Cl$. Analyses: Aerosil 380, 2.55 % Ru, 0.07 % Os; Al_2O_3 1.08 % Ru, 0.04 % Os. I.r. (Nujol): $M'O_n$ = SiO_2 2 105(w), 2 092(w), 2 080(vw), 2 064(vs), 2 056(s). 2 038(m), 2 023(vs), and 2 007(s); Al_2O_3, 2 105(w), 2 092(w), 2 081(w), 2 064(s), 2 052(s), 2 038(m), 2 023(s), 2 008(vs), 1 998(br,vs), and 1 945(m); TiO_2, 2 104(m), 2 091(w), 2 080(w), 2 064(vs), 2 053(s), 2 038(w), 2 022(s), 2 006(vs), and 1 999(br,s); ZnO, 2 102(w), 2 080(w), 2 064(m), 2 054(s), 2 023(m), 2 008(m), and 1 998(br,m); SnO_2, 2 104(vw), 2 090(vw), 2 080(w), 2 062(w), 2 052(w), and 2 000(br,s); MgO, 2 104(w), 2 063(m), 2 055(m), 2 023(m), and 2 000(br,w) cm^{-1}.

Again it was found that improved spectra were obtained when the reactions were repeated under CO.

Reaction of $|Os_3H(CO)_{10}\{S(CH_2)_3Si(OMe)_3\}|$ with oxides ($M'O_n$).

This was carried out as described for the ruthenium analogue except that the solids were extracted with Et_2O (6 h) and MeOH (6 h) in a Soxhlet apparatus. In all cases this caused some leaching but pale yellow solids were obtained. Osmium analyses: Aerosil 380, 0.36; Al_2O_3, 2.94; TiO_2, 3.17; MgO, 1.00; ZnO, 1.33 %. I.r. (Nujol): oxide = SiO_2, 2 109(m), 2 069(s), 2 058(s), and 2 024(vs); Al_2O_3, 2 109(m), 2 067(s), 2 057(s), 2 023(vs), 1 997(br,m), and 1 986(br,m);

TiO_2, 2 107(m), 2 067(s), 2 056(s), 2 023(vs), 1 998(br,m), and 1 988(br,m); ZnO, 2 108(w), 2 067(s), 2 057(s), 2 022(vs), 1 997(br,m), and 1 988(br,m); SnO_2, 2 107(w), 2 066(s), 2 056(m), 2 021(s), 1 997(br,w), and 1 985(br,w); MgO, 2 108(m), 2 067(s), 2 056(s), 2 022(vs), and 1 998(br,m) cm^{-1}.

Reaction of $|Os_3(CO)_{12}|$ with $HS(CH_2)_3Si(OMe)_{3-x}(OM'O_n)_x$.

A suspension of thiolated oxide (0.5 g) was refluxed in a toluene solution (40 cm^3) of $|Os_3(CO)_{12}|$ (0.025 g) for 6 h and allowed to cool. The mixture was filtered and the solid residue extracted with Et_2O (5 h) in a Soxhlet apparatus. No leaching occurred, and the products were obtained as yellow solids. Osmium analyses: Aerosil 200, 2.01; Al_2O_3, 2.24; TiO_2, 1.96; MgO, 0.95; ZnO, 1.95 %. I.r. (Nujol): $M'O_n$ = SiO_2, 2 108(m), 2 068(s), 2 057(s), 2 020(s), 1 999(br,s), and 1 980(br); Al_2O_3, 2 109(m), 2 067(s), 2 057(s), 2 024(s), 1 995(br), and 1 988(br); TiO_2, 2 109(m), 2 067(s), 2 057(s), 2 024(s), 1 995(br), and 1 988(br); ZnO, 2 108(m), 2 067(s), 2 057(s), 2 022(s), 1 997(br), and 1 986(br); SnO_2, 2 108(m), 2 067(s), 2 057(s), 2 022(s), 1 997(br), and 1 986(br); MgO, 2 110(m), 2 067(s), 2 057(s), 2 024(s), and 1 992(br,s) cm^{-1}.

This procedure was repeated on samples of thiolated oxides treated with $SiMe_3Cl$. Osmium analyses: Aerosil 200, 2.32; Aerosil 380, 2.74; Al_2O_3, 1.79; TiO_2, 2.13; MgO, 0.78; ZnO, 0.25 %. I.r. (Nujol): SiO_2, 2 108(m), 2 067(s), 2 059(m), 2 023(vs), 1 997(br,m), 1 987(br,m), and 1 980(sh); Al_2O_3, 2 109(m), 2 067(s), 2 058(s), 2 023(s), 1 995(br,m),

and 1 987(br,m); TiO_2, 2 109(m), 2 067(vs), 2 058(s), 2 024(s), 1 995(br,m), and 1 987(br,m); ZnO, 2 110(w), 2 067(s), 2 059(m), 2 024(s), 1 997(br,m), and 1 987(br,m); SnO_2, 2 108(m), 2 066(s), 2 056(s), 2 021(s), 1 997(br,m), and 1 988(br,m); MgO, 2 109(m), 2 066(s), 2 058(s), 2 022(s), 1 995(br,m), and 1 988(br,m) cm^{-1}.

Reaction of $|Ru_3(CO)_{12}|$ with oxides $M'O_n$

This was carried out under the same conditions as used for the reaction with thiolated oxides.
I.r. (Nujol) mull: $M'O_n$ = SiO_2, 2 060(s), 2 032(m), and 2 011(w); γ-Al_2O_3, 2 104(vw), 2 080(w), 2 064(m), 2 056(m), 2 038(m), 2 025(m), 1 990(br,m), and 1 950(br,w), decomposed (3 hrs, r.t.) to give 2 065(br,m), and 1 990(br,m); TiO_2, 2 066(br,s), and 1 998(br,m); ZnO, 2 055(br,m), and 1 970(br,m); SnO_2, 2 061(br,w), and 1 987(br,w); MgO, 2 082(w), 2 042(br,w), 1 984(vs), and 1 966(br,vs) cm^{-1}. Analyses: SiO_2, 0.21 % Ru, 0.02 % Os; γ-Al_2O_3, 1.51 % Ru, 0.04 % Os. These reactions were repeated on oxides silylated using, (a) $SiMe_3Cl$, I.r. (Nujol) mull: $M'O_n$ = SiO_2, no ν_{CO}; γ-Al_2O_3, 2 070(s), and 1 996(br,m); TiO_2, 2 064(br,vw), and 1 994(br,m); ZnO, 2 065(br,s), and 1 997(br,m); SnO_2, 2 065(br,w), and 1 993 (br,w); MgO, 2 070(br,w), and 2 000(br,vw) cm^{-1}, (b) $(SiMe_3)_2NH$, I.r. (Nujol) mull: $M'O_n$ = SiO_2, no ν_{CO}; γ-Al_2O_3, 2 068(br,vw), and 1 985(br,w); TiO_2, 2 057(br,m), and 1 985(br,w); ZnO, 2 050(br,m), and 1 967(br,w); SnO_2, 2 060(br,w), 2 030(br,w), and 1 975 (br,w); MgO, 2 040(br,m),

2 010(m), 1 993(br,w), 1 982(br,w), 1 968(br,w), 1 935(br,w), 1 925(br,w), 1 817(br,w), and 1 788(br,w) cm^{-1}.

Reaction of $|Os_3(CO)_{12}|$ with oxides ($M'O_n$)

This was carried out as described for the reaction between $|Os_3(CO)_{12}|$ and the thiolated oxides. Osmium analyses: Aerosil 380, 1.00; γ-Al_2O_3, 2.26; TiO_2, 0.93; MgO, 1.70; ZnO, 1.90 %. I.r. (Nujol) mull: SiO_2, 2 115(w), 2 078(s), 2 064(m), 2 024(vs), 2 014(sh), and 1 985(br,m); Al_2O_3, 2 021(br,s), and 1 947(br,m); TiO_2, 2 030(br,m), and 1 947 (br,w); ZnO, 2 108(w), 2 067(m), 2 059(w), 2 045(sh), 2 020(s), 2 018(sh), 2 000(br,s), 1 990(w), and 1 985(w); SnO_2, no ν_{CO} observed; MgO, 2 015(br,m), and 1 930(br,w) cm^{-1}.

A similar procedure was carried out on oxides treated with $SiMe_3Cl$. I.r./(Nujol) mull: SiO_2, 2 124(br,w), 2 114(w), 2 078(m), 2 065(m), 2 026(s), 2 014(sh), 1 999(w), and 1 987(br,w); γ-Al_2O_3, 2 106(vw), 2 060(br,m), 2 034(br,s), 1 950(br,m), and 1 925(br,w); TiO_2, 2 104(w), 2 065(m), 2 056(w), 2 026(s); ZnO, 2 025(br,m), 1 980(br,w), and 1 970 (br,w) cm^{-1}; MgO no ν_{CO} observed.

Repeating the reaction of $|Os_3(CO)_{12}|$ with oxides in refluxing toluene for 5 hours, with no Soxhlet extraction afforded different i.r. spectra for γ-Al_2O_3, TiO_2, MgO and ZnO. I.r./(Nujol) mull: γ-Al_2O_3, 2 102(w), 2 083(sh), 2 061(s), 2 048(s), 2 015(vs), 2 001(sh), 1 941(br,m), and 1 919(br,m); TiO_2, 2 117(m), 2 102(w), 2 062(w), 2 048)w), 2 015(vs), and 1 940(br,w); ZnO, 2 102(w), 2 085(w), 2 060(s),

2 047(s), 2 016(vs), 2 001(sh,s), 1 978(sh), and 1 929(br,m); MgO, 2 102(w), 2 059(m), 2 045(s), 2 033(w), 2 015(vs), 1 998 (sh,m), 1 967(sh,br,m), and 1 929(br,m) cm^{-1}.

Reaction of $|Os_3(CO)_{10}(MeCN)_2|$ with $SiPh_3OH$

A solution of $|Os_3(CO)_{10}(MeCN)_2|$ in dry benzene was prepared by gradual addition of NMe_3O in CH_3CN to $|Os_3(CO)_{12}|$ (0.066 g) and MeCN (5 cm^3) in benzene (50 cm^3). On successive additions, $|Os_3(CO)_{11}(CH_3CN)|$ (i.r./hexane: 2 105(w), 2 053(s), 2 041(s), 2 021(m), 2 000(vs), 1 984(sh), and 1 981(m) cm^{-1}) and subsequently $|Os_3(CO)_{10}(CH_3CN)_2|$ (i.r./hexane: 2 078(s), 2 052(m), 2 022(br), 1 993(sh), 1 984(s), and 1 964(m) cm^{-1}) were formed. Triphenylsilanol (2 equivalents) was added to the reaction mixture which was then left overnight. The solvent was removed and the residue chromatographed on 20 x 20 cm silica t.l.c. plates with hexane as solvent. Two main bands were obtained which afforded $|Os_3(H)(CO)_{10}(OH)|$[28] and $|Os_3(H)(CO)_{10}(OSiPh_3)|$.[29] (I.r./hexane: 2 112(w), 2 100(vw), 2 072(s), 2 063(s), 2 044(w), 2 027(s), 2 022(sh), 2 001(s), 1 997(sh), 1 990(m), 1 985(m), and 1 958(w) cm^{-1}. ^1H n.m.r./$CDCl_3$, 31 °C: δ (p.p.m.) 7.40 (m, 15 H, Ph), and -12.59 (s, 1 H, Os-H-Os).

Pyrolysis experiments on homogeneous and supported thiolate clusters

These were carried out in an evacuable heated i.r. cell, on samples prepared as pressed discs (unsupported clusters in

KBr discs) by using a disc press (5 - 10 tons, 14 mm diameter disc). In general, the PE580 i.r. spectrometer was programmed with a repetitive scan and state routine and the sample pyrolysed overnight. For the ruthenium samples the conditions used were 50 ^{o}C and vacuum (5 x 10^{-2} mm Hg) and for the osmium samples 30 → 150 ^{o}C (1 hour) and then 150 → 160 ^{o}C (overnight) with a vacuum (5 x 10^{-2} mm Hg) or a partial pressure of carbon monoxide (35 mm Hg).

References for Chapter 2.

1. J. Lieto, J.J. Rafalko, J.V. Minkiewicz, P.W. Rafalko, and B.C. Gates, in "Fundamental Research in Homogeneous Catalysis", Vol. 3, Ed. M. Tsutsui, Plenum, New York (1979).
2. J.J. Rafalko, J. Lieto, B.C. Gates, and G.L. Schroder,Jr., J.Chem.Soc.,Chem.Commun., (1978), 540.
3. R. Pierantozzi, K.J. McQuade, B.C. Gates, M. Wolf, H. Knozinger, and W. Ruhmann, J.Am.Chem.Soc., (1979), 101, 5436.
4. B.C. Gates and J. Lieto, Chem.Technol., (1980), 248.
5. T.Castrillo, H. Knozinger, J. Lieto, and M. Wolf, Inorg. Chim Acta, (1980), 44, L239.
6. S.C. Brown and J. Evans, J.Chem.Soc.,Chem.Commun., (1978), 1063.
7. S.C. Brown and J. Evans, J.Organomet.Chem., (1980), 194, C53.
8. S.C. Brown and J. Evans, J.Mol.Catal., (1981), 11, 143.
9. T.Castrillo, H. Knozinger, M. Wolf, and B. Tesche, J.Mol.Catal., (1981), 11, 151.
10. J.L. Bilhou, V. Bilhou-Bougnol, W.F. Graydon, J.M. Basset, and A.K. Smith, J.Mol.Catal., (1980), 8, 411.
11. J.A.S. Howell and P. Mathur, J.Chem.Soc.,Chem.Commun., (1981), 263.
12. M.R. Churchill, B.G. De Boar, J.F. Ratella, E.W. Abel, and R.J. Rawley, J.Am.Chem.Soc., (1975), 97, 7158.
13. C. Choo-Yin and A.J. Deeming, J.Organomet.Chem., (1977), 133, 123.

14. H. Vahrenkamp and D. Walters, J.Organomet.Chem., (1982), 224, C17.

15. J.S. Field, R.J. Haines, and D.N. Smit, J.Organomet.Chem., (1982), 224, C49.

16. F. Iwasaki, M.J. Mays, P.R. Raithby, P.L. Taylor, and P.J. Wheatley, J.Organomet.Chem., (1981), 213, 185.

17. A.A. Arduini, A.A. Bahsoun, J.A. Osborn, and C. Voelker, Angew.Chem.,Int.Ed.Engl., (1980), 19, 1024.

18. G.R. Crooks, B.F.G. Johnson, J. Lewis, and I.G. Williams, J.Chem.Soc.(A), (1969), 797.

19. V.F. Allen, R. Mason, and P.B. Hitchcock, J.Organomet.Chem., (1977), 140, 297.

20. W.D. McLeod Jr., and B. Nagy, Anal.Chem., (1968), 40, 841.

21. "Structure of metallic catalysts", Ed. J.R. Anderson, Academic Press (1975).

22. A.S. Listsyn, V.L. Kuznetsov, and Y.I. Yermankov, React.Kinet.Catal.Lett., (1980), 14, 445.

23. J. Evans and B.P. Gracey, J.Chem.Soc.,Chem.Commun., (1980), 852.

24. J. Evans and B.P. Gracey, J.Chem.Soc.,Dalton Trans., (1982), 1123.

25. T. Castrillo, H. Knozinger, and M. Wolf., Inorg.Chim.Acta, (1980), 45, L235.

26. "The Chemistry of Silica", R.K. Iier, Wiley Interscience, (1979).

27. "Organosilicon Compounds", C. Eaborn, Butterworth Scientific Publications, (1960).

28. B.F.G. Johnson, J. Lewis, and P.A. Kilty, J.Chem.Soc.(A), (1968), 2859.

29. A.K. Smith, B. Besson, J.M. Basset, P. Psaro, A. Fusi, and R. Ugo, J.Organomet.Chem., (1980), 192, C31.

30. R. Psaro, R. Ugo, G.M. Zanderighi, B. Besson, A.K. Smith, and J.M. Bassett, J.Organomet.Chem., (1981), 213, 215.

31. M. Deeba and B.C. Gates, J.Catal., (1981), 67, 303.

32. M. Deeba, B.J. Streusand, G.L. Schroder, and B.C. Gates, J.Catal., (1981), 69, 218.

33. L.A.W. Hales and R.J. Irwing, J.Chem.Soc.(A), (1967), 1932; M.I. Bruce, M. Cooke, M. Green, and D.J. Westlake, J.Chem.Soc.(A), (1969), 987.

34. G.S. McNulty, Unpublished communication.

35. V.L. Kuznetsov, A.T. Bell, and Y.I. Yermakov, J.Catal., (1980), 65, 374.

36. E. Guglieminatto, A. Zecchina, A. Bassi, and M. Camia, J.Catal., (1982), 74, 225; ibid, (1982), 74, 252; ibid, (1982), 74, 240.

37. H. Schwonk, G. Parravano, and H.L. Gruber, J.Catal., (1980), 61, 19.

38. K. Fusimoto, M. Kameyama, and T. Kunugi, J.Catal., (1980), 61, 7.

39. W.F. Graydon and M.D. Langan, J.Catal., (1981), 69, 180.

40. K.L. Watters and R.F. Howe, J.Catal., (1981), 69, 212.

41. J.L. Bihou, V. Bilhou-Bougnol, W.F. Graydon, J.M. Basset, A.K. Smith, G.M. Zanderighi, and R. Ugo, J.Organomet.Chem., (1978), 153, P.73.

42. A.K. Smith, F. Hughes, A. Theolier, J.M. Basset, R. Uso, G.M. Zanderighi, J.L. Bilhou, V. Bilhou-Bougnol, and W.F. Graydon, Inorg.Chem., (1979), 18, 3104.

43. W.M. Bowser and W.H. Weinberg, J.Am.Chem.Soc., (1981), 103, 1453.

44. B.F.G. Johnson, J. Lewis, R.D. Johnson, P.L. Josty, and I.G. Williams, Nature, (1967), 213, 901.

45. J. Robertson and G. Webb, Proc.R.Soc.London Ser.A, (1974), 341, 383.

46. A.J. Deeming, B.F.G. Johnson, and J. Lewis, J.Chem.Soc.(A), (1970), 2517.

Chapter Three

A Study of the Reactivity and Catalytic Activity of Solution and Tethered Thiolate Osmium Clusters.

The impetus to derivatise these clusters was partially provided by the need to characterise the anchored systems more fully. In addition to this a reactivity study could show up any effects on the reactivity of clusters due to the oxide environment. Finally, cluster compounds can be regarded as poisoned metal catalysts because they are often completely coated with chemisorbed material and so have no vacant sites available for substrate binding. A result of this is that if a cluster is going to be an active catalyst it needs to be able to produce a vacant site by either; ligand rearrangement, ligand loss, or M — M bond rupture. Unfortunately, $|Os_3(H)(CO)_{10}SR|$ does not readily show any of these features but derivatives do exist which show suitable properties for a cluster catalyst precursor.

The reported route[1] to these derivatives (see Scheme 3.1) involves the attack of R_3O^+ on a cluster anion. Unfortunately, this route is unsuitable for the preparation of anchored derivatives as one cannot prepare R_3O^+ when R contains a hydrolysable silyl group. However, a high yield route into this cycle was found. This involves oxidising off a carbonyl on the parent cluster by the use of trimethylamine oxide, and then trapping the nonacarbonyl cluster produced with a weakly co-ordinating ligand.

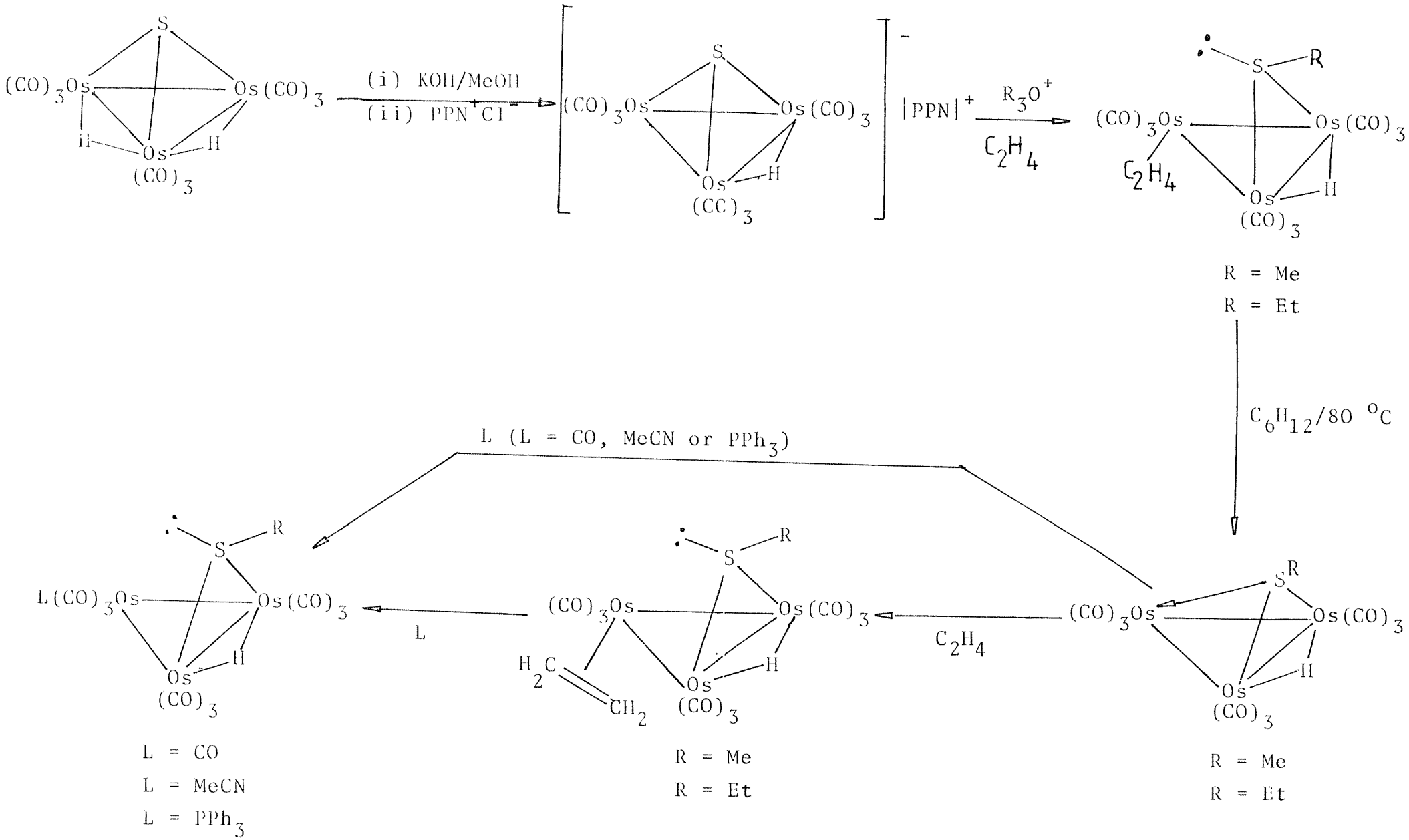
(i) KOH/MeOH
(ii) PPN+Cl-
|PPN|+
R3O+
C2H4
R = Me
R = Et
C6H12/80 °C
L (L = CO, MeCN or PPh3)
L
C2H4
L = CO
L = MeCN
L = PPh3
R = Me
R = Et
R = Me
R = Et

Scheme 3.1.

RESULTS AND DISCUSSION

(a) Some aspects of the reactivity of solution thiolate clusters.

A major problem encountered in catalysis with osmium clusters is the high thermal stability of the Os-CO bond. For example, to ^{13}CO enrich osmium carbonyl by $^{12}CO/^{13}CO$ exchange requires a temperature of about 120 - 130 °C (overnight) compared with 60 °C for $|Ru_3(CO)_{12}|$,[4] 25 °C for $|Co_4(CO)_{12}|$,[5] $|Rh_4(CO)_{12}|$,[6] and $|Fe_3(CO)_{12}|$.[7] This reluctance to undergo reactions which require a CO dissociation step can be seen in the comparatively drastic conditions required for reactions with poor nucleophiles such as olefins[8] and acetylenes[9] (120 - 130 °C, several hours), which often result in cluster fragmentation,[10] e.g.

$$|Os_3(CO)_{12}| + C_2H_4 \xrightarrow[160\ ^{o}C/4\ hrs]{20\ bar} |Os_4(CO)_{12}(C_2H_2)| + |Os_4(CO)_{12}(C_4H_8)|$$

In the case of $|Os_3(CO)_{12}|$ this problem is commonly overcome by removing one or two carbonyls by Me_3NO oxidation. The electron deficient clusters produced are "captured" by weakly co-ordinating ligands such as acetonitrile and pyridine (e.g. $|Os_3(CO)_{11}(NCMe)|$[11]). The easy replacement of this weakly co-ordinated ligand allows the preparation of species hitherto unattainable which could be of catalytic interest, e.g. $|Os_3(CO)_{11}(C_2H_4)|$.[12]

When an olefin isomerisation catalysis study was carried out on $|Os_3(CO)_{10}(H)(SPr^n)|$ (4) it was found that this compound only displayed a slight activity and then only under conditions which caused cluster decomposition (125 ^oC, 15 hrs). So, despite the presence of the thiolate ligand and the bridging hydride, none of the Os-CO bonds are activated towards dissociation. This inactivity has been overcome by preparing the nonacarbonyl derivatives directly.[1] This was achieved by reacting $|HOs_3(CO)_9S|^-$ with a cationic alkylating agent in the presence of a weakly co-ordinating ligand to trap the otherwise unstable nonacarbonyl cluster. The unstable nonacarbonyl cluster can be regenerated by heating the ethylene adduct. This is an example of a metal-ligand redox system with the sulphur ligand changing from a capping ligand (formally a five electron donor) to a bridging ligand (formally a three electron donor) when in the presence of a suitable ligand.

This ability of the sulphur to cap depends on both steric and electronic factors. The ability to cap is increased when the sulphur is more electron rich. For example, the stability of $|Os_3(CO)_9(H)_2S| >> |Os_3(CO)_9(H)(SEt)| > |Os_3(CO)_9(H)(SMe)|$. The ^1H n.m.r. spectra of these compounds provide evidence for the increased electron donation of sulphur on changing from a bridging to a capping mode. For example, the protons on the carbon attached directly to the sulphur are deshielded in the nonacarbonyl compounds compared to the substituted nonacarbonyl compounds and the

decacarbonyl compounds. For example, in $|Os_3(H)(CO)_9SPr^n|$ (13) the methylene protons come at δ 3.15 compared to δ 2.5 in $|Os_3(H)(CO)_{10}SPr^n|$ (4) and δ 2.44 in $|Os_3(H)(CO)_9(C_2H_4)(SPr^n)|$ (7). Also, the hydride shows an increased shielding when the sulphur adopts a capping configuration, e.g. -20.92 (13), compared with -17.39 (4) and -17.04 δ (7).

The greater instability of $|Os_3(CO)_9(H)SR|$ when R = Pr^n compared to when R = Et is unexpected as the propyl group should be just as strong an I+ group. A possible explanation for this discrepancy is that the greater steric size of the propyl group causes the delicate balance between the two co-ordinations to be shifted in favour of the less sterically demanding bridging species. Interestingly, the sulphur in $|Os_3(CO)_9(H)(SPr^n)|$ does not appear to cap symmetrically as its i.r. spectrum resembles closely that of the ethylene adduct. Some evidence for the proposed steric conjestion on the sulphur side of the capped cluster is given by the X-ray of $|Os_3(CO)_9(H)_2(\mu_3\text{-}S)|^-|P.P.N.|^{+13}$ in which 6 carbonyls point up and out on the sulphur side.

The stability of the nonacarbonyl compounds, $Os_3(CO)_9(\mu_2\text{-}H)(\mu_3\text{-}SR)$, relative to decacarbonyl compounds varies as one ascends the iron-ruthenium triad. That is, the equilibrium position (see diagram 3.1) changes from being far over to the left for osmium to far over to the right for iron,[14,15] with ruthenium[16] being intermediate. This is probably a reflection on the increase in the stability of the M-CO linkage from iron to osmium. The stability of the capped

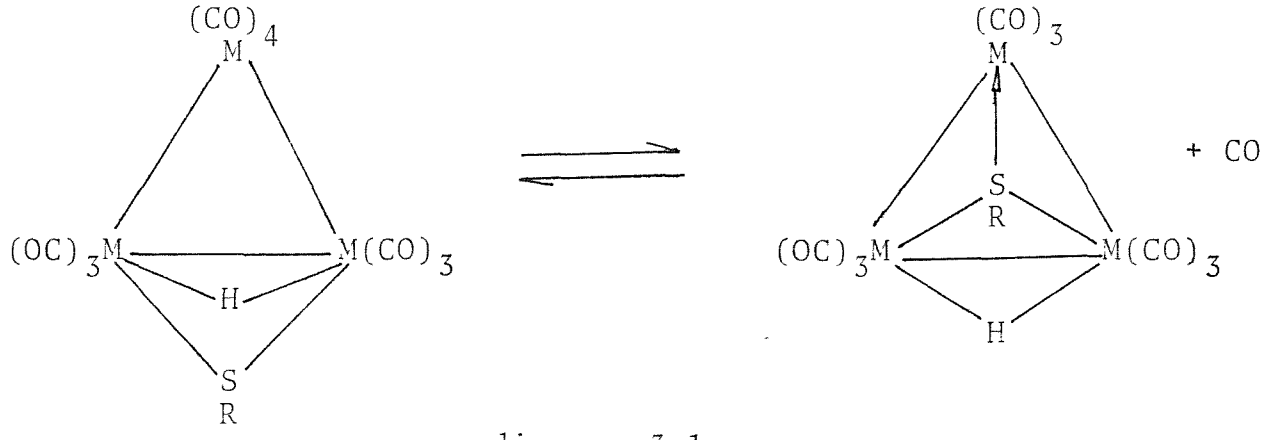

diagram 3.1

species increases dramatically from osmium and ruthenium to iron and this probably is a result of better fitting of the sulphur cap. Opposing this is the increase in M-M bond strength on descending the triad,[18] and this is seen in the relative stabilities of $|Os_3(CO)_9(H)_2(\mu_3\text{-}S)|$[13] and $|Ru_3(CO)_9(H)_2(\mu_3\text{-}S)|$.[16,17]

As $|O\{(CH_2)_3Si(OMe)_3\}_3|^+|BF_4|^-$ was not attainable another entry route to the nonacarbonyl compounds, $|Os_3(CO)_9(H)(X)SR|$ had to be devised. The alternative entry found (see Scheme 3.2), included removing a carbonyl from the decacarbonyl cluster by Me_3NO oxidation. A trapping agent was found to be required as the nonacarbonyl cluster turned out to be unstable. Two weakly co-ordinating ligands, CH_3CN and C_2H_4, were evaluated. The CH_3CN gave the best yields possibly because of its higher concentration compared with the dissolved ethylene. Indeed, when the ethylene was forced to dissolve by using an autoclave the yield was increased.

Although Lewis and co-workers[1] have prepared many of the

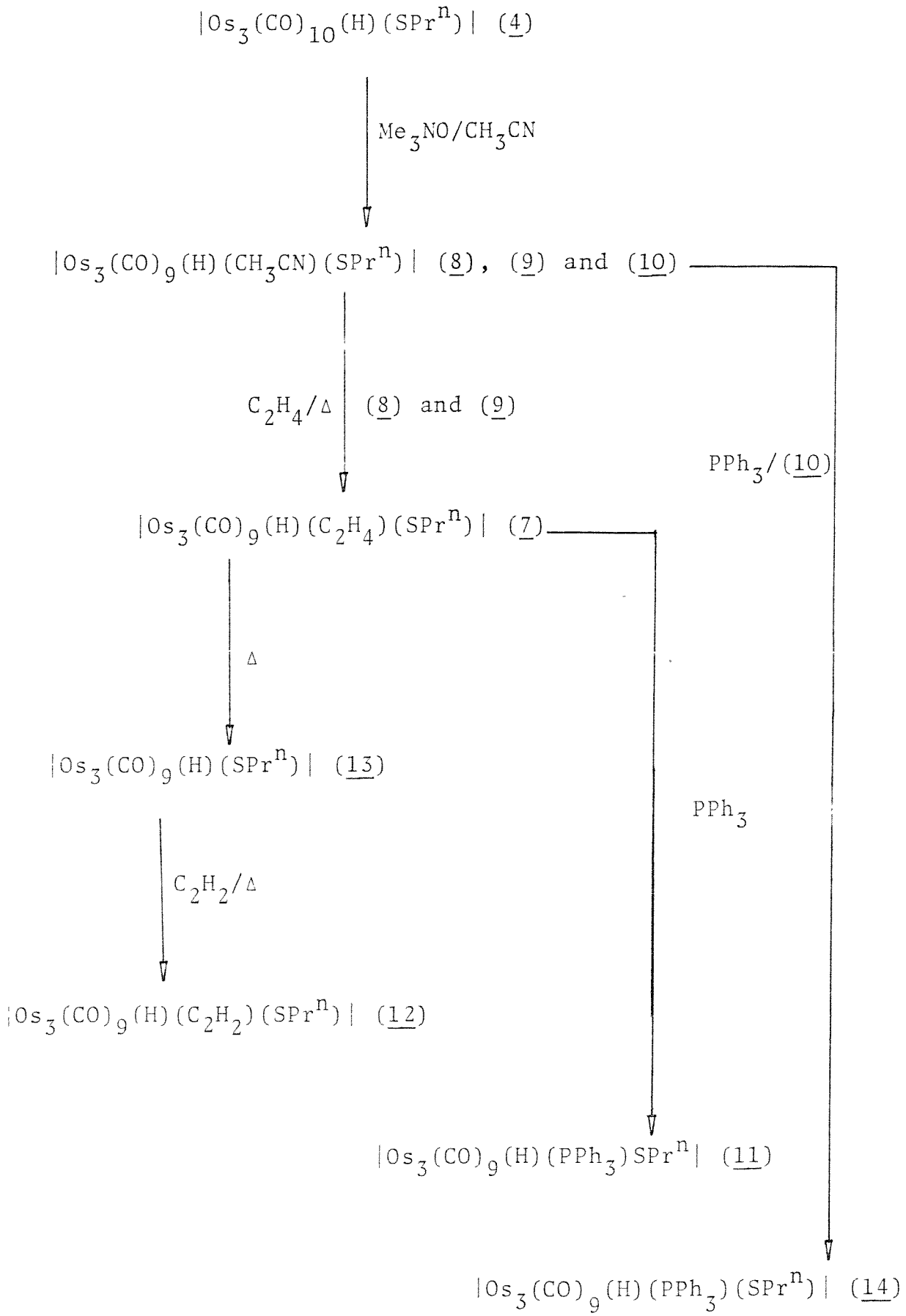
|Os3(CO)10(H)(SPrn)| (4)
Me3NO/CH3CN
|Os3(CO)9(H)(CH3CN)(SPrn)| (8), (9) and (10)
C2H4/Δ
(8) and (9)
PPh3/(10)
|Os3(CO)9(H)(C2H4)(SPrn)| (7)
Δ
|Os3(CO)9(H)(SPrn)| (13)
PPh3
C2H2/Δ
|Os3(CO)9(H)(C2H2)(SPrn)| (12)
|Os3(CO)9(H)(PPh3)SPrn| (11)
|Os3(CO)9(H)(PPh3)(SPrn)| (14)

Scheme 3.2.

compounds in Scheme 3.2, they have only determined the structure of the ethylene adduct.[19] This lack of information prompted the investigation of these compounds by ^{13}C n.m.r. The ^{13}CO enriched compounds were made from ^{13}CO enriched $|Os_3(CO)_{12}|$ in much the same way as were the unenriched compounds except identification mainly depended on the R.f. values and ^{1}H n.m.r. spectra as i.r. spectroscopy using the carbonyl fingerprint was of little use.

The structure of compounds, $|M_3(CO)_{10}(H)(SR)|$, have been determined by X-ray diffraction.[2] Both the decacarbonyl compounds prepared (M = Os; R = Pr^n (4) and $(CH_2)_3Si(OMe)_3$ (2)) gave solution ^{13}CO n.m.r. spectra in agreement with the compounds maintaining the same structure in solution as in the solid state. The $\{^1H\}$ ^{13}C n.m.r. spectrum for (4) (see Figure 3.2) displays a six line spectrum of approximate relative intensities 1:1:2:2:2:2 indicative of a plane of symmetry in the molecule. The two bands of intensity one, can be assigned to the two inequivalent axial carbonyls. The rest of intensity two, are due to the symmetry related carbonyls. The ^{1}H coupled ^{13}C n.m.r. spectrum of (4) allows one of these (Band at 169.5 p.p.m.) to be assigned to the pair of carbonyls trans to the bridging hydride because of the strong angle dependence of $^{2}J_{HC}$.[21,22] A variable temperature ^{13}C n.m.r. study showed no change from -60 ^{o}C to 60 ^{o}C indicating that (4) is rigid on the n.m.r. time scale over this temperature range. The ^{13}C n.m.r. of $|Os_3(CO)_{10}(H)(X)|$ where X = 3e donor (e.g. SEt, SPh, NBu^nH, OH, Cl, Br,

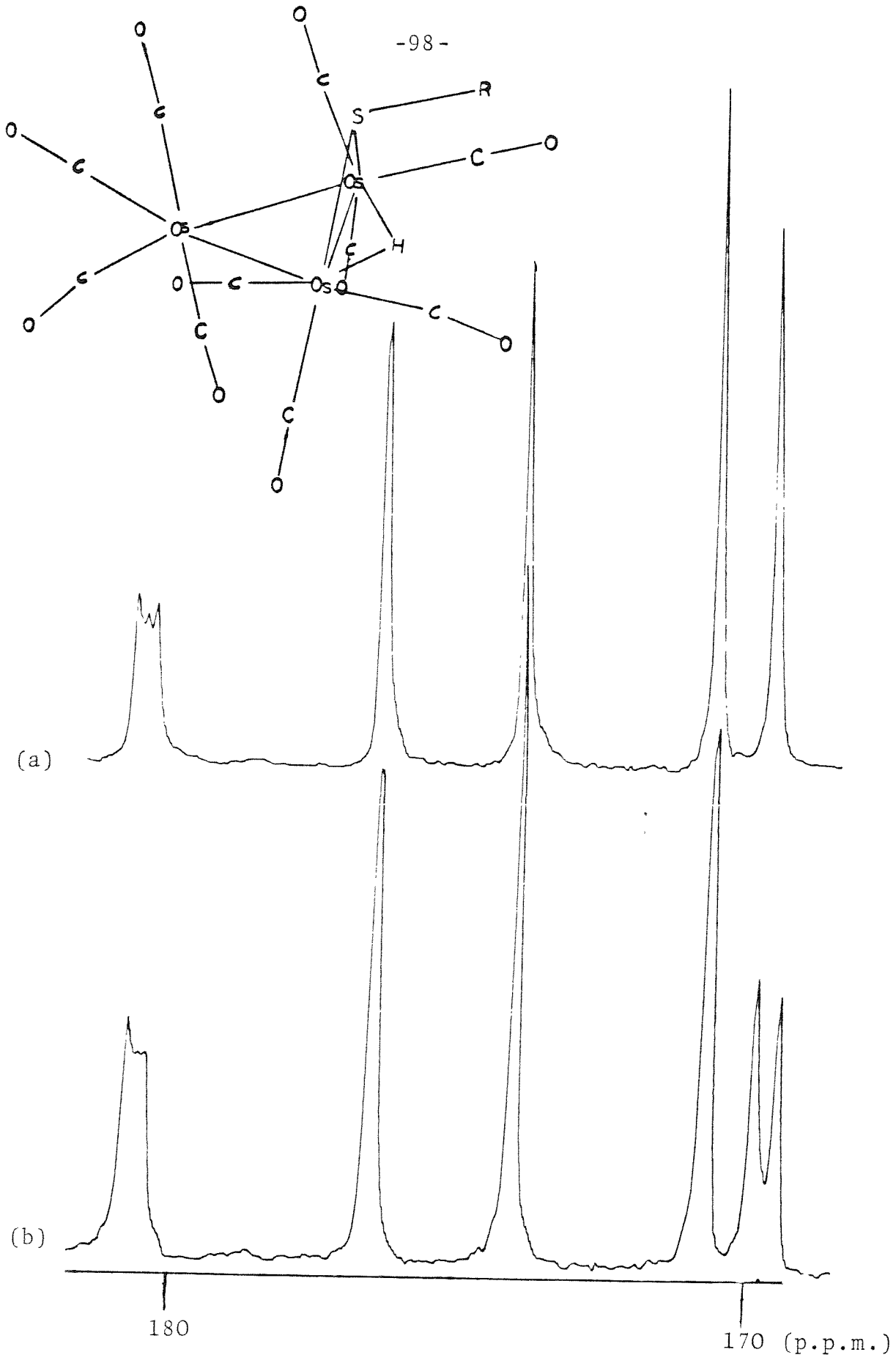

Figure 3.2. inset the structure of $|Os_3(CO)_{10}(H)(SR)|$
(a) $^{13}C-\{^1H\}$ n.m.r. spectrum of ^{13}CO enriched (2) (R = $CH_2CH_2CH_2Si(OMe)_3$) in CD_2Cl_2.
(b) ^1H coupled ^{13}C n.m.r. spectrum of ^{13}CO enriched (2) in CD_2Cl_2.

I, CO_2Me and CO_2CF_3) have been reported[23] for temperatures above 70 °C. It was found that for X = SEt, SPh, NBu^nH, Cl, Br, I and CO_2CF_3 the previously rigid clusters show a broadening of the axial carbonyl bands in conjunction with a band of intensity 2. Obviously positional exchange is starting to occur about the unique osmium, and because of the close similarities of the spectra (band of intensity 2 that broadens, X = SEt 173.7; and SPh 173.8 δ) this allows the assignment of the peaks due to the equatorial carbonyls in (4) and (2) (173.9 and 174.4 δ, respectively). The mechanism of this exchange is unknown but clearly involves only rearrangement of the carbonyls on the unique osmium atom. This rules out incidentally, mechanisms which involve rotation of the metal core within a fixed or variable carbonyl envelope,[24] and bridging carbonyl intermediates,[25] since these would be expected to cause carbonyl exchange between adjacent osmium atoms.

In the $^{13}C-\{^1H\}$ spectrum of (2) there is an unexpected extra peak between the two axial carbonyl bonds. This is probably caused by an accidental degeneracy in the inner lines of a pair of doublets caused by $^2J_{CC}$. Since the level of enrichment was only 35 % the likelihood of coupling $^2J_{c(axial)c(axial)}$ = 12 %, and $^2J_{c(axial)c(equatorial)}$ = 25 %. Thus the most likely source of the coupling is between the axial and equatorial carbonyls on the unique osmium atom. Some supporting evidence for this comes from the steric dependence of $^2J_{CC}$, $^2J_{CC(\underline{trans})}$ being usually 30 - 35 Hz and

$^{2}J_{CC}$ (90°), being 3 - 4 Hz.[26] The $^{2}J_{CC}$ from the spectrum of (2) appears to be 5 - 8 Hz and so is obviously due to $^{2}J_{CC}$ (≈ 90°). There are several reasons why the coupling is not seen for the other carbonyls. Mainly this is due to the low likelihood of there being two ^{13}C enriched carbonyls on two specified positions. In the case that it is seen, this is doubled by there being two possible equivalent sites for the second equatorial carbonyl and the intensity is also increased by the accidental degeneracy. It is interesting to note that the outer lines are not seen, presumably they are incorporated in the tails of the uncoupled peaks. Another reason why coupling is not seen for the other bands is the angle dependence of J_{CC}. In S. Aime's paper,[26] the coupling between carbonyls in highly ^{13}CO enriched $|Os_3(H)_2(CO)_{10}|$ is not seen for the carbonyls on the osmium atoms bridged by the hydride despite the coupling being seen for the <u>trans</u> and <u>cis</u> carbonyls on the unique osmium. This is presumably due to $^{2}J_{CC}$ being too small to be observed. So by analogy one would not expect to observe it for the carbonyls on the osmium atoms bridged by the sulphur, which have approximately the same relative spacial positions. In the ^{1}H coupled spectra of (2) and (4) one of the axial carbonyl bands is split by $^{2}J_{HC}$. Unfortunately, not enough is known at present about the steric effects on long range $^{1}H - ^{13}C$ coupling to assign the axial carbonyl.

The reaction of $|Os_3(CO)_{10}(H)(SPr^n)|$ (4) with Me_3NO in CH_3CN produces three major products all with the same formulae,

$|Os_3(CO)_9(H)(SPr^n)(CH_3CN)|$ (from their mass spectra). These are thought to be isomeric compounds which could be different in the position: of the acetonitrile on the triangle (either adjacent to the bridge or away); of the acetonitrile on the osmium (could be axial, equatorial, or trans to the μ_2-hydride etc); of the hydride or the SR ligand (due to inversion). The ^1H n.m.r. spectra differentiates the three isomers readily on the basis of the position of the hydride signal, but the acetonitrile resonance appears to be much less sensitive to the environment and does not help in the assignment. ^{13}C n.m.r., however, proved to be a much more sensitive tool.

In the case of (8) (see Figure 3.3) the ^{13}C n.m.r. five band pattern of approximate intensities 1:2:2:2:2 is indicative of the acetonitrile occupying an axial position on the unique osmium. The ^{13}C n.m.r. spectrum does not indicate which site is occupied but the position cis to the hydride is probably favoured on steric grounds. Some evidence for this is supplied by the X-ray structures of $|Os_3(CO)_{10}(H)(SEt)|$[20] and $|Os_3(CO)_9(H)(C_2H_4)(SMe)|$[19] in which the axial carbonyl is tilted away from the sulphur ligand due to steric interactions with the sulphur lone pair. The ^1H coupled ^{13}C n.m.r. spectra again shows a splitting of the trans carbonyls from the μ_2-hydride. The other bands in the spectrum also show a variation in relative intensities on turning off the broad band decoupler due to removal of the Overhauser effect.

Upon warming to r.t. (8) interconverts slowly with (9) but not (10) to give an equilibrium mixture of 60 % (8):40 % (9). This piece of evidence suggests that (8) and (9) are

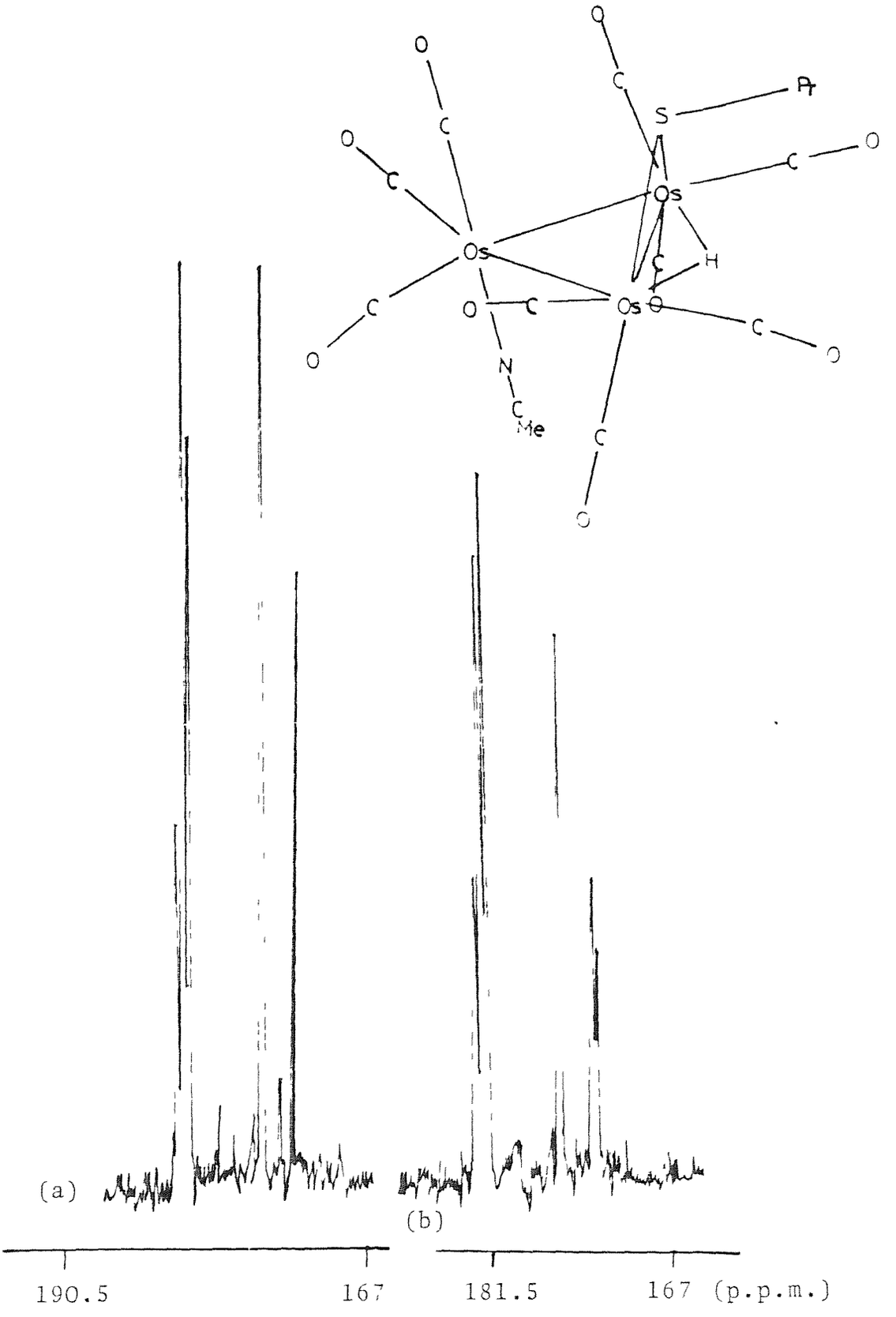

Figure 3.3. Inset the proposed structure of $'Os_3(CO)_9(H)(SPr^n)(CH_3CN)|$ (8). ^{13}C n.m.r. spectra in $CDCl_3$ at 0 ^oC of (8). (a) $\{^1H\}$ and (b) ^1H coupled.

on the same unique osmium but differ in their stereochemistries. This is confirmed by the ^{13}C n.m.r. spectrum of (9) (see Figure 3.4) which shows nine carbonyl bands, indicative of the CH_3CN occupying an equatorial position on the unique osmium. Again there is insufficient evidence to assign the carbonyl peaks except for the two due to carbonyls trans to the hydride and one of the axial carbonyls (which is also split by J_{HC}). The carbonyl peaks trans to the hydrides are in general shifted upfield either due to electron donation by the hydrides (causing increased shielding) or by virtue of their position relative to the cluster triangle.

The steric and electronic factors which govern the equilibrium between (8) and (9) are not easy to evaluate. Firstly, considering $|Os_3(CO)_{12}|$, the equatorial positions should, being trans to a M-M bond, have more electron density available for back donation than the axial positions. So the axial positions should suit σ donor ligands and the equatorial π acceptor ligands. Some evidence to support this comes from the structures of compounds of the general formula $|Os_3(CO)_{11}X|$. In the case of good σ donor ligands (poor π acceptors) they are found to go axial (X = NH_3[27] and CH_3CN[29]), whereas good π acceptor ligands tend to go equatorial (X = C_2H_4[29]). However, in the last example, steric effects may have predominated. For example, isocyanide ligands are good σ donor and moderate π acceptors. Though they are poorer σ donors than cyanides they still go axial when the ligand is small, e.g. $|Os_3(CO)_{11}CNMe|$.[31] However,

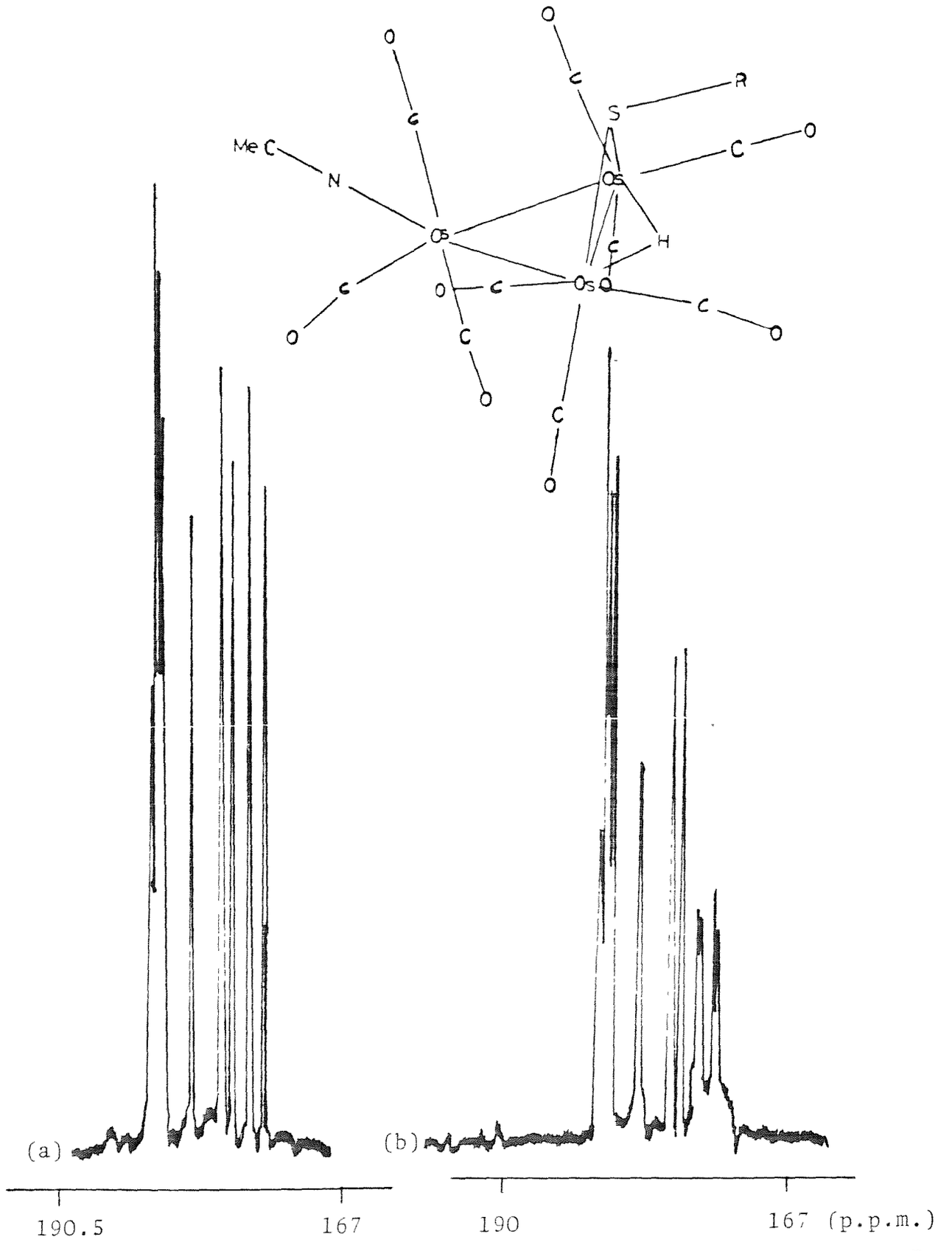

Figure 3.4. Inset the proposed structure of $|Os_3(CO)_9(H)(SPr^n)(CH_3CN)|$ (9). ^{13}C n.m.r. spectra in $CDCl_3$ at 0 °C of (9). (a) $\{^1H\}$ and (b) ^1H coupled.

as they increase in size or the cluster becomes more substituted they lose this preference and go also in equatorial positions (e.g. $|Os_3(CO)_{11}CNBu^t|$[30] exists as a mixture of both axial and equatorial isomers). This is because the equatorial positions are less sterically demanding than the axial ones. Further evidence for this is seen in the compounds $|Os_3(CO)_{11}PR_3|$ in which the phosphines go exclusively equatorial (X-ray,[3] ^{13}C n.m.r.[31]) despite their strong σ donor and poor π acceptor properties.

The situation for, $|Os_3(CO)_9(H)(CH_3CN)(SPr^n)|$ (8) or (9), is more complex both sterically and electronically. The axial position on the unique osmium is more sterically hindered than on osmium carbonyl on the sulphur side of the cluster. But on the hydride side it is probably less because there are no other axial carbonyls on the adjacent osmium atoms. The isomers of $|Os_3(CO)_9(H)(PPh_3)(Cl \text{ or } I)|$ are thought to be due to this lack of hindrance allowing the phosphine to go both equatorially and axially.[32] This line of argument suggests that the axial isomer for the CH_3CN should be even more stable than the osmium carbonyl analogue, on steric grounds. However, this is evidently not the case, a possible reason why (9) occurs is that the sulphur causes the whole unique osmium unit ($Os(CO)_4$ or $Os(CO)_3(L)$ unit) to tilt away from it (see the solid state structures of $|Os_3(CO)_{10}(H)(SEt)|$[20] and $|Os_3(CO)_9(H)(C_2H_4)(SMe)|$[19]) and so mixes the electronic preferences of the different positions on the unique osmium.

The CH_3CN derivative (10) is due to substitution next to

the bridge. The ^{13}C n.m.r. spectrum shows numerous peaks (14-18) which are in part due to its decomposition. The CO given off by this being taken up by (10) to give $|Os_3(CO)_{10}(H)(SPr^n)|$ (4). Once the peaks due to (4) are subtracted out the problem becomes more tractable with an 8 or 9 band pattern remaining. This suggests that the molecule has no plane of symmetry (as one would expect for substitution adjacent to the bridge) and has only one major isomer occurring over the temperature range scanned (-60 - 0 ^{o}C). This is in part confirmed by the ^{1}H n.m.r. spectra of the unenriched compound which show only one CH_3CN and hydride resonance over the temperature range, -60 - 30 ^{o}C. However, at 30 ^{o}C decomposition was evident after ten minutes and a weak peak in the hydride region was seen assignable to (4). Further evidence for the CH_3CN being next to the bridge is given by its reaction with PPh_3 which is discussed later.

It was found that the relative yields of ((8) + (9)):(10) could be varied by changing the reaction temperature. Lower temperatures favoured the production of (8) + (9) at the expense of (10). This is in accord with the Me_3NO becoming more specific as the temperature is lowered and reacting in preference with the least sterically hindered carbonyls but electronic effects within the cluster may also cause this preference.

The reaction of (8) + (9) with ethylene was carried out in 1,2-dichloroethane so when the solvent was blown off the freed CH_3CN is also removed so as to provide

$|Os_3(CO)_9(H)(C_2H_4)(SPr^n)|$ (7) free of (8) and (9). The X-ray structure of $|Os_3(CO)_9(H)(C_2H_4)(SMe)|$[19] shows that the ethylene ligand occupies an equatorial position (as deduced for $|Os_3(CO)_{11}(C_2H_4)|$[29]) with the C-C axis in the plane of the osmium triangle. The ethylene is bonded in the Chatt-Dewar-Duncanson bonding mode. The $^{13}C-\{^1H\}$ n.m.r. spectrum (see Figure 3.5) displays an 8 line spectrum instead of the 9 line pattern one would expect for a molecule with C_1 symmetry. This is because of an accidental degeneracy in the upfield peak. The ^1H decoupled spectrum shows a splitting of two bands (probably the two carbonyls trans to the hydride). This is only resolved for one (band at 169.8 δ), the other only shows a reduction in intensity due to a broadening (band at 172.8 δ).

The ^1H n.m.r. spectrum is unusual in the light of the ^{13}C n.m.r. results. If the ethylene was fixed in space it would have four inequivalent protons because of the C_1 symmetry of the molecule. The ^{13}C n.m.r. spectrum shows that all the carbonyls are frozen on the n.m.r. time scale. So, if the ethylene was rotating as currently thought[34] only about its M-π bond axis, one would expect to see a doublet of doublets , since only inequivalent pairs of trans protons would be interconverted. However, the ^1H n.m.r. spectrum displays only a singlet (30 °C- -114 °C) and as the compound only dissociates rapidly at 80 °C (to give the capped cluster) a dissociative mechanism for the ethylene's ^1H exchange is unlikely. A possible mechanism that would account for the

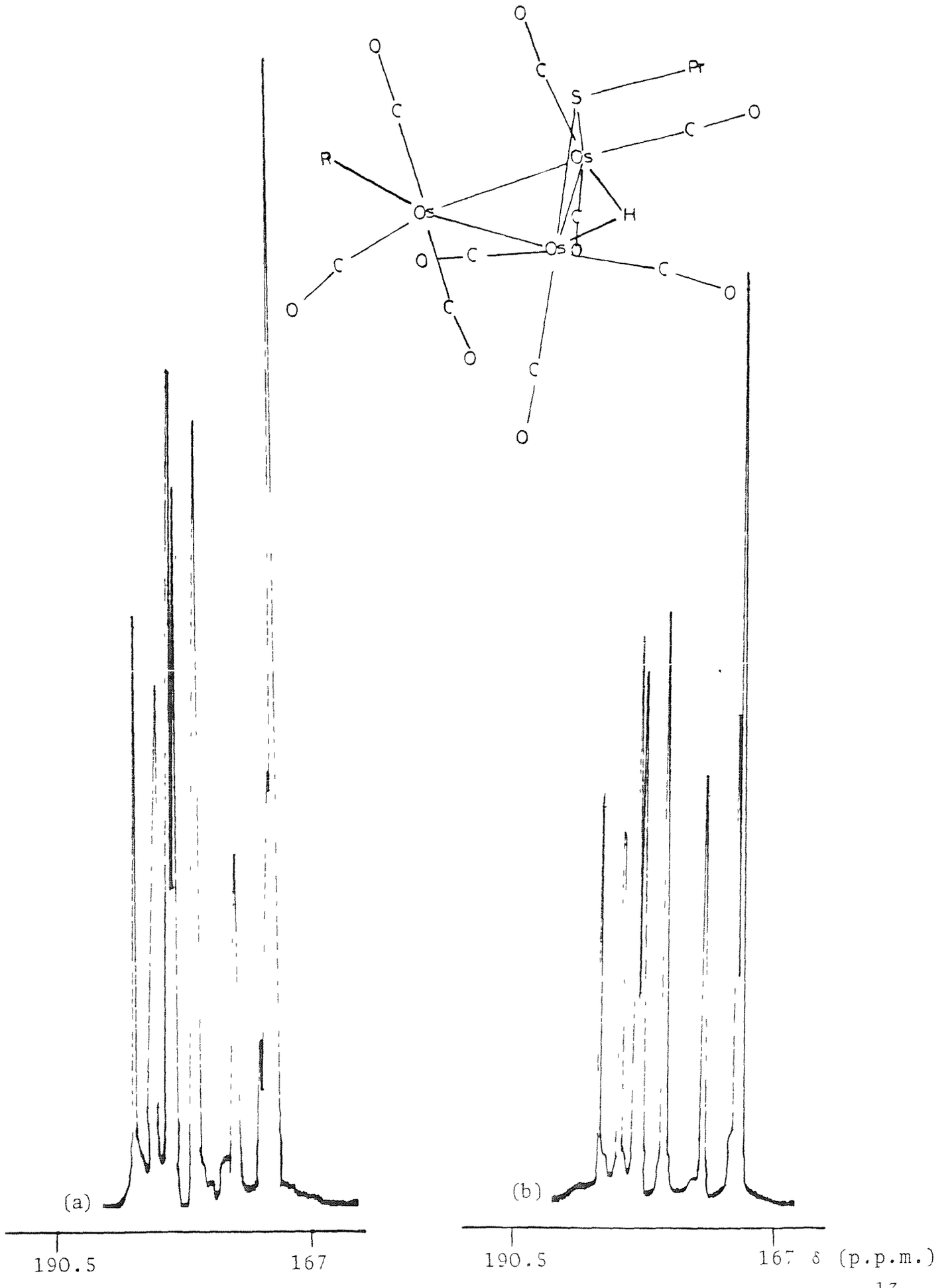

Figure 3.5. X-Ray structure of $Os_3(CO)_9(H)(SPr^n)(C_2H_4)$ (7). ^{13}C n.m.r. of (7) at $CDCl_3$/0 °C. (a) ^1H coupled and (b) $\{^1H\}$.

spectral results involves two rotations. That is, one about the π-M bond and one about the C-C bond.

The reaction of (7) or ((8) + (9)) with PPh_3 gave $|Os_3(CO)_9(H)(PPh_3)(SPr^n)|$ (11) in high yield. The ^1H n.m.r. spectrum of this compound, besides demonstrating the existence of the alkyl groups, shows only one hydride signal. This is because the phosphine is co-ordinated to the unique osmium atom away from the hydride bridge. The ^{13}C n.m.r. spectra (see Figure 3.6) show that the phosphine occupies an equatorial position on the unique osmium. Three bands (192.6 at -60 °C; 190.8 and 178.5 δ at 31 °C) show varying amounts of phosphorus coupling and so can be tentatively assigned to the three carbonyls on the unique osmium atom. Since in the ^1H coupled spectrum the band at 190.8 δ (p.p.m.) shows further splitting it can be assigned to one of the axial carbonyls. Two other bands in the low temperature spectra also show a ^1H coupling (174.8 and 172.1 δ) and can by virtue of their upfield position be assigned to the carbonyls *trans* to the hydride. On warming to 31 °C the bands broaden unevenly. The furthest downfield band (192.5 δ) broadens more than any other band, whereas the band at 191.2 sharpens to give a doublet (190.8 δ), and the three furthest upfield bands become accidentally degenerate to give a strong peak at 171.4 with a shoulder at 172.1 δ (p.p.m.). Another spectral change that occurs on warming from -60 °C to 30 °C is that the signal for the phenyl rings, in the $^{13}C-\{^1H\}$ n.m.r. spectrum, changes from a broad hump to

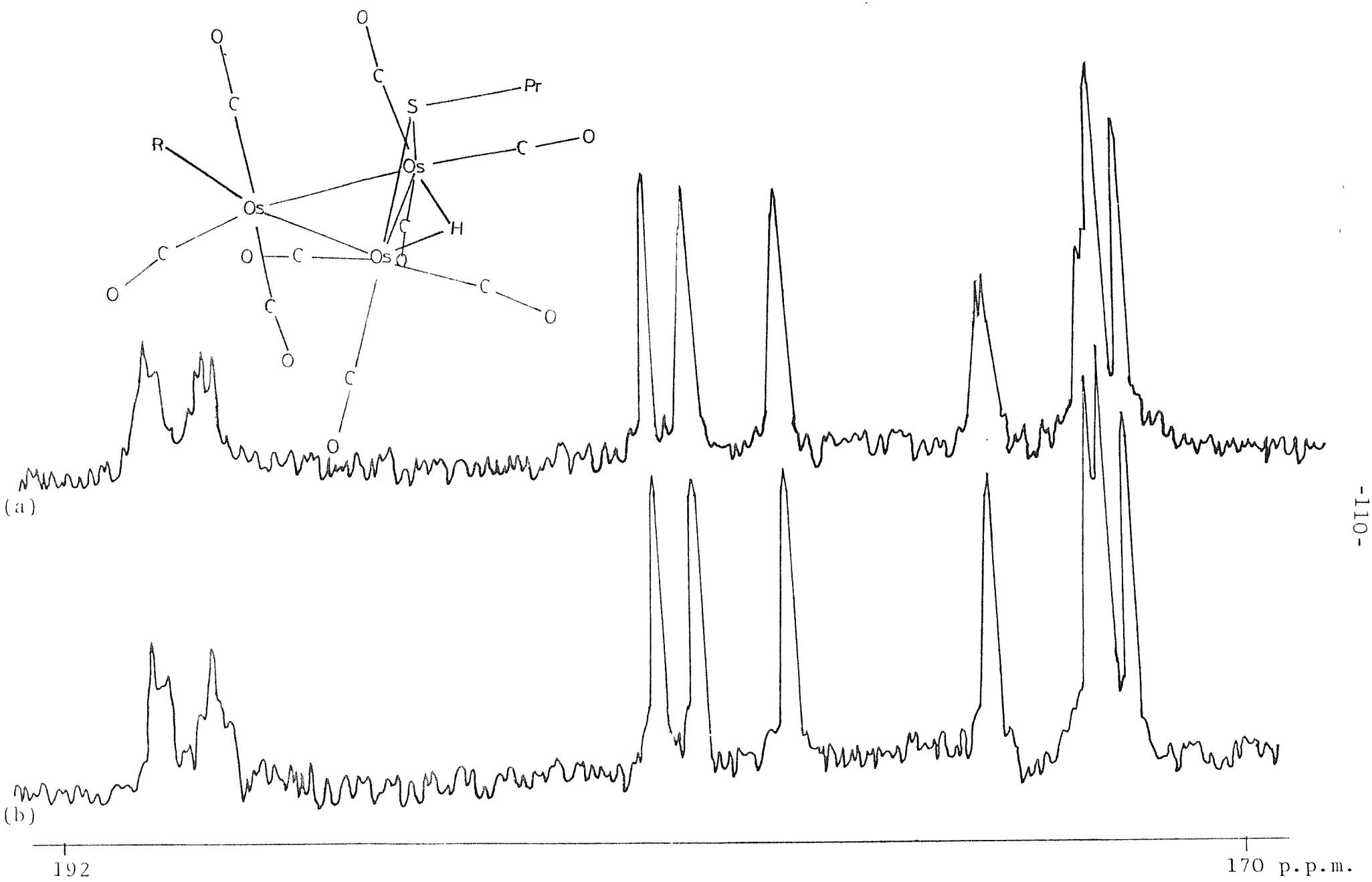

Figure 3.6. Inset, proposed structure of $|Os_3(CO)_9(H)(SPr^n)(PPh_3)|$ (11). ^{13}C n.m.r. of (11) in $CDCl_3$ at -60 ^oC (a) ^1H coupled, (b) $\{^1H\}$.

a sharp five peak equal intensity pattern (2 pairs of doublets and one singlet). These can be assigned to the ortho, meta and para carbons on the phenyl rings. The phosphine substituted carbon not being seen presumably because of poor relaxation.

These spectral changes could be caused by two fluxional processes. Firstly, at high temperatures all the ortho or meta or para carbons are equivalent. So the phosphine as well as rotating about its M-P axis must also be rotating about the P-Ph bond. At low temperatures, because of the single broad phenyl signal, one or both of these rotations must be slowed down. The broadening of particularly the axial carbonyls (band at 192.5 δ appears to be an axial carbonyl and the band at 178.6 δ an equatorial by comparison with the ^{13}C n.m.r. spectra of (4)) at low temperatures requires the invoking of a slowing of both rotational processes, since the equatorial carbonyl and the rest of the carbonyl bonds remain relatively sharp. This broadening of the axial carbonyls is probably due to a localised effect such as a restriction to the rotation of particular phenyl rings. The sharpening of one of the axial carbonyls (191.2 δ) and the broadening of the other (192.5 δ) on warming to 31 ^{o}C is hard to interpret but possibly could be caused by a combination of acceleration of the phosphine rotations, sharpening peaks, while requiring the movement of one of the axial carbonyls and so broadening its peak.

The reaction of $|Os_3(CO)_9(H)(CH_3CN)(SPr^n)|$ (10) with PPh_3

gave $|Os_3(CO)_9(H)(PPh_3)(SPr^n)|$ (14). The ^1H n.m.r. spectrum of (14) shows ^{31}P coupling to the hydride and on cooling the hydride signal is resolved to a pair of unequal doublets. This indicates that (14) exists as a mixture of two rapidly interconverting isomers with the phosphine occurring on a osmium common with the hydride. A similar situation has been reported for $|Os_3(CO)_9(H)(PPh_2Me)(SPh)|$[35] which was produced by heating $|Os_3(CO)_{10}(H)(SPh)|$ with PPh_2Me. This compound was reported to exist as two isomers. The major species gave a doublet with a splitting of 28.5 Hz while the minor species displayed only a splitting of 6.5 Hz. These two species can be assigned in the light of the current knowledge on the steric effects on J_{PH}[21] as due to trans (major isomer) and cis (minor isomer) orientations of the phosphine relative to the hydride. As both isomers of (14) display $^2J_{PH}$ values of about 6 Hz, the phosphine in both isomers must not adopt a trans configuration relative to the hydride (see Figure 3.7). That is, it must occupy positions P_1 or P_2 but not P_3. The ^{13}C n.m.r. spectra for (14) are not consistent with the two isomers differing in the position of the phosphine otherwise two sets of nine bands (ignoring phosphine and proton coupling) should be seen in the low temperature spectrum. As this is not observed these two isomers must differ in some other aspect, to which the carbonyls are insensitive, such as the relative orientations of the phenyl and propyl groups. For this to occur requires the molecule to be sterically conjested so as to stop the free rotation of the phosphine. This effect

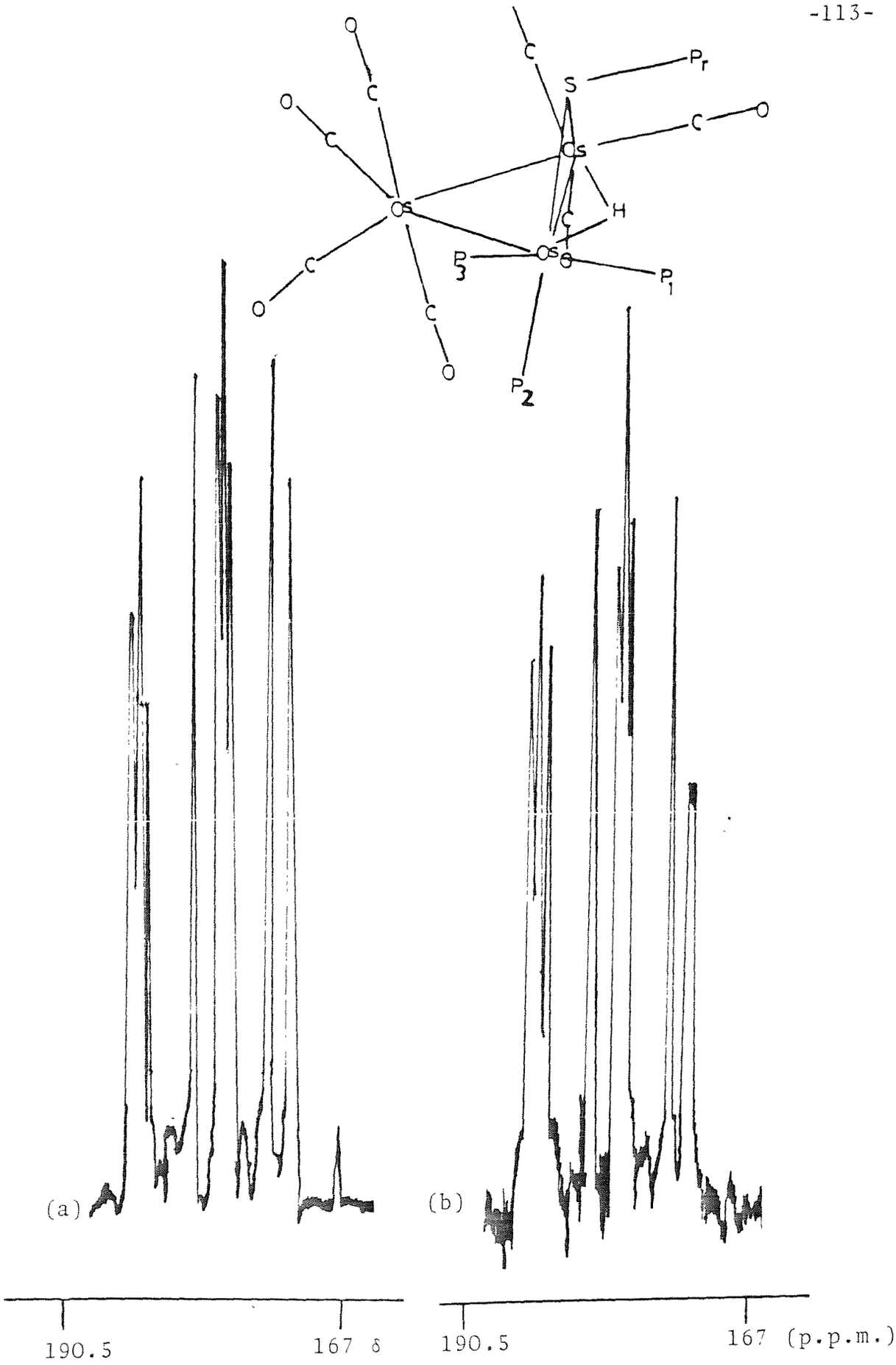

Figure 3.7. Top right the 3 possible positions for phosphine substitution next to the hydride bridge. ^{13}C n.m.r. spectra in $CDCl_3$, (a) $\{^1H\}$ and (b) ^1H coupled, for $[Os_3(CO)_9(H)(SPr^n)(PPh_3)]$ (14).

has been seen for (11) at -60 °C, in which the phosphine occupies the less sterically conjested equatorial site on the unique osmium. The ^{1}H coupled ^{13}C n.m.r. spectra of (14) show that there is only one carbonyl in the trans position to the hydride. To account for this, since the phosphine does not occupy a trans orientation to the hydrides, a partial rotation of the $M(CO)_2(PPh_3)$ unit is proposed. The driving force behind this is probably the conjestion about this osmium.

An interesting point about the ^{13}C n.m.r. spectra of (14) was that no phosphorus coupling was observed, unlike in the case of (11) with the phosphine on the unique osmium. The reason for this is the steric dependence of J_{PC} which like J_{CC} is largest for angles of 180 °C, small for angles of 90 °C and very small for intermediate angles (like those seen for the carbonyls next to the hydride bridge in $H_2Os_3(CO)_{10}$[26]).

The reaction of (7) or ((8) + (9)) with acetylene gave two main products. The major of these from its mass spectrum is formulated as $Os_3(CO)_{10}(H)(C_2H_2)(SPr^n)$ (12). The r.t. ^{1}H n.m.r. spectrum of (12) confirmed the existence of a n-propyl group, bridging hydride and an unsaturated alkyl group, probably acetylenic. This acetylenic peak on cooling broadens and "freezes" out as a distorted ab quartet (see Figure 3.1). Another possible C_2H_2 ligand besides a π bound acetylene which could give two inequivalent hydrides is a vinylidene ($M=C=CH_2$) grouping. Deeming has reported compounds which resolve this problem (see Table 3.1). Obviously from these results, (12) contains a π bound acetylene.

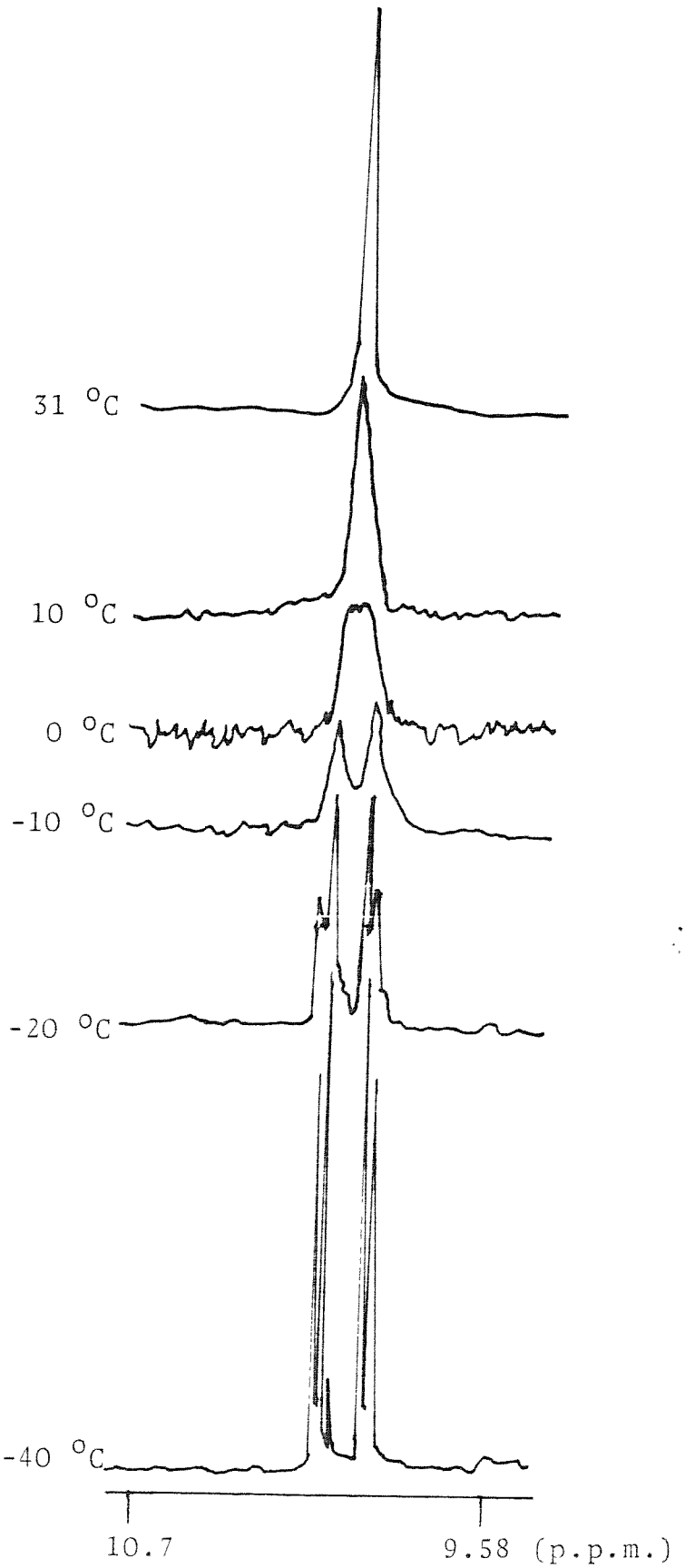

Figure 3.1. Variable temperature ^{1}H n.m.r. spectra of $|Os_3(CO)_9(H)(C_2H_2)(SPr^n)|$ (12) in the acetylenic region.

TABLE 3.1.

Compound	^1H n.m.r. of C_2H_2 ligand/δ (p.p.m.)	
(12)	10.4(s)	31 °C
	10.43(d), 9.88(d)	-40 °C
$\|Os_3(H)_2(CO)_9(CHCH)\|$[36]	9.3(s)	0 °C
	10.2(d), 9.2(d)	-120 °C
$\|Os_3(H)(AsMe_2)(CO)_9(CHCH)\|$[36]	10.52(d), 10.03(d)	
$\|Os_3(H)_2(CO)_9(CCH_2)\|$[37,29]	6.1(s), 5.6(s)	
$\|Os_3(H)(AsMe_2)(CO)_9(CCH_2)\|$[36]	5.98(s), 3.29(s)	

The ^{13}C n.m.r. spectra of (12) provide evidence that the acetylene like the ethylene occupies an equatorial site on the unique osmium. The low temperature ^{13}C spectrum displays (see Figure 3.8) an 8 line pattern indicative of the molecule having a C_1 symmetry. Incidentally, it should be a nine line pattern but there is an accidental degeneracy of two lines to give the intense upfield peak. This pattern remains unchanged upon warming to -40 °C and then broadens to give a single broad feature by 12 °C (centred at 173.7 δ). This remains broad up to 30 °C and then sharpens to give a four band spectrum at 50 °C (relative intensities 2:3:2:2). This remains unchanged up to 70 °C. This high temperature spectrum is that which would be expected if there was substitution on the unique osmium and a time averaged plane of symmetry in the molecule caused by exchange of the groups on the unique osmium, with no exchange with the other osmium

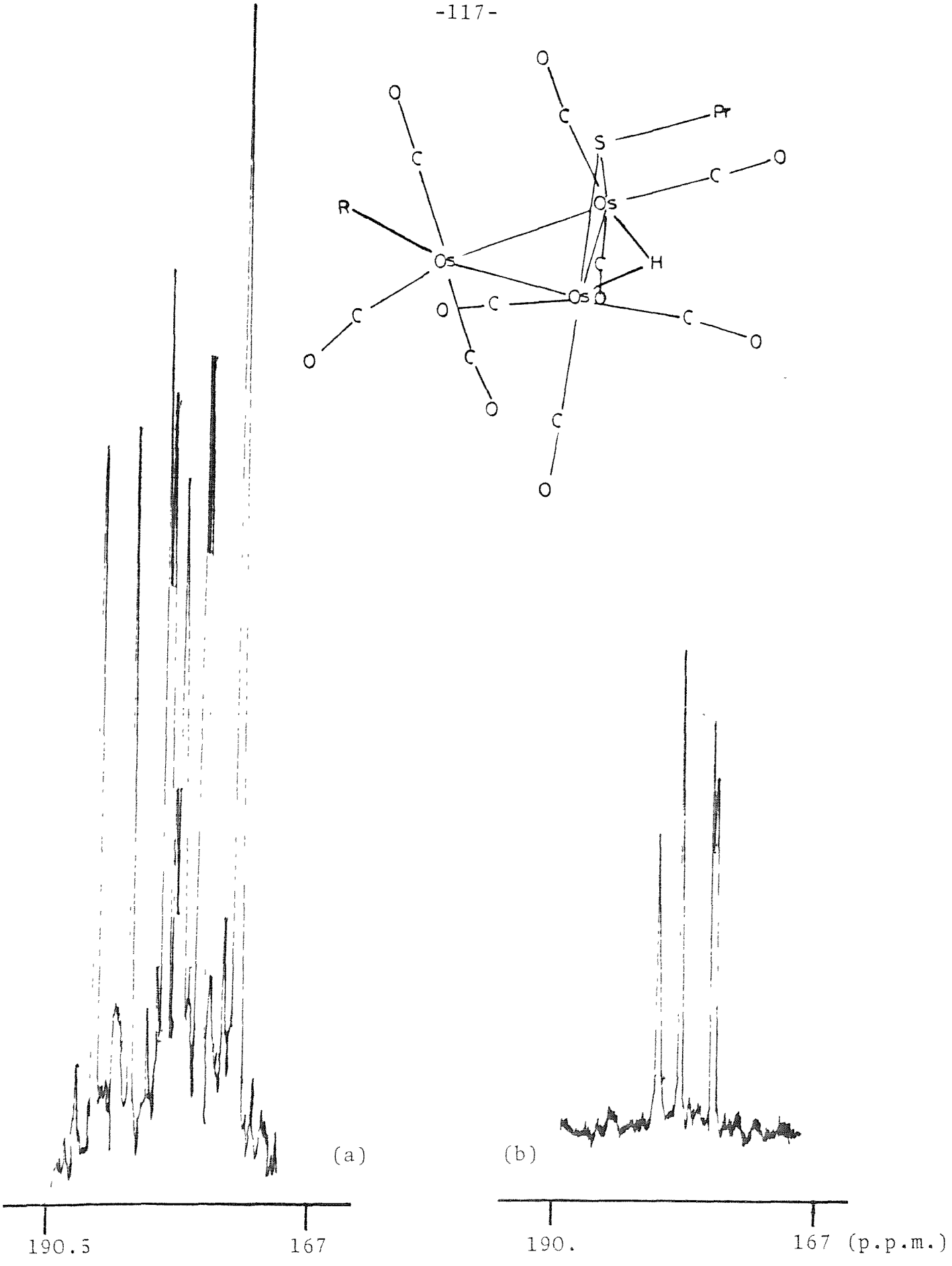

Figure 3.8. inset a possible structure for $[Os_3(CO)_9(H)(SPr^n)(C_2H_2)]$, $^{13}C-\{^1H\}$ n.m.r. spectra at (a) -60 °C and (b) 60 °C.

atoms. This lack of exchange with the two hydride bridged osmium atoms is in accord with the variable temperature ^{13}C n.m.r. spectrum of $|Os_3(CO)_{10}(H)(SR)|$ in which the bands are due to the carbonyls on the unique osmium broaden first. An important point about the two fluxional processes occurring in this molecule is that the acetylenic protons are not interconverted, at least to start with, by the CO exchange process on the unique osmium atom. As this $M(CO)_3(C_2H_2)$ exchange process coalesces and sharpens at about 20 °C above the acetylenic protons interconversion process, the mechanism for this proton interconversion probably is rotation about the metal acetylene π-bond though processes involving vinylidene intermediates cannot be ruled out.

The complete assignment of all the carbonyls in the molecule is again not possible but the low temperature ^{1}H coupled ^{13}C n.m.r. spectrum shows a broadening of two upfield bands indicative of these being due to carbonyls trans to the bridging hydride. One of these bands (168.3 δ) is part of the accidentally degenerate band. In the high temperature spectrum (50 - 70 °C) these two carbonyls trans to the hydride are now equivalent and give rise to either the peak at 171.8 or 171.6 δ (p.p.m.). Unfortunately, on turning off the broad band decoupler, broadening of one of the peaks occurs and causes an accidental degeneracy which makes it impossible to assign them to one of the two. There is some evidence in the low temperature ^{13}C n.m.r. spectrum of (12) for the co-existence of another isomer. This could be the

axially substituted adduct (on the unique osmium). In the low temperature ^{1}H n.m.r. this species gives rise to the sharp weak peak at 10.30 δ (p.p.m.) which merges with the rest on warming. In the low temperature ^{13}C n.m.r. spectra (see Figure 3.8) some weak extra peaks can be discerned and these also disappear on warming and so are not due to impurities in the sample.

The reaction of either the π-bound ethylene (7) or acetonitrile ((8) + (9)) derivatives with hydrogen proceeds through an intermediate compound to $|H_2Os_3(CO)_9S|$. Pippard[33] has also observed this intermediate and proposed a structure (see diagram 3.2) based on the products obtained by reacting hydrogen halides with the nonacarbonyl clusters. Although a route to the pure intermediate was found it proved to be too

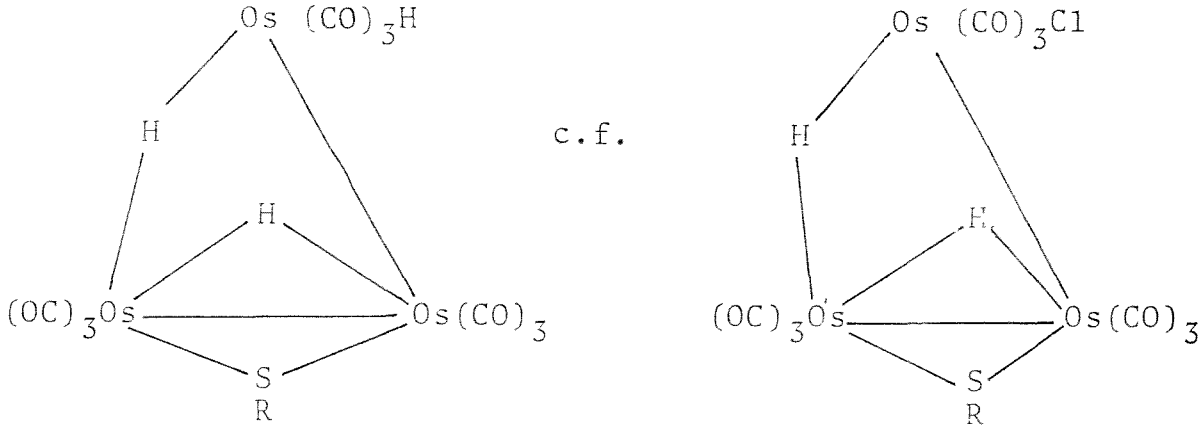

diagram 3.2.

unstable for ^{13}C n.m.r. and despite numerous attempts only a poor quality ^{1}H n.m.r. spectrum was obtained. This showed in the hydride region signals due to both terminal and bridging

hydrides. Further comment on this spectrum is not given because of its poor quality.

(b) Some aspects of the reactivity of tethered thiolate clusters.

Both (4) and (2) ($|Os_3(CO)_{10}(H)(SR)|$: R = Pr^n, (4); $(CH_2)_3Si(OMe)_3$, (2)) were found to be inactive towards olefin isomerisation under moderate conditions (< 100 °C, 72 hours), and only weakly so, under forcing conditions (125 °C, 15 hours). Some doubt exists as to the nature of the active catalyst under these conditions as extensive decomposition occurs. Obviously from these results (2) is not a good candidate for a supported catalyst. However, derivatives of the decacarbonyl clusters[1] are known which show features promising for catalysis. For example, $|Os_3(CO)_9(H)(SR)|$ exhibits a high,and more importantly, a reversible reactivity towards olefins. The reported entry into this class of compounds cannot be used to prepare the heterogeneous species, as $|R_3O|^+|BF_4|^-$ cannot be prepared when R contains a hydrolysable silyl group.[38,39] A way around this problem was found and applied to the heterogeneous systems.

Thus the entry into this class of nonacarbonyl compounds was achieved by using Me_3NO to oxidise off a carbonyl in the presence of a weakly co-ordinating ligand to trap the product. Two ligands were evaluated (CH_3CN, and C_2H_4), the CH_3CN proving to be the superior, was thus used for all subsequent experiments. These yield yellow/orange supported derivatives

whose i.r. spectra were in fairly close agreement with the homogeneous analogues (see Figure 3.9).

The reaction of the supported clusters with Me_3NO proceeded more slowly (5 - 24 hours compared to 20 minutes) and required more oxidant (5 - 25 equivalents compared with 1.1 equivalents), in all cases, than the homogeneous analogues. There are two possible reasons for this. Firstly, the Me_3NO being partially ionic is probably strongly absorbed by the oxide and secondly some Me_3NO is consumed in oxidising any excess free thiol ligand. Evidence exists for both these suggestions. For example, when (2) was reacted with the oxides it was found that a smaller excess of oxidant was required than in the case of the anchored analogue, with the same loading, prepared by reacting $|Os_3(CO)_{12}|$ with the same thiolated oxide. Obviously in this case some of the extra Me_3NO is required to oxidise the remaining free thiolate ligands. Me_3NO can be used to oxidise thiolate ligands homogeneously.[40]

<u>e.g.</u> $R\text{-}SH + Me_3NO \longrightarrow RSSR + R\text{-}S(O)\text{-}SR + RSO_2H$ <u>etc.</u>

When the reaction was repeated on samples derived from $SiMe_3Cl$ pretreated thiolated oxides a reduction in both the reaction time and amount of Me_3NO required was seen. This is probably due to the $SiMe_3Cl$ blocking the sites used for surface absorption of the Me_3NO, as a similar shortening of the reaction time was seen on going from a non-polar (<u>e.g.</u> cyclohexane, 3 days) to a co-ordinating solvent (<u>e.g.</u> CH_3CN,

Figure 3.9. I.r. spectra of (a) an equilibrium mixture of both isomers (8) and (9) of $|Os_3(CO)_9(H)(SPr^n)(CH_3CN)|$ in cyclohexane, (b) a Nujol mull of the CH_3CN derivative on thiolated aerosil 380, and (c) a Nujol mull of the CH_3CN derivative on $SiMe_3Cl$ pretreated thiolated aerosil 380.

25 hours). Since the osmium loadings are similar on both the $SiMe_3Cl$ pretreated and untreated thiolated oxides one can assume that the $SiMe_3Cl$ has not reacted with the thiolate groups. This indicates that the excess Me_3NO required is taken up by (a) reacting with free thiolate groups, and (b) permanent absorption on the oxide (since no further reaction is observed with the clusters on standing).

Several points can be made about the i.r. spectra of the supported CH_3CN derivatives. In most cases there is deliberately left some residual decacarbonyl cluster (as can be seen by bands at 2 108 and 2 065 cm^{-1}, see Figure 3.9) as excess Me_3NO was found to cause further reaction and cluster breakdown. The spectral quality in most cases (exception ZnO due to reduced loading) were improved by $SiMe_3Cl$ pretreatment (see Figure 3.9) of the oxide. The isomers (8) and (9) which predominate in the solution also appear on the support. Only one band that could be assigned to the isomer with the CH_3CN adjacent to the bridge (10) is seen (2 094 cm^{-1} compared with the band at 2 098 cm^{-1} in (10)).

The supported CH_3CN derivatives were found to convert exclusively to the C_2H_4 derivative when stirred overnight as a slurry under ethylene (40 bar, 40 ^{o}C). The i.r. spectrum (see Figure 3.10) illustrates a problem with supported cluster spectra. That is, a minor or impurity peak can be easily hidden by other peaks due to the peak broadening caused by the oxide environment. For example,

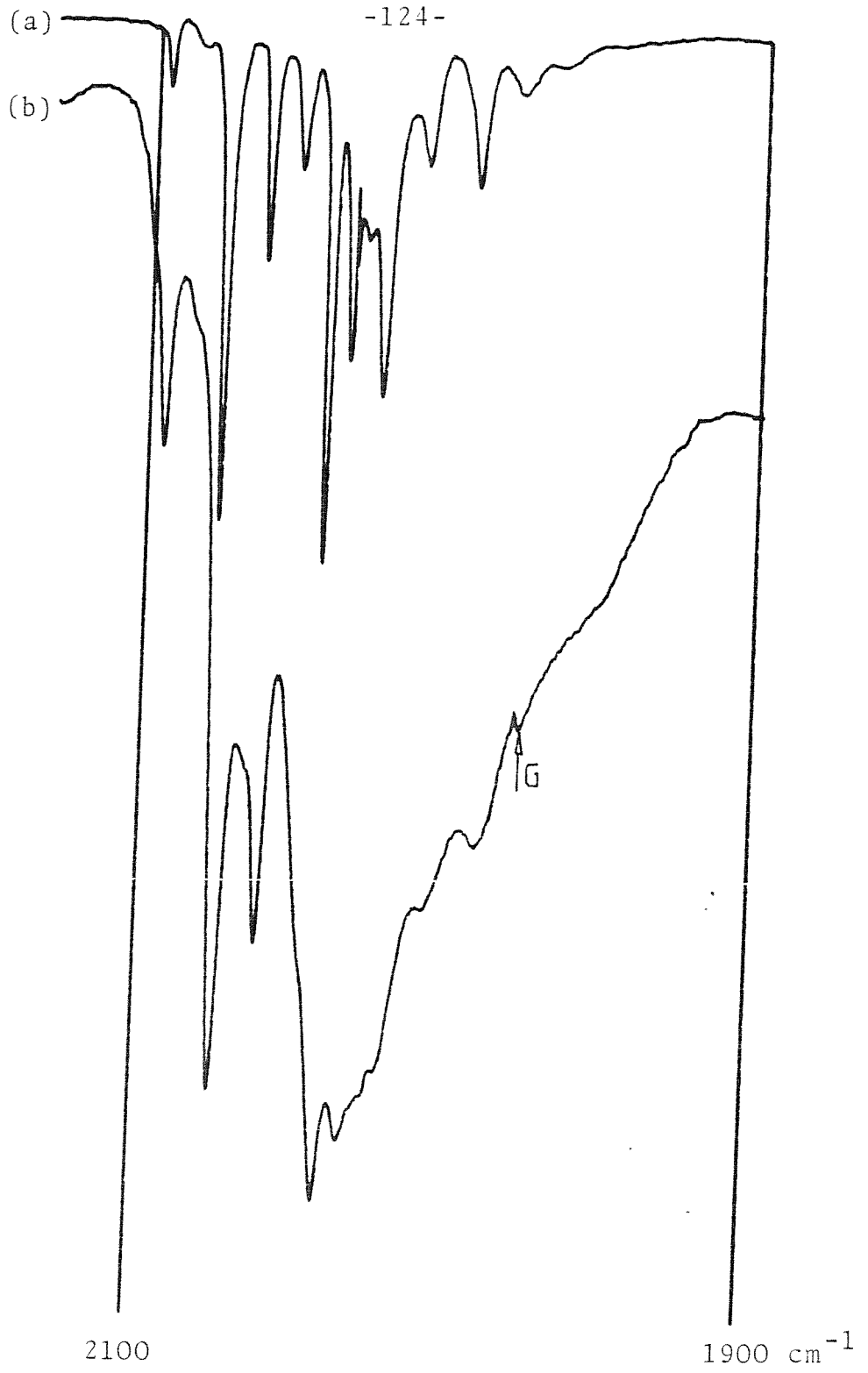

Figure 3.10. I.r. spectra of (a) $|Os_3(CO)_9(H)(SPr^n)(C_2H_4)|$ (7) in pentane, and (b) a Nujol mull of the supported analogue of (7) an aerosil 380. G = Grating change.

the peak at 2 026 cm^{-1} appears to have disappeared in the anchored species but careful comparison with the silica background spectrum shows it to exist as a shoulder on the 2 010 cm^{-1} peak.

The supported CH_3CN or C_2H_4 derivatives when stirred overnight with excess PPh_3 or refluxed in cyclohexane with a C_2H_2 bubble, convert cleanly to the PPh_3 and C_2H_2 derivatives, respectively, as can be seen from their i.r. spectra (see Figures 3.11 and 3.12). Interestingly, in all these derivatives (C_2H_4, C_2H_2 and PPh_3) the peak at 2 094 cm^{-1}, seen in the supported CH_3CN derivative case, has disappeared or is possibly obscured by peaks in the compounds but this is unlikely as when the silica backgrounds are subtracted out, the peak ratios are similar to those seen in the homogeneous compounds. Since the CH_3CN derivative (10) does not react with PPh_3 or C_2H_2 to give the same derivatives as (8) or (9) do, these results indicate that the peak at 2 094 cm^{-1} is not due to (10) but due to a new species possibly produced by oxide interaction with (8) or (9). Some evidence for this comes from the reaction in which the CH_3CN derivative is regenerated from the supported ethylene adduct, during which this band is also regenerated. Incidentally, CH_3CN itself also reacts with oxides to give bands in the carbonyl region[41] (e.g. MgO + CH_3CN gave bands at 2 190, 2 150 and 2 060) but this possibility was ruled out by control experiments.

Ideally the preparation of the capped cluster on the

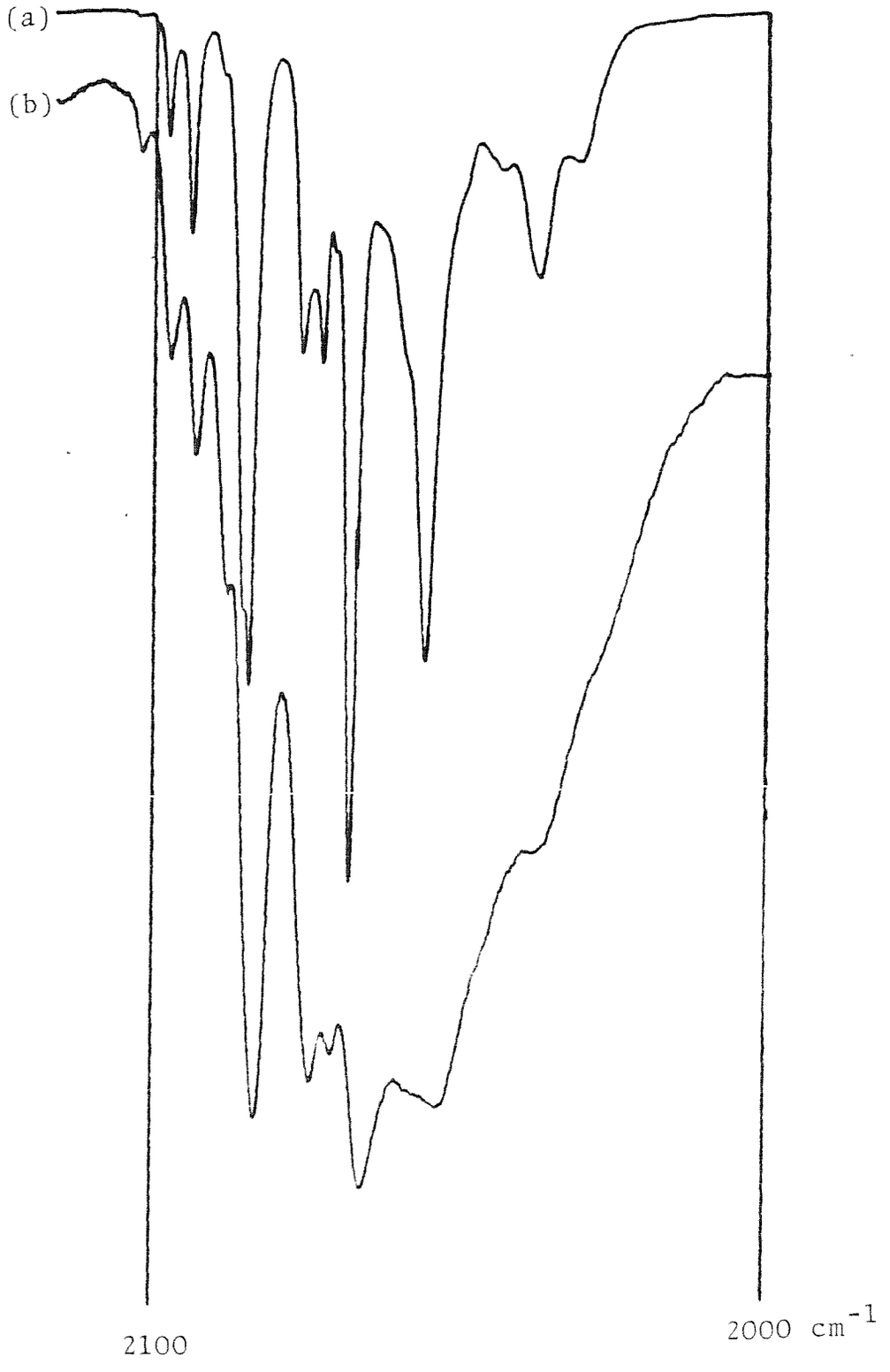

Figure 3.11. I.r. spectra of (a) $[Os_3(CO)_9(H)(SPr^n)(PPh_3)]$ (11) in cyclohexane, and (b) a Nujol mull of the supported analogue of (11) on aerosil 380.

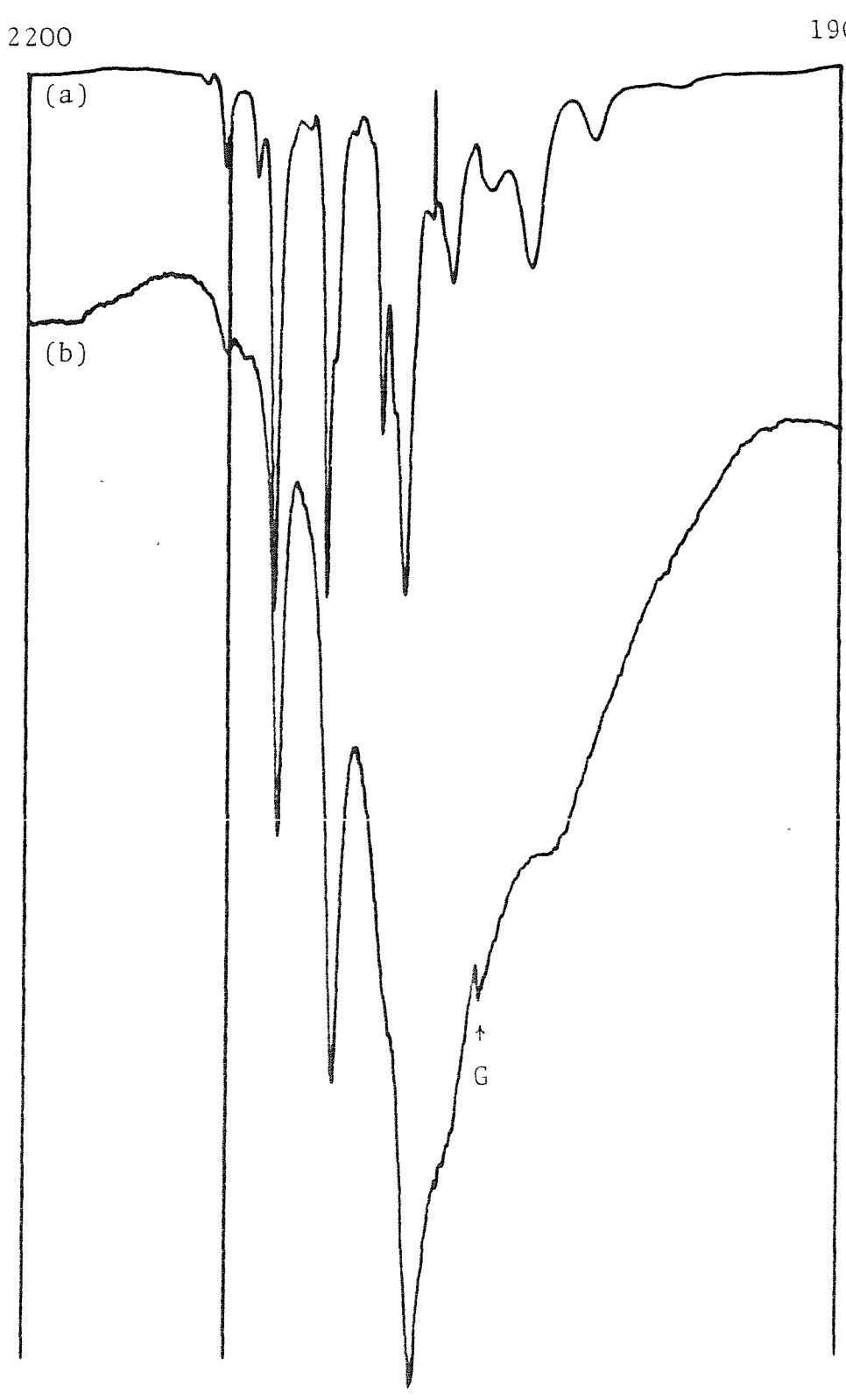

Figure 3.12. I.r. spectra of (a) $[Os_3(CO)_9(H)(SPr^n)(C_2H_2)]$ (12) in cyclohexane, and (b) the acetylene derivative on aerosil 380 (Nujol mull). G = Grating change.

surface should be more easy than in solution, as the weakly co-ordinating ligands can be desorbed by warming under vacuum, and also the capped cluster once obtained should be in effect matrix isolated because of the tethering. This, however, turned out not to be the case as the oxide itself acted as a weakly co-ordinating ligand. Evidence for this comes from the i.r. spectra (see Figure 3.13) which do not resemble the capped species (13) but rather the cluster with a phosphine on the unique osmium (11). The similarity is so good that it seems a reasonable guess that the oxide acts as a ligand in the equatorial position on the unique osmium, i.e.

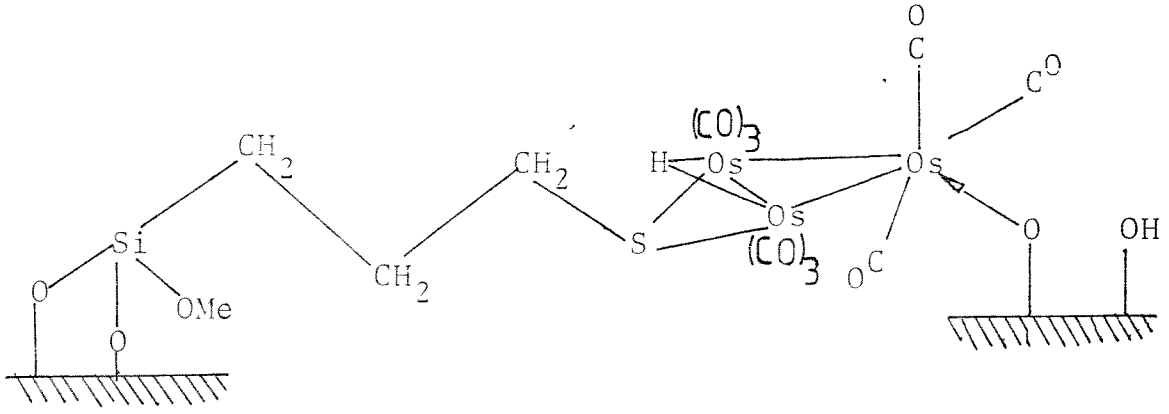

A close analogue to this compound has been reported[33] : $[Os_3(CO)_9(H)(NEt_3)(SMe)]$. The amine ligand in common with the oxide ligand should only be a σ donor. It displays νCO bands at 2 081(m), 2 050(s), 2 023(s), 1 993(ms), 1 977(m), 1 957(sh), 1 954(w), and 1 941(w) cm^{-1} which are in partial agreement with those seen for the oxide species. Attempts at producing a solution analogue for the oxide species with

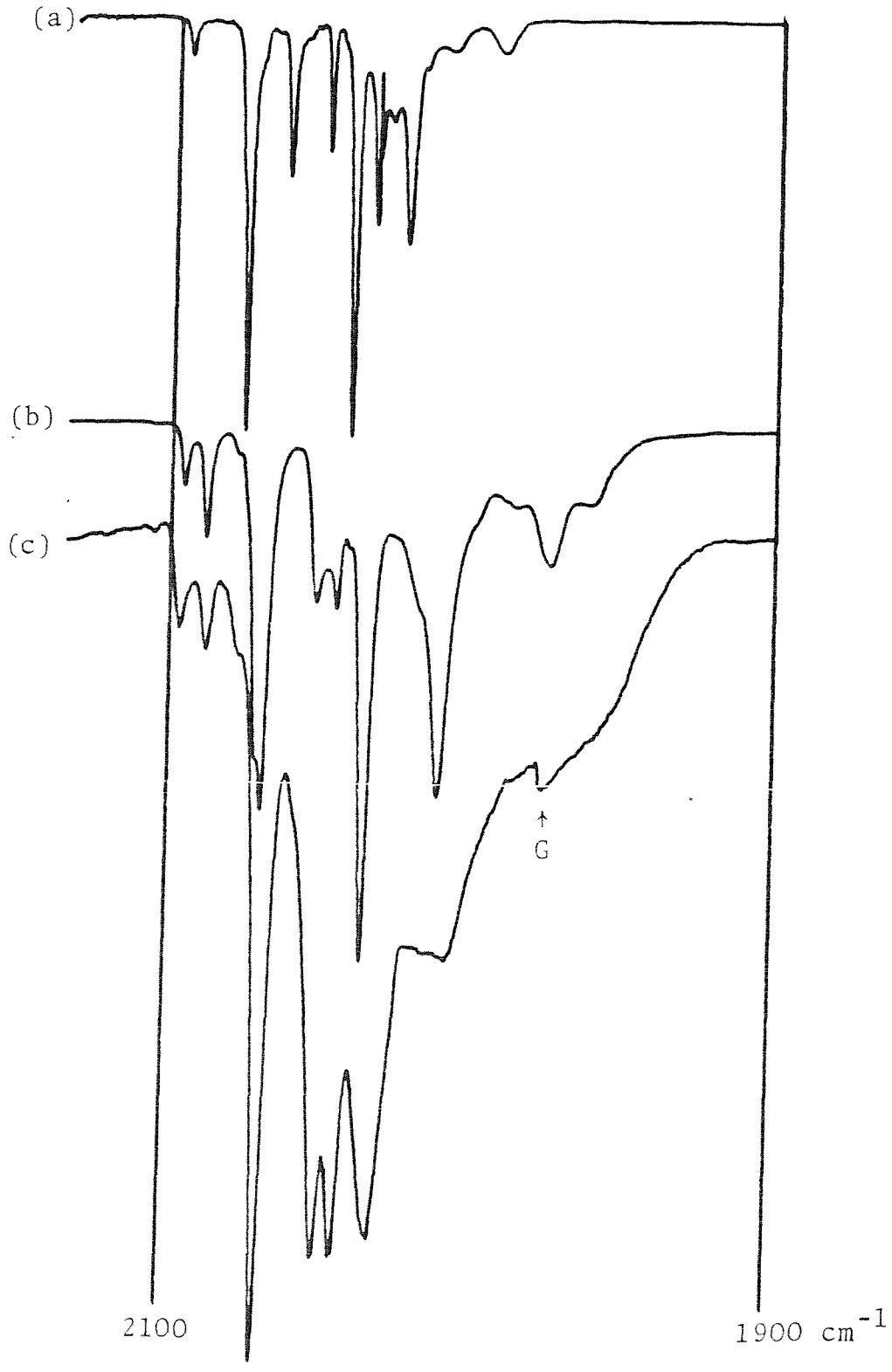

Figure 3.13. I.r. spectra of (a) the sulphur capped cluster (13) in cyclohexane, (b) the phosphine substituted cluster (11), and (c) a Nujol mull of the oxide substituted cluster on aerosil 380 with the silica background partially subtracted out. G = Grating change.

Ph_3SiOH and Me_3SiOH were unsuccessful because of its inherent instability.

Interestingly, the capped cluster has been reported[33] to react rapidly at room temperature with thiolate ligands to give $|Os_2(CO)_6(SR)_2|$. So if any thiolate ligands were still present on the surface a reaction would be expected. As no reaction is seen it must be concluded that either the Me_3NO treatment has oxidised all the free thiolate ligands or the free thiolate ligands are not close enough to react. This last possibility is unlikely since surfaces with similar loadings of phosphine ligands often display polysubstitution of anchored clusters. The oxide ligand was shown to be weakly bound by the facile regeneration of the CH_3CN and ethylene derivatives when these ligands were added.

As with the homogeneous case the acetonitrile, "oxide" and π bound ethylene supported clusters react with hydrogen to produce an intermediate before forming $|H_2Os_3(CO)_9S|$ (see Figure 3.14). The impurity band at 2 094 cm^{-1} is evident in all the spectra regardless of their origin, but there is no further evidence as to what it is due to, except that it cannot be caused by the "oxide" species as it is too intense for no other bands of this species to be seen. This stripping of the cluster by hydrogen provides firm evidence for the existence of these supported sulphur clusters.

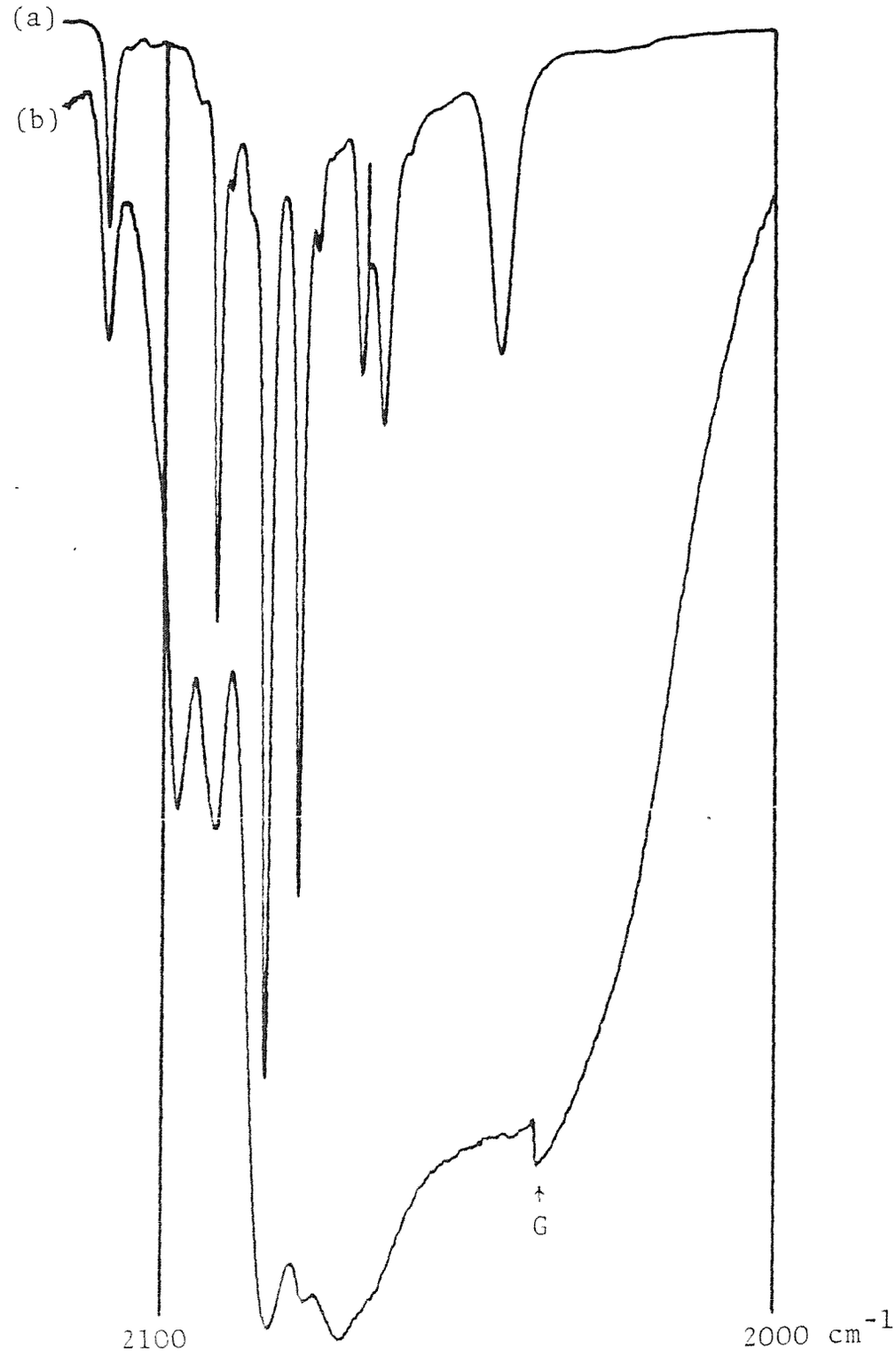

Figure 3.14. I.r. spectra of (a) the hydrogenation intermediate obtained from the C_2H_4 derivative (7) in n-hexane, and (b) the heterogeneous hydrogenation intermediate obtained from the supported CH_3CN derivative on $SiMe_3Cl$ pretreated thiolated alumina (Nujol mull). G = Grating change.

(C) The catalytic behaviour of the homogeneous and heterogeneous thiolate cluster systems.

The parent clusters $|Os_3(CO)_{10}(H)(SR)|$ (R = Pr^n (4) and $(CH_2)_3Si(OMe)_3$ (2)) were found only to display olefin isomerisation activity under forcing conditions which caused cluster breakdown. So the nature of the active catalyst under these circumstances is uncertain and could be either the cluster or its breakdown products. This was not unexpected as these clusters demonstrate a similar stability towards reactions involving Os — CO bond cleavage, as $|Os_3(CO)_{12}|$. For example, to cause substitution of both $|Os_3(CO)_{12}|$ and (4) with PPh_2Me requires temperatures of 110 ^oC[42] and 80 ^oC[35], respectively.

This inactivity of the decacarbonyl clusters towards olefins provided the impetus to produce the nonacarbonyl clusters with weakly co-ordinating ligands. These can be readily lost to give the capped cluster (13), whose incipient unsaturation should make it a suitable candidate for a catalyst. Unfortunately, (13) proved to be too unstable for purification and catalytic testing. Instead the acetonitrile ((8) and (9)) and ethylene (7) derivatives were used. They both proved to be olefin isomerisation catalysts and caused both double bond migration and cis-trans isomerisation. Under identical conditions the acetonitrile derivative proved to be about twice as active as the ethylene. As both these clusters react by losing the weakly co-ordinating ligand to produce the capped cluster which then reacts rapidly with the

incoming ligand (see diagram 3.4) and since the concentrations of the pentene, cluster and therefore the amount of X is constant, in both the C_2H_4 and CH_3CN derivative catalysis runs, the differences in catalytic acticity between them must be caused by different dissociation constants for the cluster X bonds. Incidentally, significant catalysis by the decomposition products of these clusters was ruled out by extended catalysis experiments, during which the catalytic activity decreased as the cluster decomposed.

The rate determining step for the reaction of $|Os_3(CO)_9(X)(H)SPr^n|$ adducts with ligands is the dissociation step rather than the association one. For example, the capped species (13) reacts instantaneously with PPh_3, whereas the CH_3CN or C_2H_4 derivatives take about 30 minutes at r.t.. This dissociation step is many times more rapid than the observed rate of catalysis. So the rate of formation of the pentene adduct is greater than the rate of catalysis. Control experiments carried out to identify the pentenes attached to the clusters after catalysis runs showed that the pentene adduct was formed rapidly from the capped cluster and had the same general structure as the ethylene adduct (i.r. spectra were almost identical). However, the ^1H n.m.r. spectra proved to be too complex for easy assignment of which pentene was co-ordinated. These pentene derivatives were found to be less stable than the ethylene derivatives (towards dissociation). This is as expected as the pentene is larger sterically than ethylene and the +I alkyl groups should also

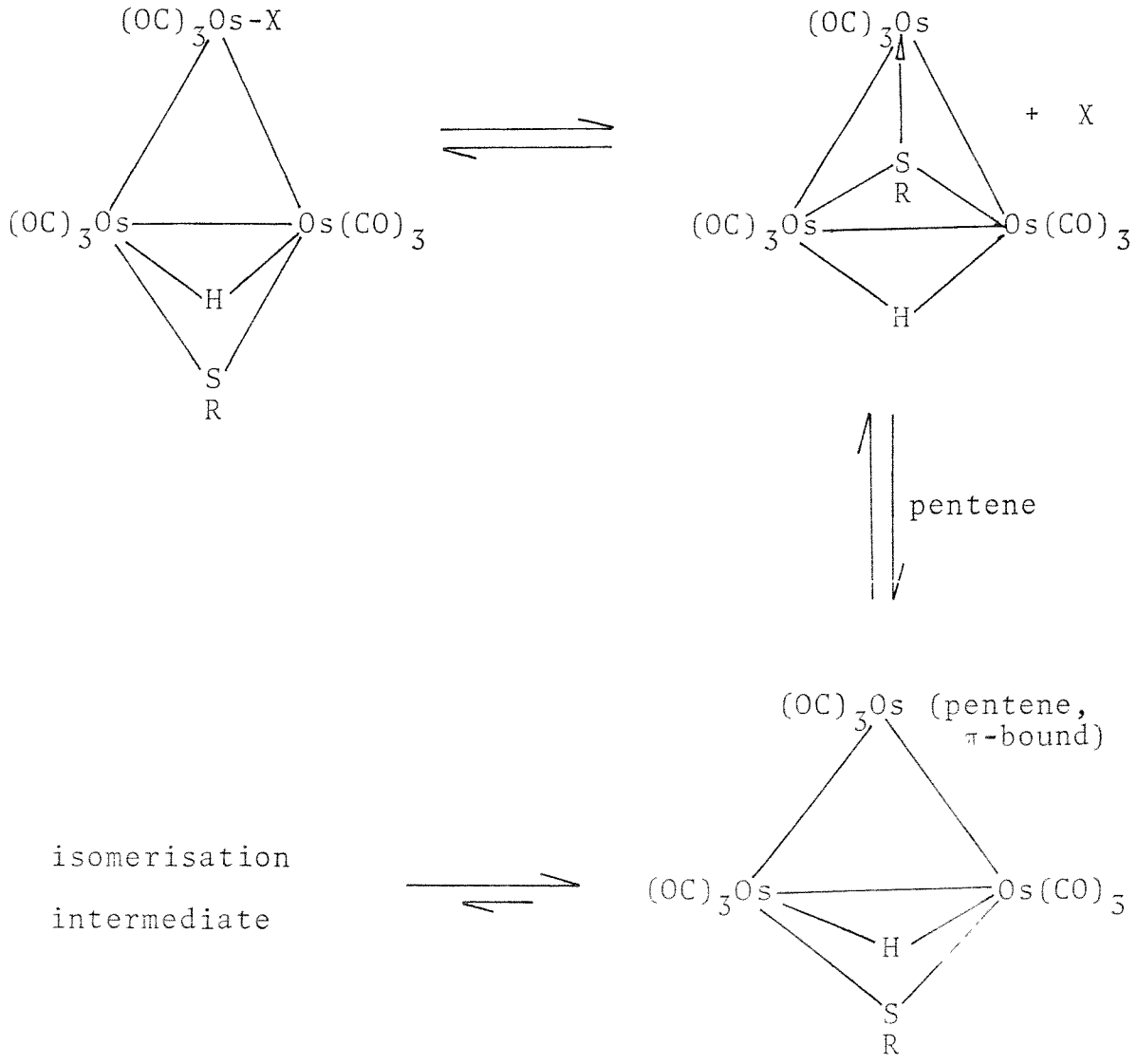
(OC)3Os-X
(OC)3Os
Os(CO)3
H
S
R
+ X
pentene
isomerisation
intermediate
(OC)3Os (pentene,
π-bound)

Diagram 3.4.

make it a poorer π acceptor. This facile reaction and dissociation of the pentene from the capped cluster is important since it indicates that the rate of isomerisation is slower than the rate of formation of the pentene species. That is,the olefin is not isomerised every time it is co-ordinated.

This indicates that the isomerisation probably occurs via an intermediate formed from the π-bound olefin. Two possible intermediates are a π-bound allyl species and a protonated olefin (see diagram 3.5). The formation of the π-bound allyl species requires the cluster to act as a base and a similar reaction occurs when the capped cluster is treated with hydrogen chloride.[33] The formation of the protonated olefin intermediate requires the cluster to act as an acid. Some evidence for this possibility[43] is provided by dissociation of the analogous compound $|Fe_3(CO)_9(H)(SR)|$ to give $|Fe_3(CO)_9(SR)|^-$ (pKs = 3-4).

An interesting feature of the isomerisation of 1-pentene by the CH_3CN and C_2H_4 derivatives is the occurrence of cis-2-pentene in above thermodynamic proportions, in the product mixture. The cause of this imbalance may be a sterically demanding intermediate in the isomerisation reaction. Some evidence for the importance of the dissociation to produce the capped species is seen in the negligible activity of the acetylene (12) and PPh_3 (11) derivatives towards pentene isomerisation.

An alternative way to visualise these catalysts is to

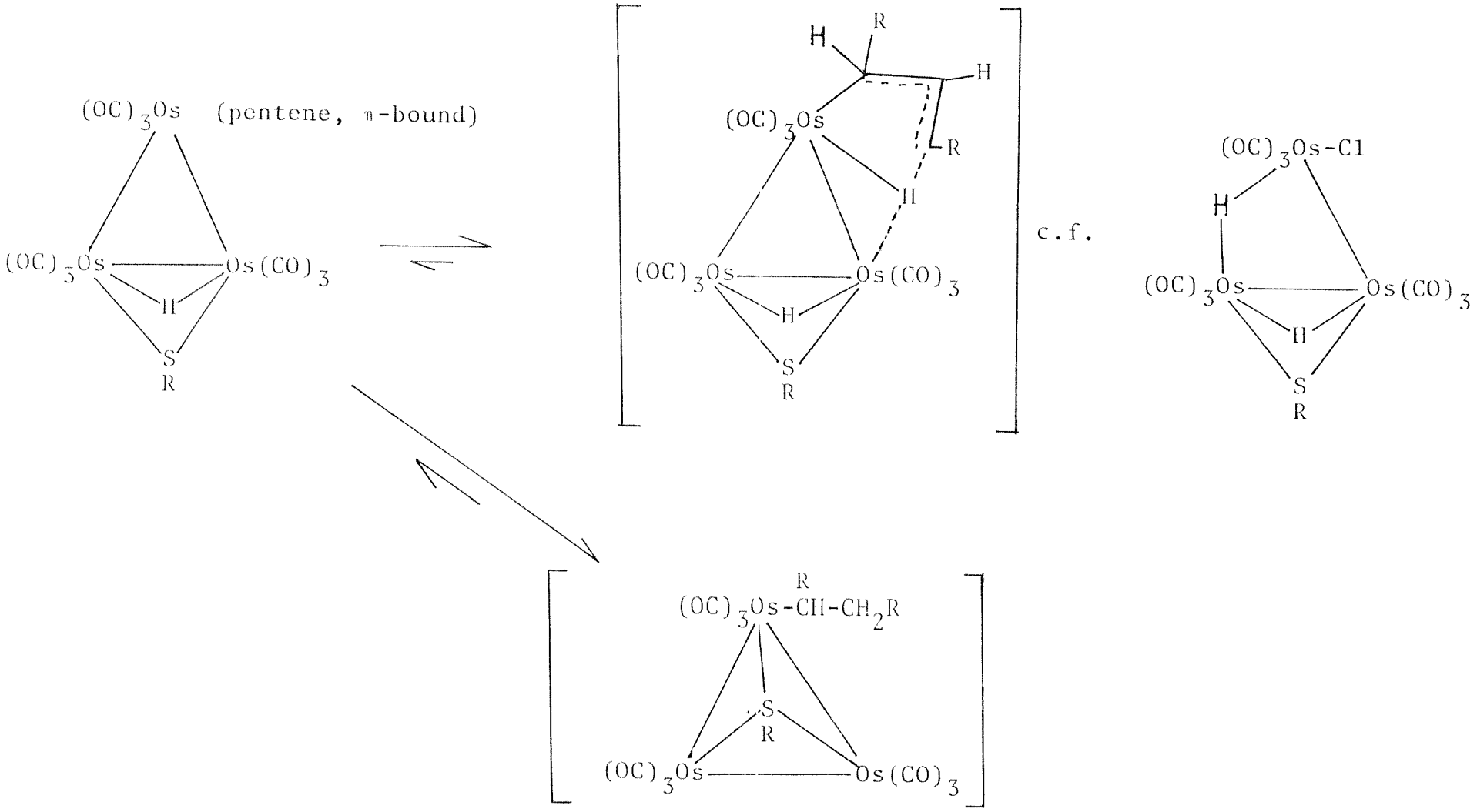
(OC)3Os (pentene, π-bound)
(OC)3Os
Os(CO)3
H
S
R
R
H
H
R
H
c.f.
(OC)3Os-Cl
H
R
(OC)3Os-CH-CH2R
S
R

Diagram 3.5.

consider the heterogeneous approach. That is, to assume that there are two ligands competing for a single type of site on a metal particle. One ligand being X, the ligand in $|Os_3(CO)_9(H)(SR)X|$ and the other the pentene. Obviously the fractional coverage of the pentene and hence the catalytic activity depends on the other ligands strength of adsorption and concentration. So the approximate strength of the catalyst poisons X are PPh_3, C_2H_2, CO > C_2H_4 > CH_3CN.

Although homogeneously $|Os_3(CO)_{10}(H)(SR)|$ ((4) and (2)) showed no catalytic activity for pentene isomerisation up to 80 °C, the heterogeneous analogue (prepared by reacting $|Os_3(CO)_{12}|$ with thiolated oxide) did. It is interesting to note that its catalytic activity is oxide dependent (TiO_2 > MgO > SiO_2 > ZnO > γ-Al_2O_3) which suggests that there is oxide participation in the catalytic species. To check this, the catalysis experiments were repeated as closely as possible using $SiMe_3Cl$ pretreated thiolated oxides. In all cases there was a general reduction in the catalytic activity of the samples which confirms the oxide participation. At this point there seemed to be 3 distinct possibilities for the active catalyst. That is by: oxide activation of the intact sulphur cluster (e.g. by protonation, deprotonation or polarisation); oxide induced breakdown products of the sulphur cluster; or products from the direct interaction of $|Os_3(CO)_{12}|$ with the oxide.

The first possibility was ruled out by repeating the catalysis experiments with samples prepared by reacting (2)

($|Os_3(CO)_{10}(H)\{S(CH_2)_3\}Si(OMe)_3|$) with oxides, under mild conditions (see Chapter 2) during which production of products of the second type (decomposition of the sulphur cluster by the oxide) should be minimised and of the last sort eliminated (by interaction of $|Os_3(CO)_{12}|$ with oxides). In this case no activity was seen for any of the oxide samples.

In order to determine which of the two remaining possibilities were responsible, a series of control experiments were carried out with samples prepared by reacting the oxide with $|Os_3(CO)_{12}|$ under identical conditions to those used in the anchoring reaction for thiolated oxides. These oxides displayed in most cases i.r. spectra indicative of an oxide bridged species together with mono-nuclear species (see Chapter 2). The exception to this being silica which displayed the i.r. spectrum solely of $|Os_3(CO)_{10}(H)(O\text{-}SiO_2)|$ with no impurity peaks. Again oxide dependent catalytic activity was observed. However, interpretation of these results is hindered by the co-existence of several species whose distribution varies during the catalytic run (e.g. the bridged species decomposed to give "mononuclear" species). An important point that can be made is that the activity of these species is too low for them to be responsible for the isomerisation activity observed for the thermally anchored cluster ($|Os_3(CO)_{12}|$ + thiolated oxide) because in the latter cases their levels are too low to be detected by i.r. spectroscopy.

To see if the trinuclear oxide bridged species (e.g.

$|Os_3(CO)_{10}(H)(O\text{-}M'O_n)|$) or "mononuclear" species are responsible for the low levels of activity observed on these oxides, a catalysis run was carried out on a sample of the oxide bridged species (i.e. $|Os_3(CO)_{10}(H)(O_{SiO_2})|$) pyrolysed to give a peak pattern indicative of "mononuclear" species. This pyrolysed sample showed no catalytic activity and hence indicates that the active catalyst in these systems (e.g. $|Os_3(CO)_{12}|/M'O_n$) could be the oxide bridged species. Though the existence of a minor active species, not seen in the i.r., which was also destroyed in the pyrolysis cannot be ruled out.

In the case of the anchored osmium thiolate clusters (produced by reacting $|Os_3(CO)_{12}|$ with functionalised oxides) the remaining possibility for the catalyst is that it is a product from the reaction of the thiolate cluster with either the oxide or excess sulphur ligands. To test this a sample of $|Os_3(CO)_{10}(H)\{S(CH_2)_3Si(OMe)_{3-x}(O_{SiO_2})_x\}|$ was pyrolysed (160 °C, 3 days) in vacuo until it gave a spectrum indicative of only mononuclear species. This sample exhibited a very low level of olefin isomerisation activity.

To conclude, these results indicate that the active catalyst or catalysts in the thermally anchored thiolate osmium clusters are not the intact clusters or the products from the interaction of $|Os_3(CO)_{12}|$ with oxides but rather intermediates in the breakdown of the anchored sulphur clusters (and not the final species observed in pyrolysis). A possible such species, $|Os_3(CO)_9(H)(oxide)\{S(CH_2)_3Si(OMe)_{3-x}(O\text{-}M'O_n)_x\}|$, can be made by pumping on the supported acetonitrile and ethylene derivatives.

The catalytic activity of the supported acetonitrile derivative (on $SiMe_3Cl$ pretreated thiolated oxides) was found to be of the same order as the homogeneous case but the activity was found to vary with the oxide (e.g. TiO_2 > SiO_2 > γ-Al_2O_3). This is probably caused by oxide involvement in a species like that proposed for the capped cluster with an oxide ligand. Indeed in the recovered samples the i.r. spectra showed bands symptomatic with the presence of both the acetonitrile and oxide species. However, the situation is not straightforward, as cluster decomposition is also evident, particularly on the samples which show the highest activity (e.g. TiO_2).

Homogeneously, the ruthenium decacarbonyl cluster, $|Ru_3(CO)_{10}(H)(SPr^n)|$ (3), at 47 °C, catalyses both cis-trans and olefin migration isomerisation and is recovered unchanged. At 80 °C it is three times as active but it is not recovered. A possible candidate for the active catalyst is $|Ru_3(CO)_9(H)(SPr^n)|$ (13) (which has the same structure as the osmium analogue). This ruthenium nonacarbonyl cluster was observed as one of the products from the 80 °C catalysis runs but it may not be the sole catalyst at this temperature as there is a plethora of other unstable products formed. The reason why (13) is not observed in the 47 °C catalysis runs is probably that under these conditions (3) can dissociate reversibly without side products (produced at higher temperatures) scavenging the liberated carbon monoxide.

In the heterogeneous cases (samples prepared by reacting

$|Ru_3(CO)_{12}|$ with $SiMe_3Cl$ pretreated thiolated oxides) some cluster decomposition was evident (by i.r.) in the 47 °C catalysis runs. The heterogeneous catalysts proved to be about six times as active as the homogeneous analogue (3). This is an example of oxide promoted catalysis. When a control run was carried out on a sample prepared by reacting $|Ru_3(CO)_{12}|$ with plain oxide, little or no activity was observed for pentene isomerisation though its i.r. spectrum did change. This indicates that it is either the supported ruthenium cluster or its breakdown products which provide the active catalysts.

When comparing the activity of the supported catalysts to their homogeneous analogues care must be taken for numerous reasons apart from the uncertainty in the species present. Some of these are;

(i) The concentrations of the supported catalysts are different from their homogeneous analogues. For example, the homogeneous analogues should be ideally randomly distributed throughout the reaction solution whereas the heterogeneous analogues will be concentrated on oxide particles.

(ii) The surfaces may have a concentrating effect on the substrate. For example, the pentene may be adsorbed on the oxide in preference to the solvent. This is probably best avoided by using polar solvents like methanol and methylene chloride.

(iii) Homogeneously the rate constant for a reaction is given by the Arrhenius equation $R = A_{exp}^{(-E/RT)}$. The "A" term can be divided into a term for the collision rate and a steric term which is important when the relative orientations of the substrate and catalyst are crucial. Obviously the surface environment will effect both these terms. For example, in the homogeneous case the catalyst will have collisions with the substrate molecules from all directions, whereas in the heterogeneous case the collisions with the substrate will be more likely to come from the direction away from the surface (if the pentene is not physisorbed by the oxide). The oxide/solvent interface could also cause a preferred orientation to be taken up by the cluster and substrate (in much the same manner as detergent molecules in an oil/water mixture) and this will affect the steric term.

(iv) An alternative way of considering catalysis is by transition state theory. This gives rise to a new form of the Arrhenius equation (see below) where $\neq$ denotes the activated complex.

$$R = \frac{KT}{h} \exp^{(\Delta S^{\neq}/R)} \exp^{(-\Delta H^{\neq}/RT)}$$

On going from a homogeneous to a heterogeneous system the entropy term will become less because the transition state is immobilised on the catalyst/oxide with the consequential loss of translational freedom.

When tested for olefin hydrogenation activity (80 ^{o}C, 40 bar H_2, 24 h, 1-pentene 25 equivalents w.r.t. the cluster), the clusters with strongly co-ordinated ligands ($|Os_3(CO)_9(H)(X)(SPr^n)|$, (X = CO (4), PPh_3 (11) and C_2H_2 (12)) were recovered unchanged and showed negligible activity. Unfortunately, it was found that the species with weakly co-ordinating ligands (X = CH_3CN (8) + (9), C_2H_4 (7)) which should be active reacted with hydrogen rapidly to produce $|H_2Os_3(CO)_9S|$ and so rendering them useless for heterogeneous hydrogenation catalysts.

Conclusion.

The compounds $|Os_3(CO)_9(H)(SPr^n)(X)|$ (where X = CO (4); CH_3CN (8), (9) and (10); PPh_3 (11) and (14); C_2H_4 (7) and C_2H_2 (12)) have been prepared and characterised. Carbon-13 n.m.r. proved to be a powerful technique in the elucidation of their structures. This technique confirmed that the solution structures for (4) and (7) are the same as reported for analogous compounds in the solid state. In order to explain the ^{1}H n.m.r. spectrum of (7) (in the light of the ^{13}C n.m.r. results) an unusual mode of rotation (i.e. about the C-C bond axis) had to be proposed to occur simultaneously with the more conventional rotation about the M-π bond.

The CH_3CN adducts proved to be isomeric in their position of substitution and (8) was shown to differ from (9) only in the position of substitution on the unique osmium atom. That is, (8) occupies an axial position and (9) occupies an

equatorial one. In (10) the CH_3CN is thought to occur on one of the bridged osmium atoms but due to the poor quality of the ^{13}C n.m.r. spectra its position on the osmium atom could not be detected.

The positions of the CH_3CN on the osmium triangle were confirmed by PPh_3 substitution. Substitution of (10) with PPh_3 gave (14) whereas (8) and (9) gave (11) ((7) gave (11) also). (14) displays a phosphine coupling to the bridging hydride unlike (11) which does not. This indicates that in (14) the phosphine occurs on one of the bridged osmium atoms, and the magnitude of $^2J_{PH}$ indicates that it is in a cis position relative to the bridging hydride. However, the ^{13}C n.m.r. spectra of (14) only shows the existence of one trans carbonyl to the hydride and in order to explain this a partial rotation of the $|Os(CO)_2PPh_3|$ unit is proposed. Presumably caused by steric conjestion about the osmium and this is thought also to be responsible for the two isomers observed in the low temperature ^1H n.m.r. spectrum. Steric effects are also seen in (11) whose spectra show that at low temperatures the rotations of the phosphine stop. Carbon-13 n.m.r. and ^1H n.m.r. spectra of (11) confirm the position of the phosphine on the equatorial site on the unique osmium atom.

The compound (12) is thought to contain a π-bound acetylene by comparison with the ^1H n.m.r. spectra of literature compounds. Variable ^{13}C n.m.r. spectra of (12) show the acetylene occupies the equatorial site on the unique osmium atom, though there is slight evidence for the

co-existence of another structural isomer presumably occupying an axial site on the unique osmium. Two fluxional processes were identified, a lower energy M-π bond axis rotation of the acetylene and a higher energy $|M(CO)_2(C_2H_2)|$ unit rotation.

All these species were produced in heterogeneous form by using the Me_3NO/CH_3CN entry developed in this work despite problems with the Me_3NO reacting with the free thiol groups and the oxide. The heterogeneous species were identified by comparative i.r. and this was further confirmed by their reactivity. However, when the synthesis of the capped species was attempted heterogeneously a loosely co-ordinated oxide adduct was obtained (similar in structure to (11)) which had a similar reactivity to the other loosely co-ordinated adducts (e.g. C_2H_4 (7)). The hydrogenation of these loosely co-ordinated adducts both homo- and heterogeneously gave first an unstable intermediate which then converted to $|H_2Os_3(CO)_9S|$. The isolation of this from the heterogeneous samples provides firm proof of the existence of the thiolated osmium clusters on the surface.

Pentene isomerisation activity was tested for. Homogeneously this activity was found under moderate conditions to occur only for compounds which had a loosely co-ordinated ligand and so could generate $|M_3(CO)_9(H)(SPr^n)|$. For example, $|Os_3(CO)_9(H)(SPr^n)(x)|$ where X = CO (4), PPh_3 (11), and C_2H_2 (12), are inactive, whereas C = C_2H_4 (7) and CH_3CN ((8) + (9)) are. The cluster $|Ru_3(CO)_{10}(SPr^n)(H)|$ is also active due to its ready CO loss. Heterogeneously the situation proved to

be more complex with both species, $|M_3(CO)_{10}(H)\{S(CH_2)_3$-$Si(OMe)_{3-x}(O\text{-}M'O_n)_x\}|$ (M = Ru and Os, produced by $M_3(CO)_{12}$ + thiolated oxide), being more active than their homogeneous counterparts. In the case of M=Os this was shown to be due to breakdown products of the sulphur cluster produced during the anchoring reaction. Heterogeneously the osmium CH_3CN adduct proved to be as active as its homogeneous counterpart but due to the inherent complexities of heterogeneous catalysis little could be said about the variation in activity observed on varying the oxide.

Experimental

Reaction of $|Os_3(H)(CO)_{10}SPr|$ (4) with Me_3NO.

A solution of Me_3NO (resublimed, 4 mg/cm^3, in dry methanol) was added dropwise to (4) (25 mg) dissolved in cyclohexane (pure). The reaction was monitored by i.r. spectroscopy. When the peaks due to (4) (particularly those at 2 108 and 2 065 cm^{-1}) had almost disappeared, the addition was stopped and the solvent removed under reduced pressure. The yellow-brown solid was then separated by t.l.c. (eluted, CH_2Cl_2:hexane, 15:85). This gave principally residual (4) and two other products. The major of which was $|Os_3(H)(CO)_9SPr|$ (13) (identified by its i.r. spectrum, yield < 1 %).

Reaction of (4) with Me_3NO and ethene

The reaction was repeated as in the previous experiment except that the nitrogen was replaced by ethene. T.l.c. this time afforded $|Os_3(H)(CO)_9SPr(C_2H_4)|$ (7) as the major product in 15 % yield, together with the other bands previously mentioned. In order to increase the yield the reaction was repeated in an autoclave charged with C_2H_4 (50 bar) and a stoichiometric amount of Me_3NO. This served to increase the yield of (7) (25 %) but did not remove the side products.

Reaction of (4) with Me_3NO and acetonitrile.

This turned out to be the best entry into the nona-carbonyl compounds. Trimethylamine oxide in CH_3CN (1 mg/cm^3) was added dropwise to a solution of (4) (100 mg) in aceto-nitrile (50 cm^3) until the i.r. spectrum of (4) had dis-appeared. T.l.c. (40 - 60 petroleum ether:CH_3CN:CH_2Cl_2, 70:1:29) gave three main yellow bands, (8) and (9) (> 60 %. R.f. 0.8 and 0.75, respectively), and (10) (< 15 %, R.f. 0.4) assignable to different isomers of $|Os_3(H)(CO)_9(SPr^n)(CH_3CN)|$. It was found subsequently that the yield of the minor isomer could be markedly reduced by repeating the reaction at 0 °C rather than at r.t.

I.r./cyclohexane:

(8) 2 079(w), 2 050(vs), 2 032(vs), 2 010(vs), 1 989(vs), 1 980(vs), 1 971(s), 1 959(m), and 1 934(w) cm^{-1}.

(9) 2 082(w), 2 051(vs), 2 030(vs), 2 010(w), 1 997(m), 1 980(vs), and 1 960(w) cm^{-1}.

(10) 2 098(s), 2 054(vs), 2 016(vs), 2 005(s), 1 991(m), 1 981(s), 1 973(s), 1 958(w), and 1 950(s) cm^{-1}.

^1H n.m.r./$CDCl_3$, 0 °C: δ (p.p.m.).

(8) 2.58 (s, 3 H, $\underline{CH_3}CN$), 2.46 (t, 2 H, S-$\underline{CH_2}$-), 1.62 (m, 2 H, $SCH_2\underline{CH_2}$), 1.0 (t, 3 H, S-$CH_2CH_2\underline{CH_3}$) and -16.6 (s, 1 H, Os-H-Os).

(9) 2.57 (s, 3 H, $\underline{CH_3}CN$), 2.46 (t, 2 H, S-$\underline{CH_2}$-), 1.62 (m, 2 H, $SCH_2\underline{CH_2}$-), 1.0 (t, 3 H, S-$CH_2CH_2\underline{CH_3}$) and -16.4 (s, 1 H, Os-H-Os).

(10) 2.58 (s, 3 H, $\underline{CH_3}CN$), 2.46 (t, 2 H, S-$\underline{CH_2}$), 1.62 (m, 2 H, S-$CH_2\underline{CH_2}$), 1.0 (t, 3 H, $SCH_2CH_2\underline{CH_3}$) and -15.81 (s, 1 H, Os-H-Os).

Mass spectrum: All three showed a weak parent (945 a.m.u. ^{192}Os), followed by a strong peak (904 a.m.u.) assignable to $|Os_3(H)(CO)_9SPr^n|^+$. After this their fragmentation patterns were too complex for accurate assignment except a series of peaks which could be discerned corresponding to nine stepwise carbonyl losses.

Preparation of $|Os_3(H)(CO)_9SPr^n(C_2H_4)|$ (7)

$|Os(H)(CO)_9SPr^n(CH_3CN)|$ (8) + (9) (40 mgs) in 1,2-dichloromethane (30 cm^3) was heated (40 ^oC) in an autoclave pressurised with ethene (50 bar) and stirred overnight. The solvent was removed from the lemon yellow solution by a rapid stream of ethylene to yield a slightly heat sensitive lemon yellow solid (> 99 % yield).

I.r./pentane: 2 093(w), 2 062(s), 2 041(m), 2 026(w), 2 011(s), 2 001(m), 1 993(m), 1 982(w), 1 969(w), and 1 938(w) cm^{-1}.

^1H n.m.r./$CDCl_3$, 30 - 0 ^oC; $CD_2Cl_2/CFCl_2H$, 0—-114 ^oC: δ (p.p.m.) all the signals remained unchanged over the temperature ranges. 2.5 (s, 4 H, C_2H_4), 2.44 (t, 2 H, S-$\underline{CH_2}$-), 1.64 (m, 2 H, S-$CH_2\underline{CH_2}$-), 1.1 (t, 3 H, $SCH_2CH_2\underline{CH_3}$) and -17.04 (s, 1 H, Os-H-Os).

Mass spectrum: This exhibited a very weak parent (952 a.m.u., ^{192}Os) followed by a relatively strong band (904 a.m.u., ^{192}Os, $|Os_3(H)(CO)_9SPr^n|^+$) and bands caused by successive carbonyl losses and fragmentation of the alkyl group.

Preparation of $|Os_3(H)(CO)_9SPr^n(C_2H_2)|$ (12).

(7) or (8) + (9) was heated under C_2H_2 in refluxing cyclohexane until its i.r. spectrum had disappeared (45 - 60 minutes). Work up by t.l.c. (40 - 60 petroleum ether: Et_2O, 5:1) gave two main products. A major pale yellow band due to (12) (70 %, R.f. 0.8) and a more intense yellow band (20 %, R.f. 0.5, (15)).

I.r./hexane:

(12) 2 111(vw), 2 101(w), 2 086(w), 2 077(vs), 2 061(w), 2 052(vs), 2 048(sh), 2 024(m), 2 018(sh), 2 013(vs), 2 000(w), 1 994(m), 1 986(m), 1 975(m), 1 959(m), and 1 939(vw) cm^{-1}.

(15) 2 083(s), 2 076(vw), 2 068(vw), 2 060(vw), 2 050(vs), 2 020(vs), 2 000(w), 1 985(m), 1 977(m), and 1 960(s) cm^{-1}.

^1H n.m.r./$CDCl_3$, 31——-60 °C: δ (p.p.m.)

(12) (see Figure 3.1). At 31 °C, 10.14 (s, 2 H, H-C≡C-H), 2.25 (t, 2 H, S-$\underline{CH_2}$), 1.3 (m, 2 H, S-$CH_2\underline{CH_2}$), 0.9 (t, 3 H, $SCH_2CH_2\underline{CH_3}$), and -17.83 (s, 1 H, Os-H-Os).

Only the acetylenic peak changed on varying the temperature, i.e. 10 °C, broadened singlet; 0 °C, coalescence; -10 °C, two broad signals; -20 °C, distorted pair of broad doublets; -40 °C, a sharp pair of distorted doublets with peaks at 10.47, 10.38, 9.93, 9.84, together with a sharp weak band at 10.30.

(15) The n.m.r. spectrum of this compound varies with temperature and is very complex. However, it can be discerned

that the propyl group is still present (signals at 2.4, 2.0, and 1.0 δ), the hydride is absent and that the compound exists as several interconverting isomers. This last fact was deduced from the plethora of free and co-ordinated olefinic signals which varied in a complex manner with temperature.

Mass spectrum.

(12) gave a parent at 930 a.m.u. (^{192}Os) followed by a complex pattern which showed 9 successive carbon monoxide losses.

(15) gave a parent at 951.9 a.m.u. corresponding to a plausible formula of $|Os_3(CO)_9SPr^n(C_4H_{5-6})|$. Further weight is added to this by the fragmentation pattern which shows nine successive losses of 28 a.m.u.

Preparation of $|Os_3(H)(CO)_9(SPr^n)(PPh_3)|$ (11).

A solution of PPh_3 was added dropwise to a CH_2Cl_2 solution of (7) or ((8) + (9)), until the i.r. spectra of the starting materials had disappeared. T.l.c. (40 - 60 petroleum ether:CH_2Cl_2; 70:30) gave one major bright yellow band (R.f. 0.75, 75 %).

I.r./cyclohexane: (11) 2 094(w), 2 083(m), 2 056(sh), 2 052(vs), 2 028(s), 2 018(s), 2 003(vs), 1 987(sh), 1 984(vs), 1 965(w), 1 956(m), and 1 945(w) cm^{-1}.

^1H n.m.r./$CDCl_3$, 31 °C: δ (p.p.m.) 7.4 (m, 15 H, Ph), 2.3 (t, 2 H, S-$\underline{CH_2}$), 1.6 (m, 2 H, S-$CH_2\underline{CH_2}$), 1.0 (t, 3 H, $SCH_2CH_2\underline{CH_3}$) and -16.93 (s, 1 H, Os-H-Os).

Mass spectrum. This gave a parent (1166 a.m.u., ^{192}Os) followed by a complex fragmentation pattern.

Analysis calculated C, 31.6 %; H, 2.9 %.

found C, 30.9 %; H, 2.0 %.

Preparation of $|Os_3(H)(CO)_9(SPr^n)(PPh_3)|$ (14).

PPh_3 (1.1 equivalents) was added to a CH_2Cl_2 solution of (10) and stirred overnight. T.l.c. (hexane:CH_2Cl_2, 70:30) gave one broad yellow band (14) (30 %, R.f. 0.5). I.r./hexane: 2 077(w), 2 067(m), 2 051(w), 2 026(vs), 2 018(vw), 2 003(s), 1 997(s), 1 989(s), 1 982(s), 1 969(s), and 1 958(s) cm^{-1}.

^1H n.m.r./$CDCl_3$, 31- -60 °C: δ (p.p.m.) 31 °C, 7.4 (m, 15 H, Ph), 2.4 (t, 2 H, $S\underline{CH_2}$-), 1.7 (m, 2 H, S-$CH_2\underline{CH_2}$-), 1.0 (t, 3 H, $SCH_2CH_2\underline{CH_3}$) and -16.45 (d, 1 H, Os-H-Os, $^2J_{PH}$ = 7 Hz). Only the hydride signal varies with temperature. At -20 °C the low temperature limiting spectrum is obtained, i.e. -15.5 (d, 1 H, Os-H-Os, $^2J_{PH}$ = 6 Hz, isomer 1), and -16.7 (d, 1 H, Os-H-Os, $^2J_{PH}$ = 6 Hz, isomer 2). The relative intensities were isomer 1:isomer 2 = 3:1.

Attempted preparation of $|Os_3(H)(CO)_9SPr^n|$ (13)

The i.r. spectrum was monitored of a refluxing cyclohexane solution of (7) or ((8) + (9)). As the solution darkened the i.r. of (13) was observed. Attempted purification of (13) by t.l.c. and crystallisation was unsuccessful due to decomposition. A ^1H n.m.r. spectrum was obtained by heating a sample of (7) in situ.

I.r./cyclohexane: 2 095(w), 2 065(vs), 2 045(m), 2 025(m), 2 013(vs), 2 002(s), 1 993(m), 1 983(s), and 1 970(w) cm^{-1}. ^1H n.m.r./$CDCl_3$, 40 °C: δ (p.p.m.) most of the alkyl signals were swamped by residual (7) and the side products (mostly (4)) but a triplet was observable at 3.15 (t, 2 H, S-$\underline{CH_2}$) and a new hydride signal at -20.92 (s, 1 H, Os-H-Os).

Preparation of $|Os_3(H)_2(CO)_9S|$

This was prepared according to the literature[2] to give a pale yellow powder.
I.r./n-octane: 2 118(m), 2 085(vs), 2 058(vs), 2 036(vs), 2 012(vs), 1 997(s), 1 991(w), and 1 984(m) cm^{-1}.
^1H n.m.r./$CDCl_3$: δ (p.p.m.) -20.9 (s, 2 H, Os-H-Os).
Mass spectrum. A parent was seen (862 a.m.u., ^{192}Os) followed by nine strong peaks due to successive carbon monoxide losses.

Reaction of $|Os_3(H)(CO)_9SPr^n(CH_3CN((8)$ or $(9))$ or $C_2H_4(7))|$ with H_2.

A dilute solution (3 mg/cm^3) of (7) or ((8) + (9)) in hexane was put into a glass liner of a 100 cm^3 autoclave with a magnetic follower. The autoclave was charged with H_2 (30 - 40 bar) and heated (50 °C) with stirring for two hours. It was allowed to cool, vented and the i.r. immediately run on the pale yellow solution. A sample for ^1H n.m.r. was prepared by repeating the experiment with a concentrated solution in $CDCl_3$.

I.r./hexane: 2 128(w), 2 075(s), 2 050(vs), 2 034(vs), 2 025(w), 2 004(m), 1 997(m), and 1 968(m) cm^{-1}.

^1H n.m.r./$CDCl_3$, 0 °C: δ (p.p.m.) -10.6? and -10.8 (s, 1 H, Os-H) and -15.4 (s, 1 H, Os-H-Os).

The signals in the alkyl region were swamped by residual (7) or ((8) + (9)). This compound on gentle warming or when left overnight yielded $|H_2Os_3(CO)_9S|$ and traces of $|Os_3(H)(CO)_{10}SPr^n|$.

The preparation of ^{13}CO enriched thiolate clusters.

A sample of ^{13}CO enriched $|Os_3(CO)_{12}|$ (prepared as in the literature,[3] 50 % enrichment by m.s.) was converted into $|Os_3(H)(CO)_{10}SR|$ ((4) and (2)). The ^{13}CO enriched compounds $|Os_3(H)(CO)_9(SPr^n)(L)|$ (where L = CH_3CN, C_2H_4, PPh_3, and C_2H_2) were obtained by repeating the preparations used for the unenriched samples. The ^{13}C n.m.r. spectra all used $Cr(acac)_3$ as a spin relaxant and the chemical shifts are relative to t.m.s. ($Si(CH_3)_4$) in p.p.m..

^{13}C n.m.r. results

(a) = broad band $\{^1H\}$ and (b) = ^1H coupled spectra.

$|Os_3(CO)_{10}(H)(SPr^n)|$ (4)/$CDCl_3$, 31 - 60 °C:

(a) Position	No. of carbonyls
180.8 s	1
180.5 s	1
176.4 s	2
173.9 s	2
170.7 s	2
169.5 s	2

(b)

Position	No. of carbonyls	
180.8 s	1	
180.6 d	1	$^{2}J_{HC}$ = 5 Hz
176.4 s	2	
173.9 s	2	
170.7 s	2	
169.5 d	2	$^{2}J_{HC}$ = 10 Hz

$|Os_3(CO)_{10}(H)\{S(CH_2)_3Si(OMe)_3\}|$ (2)/CD_2Cl_2, 31 °C:
(see Figure 3.2).

(a)

Position	No. of carbonyls	
181.4 s	1	
181.5 d	1	$^{2}J_{CC}$ = 3 Hz
177.0 s	2	
174.4 s	2	
171.0 s	2	
170.0 s	2	

(b)

181.4 s	1	
181.15 d	1	broadened
177.0 s	2	
174.4 s	2	
171.0 s	2	
170.0 d	2	J_{HC} = 11 Hz

$|Os_3(CO)_9(H)(SPr^n)(CH_3CN)|$ (8)/$CDCl_3$, 0 °C:
(see Figure 3.3)

(a)

Position	No. of carbonyls
181.9 s	1
181.3 s	2

	181.0 s	2	
	175.2 s	2	
	172.4 s	2	
(b)	181.9 s	1	
	181.3 s	2	
	181.0 s	2	
	175.2 s	2	
	172.4 d	2	$^2J_{HC}$ = 9 Hz

$|Os_3(CO)_9(H)(SPr^n)(CH_3CN)|$ ($\underline{9}$)/$CDCl_3$, 0 °C:
(see Figure 3.4)

(a)	Position	No. of carbonyls	
	181.9 s	1	
	181.5 s	1	
	181.3 s	1	
	180.9 s	1	
	178.7 s	1	
	176.1 s	1	
	175.2 s	1	
	173.8 s	1	
	172.4 s	1	
(b)	182.0 d	1	$^2J_{HC}$ = 9 Hz
	181.5 s	1	
	181.3 s	1	
	181.0 s	1	
	178.7 s	1	
	176.0 s	1	

175.2 s	1	
173.7 d	1	$^2J_{HC}$ = 6 Hz
172.4 d	1	$^2J_{HC}$ = 7 Hz

$|Os_3(H)(CO)_9(SPr^n)(CH_3CN)|$ (10)/$CDCl_3$, 0 - 30 °C, and -60 °C: No significant changes occurred on varying the temperature. This compound appears to exist as only one isomer but the assignment is confused by decompostion of the sample which causes deterioration in the quality of the n.m.r. spectrum as well as peaks indicative of (4). Peaks at -60 °C ((4) subtracted out, $\{^1H\}$), 182.3, 181.3, 181.1, 177.6, 177.3, 173.7, 173.5, 171.9, 171.4 (all of intensity one) p.p.m.

$|Os_3(CO)_9(H)(SPr^n)(C_2H_4)|$ (7)$CDCl_3$, °C:
(see Figure 3.5)

(a) Position	No. of carbonyls
182.4 s	1
180.2 s	1
178.8 s	1
178.5 s	1
176.4 s	1
172.8 s	1
169.8 s	1
169.4 s	2

(b)	
182.5 s	1
180.2 s	1
178.8 s	1
178.5 s	1

176.4 s	1	
172.8 s	1	broadened
169.8 s	1	broadened
169.4 s	2	

$|Os_3(CO)_9(H)(SPr^n)(PPh_3)|$ (11)/CD_2Cl_2, 31 °C- -60 °C: (see Figure 3.6), at 31 °C.

(a)

Position	No. of carbonyls	
192.5 s	1	
190.8 d	1	$^2J_{PC}$ = 8 Hz
181.1 s	1	
180.6 s	1	
178.5 d	1	$^2J_{PC}$ = 5 Hz
174.8 s	1	
172.1 s	1	
171.4 s	2	

(b)

192.5 s	1	
190.8 d	1	$^2J_{PC}$ = 8 Hz
181.1 s	1	
180.6 s	1	
178.5 d	1	$^2J_{PC}$ = 5 Hz
174.8 s	1	broadened
172.1 s	1	broadened
171.4 s	2	

$\{^1H\}$ Ph ring carbons at 31 °C, 133.4 (d, 6 C, ortho or meta carbons, $^2J_{PC}$ = 12 Hz), 130.9 (s, 3 C, para-carbon), and 128.9 (d, 6 C, ortho or meta carbons, $^2J_{PC}$ = 10 Hz) p.p.m.

at -60 °C the signals are:-

	Position	No. of carbonyls	
(a)	192.5 s	1	broadened
	191.2 s	1	broadened
	181.5 s	1	
	180.7 s	1	
	178.6 s	1	
	174.3 s	1	
	172.2 s	1	
	171.9 s	1	
	171.4 s	1	
	134-128 br	phenyl ring carbons	
(b)	192.4 s	1	
	191.0 d	1	$^2J_{HC}$ = 6 Hz
	181.5 s	1	
	180.6 s	1	
	178.6 s	1	
	174.3 d	1	$^2J_{HC}$ = 4 Hz
	172.2 s	1	broadened
	171.9 s	1	
	171.4 s	1	

$\{Os_3(CO)_9(H)(SPr^n)(PPh_3)\}$ (14)/$CDCl_3$, 31- -60 °C:
(see Figure 3.7).

The spectra varied only slightly on going from 31 °C to -60 °C.

(a)	Position	No. of carbonyls	
	183.7 s	1	
	183.0 d	1	$^2J_{PC}$ = 6 Hz
	182.2 s	1	
	178.3 s	1	
	176.1 d	1	$^2J_{PC}$ = 4 Hz
	175.8 s	1	
	175.4 s	1	
	171.9 s	1	
	170.5 s	1	

(b)			
	183.6 s	1	
	183.0 d	1	$^2J_{PC}$ = 6 Hz
	182.2 s	1	
	178.3 s	1	
	176.0 d	1	$^2J_{HC}$ = 8 Hz?
	175.8 s	1	
	175.4 s	1	
	171.9 s	1	
	170.5 d	1	$^2J_{HC}$ = 7 Hz

$[Os_3(CO)_9(H)(SPr^n)(C_2H_2)]$ (12)/$CDCl_3$, 0 - -60 °C: d^8-toluene 0 - -70 °C: (see Figure 3.8)

The ^{13}C n.m.r. spectra varied with temperature. The low temperature limiting spectrum was obtained at -40 °C.

at -40 °C:

(a)	Position	No. of carbonyls
	181.2 s	1
	178.1 s	1

	175.0 s	1	
	174.7 s	1	
	173.4 s	1	
	171.7 s	1	
	171.4 s	1	
	168.3 s	2	
(b)	181.2 s	1	
	178.0 s	1	
	175.0 s	1	
	174.7 s	1	
	173.4 s	1	broadened
	171.7 s	1	
	171.4 s	1	
	168.3 s	2	broadened

On warming these peaks broaden, by 12 ^{o}C only a broad feature is seen (~ 173.7 p.p.m.) which remains broad up to 30 ^{o}C. At 40 ^{o}C it sharpens to give a spectrum which remains unchanged up to 70 ^{o}C.

at 40 - 70 ^{o}C:

(a)	Position	No. of carbonyls	
	176.9 s	2	
	174.8 s	3	
	171.8 s	2	
	171.6 s	2	
(b)	176.9 s	2	
	174.8 s	3	
	171.7 s	4	(broadening of one peak caused the accidental degeneracy)

Preparation of derivatives of $|Os_3(H)(CO)_9SR|$ where R = thiolated oxide.

Two entries into the cycle were evaluated. The more specific, CH_3CN, one was subsequently adopted for all the oxides.

(i) via $|Os_3(H)(CO)_9SR(C_2H_4)|$.

A solution of Me_3NO (1 mg/cm^3 in methanol) was added dropwise to a methylene chloride slurry of $|Os_3(H)(CO)_{10}\{S(CH_2)_3Si(OMe)_{3-x}(O_{\gamma}\text{-}Al_2O_3)_x\}|$ while ethylene was bubbled through. The i.r. spectrum of the oxide was run at hourly intervals. The reaction took twenty four hours to complete and required approximately twenty equivalents of Me_3NO. I.r./Nujol mull: 2 107(s), 2 093(m), 2 078(w), 2 062(s), 2 049(s), 2 040(s), 2 020(s), 2 009(s), and 1 996-1 930(vbr,s) cm^{-1}.

(ii) via $|Os_3(H)(CO)_9SR(CH_3CN)|$.

In general, a solution of Me_3NO in acetonitrile (1 mg/cm^3) was added to a slurry of $|Os_3(H)(CO)_{10}\{S(CH_2)_3Si(OMe)_{3-x}(O\text{-}M\ O_n)_x\}|$ in acetonitrile and the i.r. monitored by removing samples at hourly intervals. The reactions typically took fifteen hours to complete and ten to fifteen equivalents of oxidising agent (depending on the oxide). When the reactions were repeated on $SiMe_3Cl$ pretreated thiolated oxide samples both the reaction time (6 hours) and the amount of Me_3NO (5-7 equivalents) were reduced. All the solids were yellow-orange in colour.

I.r./Nujol mull: (see Figute 3.9), $M'O_n = SiO_2$, 2 094(m), 2 079(w), 2 049(vs), 2 025(vs), 2 008(s), 1 994(sh), 1 984 (vbr,vs), and 1 950(sh);

γ-Al_2O_3, 2 093(m), 2 079(m), 2 048(vs), 2 025(vs), 2 009(s), 1 995(br,s), and 1 981(vbr,vs);

TiO_2, 2 092(m), 2 078(m), 2 048(vs), 2 025(vs), 2 008(s), 1 995(br,s), and 1 979(vbr,vs);

ZnO, 2 094(w), 2 079(m), 2 047(vs), 2 026(s), 2 008(s), 1 995(s), 1 984(vbr,vs), and 1 979(vbr,vs);

MgO, 2 093(w), 2 079(m), 2 047(vs), 2 026(vs), 2 011(s), 1 994(br,s), and 1 983(vbr,vs) cm^{-1}.

$(Me_3Si)_yM'O_n$ =

SiO_2, 2 107(vw), 2 094(m), 2 080(m), 2 062(sh), 2 049(vs), 2 028)vs), 2 012(s), 1 996(br,s), 1 986(br,s), 1 977(br,s), and 1 956(sh);

γ-Al_2O_3, 2 107(vw), 2 094(m), 2 079(m), 2 065(sh,vw), 2 048(vs), 2 027(s), 2 012(s), 1 995(br,s), 1 985(br,sh), and 1 977(br,s);

TiO_2, 2 107(vw), 2 092(m), 2 078(m), 2 065(sh), 2 048(vs), 2 025(s), 2 009(s), 1 996-1 970(br,s), and 1 950(sh);

ZnO, 2 107(vw), 2 093(m), 2 078(m), 2 064(sh), 2 047(vs), 2 027(s), 2 014(vs), 1 995(br,s), and 1 985(br,vs) cm^{-1}.

Preparation of $|Os_3(H)(CO)_9(C_2H_4)\{S(CH_2)_3Si(OMe)_{3-x}(O\text{-}M'O_n)_x\}|$.

A slurry of the supported CH_3CN derivative in cyclohexane was heated (50 °C) and stirred overnight in an autoclave charged with ethylene (50 bar). It was then cooled and the excess ethylene vented off. The product was recovered by filtration and dried <u>in vacuo</u> to yield a lemon yellow powder.

I.r./Nujol mull: (see Figure 3.10), $M'O_n$ =

SiO_2, 2 093(m), 2 062(vs), 2 041(s), 2 010(s), 2 005-1 970 (br,vs), and 1 968(sh,vw);

γ-Al_2O_3, 2 093(m), 2 062(vs), 2 051(m), 2 040(s), 2 009(br,vs), 2 000-1 970(br,vs), and 1 968(sh);

TiO_2, 2 093(m), 2 078(vw), 2 062(vs), 2 050(s), 2 041(s), 2 010-1 977(br,vs), and 1 966(m) cm^{-1}.

$(Me_3Si)_yM'O_n$ =

SiO_2, 2 093(m), 2 078(sh,vw), 2 062(vs), 2 041(s), 2 010(vs), 1 999-1 989(sh), 1 979(sh), 1 966(s), and 1 938(sh);

γ-Al_2O_3, 2 093(m), 2 062(vs), 2 051(s), 2 041(s), 2 009(br,vs), 1 998(br,vs), 1 989(sh), 1 967(sh), and 1 938(sh);

TiO_2, 2 093(m), 2 078(w), 2 062(vs), 2 050(sh,w), 2 041(s), 2 010(br,vs), 1 998-1 977(sh), 1 966(m), and 1 936(m);

ZnO, 2 093(m), 2 077(vw), 2 062(vs), 2 041(s), 2 010(br,vs), 2 000-1 975(sh), 1 966(m), and 1 938(w);

MgO, 2 093(m), 2 062(vs), 2 051(vw), 2 041(s), 2 026(sh), 2 011(br,vs), 2 000-1 976(sh), 1 970(sh), and 1 938(w) cm^{-1}.

Preparation of $[Os_3(H)(CO)_9(PPh_3)\{S(CH_2)_3Si(OMe)_{3-x}(O\text{-}M'O_n\}]$.

A slurry of the C_2H_4 or CH_3CN supported derivatives in methylene chloride was stirred overnight with an excess of PPh_3, filtered, and washed (3 x CH_2Cl_2) to give a bright yellow solid.

I.r./Nujol mull: (see Figure 3.11), $M'O_n$ =

SiO_2, 2 092(w), 2 080(w), 2 050(m), 2 025(s), 2 012(sh), and 1 999-1 955(br,vs) cm^{-1}.

$(Me_3Si)_y M'O_n$ =
SiO_2, 2 107(vw), 2 093(m), 2 080(m), 2 065(sh), 2 050(s), 2 023(s), 2 012(s), 1 999(vs), 1 980(br,s), and 1 955(sh); γ-Al_2O_3, 2 107(sh), 2 092(m), 2 079(m), 2 065(sh,vw), 2 049 (br,vs), 2 021(s), 2 010(s), 1 997(br,vs), and 1 978(br,s); TiO_2, 2 112(br,w), 2 093(m), 2 080(m), 2 065(sh), 2 050(br,s), 2 021(br,s), 1 998(br,s), and 1 978(br,s) cm^{-1}.

Preparation of $|Os_3(H)(CO)_9(C_2H_2)\{S(CH_2)_3Si(OMe)_{3-x}(O\text{-}M'O_n)_x\}|$.

A slurry of either the supported CH_3CN or C_2H_4 derivative was refluxed in cyclohexane, under C_2H_2 for one hour, filtered and washed (3 x CH_2Cl_2). This afforded pale yellow powders in the cases of γ-Al_2O_3 and TiO_2, and a purple powder in the case of SiO_2.
I.r./Nujol mull: (see Figure 3.12), $M'O_n$ =
SiO_2, 2 102(w), 2 094(w), 2 076(s), 2 047(s), and 2 009(br,vs);
$(Me_3Si)_y M'O_n$ =
SiO_2, 2 102(w), 2 093(w), 2 076(s), 2 048(s), 2 021(sh), 2 009(vs), 1 996(br,sh), 1 971(br,sh);
γ-Al_2O_3, 2 102(w), 2 092(w), 2 075(s), 2 048(s), 2 008(vs), and 1 973(vbr,sh);
TiO_2, 2 102(w), 2 092(w), 2 076(m), 2 048(s), 2 008(vs), and 1 975(br,sh) cm^{-1}.

Attempted preparation of the supported capped cluster.

Samples of either the CH_3CN or C_2H_4 supported clusters were evacuated (10^{-1} mm Hg) and heated (40 ^{o}C) overnight to

give pale yellow solids with new i.r. spectra.

I.r./Nujol mull: (see Figure 3.13) $(Me_3Si)_yM'O_n$ =

(a) from the CH_3CN derivative:

SiO_2, 2 107(vw), 2 094(m), 2 080(m), 2 065(sh), 2 051(vs), 2 022(vs), 2 013(vs), 1 997(br,vs), 1 981(sh), and 1 946(sh,vw);

γ-Al_2O_3, 2 107(vvw), 2 094(m), 2 080(m), 2 066(sh), 2 050(vs), 2 021(s), 2 012(vs), 1 997(vs), and 1 978(br,s);

TiO_2, 2 107(w), 2 094(m), 2 079(m), 2 065(sh), 2 050(vs), 2 022(sh), 2 013(vs), 1997(br,s), and 1 981(br,s) cm^{-1}.

(b) from the C_2H_4 derivative:

SiO_2, 2 107(vw), 2 094(m), 2 080(m), 2 064(sh), 2 051(vs), 2 022(vs), 2 013(vs), 1 997(br,vs), 1 982(vbr,sh), and 1 952(vbr,sh);

γ-Al_2O_3, 2 107(vvw), 2 093(m), 2 080(m), 2 065(sh), 2 050(vs), 2 021(s), 2 012(vs), 1 996(br,vs), and 1 977(br,s);

TiO_2, 2 107(w), 2 093(m), 2 080(m), 2 065(m), 2 050(vs), 2 022(s), 2 013(vs), 1 997(br,vs), and 1 978(sh);

ZnO, 2 105(vw), 2 090(vw), 2 078(w), 2 065(sh), 2 051(s), 2 018(vbr,vs), 1 997(br,m), and 1 985(br,m) cm^{-1}.

$M'O_n$ = SiO_2, 2 107(vvw), 2 095(m), 2 080(m), 2 065(sh,w), 2 050(vs), 2 021(vs), 2 013(vs), and 1 990(vbr,vs) cm^{-1}.

Reactions of the supported "capped" cluster.

(i) with CH_3CN

When a suspension of this derivative in acetonitrile was stirred overnight, filtered and washed (3 x CH_2Cl_2), the i.r. spectrum of the CH_3CN derivatives was reobtained.

I.r./Nujol mull: $(Me_3Si)_y M'O_n$ =

SiO_2, 2 107(vw), 2 094(m), 2 079(m), 2 065(sh), 2 048(s), 2 027(s), 2 012(s), 1 996(br,vs), 1 977(vbr,s), 1 957(s);

γ-Al_2O_3, 2 107(vw), 2 092(m), 2 078(m), 2 065(sh), 2 048(vs), 2 025(s), 2 011(s), 1 995(br,s), and 1 982(vbr,s);

TiO_2, 2 107(vw), 2 093(m), 2 079(m), 2 065(sh), 2 048(vs), 2 025(s), 2 009(s), 1 996-1 965(br,s), and 1 950(sh) cm^{-1}.

(ii) with C_2H_4

When a slurry of this derivative was stirred overnight in an autoclave charged with ethylene (50 bar) the i.r. of the ethylene derivative was reobtained.

I.r./Nujol mull: $(Me_3Si)_y M'O_n$ =

SiO_2, 2 093(m), 2 062(s), 2 051(s), 2 041(s), 2 021(sh), 2 010(vs), 1 99(s), 1 989(sh), 1 977(sh), and 1 965(sh);

γ-Al_2O_3, 2 093(m), 2 078(vw), 2 062(s), 2 050(vs), 2 041(s), 2 021(s), 2 010(vs), 1 997(br,s), and 1 978(br);

TiO_2, 2 107(sh), 2 093(m), 2 078(w), 2 062(s), 2 050(s), 2 041(s), 2 022(sh), 2 011(vbr,vs), 1 997(br,s), 1 985(sh), 1 978(sh), and 1 964(sh) cm^{-1}.

Demonstration of the reversibility of the $CH_3CN \rightarrow C_2H_4$ step.

A sample of the ethylene supported cluster was stirred overnight in acetonitrile, filtered and washed (3 x CH_2Cl_2) to afford a yellow powder.

I.r./Nujol mull: $(Me_3Si)_y M'O_n$ =

SiO_2, 2 107(vw), 2 094(m), 2 080(m), 2 065(sh), 2 049(s), 2 027(s), 2 012(s), 1 997(s), 1 986(br,s), 1 977(br,s), and 1 957(sh);

γ-Al_2O_3, 2 107(vw), 2 093(m), 2 079(m), 2 065(sh), 2 048(vs), 2 025(s), 2 011(s), 1 996(vbr,s), and 1 980(vbr,s);
TiO_2, 2 107(vw), 2 092(m), 2 079(m), 2 065(sh), 2 049(vs), 2 025(s), 2 008(s), and 1 997-1 960(br,s) cm^{-1}.

Preparation of the hydrogenation intermediate on the surface.

When a sample of either the "capped", CH_3CN or C_2H_4, supported clusters was subjected to the same conditions used for the homogeneous analogues, filtration gave very pale yellow powders, which displayed the similar i.r. spectra to the homogeneous adduct.

I.r./Nujol mull: (see Figure 3.14), $(Me_3Si)_y M'O_n$ =
SiO_2, 2 128(m), 2 094(m), 2 075(s), 2 048(s), 2 031(s), and 2 013(s);
γ-Al_2O_3, 2 128(m), 2 094(s), 2 075(s), 2 048(s), 2 031(s), and 2 013(s) cm^{-1}.

The removal of the cluster from the surface by hydrogen.

A sample of $\{Os_3(H)(CO)_9(C_2H_4$ or $CH_3CN)\{S(CH_2)_3Si(OMe)_{3-x}(O\text{-}M'O_n)_x(Me_3Si)_y\}\}$ was placed in a Soxhlet thimble and extracted with clean hexane while the whole apparatus was purged with hydrogen. After two and a half hours the hexane was removed under reduced pressure and the residue taken up in hexane.

I.r./hexane: 2 118(w), 2 085(s), 2 058(s), 2 036(m), 2 012(vs), 2 012(vs), 1 997(s), 1 991(w), and 1 984(m) cm^{-1}.

^1H n.m.r.: insufficient sample.

Mass spectrum: gave a weak parent (862 a.m.u., ^{192}Os).

Catalysis experiments.

All the catalysis experiments were conducted in pairs. The homogeneous catalysis experiments were conducted in a glass ampoule sealed by a P.T.F.E. tap. In a typical experiment, the cluster and pentene, 25 fold excess with respect to the cluster in CH_2Cl_2 (1.75×10^{-3} molar) were degassed in the ampoule by two freeze-evacuation-thaw cycles. Then put into a Grant G.E. constant temperature bath and stirred using a P.T.F.E. magnetic follower. At the end of the catalysis run the organic fraction was collected in a liquid nitrogen cooled U-tube by r.t. vacuum distillation and analysed by g.l.c. The remaining inorganic fraction was analysed by i.r. and, if necessary, separated by t.l.c.

In the heterogeneous experiments the procedure was the same except the ampoule was modified by having a P.T.F.E. "O" ring ball joint immediately under the tap. This facilitated loading and unloading of the solid. The amount of solid and volume of the pentene solution were kept at 100 mg and 3 cm^3, respectively.

The isomeric pentenes were separated on a 1/8" o.d., 4 m column packed with 11 % $AgNO_3$ and 21 % phenylacetonitrile on Chromosorb P 60 - 80 mesh, at 30 ^oC with nitrogen carrier gas (25 cm^3 min^{-1}). Since the peak shapes (1-, cis-, and trans-) for all three were exactly the same, the relative abundances were measured using peak height.

Homogeneous catalysis results

The catalytic activity is given in turnovers per cluster.

$|Os_3(CO)_{10}(H)SPr^n|$ (4)

T/°C	t/hr	Pentene	I.r. result	g.l.c. result
47-48	72	1-	no change	no catalysis
47-48	72	cis-	no change	no catalysis
47-48	96	trans-	no change	no catalysis
77-78	72	1-	no change	no catalysis
77-78	72	cis-	no change	no catalysis
77-78	72	trans-	no change	no catalysis
125-126	15	1-	slight decomposition	1 turnover
125-126	15	cis-	slight decomposition	2 turnovers
125-126	15	trans-	slight decomposition	no catalysis

$|Os(CO)_{10}(H)\{S(CH_2)_3Si(OMe)_3\}|$ (2)

No catalysis was observed at 47 and 78 °C.

$|Os_3(CO)_9(CH_3CN)(H)(SPr^n)|$ ((8) + (9))

t/°C	t/hr	Pentene	I.r. result	g.l.c. result
47-48	48	1-	((8)+(9)) + traces	4 turnovers
47-48	48	cis-	of (4) and olefin	9 turnovers
47-48	48	trans-	adducts	0.8 turnovers
77-78	48	1-	gross decomposition	7 turnovers
77-78	48	cis-	+ (4) and olefin	7 turnovers
77-78	48	trans-	adducts	2 turnovers

$|Os_3(CO)_9(C_2H_4)(H)(SPr^n)|$ (7)

T/°C	t/hr	Pentene	I.r. result	g.l.c. result
47-48	72	1-	traces (13)+(4)	2 turnovers
47-48	72	cis-	mostly olefin	4 turnovers
47-48	72	trans-	adducts and slight decomposition	1 turnover

The g.l.c. also showed ethylene in trace amounts.

$|Os_3(CO)_9(C_2H_2)(H)(SPr^n)|$ (12)

T/°C	t/hr	Pentene	I.r. result	g.l.c. result
47-48	96	1-	no change	no catalysis
47-48	96	cis-	no change	no catalysis
47-48	96	trans-	no change	no catalysis
77-78	72	1-	no change	1 turnover
77-78	72	cis-	slight	0.5 turnover
77-78	72	trans-	decomposition	0.2 turnover ?

$|Os_3(CO)_9(PPh_3)(H)(SPr^n)|$ (11)

T/°C	t/hr	Pentene	I.r. result	g.l.c. result
47-48	96	1-	no change	no catalysis
47-48	96	cis-	no change	no catalysis
47-48	96	trans-	no change	no catalysis
77-78	72	1-	no change	0.5 turnovers
77-78	72	cis-	slight	0.5 turnovers
77-78	72	trans-	decomposition	0.4 turnovers

$|Ru_3(CO)_{10}(H)(SPr^n)|$ (3)

T/°C	t/hr	Pentene	I.r. result	g.l.c. result
47-48	48	1-	no change	8 turnovers
47-48	48	cis-	no change	5 turnovers
47-48	48	trans-	no change	2 turnovers
79-80	48	1-	traces $|Ru_3(CO)_9$-	20 turnovers
79-80	48	cis-	$H(SPr^n)|$ but mainly	16.7 turnovers
79-80	48	trans-	a plethora of	3 turnovers
			unstable products	

Heterogeneous catalysis results

Only cis-2-pentene was used. Control experiments with plain oxides in all cases showed no activity, under the conditions used (47 ± 0.5 °C, 72 hrs).

$|Os_3(CO)_{12}|$ + $HS(CH_2)_3Si(OMe)_{3-x}(O\text{-}M'O_n)_x$.

$M'O_n$	Os loading/p.p.m.	turnovers per Os
$\gamma\text{-}Al_2O_3$	22 350	1
SiO_2	20 100	4.2
TiO_2	19 550	7.5
ZnO	19 550	1.4
MgO	9 450	6

$|Os_3(CO)_{12}|$ + $HS(CH_2)_3Si(OMe)_{3-x}(O\text{-}M'O_n)_x(Me_3Si)_y$

$M'O_n$	Os loading/p.p.m.	turnovers per Os
$\gamma\text{-}Al_2O_3$	17 900	0.9
SiO_2	23 200	1.8
TiO_2	21 300	1.6
ZnO	2 450	0
MgO	7 800	0

$|Os_3(H)(CO)_{10}\{S(CH_2)_3Si(OMe)_3\}|$ + $M'O_n$

$M'O_n$	Os loading/p.p.m.	turnovers per Os
γ-Al_2O_3	29 400	0
SiO_2	3 550	0
TiO_2	31 660	0
ZnO	13 300	0
MgO	9 950	0

$|Os_3(CO)_{12}|$ + $M'O_n$

$M'O_n$	Os loading/p.p.m.	turnovers per Os
γ-Al_2O_3	22 550	6.1
SiO_2	9 950	0.7
TiO_2	17 000	0.6
ZnO	19 040	0.7
MgO	17 000	0

$|Os_3(CO)_{10}(H)\{S(CH_2)_3Si(OMe)_{3-x}(O_{SiO_2})_x\}|$ pyrolysed (160 °C, 3 days, vacuum)

$M'O_n$	Os loading/p.p.m.	tunrovers per Os
SiO_2	27 400	5.04

$|Os_3(CO)_{10}(H)(O_{SiO_2})|$ pyrolysed (160 °C, 15 hr, vacuum)

Os loading/p.p.m.	turnovers per Os
9.950	0

$|Os_3(CO)_9(H)(CH_3CN)\{S(CH_2)_3Si(OMe)_{3-x}(O\text{-}M'O_n)_x(Me_3Si)_y\}|$.

$M'O_n$	Os loading/p.p.m.	turnovers per Os
γ-Al_2O_3	17 900	1.7
SiO_2	23 200	2.6

TiO_2	21 300	4.0
ZnO	2 450	2.9
MgO	7 800	2.3

$|Ru_3(CO)_{10}(H)\{S(CH_2)_3Si(OMe)_{3-x}(O\text{-}M'O_n)_x(Me_3Si)_y\}|$.

$M'O_n$	Ru loading/p.p.m.	turnovers per Ru
$\gamma\text{-}Al_2O_3$	10 800	10.0
SiO_2	25 500	10.6

$|Ru_3(CO)_{12}| + M'O_n$

$M'O_n$	Ru loading/p.p.m.	turnovers per Ru
$\gamma\text{-}Al_2O_3$	15 110	0.6
SiO_2	2 090	0.0

References for Chapter 3.

1. B.F.G. Johnson, J. Lewis, and D.A. Pippard, J.Organomet. Chem., (1981), 213, 249.

2. A.J. Deeming and M. Underhill, J.Organomet.Chem., (1972), 42, C60.

3. A. Forster, B.F.G. Johnson, J. Lewis, T.W. Matheson, B.H. Robinson, and W.G. Jackson, J.Chem.Soc.,Chem.Commun., (1974), 1042.

4. L. Milone, S. Aime, E.W. Randall, and E.J. Rosenberg, J.Chem.Soc.,Chem.Commun., (1975), 452.

5. J. Evans, B.F.G. Johnson, J. Lewis, and T.W. Matheson, J.Am.Chem.Soc., (1975), 97, 1245.

6. J. Evans, B.F.G. Johnson, J. Lewis, J.R. Norton, and F.A. Cotton, J.Chem.Soc.,Chem.Commun., (1973), 807.

7. A. Forster, B.F.G. Johnson, J. Lewis, T.W. Matheson, B.H. Robinson, and W.G. Jackson, J.Chem.Soc.,Chem.Commun., (1974), 1042.

8. A.J. Deeming and M. Underhill, J.Chem.Soc.,Dalton Trans., (1974), 1415.

9. S. Aime, L. Milone, and A.J. Deeming, J.Chem.Soc.,Chem. Commun., (1980), 1168.

10. R. Jackson, B.F.G. Johnson, J. Lewis, P.R. Raithby, and S.W. Sankey, J.Organomet.Chem., (1980), 193, C1.

11. B.F.G. Johnson, J. Lewis, and D.A. Pippard, J.Organomet. Chem., (1978), 145, C4.

12. B.F.G. Johnson, J. Lewis, and D.A. Pippard, J.Chem.Soc., Dalton Trans., (1981), 407.

13. B.F.G. Johnson, J. Lewis, D.A. Pippard, P.R. Raithby, G.M. Sheldrick, and K.D. Rouse, J.Chem.Soc.,Dalton Trans., (1979), 616.

14. J.A. De Beer and R.J. Haines, J.Organomet.Chem., (1970), 24, 757.

15. R. Bau, B. Don, R. Greatex, R.J. Haines, R.A. Love, and R.D. Wilson, Inorg.Chem., (1975), 14, 3021.

16. A.J. Deeming, R. Ettone, B.F.G. Johnson, and J. Lewis, J.Chem.Soc.(A), (1971), 1797.

17. E. Sappa, O. Gambino, and G. Centini, J.Organomet.Chem., (1972), 35, 375.

18. K. Wade, J.Organomet.Chem., (1981), 213, 35.

19. B.F.G. Johnson, J. Lewis, D. Pippard, and P.R. Raithby, Acta Crystallogr., (1980), 36, 703.

20. V.F. Allen, R. Mason, and P.B. Hitchcock, J.Organomet. Chem., (1977), 140, 297.

21. B.E. Mann, Ad.Organomet.Chem., (1974), 12, 135.

22. H.D. Kaesz and R.B. Saillant, Chem.Rev., (1972), 72, 231.

23. E.G. Bryan, A. Forster, B.F.G. Johnson, J. Lewis, and T.W. Matheson, J.Chem.Soc.,Dalton Trans., (1978), 196.

24. J. Evans, Adv.Organomet.Chem., (1977), 16, 319.

25. B.F.G. Johnson, J. Lewis, and T.W. Matheson, J.Chem.Soc., Chem.Commun., (1974), 441.

26. S. Aime and D. Osella, J.Chem.Soc.,Chem.Commun., (1981), 500.

27. G. Süss-Fink, Z.Naturforsch., (1980), 35B, 454.

28. P.A. Dawson, B.F.G. Johnson, J. Lewis, J. Puga, P.R. Raithby, and M.J. Rosales, J.Chem.Soc.,Dalton Trans., (1982), 233.

29. G.S. McNulty, personal communication.

30. M.J. Mays and P.D. Gavens, J.Chem.Soc.,Dalton Trans., (1980), 911.

31. R. Benfield, B.F.G. Johnson, P. Raithby, and G.M. Sheldrick, Acta Crystallogr., (1978), B34, 666.

32. B.F.G. Johnson, J. Lewis, B.E. Reichert, and K.T. Schorpp, J.Chem.Soc.,Dalton Trans., (1976), 1403.

33. D.A. Pippard, Ph.D. Thesis, University of Cambridge, 1978.

34. T.A. Albright, Acc.Chem.Res., (1982), 15, 149.

35. A.J. Deeming, B.F.G. Johnson, and J. Lewis, J.Chem.Soc.(A), (1970), 2517.

36. A.J. Deeming, personal communication.

37. A.J. Deeming and M. Underhill, J.Chem.Soc.,Dalton Trans., (1974), 1415.

38. H. Meerwein, Org.Synth., (1966), 46, 113.

39. H. Meerwein, Org.Synth., (1966), 46, 120.

40. The Chemistry of the Thiol Group, (The Chemistry of the Functional Groups), Ed. S. Patai, "An Interscience Publication", J. Wiley and Sons (1974).

41. F. Koubowetz, J. Latzel, and H. Noller, J.Colloid Interface Sci., (1980), 74, 322.

42. A.J. Deeming, B.F.G. Johnson, and J. Lewis, J.Chem.Soc.(A), (1970), 897.

43. W. Andreas, Z. Lazlo, and H. Gattfried, Chem.Ber., (1982), 4, 1286.

Chapter 4

Anchoring Clusters

— Some Complications —

Thiols[1] and amines[2] react with $|Os_3(CO)_{12}|$ to give complexes of the general formula $|Os_3(CO)_{10}(\mu_2\text{-}H)(\mu_2\text{-}XR)|$ in which both groups bridge the same edge.[3,4] The bridging thiol ligand (see Chapter Two) proved to be a better anchoring ligand than the monodentate phosphine. That is, it gave the clusters greater stability towards fragmentation and this provided the impetus to investigate the use of amine ligands for anchoring and prevention of cluster fragmentation.

In addition to this primary amine ligands by virtue of processing two activated hydrogens (like $PhPH_2$ and H_2S) can also form capped clusters, e.g. $|H_2Os_3(NR)(CO)_9|$[5] (c.f. $|H_2Os_3(PPh)(CO)_9|$[6] and $|H_2Os_3(S)(CO)_9|$[7]). This nitrogen cap has been shown to confer an increased stability upon the cluster. For example,[8] the cap remained intact when $|H_2Os_3(CO)_9(NR)|$ was pyrolysed at 198 °C for several hours. This reaction yielded a new tetrahedral cluster $|Os_4(CO)_{12}(NCH_3)|$ in moderate yield, whereas most other osmium clusters under these conditions would have decomposed to mononuclear species or osmium metal. This illustrates what could be an important future use for anchored ligands. That is, they could be used to provide sites for controlled metal particle growth. This template effect of certain ligands for cluster growth is not limited to amines and has been seen for other ligands such as phosphines and isocyanides, e.g.

$$HC(PPh_2)_3 + Ni(CO)_4 \longrightarrow |HC(PPh_2)_3Ni_3(CO)_6| \qquad \text{(ref. 11)}$$

$$|(PPh)Ru_3(CO)_9(H_2)| \xrightarrow[\Delta]{} |Ru_4(CO)_{11}(PPh)_2| + |Ru_5(CO)_{15}(PPh)| \qquad \text{(Ref. 9)}$$

$$|Os_3(CO)_{11}CNR| \xrightarrow[\Delta]{} |Os_6(CO)_{17}(CNR)| \qquad \text{(Ref. 10)}$$

Another reason for investigating the use of isocyanides as possible anchoring ligands is the existence of compounds $|(\mu_2\text{-H})Os_3(CO)_9(\mu_3\text{-}\eta^2,HC{=}NPh)|$,[12] which fulfil two criteria for a durable oxide tethered metal cluster. That is, it contains a bridging ligand and has some incipient unsaturation.[13] It is obtained by the thermolysis of $|H_2Os_3(CO)_{10}CNPh|$ which proceeds <u>via</u> a hydrogen migration reaction to $|HOs_3(CO)_{10}(\mu\text{-}\eta^2\text{-}HC{=}NPh)|$ and then by CO loss to the desired product. Synthesis of oxide anchored versions of these was, therefore, attempted.

A reason for the expansion of ligand anchoring to surfaces besides silica (see Chapter 2) was the prospect of oxide effects on catalysis.[14] The alkylidyne tricobalt ennea-carbonyls, $|RCCo_3(CO)_9|$, are ideal candidates for investigating this. Since studies[15,16,17] of methinyltricobalt ennea-carbonyls have shown that there is extensive electron delocalisation throughout the Co_3C unit and as a result of this the co-ordination behaviour of the cobalt is markedly affected by the type of apical substituent R. So in order to study the electronic and stereochemical behaviour of the oxides on clusters, the synthesis of $|Cl_3SiCCo_3(CO)_9|$[59] was carried out.

Particle size effects on the catalytic activity of materials derived from oxide supported metal carbonyl clusters have been suggested.[19] However, this suggestion has not been possible to test to date since a general method of tethering clusters of differing nuclearity by a standard link has not been reported. The combination of the new techniques of radical anion catalysed substitution[20] and purification by flash chromatography[21] offer the opportunity to realise this. So the application of these to ruthenium clusters of varying nuclearity was investigated.

Results and Discussion

(a) Amine ligands

The reported route[5] to the capped and bridged species (i.e. $|Os_3(CO)_{10}(H)\{N(H)R\}|$ and $|Os_3(CO)_9(NR)(H)_2|$) involves the initial preparation of a formamido complex, $|Os_3(CO)_{10}(H)\{OCN(H)R\}|$, and then the conversion of this on heating to the other species. With this in mind the complexes $|Os_3(CO)_{10}(H)\{OCN(H)R\}|$ (where R = Pr^n (16). and $(CH_2)_3Si(OEt)_3$ (18)) were prepared. (16) converted on heating to the bridged species $|Os_3(CO)_{10}(H)\{N(H)Pr^n\}|$ (17) as expected, however, (18) proved to be unstable when heated and produced an insoluble material. So ways of overcoming this problem were investigated.

(16) was found to convert to (17) by using Me_3NO to remove a carbonyl but the yields of this reaction were found to be too low (< 15 %) to make this suitable for producing an anchored bridged species. The bridged species has also bee reported[8] to be formed by the reaction of $|Os_3(CO)_{10}(CH_3CN)_2|$ with amines. However, this reaction concurrently produces the formamido complex and since the R.f. values of both species are similar (e.g. R.f. values from t.l.c. eluted with 50 % light petroleum and 50 % Et_2O are; (16) = 0.8 and (17) = 0.75) the pure silyl derivative would be inaccessible. The reason for this is that t.l.c. cannot be used for separating compounds containing a hydrolysable silyl group (e.g. $-Si(OEt)_3$, $-SiCl_3$) as this reacts with the oxide support and causes smearing and anchoring. Recently, flash

chromatography has been found to offer a way around this problem. This is because its higher speed of development (i.e. 2-5 minutes compared to 30-60 minutes for t.l.c) minimises the interactions with the oxide. However, some smearing still occurs and as a result only easy separations can be achieved (i.e. R.f. values different, > 0.2).

An alternative route to the bridged species is suggested by the work of Süss-Fink,[45] who found that ammonia reacts with $|Os_3(CO)_{11}(CH_3CN)|$ to produce the terminal amine, $|Os_3(CO)_{11}(NH_3)|$, which on heating converts in good yield to the bridged cluster, $|Os_3(CO)_{10}(H)(NH_2)|$. However, when $|Os_3(CO)_{11}CH_3CN|$ was reacted with $NH_2(CH_2)_3Si(OEt)_3$ only traces of the terminal cluster was produced. The major product obtained was the formamido cluster (18). This difference in reactivity is probably a reflection on the greater steric size of the primary amine precluding substitution directly on the osmium and causing it to go in preference on the less sterically hindered carbonyl site.

An insight was obtained as to why $|Os_3(CO)_{10}\{OCN(H)-(CH_2)_3Si(OEt)_3\}|$ (18) is unstable at r.t. (unlike $|Os_3(CO)_{10}-\{OCN(H)(CH_2)_2CH_3\}|$ (16) which is). When (18) was reacted with oxides a new compound is formed (see Figure 4.1). To investigate its identity (16) was reacted with Ph_3SiOH (an analogue of a surface hydroxyl group). Though no reaction occurred on standing at r.t. for long periods of time, warming to 40 - 60 ^{o}C caused rapid decomposition to give initially similar solution i.r. spectra to those seen on the surfaces.

Figure 4.1. I.r. spectra of; (a) $|HOs_3(CO)_{10}(OCN(H)Pr^n)|$ in cyclohexane, (b) $|HOs_3(CO)_{10}\{OCN(H)(CH_2)_3Si(OEt)_3\}|$ + γ-Al_2O_3 Nujol mull, and (c) Nujol mull of the product of heating aminated silica with osmium carbonyl (method 1).

Probably the mechanism of attack on the cluster involves nucleophilic substitution at the formamido group by the Si-OH, as in the alcoholysis of organic amides. So the surface probably initially converts the formamide cluster to an ester cluster which then decomposes. This would explain why (18) is unstable since the $-Si(OEt)_3$ group can act as a source of ethanol. Interestingly, the initial major side product on reacting (18) with oxides or $|Os_3(CO)_{11}CH_3CN|$ and $|Os_3(CO)_{12}|$ with aminated oxides (see Figure 4.1), displays a similar i.r. spectra to the terminal amine cluster, $|Os_3(CO)_{11}NH_3|$ (e.g. $Os_3(CO)_{11}NH_3$ in CH_2Cl_2, 2 096(w), 2 042(s), 2 024(s), 2 010(m), 1 989(vs), 1 980(sh), and 1 955(sh) cm^{-1}; the "impurity" bands in (18) + γ-Al_2O_3 samples = 2 089(w), 2 042(s), 2 023(s), 2 010(s), 1 967(w), and 1 954(w) cm^{-1}). Unfortunately, the product from the reaction of Ph_3SiOH with (16) which displayed a similar i.r. spectrum could not be isolated because it reacted with the t.l.c. plates and was also too unstable for purification by crystallisation. The available evidence suggests that this intermediate on a surface is possibly a terminal oxide cluster (e.g. $|Os_3(CO)_{11}(O_{SiO_2})|$. On standing all the supported formamido clusters initially decompose to give this species before fragmenting to give mononuclear species.

(b) isocyanides

For 90 years after their discovery by Gautier[32] and Hoffmann[33] the synthesis of isocyanides was dominated by the two classical methods. That is the reaction of silver cyanide (or cuprous cyanide) with an alkyl iodide reported by Hoffmann or the carbylamine reaction discovered by Gautier. e.g.

$$R-I + AgNC \longrightarrow |R-NCAgI| \xrightarrow[KCN]{} R-NC \quad < 55\ \%\ \text{yield}$$

$$R-NH_2 + CCl_2 \xrightarrow[\substack{CHCl_3\\Base}]{} |R-\overset{+}{N}H_2-CCl_2| \xrightarrow{\beta\text{elim}} |R-N=CHCl| \xrightarrow{\alpha\text{elim}} R-NC \quad < 50\ \%\ \text{yield}$$

The principal disadvantage of these routes are the poor yields (55 % is a maximum, the yields are usually 10-15 %) and the problems involved in purifying the products. These two methods have been displaced since the early 1960's by the dehydration of N-monosubstituted formamides.[34] A wide variety of acylating agents (e.g. $COCl_2$, $SOCl_2$, p-toluene sulphonyl chloride, and PPh_3) can be used to dehydrate the N-monosubstituted formamide in the presence of bases (e.g. trialkylamines, pyridine, and quinoline). e.g.

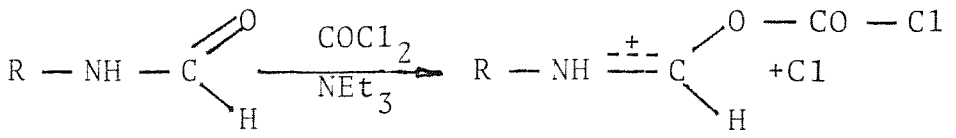

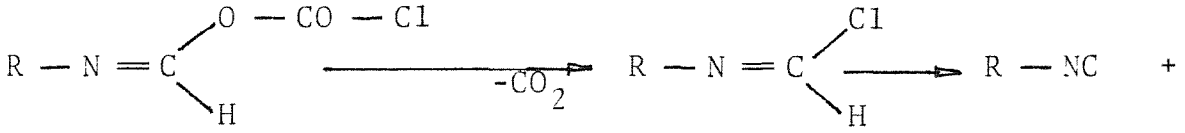

$$Et_3\overset{+}{N}HCl^- \quad + \quad CO_2$$

The choice of which pair to use depends on the isocyanide. In the two preparations carried out in this work the acylating agents and bases were chosen to allow easy separation of the isocyanide. For example, in the case of the ^tBuNC preparation[23] the product could be distilled directly from the less volatile reactants and other products, i.e.

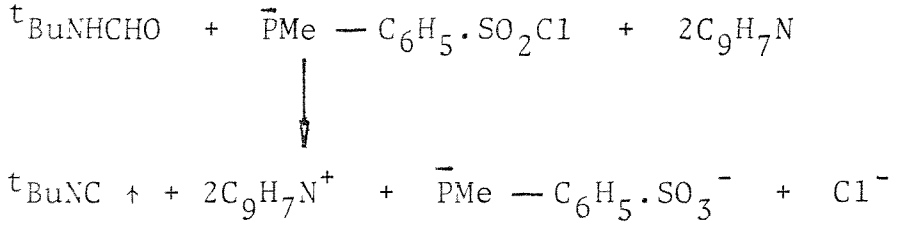

The n-alkyl formamides are generally readily available from primary aliphatic amines and the calculated quantity of either formic acid or ethylformate in refluxing benzene or toluene with the azeotrope being removed.

e.g.

Interestingly for $|(EtO)_3Si(CH_2)_3NC|$ a $^2J_{NH}$ = 2 Hz was observed for $CN-\underline{CH_2}-$. Obviously the nuclear quadrupole

coupling in isonitriles is very low[35] and this indicates that there must be a near zero electric field gradient about the nitrogen[36] in isocyanides. The literature values for $^{2}J_{NH}$ in isocyanides range from 2-4 Hz which is in accord with the observed value.

When the isocyanide was supported on silica a new isocyanide band was observed in addition to the band seen for the free isocyanide (see Figure 4.2, free isocyanide 2 148 cm^{-1} and new band 2 160 cm^{-1}). The anchoring of this isocyanide to silica has also been reported by Howell and Berry[37] and they only observed the band at 2 160 cm^{-1}. It is well known that ν_{NC} increases with increasing solvent popularity (e.g. $^{t}BuNC$ ν_{NC} = 2 134 cm^{-1} gas phase, 2131.3 cyclohexane and 2137.8 in acetonitrile). This is apparently due to the polar solvent enhancing the contribution of the polar triple bonded structure, e.g. $RN{=}C{=}$ $\quad$ $R{-}N{\equiv}C$. However, this effect is only of the order of $\sim$ 6 cm^{-1} for nonhydroxylitic solvents and the observed shift is 12 cm^{-1}. Hydrogen bonding (by alcohols[38,39]) solvents can cause a shift of this magnitude. So the peak at 2 160 cm^{-1} is probably due to surface hydroxyl groups hydrogen bonding the isocyanide (this should stabilise the triply bonded canonical form), e.g.

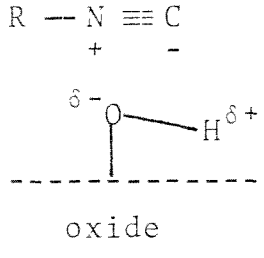

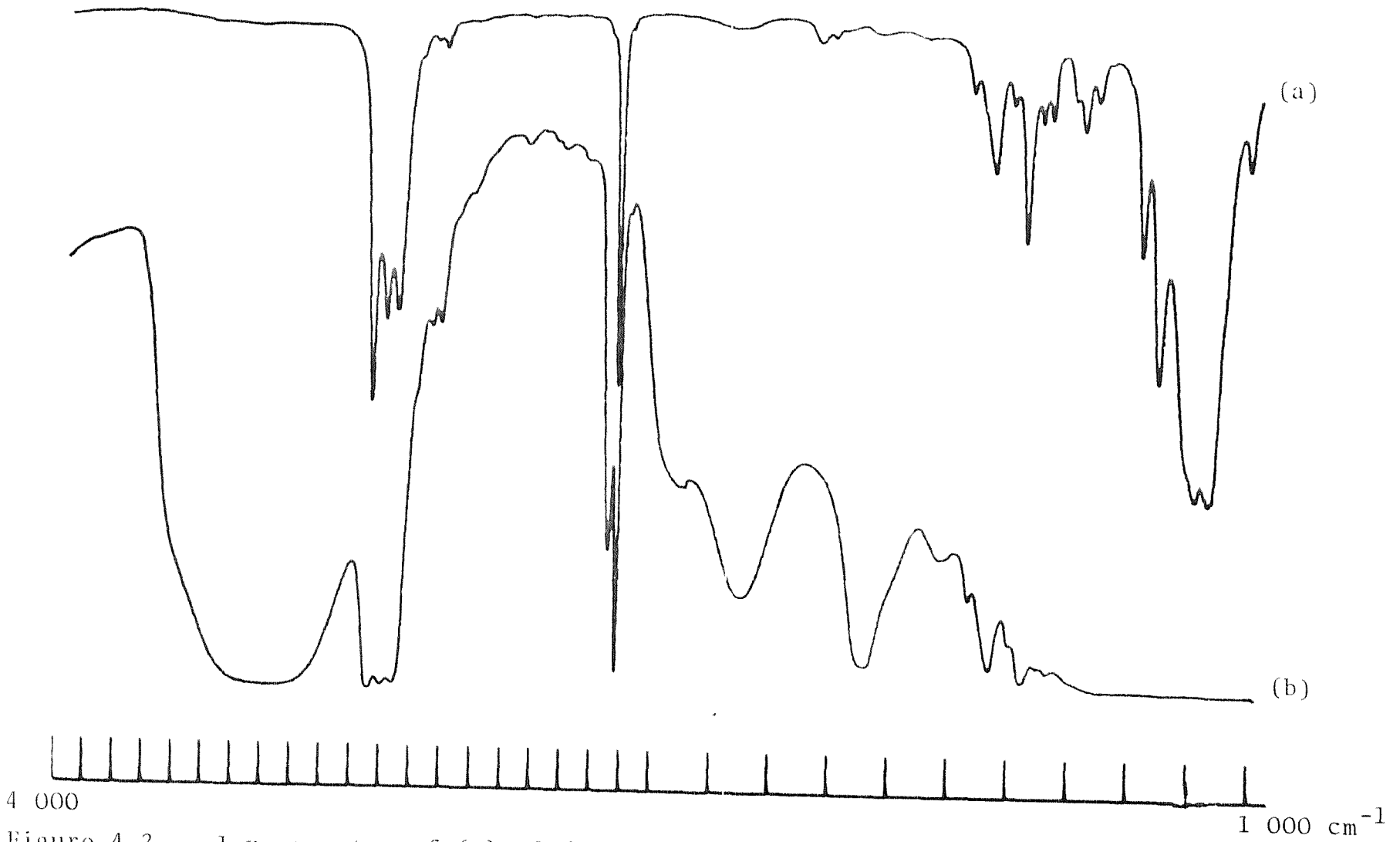

Figure 4.2. i.r. spectra of (a) $CN(CH_2)_3Si(OEt)_3$ film between KBr discs, and (6) a disc of isocyanide liganded silica.

The ν_{NC} also shifts on co-ordination and this can be explained in terms of either σ-donation or σ-donation and d-π^* back donation. In isocyanides the bond order is intermediate between 2-3 and probably nearer to 3 than 2. For example, ν_{CN} for cyanides (bond order 3) is 2 260-2 200 cm^{-1} whereas for $|(Fe(Cp)(CO))_2(\mu_2\text{-}CO)(\mu_2\text{-}CNPh)|$[40] (CN bond order ∿ 2, as C — N — Ph = 131°) ν_{NC} = 1 704 cm^{-1} compared with 2 117 cm^{-1} for the free ligand. So for isonitriles if they acted solely as σ donors on co-ordination one would expect a slight increase in ν_{NC} as the "charged" canonical form would be favoured. Cotton and Zingales[41] have proposed that in addition to this a slight increase in ν_{NC} should also occur due to a kinematic coupling of the M — C and C — N bonds. In the case of transition metals because of their ability to d → π^* backbond, one would expect to observe a drop in ν_{NC}.[41] However, in the substituted clusters, $|H_2Os_3(CO)_{10}CNR|$ and $|Os_3(CO)_nCNR|$ ν_{NC} is raised rather than lowered, e.g.

Molecule	$\Delta\nu/cm^{-1}$ (compared to free isocyanide)
$\|H_2Os_3(CO)_{10}CNBu^t\|$	+64
$\|H_2Os_3(CO)_{10}CN(CH_2)_3Si(OEt)_3\|$	+76
$\|Os_3(CO)_{11}CNBu^t\|$	+48 major, +40 minor
$\|Os_3(CO)_{11}CN(CH_2)_3Si(OEt)_3\|$	+75 and +54

This must be because the carbonyls are better d → π^* acceptors than the isocyanide and so are acting as an electron sink and causing the isocyanide to act predominantly as a σ donor

ligand. Several pieces of evidence exist to support this suggestion. Firstly, for clusters of the formula $|Os_3(CO)_{12-n}(CNR)_n|$ it has been observed[42] as n increases, ν_{NC} and ν_{CO} decrease. This suggests that relatively more charge is delocalised into the CNR π^* orbitals as the number of CO groups available for this purpose decreases and that the ν_{CO} decreases because the CNR ligands are acting as stronger electron donors than the replaced CO ligands. Secondly, for n = 1, 2 and 3 a ^{13}C n.m.r. study has shown that isonitriles occupy axial positions when not forced into equatorial positions on steric grounds. This would fit in with the current view on the electronic environments of the axial and equatorial sites on osmium carbonyl. That is, equatorial sites suit $d \rightarrow \pi^*$ acceptor ligands whereas axial sites being more electron defficient suit σ donor ligands better.

This difference between axial and equatorial sites is seen for the cases where n = 3. A ^{13}C n.m.r. study[42] on these compounds suggest that they exist as a dynamic mixture of two isomers, one of which possesses an isocyanide in the equatorial position. Interestingly in these cases two unequal ν_{NC} bands are seen in the i.r., a major higher frequency one and a minor lower frequency one. The minor lower frequency one is probably due to the isocyanide in the equatorial position, since an isocyanide on an equatorial site should have more $d \rightarrow \pi^*$ character in its bonding than one on an axial site. Unfortunately, for $|Os_3(CO)_{11}CNBu^t|$ (which exists as an equilibrium mixture of equatorial and predominantly axial isomers) though the major band is readily seen the minor

band is too weak for a firm assignment to confirm this ν_{NC} shift on different site occupancy.

In the case of the silyl cluster $|Os_3(CO)_{11}CNR|$ (R = $(CH_2)_3Si(OEt)_3$) two bands of about equal intensity are seen in the ν_{NC} region. These could be due to axial and equatorial isomers as seen for $|Os_3(CO)_{11}CNBu^t|$ but this is unlikely since the silyl ligand is sterically smaller than the ^tBu ligand. Another possibility is that these differ in the conformation of the R group, for example, the silyl group could be hydrogen bonded to isocyanide.

$CN(CH_2)_3Si(OEt)_3$ reacts readily at room temperature with $|H_2Os_3(CO)_{10}|$ as observed for other isonitriles to yield $|H_2Os_3(CO)_{10}\{CN(CH_2)_3Si(OEt)_3\}|$ which shows at 0 °C in the ^1H n.m.r. (CD_2Cl_2 solvent) two sets of terminal bridging hydride resonances due to major and minor isomers. This has been observed for other compounds of the formula $|H_2Os_3(CO)_{10}CNR|$ but interestingly the minor more upfield isomer is more prevalent in the silyl compound (major:minor ∿ 3:1) than for the other reported compounds. For example, for $|H_2Os_3(CO)_{10}CNBu^t|$ the ratio is ∿ 6:1. The coupling $^2J_{H_{terminal}H_{bridge}}$ is a constant 4 Hz independent of the isomer. This indicates that the relative orientations of the two hydrides are constant in both isomers (the angle dependence of $^2J_{HH}$ is well documented). The two isomers probably differ in the orientation of the isonitrile to the terminal hydride ligand (i.e. either cis or trans), e.g.

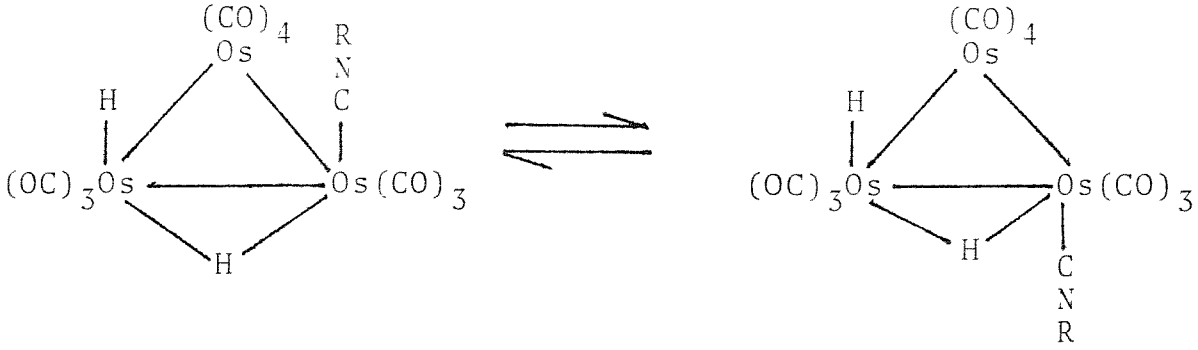

A single-crystal X-ray study of $|H_2Os_3(CO)_{10}CNBu^t|$[12] shows that in the solid state the trans isomer predominates with the isocyanide occupying an axial site. The hydrides in $|H_2Os_3(CO)_{10}CNR|$[12] (R = Bu^t, CH_3, C_6H_5) are also fluxional and are only "frozen" out on the ^1H n.m.r. time scale at temperatures around -60 °C. Surprisingly in the light of this $|H_2Os_3(CO)_{10}CN(CH_2)_3Si(OEt)_3|$ (19) is frozen out at 0 °C. This is unexpected since the proportions of the two isomers is more even for (19) than for the other substituted clusters. So one would expect the relative energies of the two isomers for (19) to be more equal. The fluxional process interconverts both the isomers, since the hydride signals collapse on warming to give a single line. Obviously in the case of (19) there is a higher energy barrier towards this interconversion and this in part favours the minor isomer which is probably the cis isomer (the X-ray of $|H_2Os_3(CO)_{10}CNBu^t|$[12] shows the trans isomer).

It is interesting to speculate that this barrier is due to hydrogen bonding in (19) between the $Si(OEt)_3$ and the terminal hydride and this would also explain the higher proportion of

the cis isomer (in (19) compared with the other derivatives). For hydrogen bonding to occur the polarity of the M — H needs to be $M^{\delta-} — H^{\delta+}$. Similar acidic behaviour of terminal and bridging hydride ligands has been seen, e.g.

Compound	K_a	Solvent	Ref.
$\|Fe_3(CO)_9(H)(SR)\|$	3 or 4	variable	54
$\|HCo(CO)_4\|$	2	H_2O	55
$\|HCo(CO)(PF_3)_3\|$	2	H_2O	56
$\|H_2M(PF_3)_4\|$ (M = Fe, Ru, Os)	weakly acidic	H_2O	57

Although it is tempting to relate the acid strength directly to the polarity of the metal-hydrogen bond, other thermodynamic factors must also be considered. Of these factors one of the most important is the solvation energy of the proton and the corresponding anionic metal species.

$|H_2Os_3(CO)_{10}CNBu^t|$[12] undergoes a (NEt_3) base catalysed rearrangement to give $|HOs_3(CO)_{10}(CN(H)Bu^t)|$ and it cannot be made to undergo this reaction without base catalysis. However, (19) undergoes this reaction slowly at r.t. and rapidly on heating without a catalyst. This could be due to speculated hydrogen bonding catalysing the reaction, e.g.

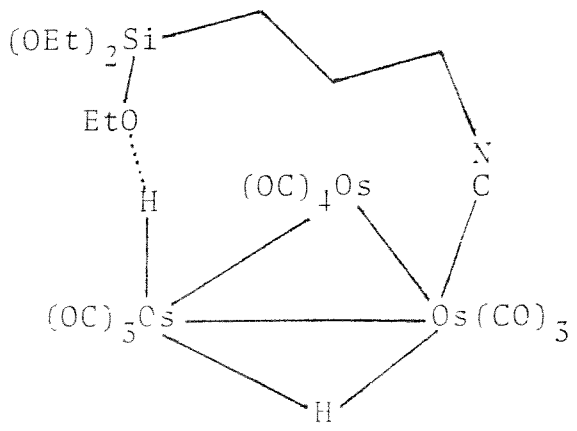

Some further evidence for this was obtained during the attempted anchoring of (19), when it changed rapidly even at low temperatures to $|HOs_3(CO)_{10}CN(H)(CH_2)_3Si(OEt)_{3-x}(M'O_n)_x|$ (identified by comparative i.r. with (20), see Figure 4.3). This isomerisation must have been catalysed by hydrogen bonding by the surface hydroxyl groups rather than by base catalysis since all the oxides catalysed it. For example, the silica used was acidic and possessed no Lewis base sites (unlike γ-Al_2O_3 and TiO_2) but still promoted isomerisation . Firmly anchored versions of (20) could be obtained by refluxing oxide suspensions in cyclohexane solutions of (19) or (20) for two hours. Substitution of ethoxide groups by surface oxygens to form $|HOs(CO)_{10}(CN(CH_2)_3Si(OEt)_{3-x}(O\text{-}M'O_n)_x)|$ was evident as ethanol was detected by g.l.c.

CH_2Cl_2 Solutions and alumina anchored versions of (20) were monitored for pentene isomerisation activity at 47 and 80 ^oC. In solution ((20) 4.3×10^{-3}M and pentene 1×10^{-1} M), only slight activity was detected at 47 ^oC after three days. After six days at 80 ^oC, little trans-2-pentene had isomerised but the degree of conversion of terminal to internal olefin (7 turnovers) and cis to trans-2-pentene (12 turnovers), did increase. The alumina anchored complex exhibited similar activity at 47 ^oC, e.g. 3 turnovers for 1-pentene going to 2-pentene but less than 10 % of the activity of (20) at 80 ^oC. The i.r. spectra of this recovered sample indicated some complex decomposition, but it appears that the oxide environment also deactivates the intact cluster.

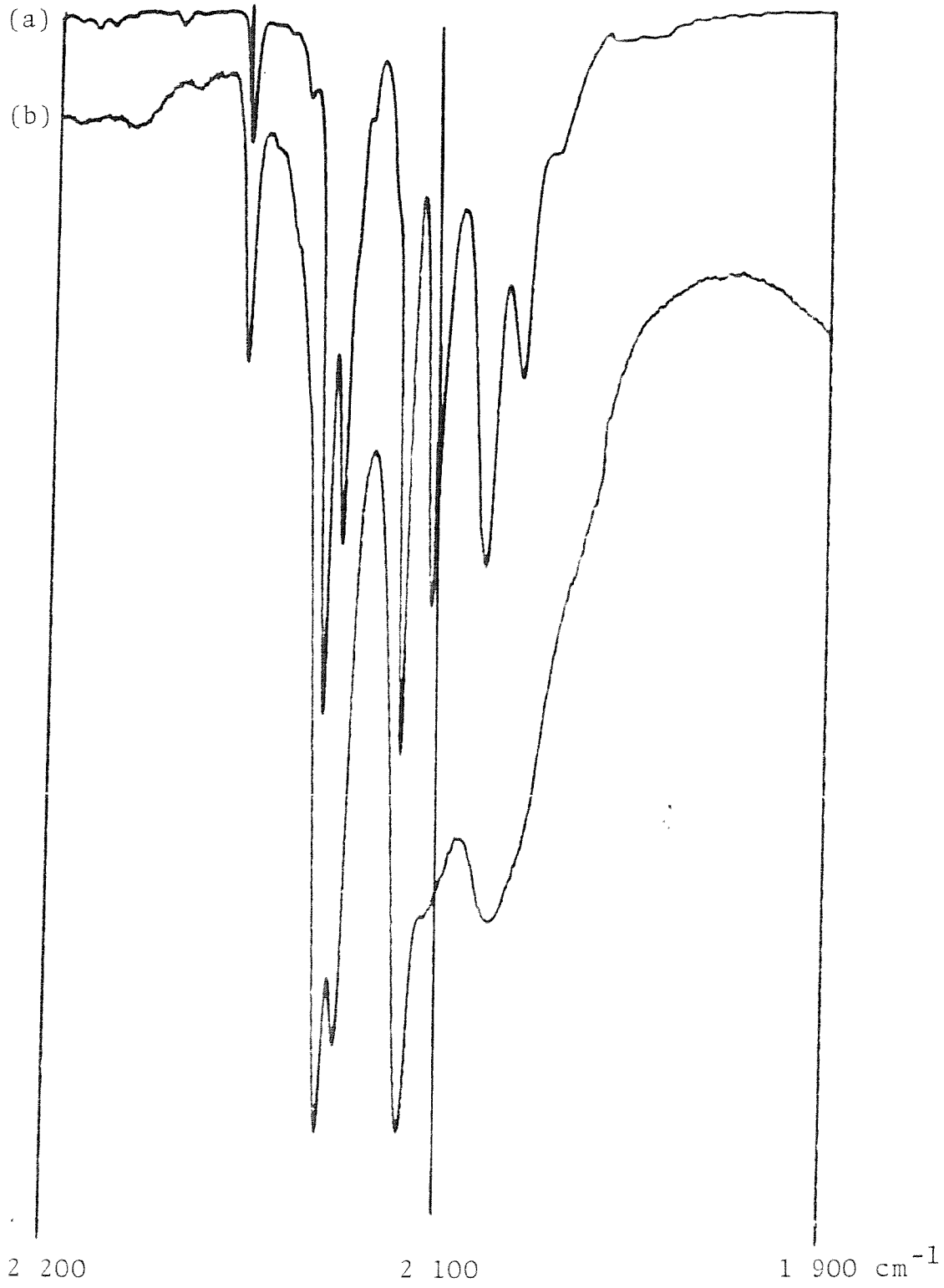

Figure 4.5. I.r. spectra of (a) $\{HOs_3(CO)_{10}[CN(H)(CH_2)_3Si(OEt)_3]\}$ (20) in cyclohexane, and (b) (20) on γ-Alumina.

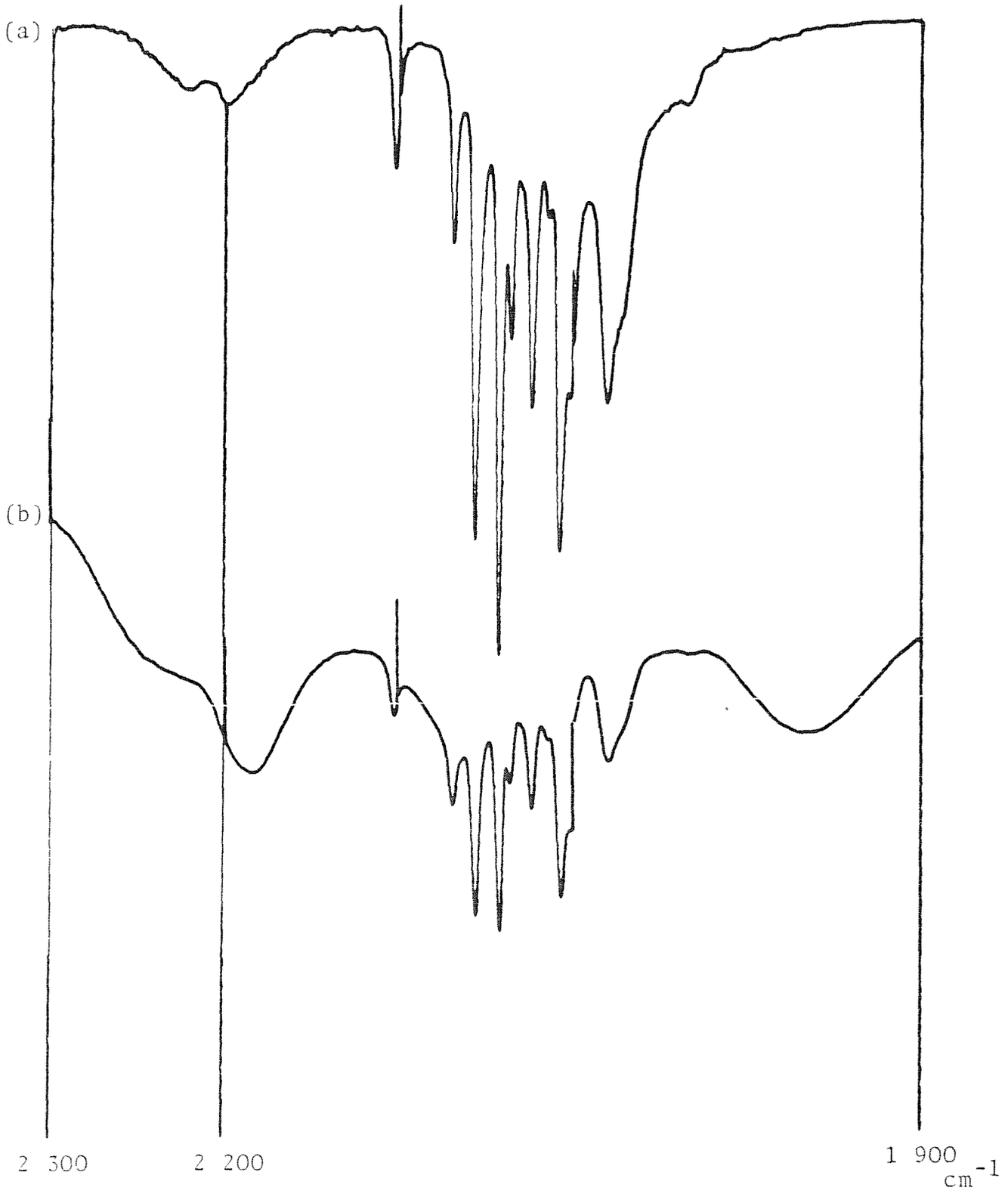

Figure 4.4. I.r. spectra of: (a) $\{Os_3(CO)_{11}\{CN(CH_2)_3Si(OMe)_3\}\}$ (21) in cyclohexane, (b) Nujol mull of (21) + γ-Al_2O_3.

The anchoring of $|Os_3(CO)_{11}CNR|$ analogues was carried out without complications by two main routes. That is by interacting either $|Os_3(CO)_{11}CN(CH_3)_3Si(OEt)_3|$ (21) with oxides or $|Os_3(CO)_{11}NCCH_3|$ with isocyanide liganded oxide, (see Figure 4.4). (21) exists from the i.r. as two isomers and this explains the complexity of its spectrum. Catalysis runs on (21) showed it to be inactive towards pentene isomerisation.

(c) alkylidene clusters

The alkylidene clusters investigated are of the robust alkylidynetricobalt nonacarbonyl series.[44] These contain a tetrahedral CCo_3 cluster unit in which the apical carbon is co-ordinated symmetrically, apparently via σ bonds to 3 cobalt atoms.

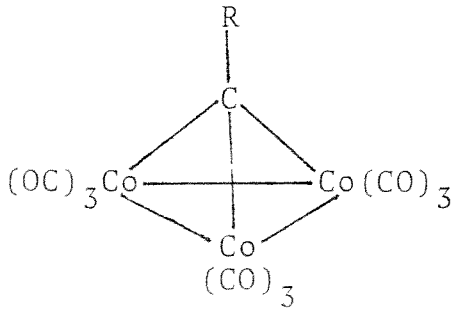

Each cobalt atom may be regarded as achieving a closed shell configuration by σ bonding to two other cobalt atoms. The arrangement of the carbon monoxide ligands is such that six of the nine carbon monoxide ligands are disposed upward in the general direction of the apical carbon atom and its substituent and as a result any reactions at the apical carbon or at is substituent group will be subject to substantial steric hindrance. This will make the Cap fairly inert to chemical

attack and thereby make these clusters resistant to fragmentation and suitable for catalysis study.

It has been shown[16] both that there is extensive electron delocalisation throughout the Co_3C unit and that the co-ordination behaviour of the cobalt is markedly affected by the type of apical substituent. Robinson et al.[16] investigated this by preparing teriary phosphine and arsine derivatives of compounds with a range of R groups on the capping carbon. They found that the cap stabilised the cluster towards fragmentation by Lewis bases (compared with $|Fe_3(CO)_{12}|$ and $|Ru_3(CO)_{12}|$, which gives mono or dinuclear species under similar conditions). In addition to this they also found that the reactivity varied with the R group. For example, only certain disubstituted clusters could be made, e.g.

$|RCCo_3(CO)_7L_2|$

R =	PPh_3	$PhEt_2P$	$PhMe_2As$
Cl	-	-	-
Ph	-	✓	-
Me	✓	✓	✓

It has also been observed that the stability of the derivatives also varies with R. For example, with the arene complexes[17] $|RCCo_3(CO)_6(arene)|$ it is Ph > F > Me.

This variation in reactivity with R groups could be useful in oxide supported catalysts, as oxide effects could be transmitted through the R group to the cluster. To test this the compounds $R_3SiCCo_3(CO)_9$ (R = Cl (23), Et (22) and OH (24)) were made by literature methods.[59] The i.r. spectra of these

compounds illustrate that the groups on the silicon do effect the electron density on the cluster and hence probably the clusters reactivity. For example, the carbonyl bonds in (22) are shifted to a lower frequency than in (23) because of the +I effect of the ethyl groups compared with the -I effect of the chlorines. (23) anchored well on most dry oxides ar r.t. from CH_2Cl_2 solution, (silica required gentle heating). A dry oxide is required otherwise the reaction shown below occurs (this can be used to prepare (24))

$$|Cl_3SiCCo_3(CO)_9| \xrightarrow{\text{"}H_2O\text{"}} 3HCl + |(HO)_3SiCCo_3(CO)_9| \quad (24)$$

The supported clusters gave purple powders whose i.r. spectra varied slightly with the oxides (SiO_2 appears to be a better electron donor than the other oxides) and agree well with the spectra for (23) and (24) but not (22) as would be expected (see Figure 4.5), as the supported species should be electronically closer to (23) than (22).

The catalysis studies though illustrating that the reactivity of the CCo_3 clusters varies with the R group do however, demonstrate the need for a stabilising carbon monoxide atmosphere as all the clusters decomposed at 80 ^{o}C. Of the two silyl clusters ((22) and (25)) tested only the triethyl one showed any catalysis and then for only 1-pentene. This is as expected since the methyinyl tricobalt enneacarbonyls are more reactive when the R substituent is a +I rather than a -I group. The reason why only one pentene is isomerised is probably because it is the least sterically hindered of the

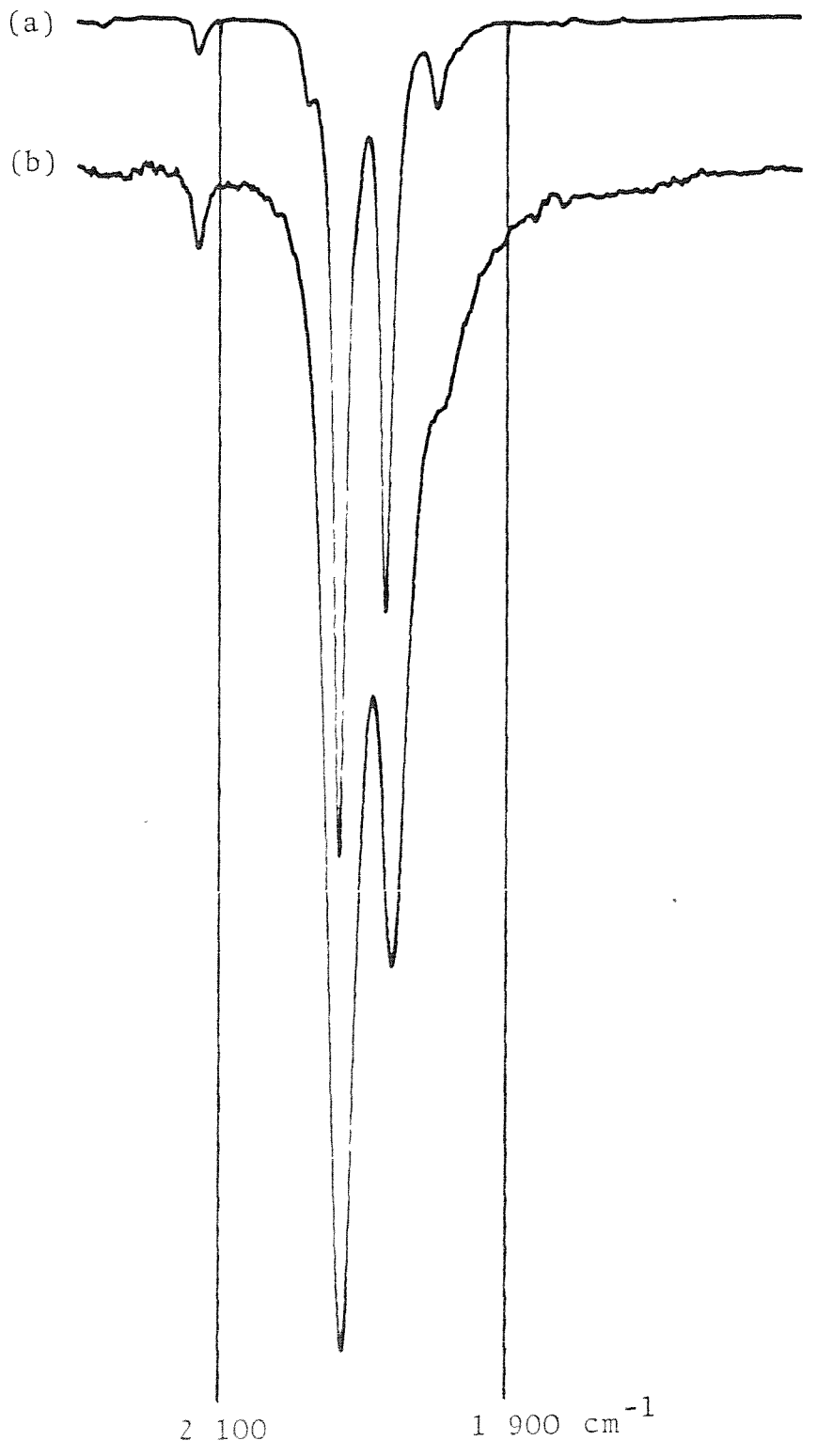

Figure 4.5. I.r. spectra of (a) $|Cl_3SiCCo_3(CO)_9|$ in cyclohexane, and (b) Nujol mull of $|(CO)_9Co_3CSi(Cl)_{3-x}(O_{Al_2O_3})_x|$ with the γ-Al_2O_3 background subtracted out.

three isomeric pentenes tested. The fact that when the $|Cl_3SiCCo_3(CO)_9|$ cluster decomposed at 80 °C no catalysis was observed indicates that it is the intact cluster or some derivative of it that is the active catalyst. The catalytic activity of $|HCCo_3(CO)_9|$ was quite different to (22) in that besides causing isomerisation of all 3 pentenes it also caused polymerisation particularly for the 1-pentene. Various $|RCCo_3(CO)_9|$ complexes have been shown[47,48] to be initiators of olefin polymerisation. With the complexes in which R = H, Cl or Br one might speculate that the initiating process involves reaction at the apical carbon atom in view of the known $|HCCo_3(CO)_9|$/olefin[49,50] reactions, and the reported reactions of $|BrCCo_3(CO)_9|$ with olefins.[50,51]

<u>e.g.</u>

$$|BrCCo_3(CO)_9| + C_2H_4 \longrightarrow |C_2H_5CCo_3(CO)_9| + |CH_3CH=C(CH_3)CCo_3(CO)_9|$$

However, the fact that complexes in which R = Ph, F, Me_2CH and C_2F_5 also initiate polymerisation of acrylonitrile suggests that chemistry of the cobalt may be involved instead. The displacement of carbon monoxide ligands by diolefins to give stable complexes of type $|RCCo_3(CO)_9(norbornadiene)|$ have been reported,[52,53] so such a process is entirely feasible.

Since in this case ($HCCo_3(CO)_9$) the starting cluster was recovered (in over 95 % yield from the catalysis experiments) mostly unchanged, the active catalyst probably like in the case of $|Et_3SiCCo_3(CO)_9|$ involves substitution at the cobalt.

Attempts to isolate the postulated olefin adduct were unsuccessful possibly because of an inherent instability, so doubt still remains about the active catalyst. When the catalysis experiments were repeated on the anchored clusters $|(CO)_9Co_3CSiCl_{3-x}(O\text{-}M'O_n)_x|$ ($M'O_n = SiO_2$, Al_2O_3) no catalysis was seen. Obviously the -I effect of the oxide inhibits its catalytic activity like the chlorines in the parent cluster $|(CO)_9Co_3CSiCl_3|$.

Interestingly, both $|PhCCo_3(CO)_9|$ and $|(\mu_4\text{-Ph-P})_2Co_3(CO)_8(\mu\text{-CO})_2|$ have been shown to catalyse hydroformylation.[58,18] Under the conditions reported (110 ^oC, 100-25 hrs) the $|PhCCo_3(CO)_9|$ would be unstable if it was not for the presence of a stabilising carbon monoxide atmosphere. This result indicates, despite that the clusters decomposed under the isomerisation conditions, they still could be possible hydroformylation catalysts. Also because of the general ease of synthesis of these from any R_3SiH and $|HCCo_3(CO)_9|$, the possibility exists to tailor these catalysts by preparing these compounds with various (e.g. $|Cl_2RSiCCo_3(CO)_9|$) R groups (useful R groups could be electron donor ones or even chiral alkyl groups).

(d) Phosphine ligands

One of the major problems encountered in the anchoring of clusters has been the specificity of the anchoring reaction. For example, Gates et al. have claimed the specific anchoring of $H_4Ru_4(CO)_{12}$ onto phosphinated polystyrene,[60] to produce samples which are uniquely either, $|H_4Ru_4(CO)_{11}"P"|$,

$|H_4Ru_4(CO)_9"P_3"|$ or $|H_4Ru_4(CO)_8"P_4"|$ (where "P" = phosphinated polystyrene), by comparative i.r. with $|H_4Ru_4(CO)_{12-n}(PPh_4)_n|$ (n = 1, 2 3, and 4). They claimed that this specificity was obtainable by using block polymers, however, on comparison with the PPh_2Et derivatives, which are close analogues of the PPh_2R (R = polystyrene) groups on the polymer, all three reported cases appear to be a mixture of the different n values, with the reported n value predominating.

This problem of polysubstitution has been reported by Brown and Evans,[61] for the thermal anchoring of $|Os_3(CO)_{12}|$ onto phosphinated silica. They observed polysubstitution by i.r. (i.e. $|Os_3(CO)_{12-n}\{PPh_2CH_2CH_2Si(OEt)_{3-x}(O_{SiO_2})_x\}_n|$, n = 1, 2, and 3), for the supported species. This problem can be overcome by using a route by which specific substitution can be obtained. For example,[61] polysubstitution in the case of $|Os_3(CO)_{12}|$/phosphinated silica system was overcome by preparing first a cluster with a weakly co-ordinating ligand (i.e. $|Os_3(CO)_{11}CH_3CN|$) and then reacting this under mild conditions with the liganded support (e.g. r.t., 60 minutes) and because CO substitution requires more forcing conditions (refluxing toluene) this reaction yields specifically $|Os_3(CO)_{11}\{PPh_2CH_2CH_2Si(OEt)_{3-x}(O_{SiO_2})_x\}|$. This method is of limited use as the routes by which specific substitution can be obtained are themselves limited. Other specific syntheses used to date involve the addition of phosphines to clusters: with incipient unsaturation[61,62] (e.g. $|H_2Os_3(CO)_{10}|$ + $\{PPh_2(CH_2)_2Si(OEt)_{3-x}(O_{SiO_2})_x\}$); for which the first addition

has the lowest activation energy[63] (e.g. $|Ru_5C(CO)_{17}|$ + phosphinated silica) and for which substitution at a particular site is favoured[64] (e.g. mixed metal clusters containing gold such as $|HAuOs_3(CO)_{10}\{PPh_2CH_2CH_2Si(OEt)_{3-x}(O_{SiO_2})_x\}|$).

Side products, however, present a constant problem even in these cases. For example, in Chapter 3, despite the reaction of $Os_3(CO)_{12}$ with thiolated oxide giving an i.r. spectrum indicative of the pure supported species, $|Os_3(H)(CO)_{10}\{S(CH_2)_3Si(OMe)_{3-x}(O\text{-}M'O_n)_x\}|$, some pentene isomerisation activity was observed. This was shown by control experiments to be due to minor impurities (not detectable by i.r.) formed during the preparation of these samples, by oxide interaction. A route avoiding this problem is to prepare the silyl liganded cluster and then attach it to the oxide. This method was pioneered by Brown and Evans[61] for clusters, though it has been reported previously for mononuclear species.[65] The major advantage of this route is that the cluster can be purified before anchoring. However, a disadvantage is that the forcing conditions required to anchor it firmly to silica can often cause loss of cluster integrity. In Chapter 2 this method was expanded to oxides besides silica and these proved to be much more reactive towards the silane (probably because these oxides possess Lewis acid/base sites which silica does not ordinarily process[66]) and so allowed gentle anchoring of these clusters.

This approach itself though expanding the range of available chemistry for anchoring was still limited until

recently to reactions which gave in high yield one product which could be purified by sublimation or on solubility or by crystallisation, as chromatography could not be used. This is because the hydrolysable silane interacts strongly with the hydroxyl groups of the chromatographic support and causes tailing, anchoring and partial hydrolysis of any recovered compound. This problem has been overcome by flash chromatography.[21] Flash chromatography is basically a compressed air or nitrogen driven hybrid of medium pressure and short column chromatography which has been optimised for particularly rapid separations. It can achieve moderate resolution (ΔR.f. = 0.1) compared to t.l.c. ΔR.f. = 0.05) despite its rapidity (time to develop a column $\approx$ 2-5 minutes compared to $\approx$ 30 minutes for a t.l.c. plate). This method due to its rapidity reduces the problem of silane interaction with the oxide and as a result only slight tailing of silanated compounds occurs and this allows separation of silane compounds having fairly close R.f. values (requires ΔR.f. for monosubstituted silane compounds to be > 0.15).

The attempted thermal anchoring of $[Ru_3(CO)_{12}]$[67] and $[Os_3(CO)_{12}$ onto phosphinated silica yielded compounds of the formulae $[M_3(CO)_{12-n}\{PPh_2CH_2CH_2Si(OEt)_{3-x}(O_{SiO_2})_x\}_n]$, where n is mainly 2 or 3. This illustrates a common problem with phosphine substitution, that is, good yields of the monosubstituted product are generally hard to obtain since attached phosphines appear to have a labilising effect on the clusters. For example, for $[Ru_3(CO)_{12}]$,[68] $[Os_3(CO)_{12}]$,[69] $[H_4Ru_4(CO)_{12}]$,[70]

$|Rh_4(CO)_{12}|$,[71] and $|Ir_4(CO)_{12}|$,[72] the first substitution appears to have the highest activation energy. This is opposite to what is observed for mononuclear carbonyls with phosphines where successive substitutions become increasingly difficult due to electronic effects which lead to M-CO strengthening as PR_3 ligands are added. In clusters this would account for the general occurrence of monosubstitution at a metal centre by monodentate phosphines (e.g. $H_4Ru_4(CO)_{12-n}\{P(OMe)_3\}_n$, n = 1, 2, 3, 4). The i.r. spectra of clusters as n increases generally show a decrease in ν_{CO}, which is in accord with the phosphine replacing a better π acceptor ligand and so leaving excess electron density on the cluster which is partially dissipated in increased d-π backbonding to the CO ligands. This should serve to increase the M-C bond strength and decrease the reactivity of the cluster by mechanisms involving rate determining M-C cleavage. The observed labilising effects of the phosphines probably arises from two effects seen in the single crystal X-ray structures of phosphine substituted clusters (e.g. X-ray, $Os_3(CO)_{11}P(OMe)_3$,[73] $Ru_3(CO)_{11}PPh_3$,[74] and $Fe_3(CO)_{11}PPh_3$ (both structures)[75]) that is a general expansion of the ligand envelope, to allow for the more bulky ligand, together with an increase in the M-M distances on phosphine substitution. The increase in the M-M distances is thought to be caused by both steric and electronic factors. For example, in $|Os_3(CO)_{11}P(OMe)_3|$ the M-M edge cis to the phosphine is lengthened more than the other two and this is possibly due to a steric interaction.

The general expansion of the metal triangle is thought to be due to the expansion of the ligand envelope together with the increased electron density on the cluster being taken up by the expansion of the metal triangle.

The reaction of $Ru_3(CO)_{12}$ with phosphines has been studied in detail.[76] Several mechanisms have been proposed to explain the observed kinetics. For the monosubstitution step there appears to be two rate determining routes; a CO dissociation step (1st order) and a phosphine attack (2nd order route). In the case of polysubstitution the proposed mechanisms involve both M-M cleavage and an increase in the rate on phosphine substitution. This could be explained in terms of a weakening of the M-M bonds together with an increased steric relief on opening the triangle of phosphinated clusters. The increased pentene isomerisation activity of clusters,[77] $|H_4Ru_4(CO)_{12-n}(PR_3)_n|$ as n increases (activity 4 > 3 > 2 > 1) or the basicity of the phosphine increases (e.g. $P(OEt)_3 > P(OPh)_3 > PPh_3 > CO$) could be due to this postulated M-M weakening, on feeding more electron density into the cluster.

Some evidence for the occurrence of M-M cleavage mechanisms in cluster substitution chemistry is seen in the reversible reaction of $|Ru_5C(CO)_{15}|$ with acetonitrile in which a possible intermediate in phosphine substitution is observed. A single crystal X-ray study on $|Ru_5C(CO)_{15}MeCN|$ shows a cleaved M-M bond, to accommodate the weakly co-ordinated ligand.[78] The substitution of $|Ru_5C(CO)_{15}|$ with phosphines

leads to products involving CO loss, i.e. $|Ru_5C(CO)_{14or13}(PR_3)_{1or2}|$. The reaction probably occurs via a S.N.2 type of attack by the phosphine on the least sterically hindered side of the cluster, that is from underneath the square face. The phosphine then probably forms an intermediate like the acetonitrile but because of the greater M-P strength it is not reversible and CO loss occurs to yield the product $|Ru_5C(CO)_{14}(PR_3)|$. A solid state X-ray structure[79] on this compound (PR_3 = PPh_3) shows that the phosphine occupies an axial site underneath the square base. The crystal structure of $|Ru_5C(CO)_{13}(PPh_3)|$ shows[79] that the second phosphine also occupies an axial site trans (across the base) to the first substituted ruthenium. Obviously the second phosphines position on the base of the square face of the cluster is determined on steric grounds. This steric hindrance to the second substitution probably explains the lower rate observed for the 2nd substitution. Interestingly, polysubstitution, n > 2, has not been seen to occur under gentle conditions except in the case of bidentate phosphines (e.g. $|Ru_5C(CO)_{11}(dppm)_2|$, see Chapter 5).

The distribution of the products from the reaction of $|Ru_6C(CO)_{17}|$[63,80] with phosphines, shows that there is a lower activation energy barrier for the initial substitution than for the subsequent ones. The reason for this is not obvious but if the reaction involves attack at the bridged carbonyl, this would be much less favourable in the monosubstituted adduct if the single crystal X-ray structure of $|Ru_6C(CO)_{16}PPh_2Et|$[63] represents the major time conformer in the solution

state. Since this shows that the phosphine is placed asymmetrically over the bridging carbonyl and so sterically could protect it from attack. The idea that the site of attack involves the bridging carbonyl is partially supported by the observation that $|Rh_4(CO)_{12}|$, which possesses bridging carbonyls, reacts about 10^7 faster with phosphines than $|Ir_4(CO)_{12}|$, which does not. This difference in reactivity is too great to be accounted for in terms of differences in the M-M and M-CO bond strengths and so must be due to the differences in structure. Another supporting piece of evidence is that for $|Ru_6C(CO)_{15}(P(OMe)_3)_2|$, Brown[67] has deduced that the major solution isomer is the cis- not the trans-isomer one would expect from steric considerations. Incidentally, the product from the attack at the bridging carbonyl in the solid state structure of $|Ru_6C(CO)_{16}PPh_2Et|$ should be the cis-isomer.

This lower first activation energy for Ru_6 and Ru_5 carbide clusters allowed the preparation of $|Ru_6C(CO)_{16}\{PPh_2(CH_2)_2Si(OEt)_3\}|$ (28) and $|Ru_5C(CO)_{14}\{PPh_2(CH_2)_2Si(OEt)_3\}|$ (27), though purification by flash chromatography in both cases showed the presence of some disubstituted product which was not evident from the i.r. spectra of the unpurified products. Brown and Evans[63] have anchored $|Ru_6C(CO)_{1}-|$ onto phosphinated silica and obtained the monosubstituted product which on mild heating converted to the disubstituted species, by reacting with the excess phosphines present on the surface. Similarly it was found that when $|Ru_5C(CO)_{15}|$ was reacted with phosphinated

alumina under conditions used to obtain monosubstitution, the monosubstituted anchored product was initially obtained but this on standing reacted with residual phosphine to produce traces of the disubstituted product detectable in the i.r. (see Figure 4.7). This problem of residual phosphine was overcome by reacting (28) and (27) with the unfunctionalised oxides (see Figures 4.11 and 4.10) and these red/brown and purple oxides, respectively, gave i.r. spectra in close agreement with those of the monosubstituted solution analogues.

The preparation of the monosubstituted Ru_3 and Ru_4 clusters represents a problem as the yield of the monosubstituted product is poor for the thermal reaction.[68] A moderate yield synthesis has been reported[81] for the monosubstituted product of PPh_3 and $|H_4Ru_4(CO)_{12}|$. However, when it was repeated heterogeneously with phosphinated silica or γ-alumina more than one product was obtained as can be seen by comparing the ν_{CO} bands in the i.r. spectrum (see Figure 4.6) with those of $|H_4Ru_4(CO)_{12-n}(PPh_2Et)_n|$, (n = 1, 2, 3, see Chapter 5) in cyclohexane. The weak absorptions at 2 092 and 2 083 cm^{-1} correlate well with the bands observed for the monosubstituted product. There are many coincidences between the absorptions of the different substitution products but the presence of the strong broad absorption at 1 990 cm^{-1} indicates there is probably also an appreciable concentration of the trisubstituted product. This synthesis failed partially because $PPh_2(CH_2)_3Si(OEt)_3$ is more reactive than PPh_3[63] and also because of a template effect on the anchored cluster. That is the anchored cluster is held in position to react with

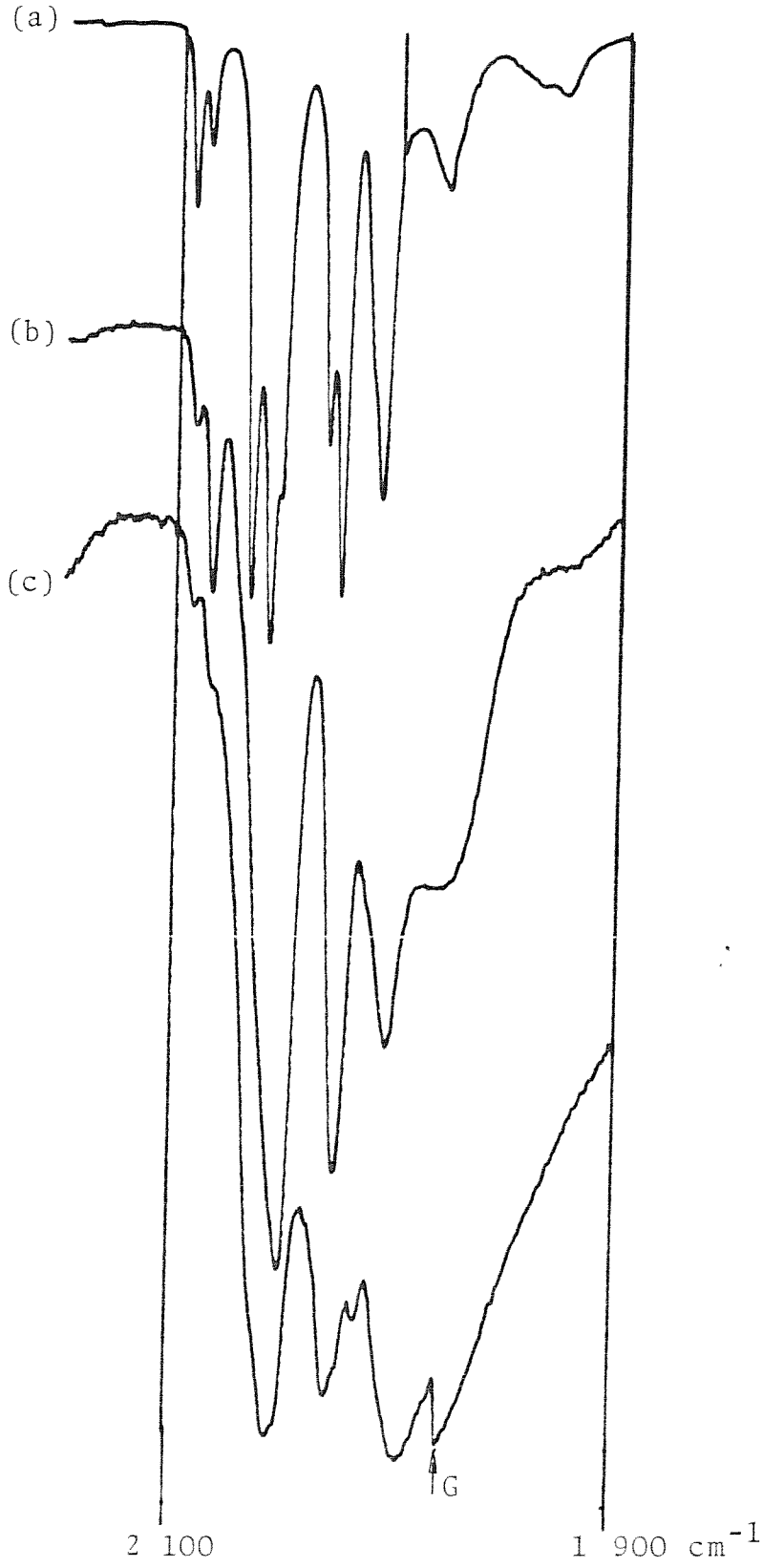

Figure 4.6. I.r. spectra of (a) $[H_4Ru_4(CO)_{11}PPh_2Et]$ in cyclohexane, (b) Nujol mull of the product from $[H_4Ru_4(CO)_{12}]$ with phosphinated silica by the photochemical method, and (c) Nujol mull of the product from $[H_4Ru_4(CO)_{12}]$ with phosphinated silica by the thermal method (G = Grating change).

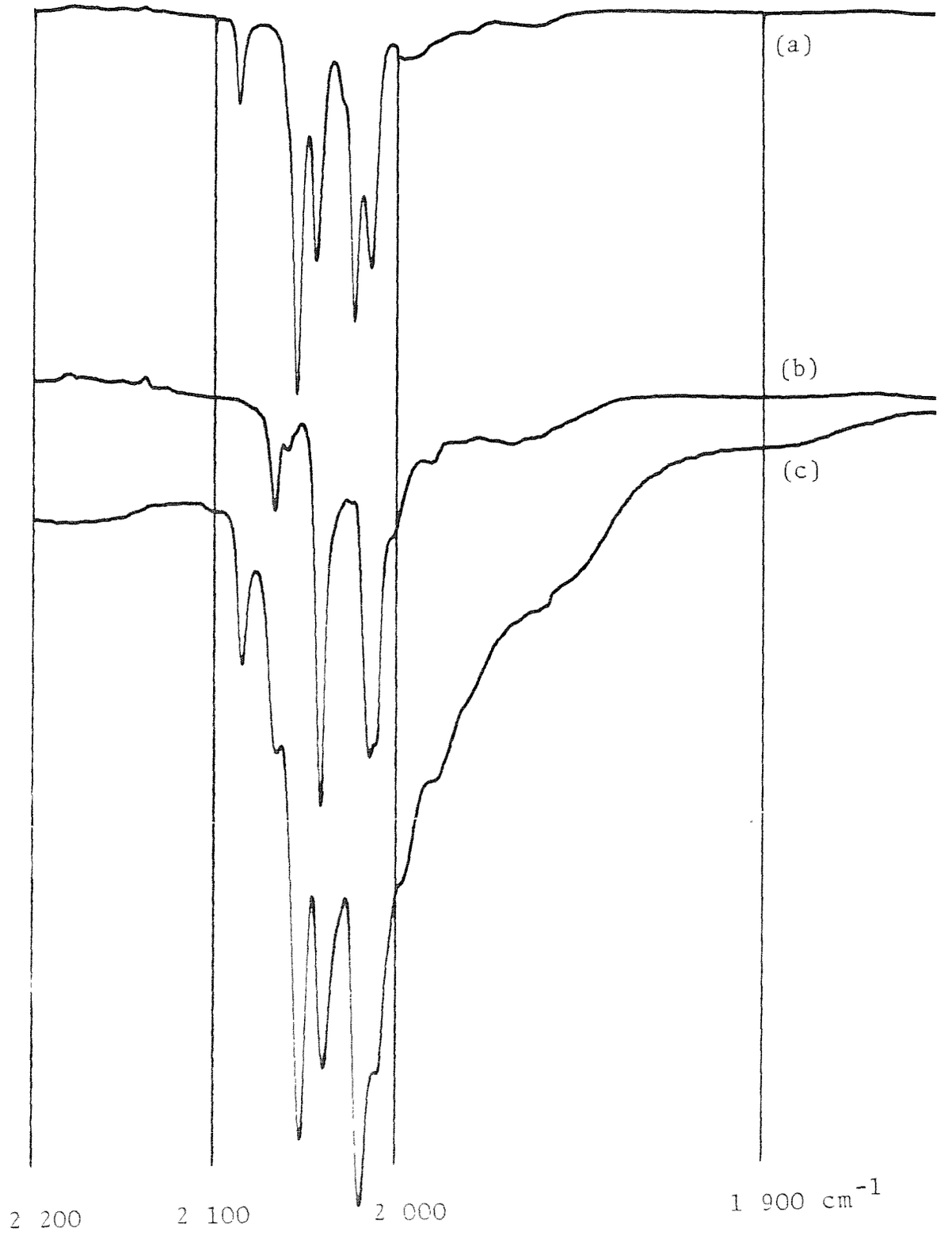

Figure 4.7. I.r. spectra of, (a) $[Ru_5C(CO)_{14}PPh_2Et]$ and (b) $[Ru_5C(CO)_{15}(PPh_2Et)_2]$, in cyclohexane, and (c) the product of reacting $[Ru_5C(CO)_{15}]$ with phosphinated alumina under the conditions for monosubstitution, (Nujol mull).

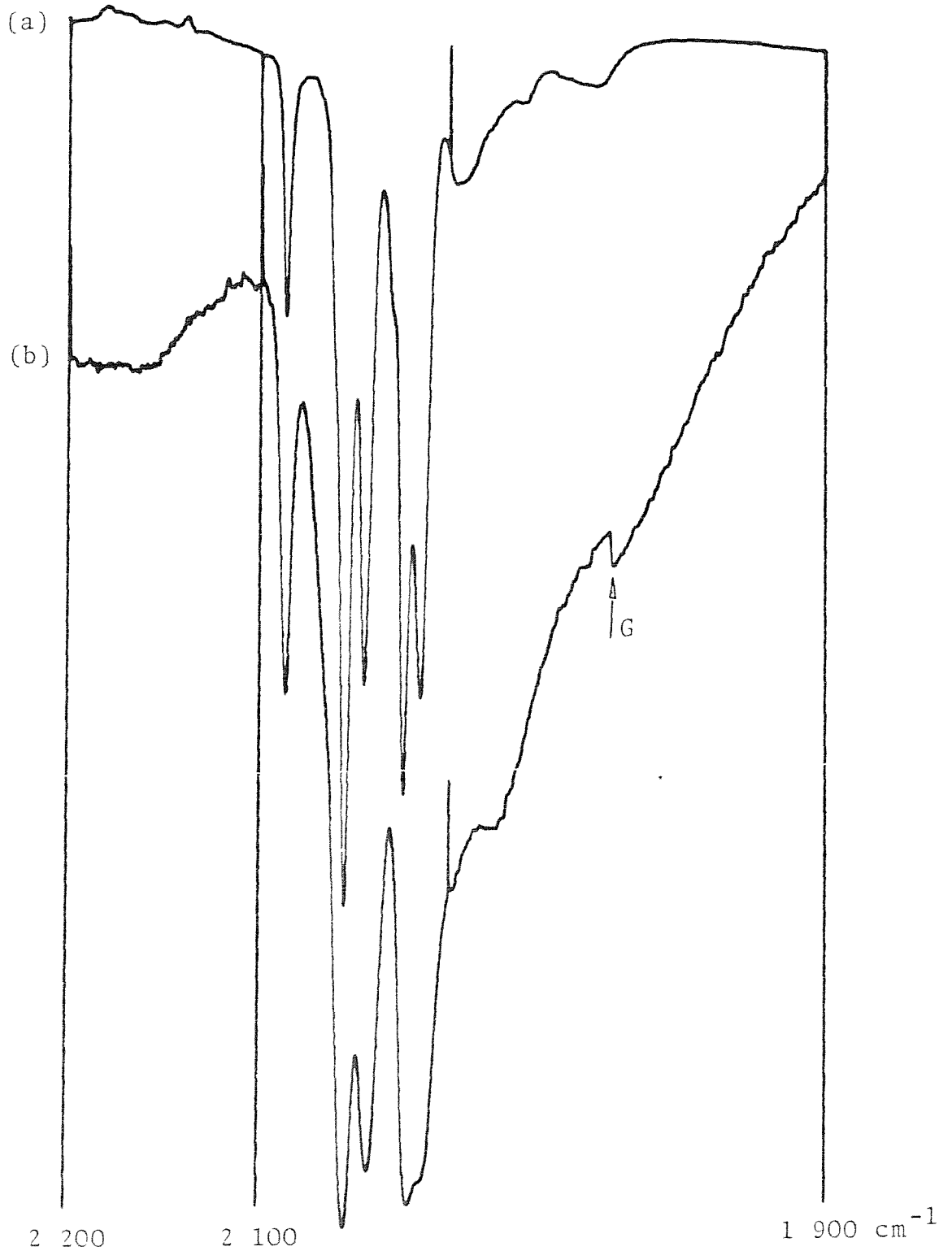

Figure 4.10. I.r. spectra of (a) $Ru_3C(CO)_{14}\{PPh_2(CH_2)_2Si(OEt)_3\}$ (27) in cyclohexane, and (b) a Nujol mull of (27) + γ-Al_2O_3. (G = Grating change).

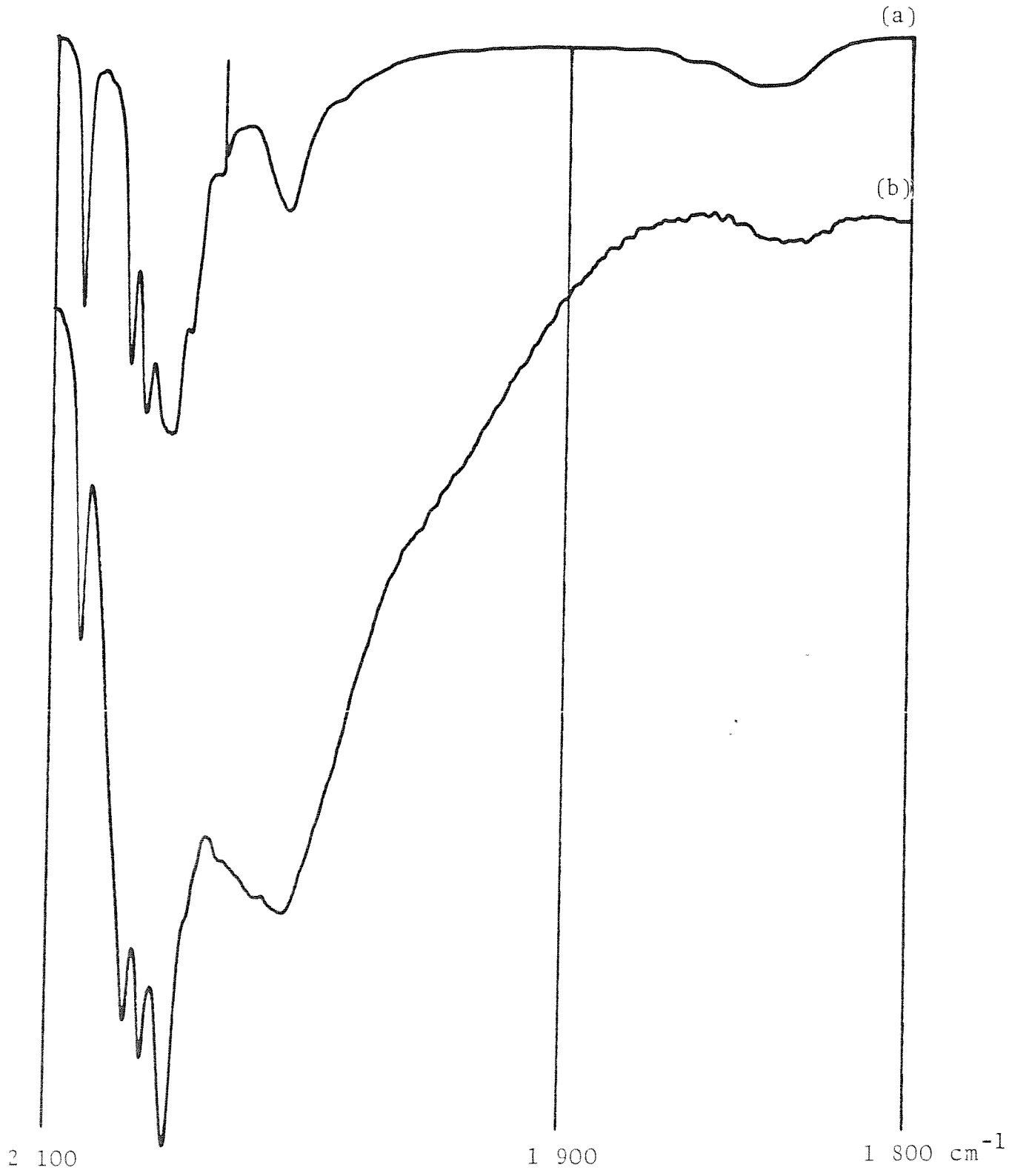

Figure 4.11. I.r. spectra of (a) $[Ru_6C(CO)_{16}\{PPh_2(CH_2)_2Si(OEt)_3\}]$ (28) in cyclohexane, and (b) a Nujol mull of (28) + γ-Al_2O_3, the approximate contribution by the alumina background is shown by the dotted line.

any other neighbouring free phosphines. It is interesting that the control of thermal substitution has been partially effected on phosphinated polystyrene divinylbenzene copolymers by altering the polymer structure.[60]

Photochemical induced anchoring was attempted on phosphinated silica and γ-alumina under conditions reported to afford quantitatively $|Ru_4H_4(CO)_{11}PPh_3|$ even with a large excess of PPh_3.[82] A substantially longer irradiation time was required to give reasonably strong ν_{CO} bands than to cause monosubstitution in solution (35 rather than 7 minutes). The spectra initially differed from those obtained by the thermal reaction (see Figure 4.6) with the bands at 2 092 and 2 083 cm^{-1} being markedly more intense. All the bands could be assigned assuming a mixture of mono- and di-substituted products. On standing for several weeks the spectra of these two materials converted into that obtained for the thermal reaction indicating the presence of residual phosphine. Whilst the anchoring of the tetraruthenium cluster had been achieved on silica and alumina by these two routes the lack of specificity was undesirable.

Recently a novel method of introducing a variety of 2e donor ligands into metal clusters in specific, stepwise reactions has been reported[20] using a radical catalysed reaction similar to those seen in organic systems. For example, the chain reaction for $|Ru_3(CO)_{12}$ is thought to occur by equations (i), (ii), and (iii).

$$|Ru_3(CO)_{12}| + Ph_2\dot{C}O^- \longrightarrow |Ru_3(CO)_{12}|^{\cdot -} + Ph_2CO \qquad (i)$$

$$|Ru_3(CO)_{12}|^{\cdot -} + L \longrightarrow |Ru_3(CO)_{11}L|^{\cdot -} + CO \qquad (ii)$$

$$|Ru_3(CO)_{11}L|^{\cdot -} + |Ru_3(CO)_{12}| \longrightarrow |Ru_3(CO)_{11}L| + |Ru_3(CO)_{12}|^{\cdot -} \qquad (iii)$$

The reactive species is thought to be the radical anion $|Ru_3(CO)_{12}|^{\cdot -}$ which is generated by adding a solution of sodium diphenylketyl to the cluster. The excess electron in this species is possibly in a Ru-Ru antibonding orbital and this would lead to a weakened Ru-Ru bond. Cleavage of which would give rise to a 17e Ru centre which could react with the ligand and then by reformation of the Ru-Ru bond and ejection of CO (see equation (ii)) would give $|Ru_3(CO)_{11}L|^{\cdot -}$. If the incoming ligand is less π acidic than CO the electron transfer from the substituted to the unsubstituted cluster would be favoured (see equation (iii)) and this new unsubstituted cluster radical anion could continue the catalytic cycle. This type of reaction has been shown to be general for systems in which; (a) the radical cluster anion can be formed and has sufficient stability to react without fragmentation, (b) the incoming ligand is a poorer π acceptor than the replaced CO and (c) the ligand does not react with the Ph_2CO or $Na^+Ph_2\dot{C}O^-$.

Using this method together with flash chromatography, $|Ru_3(CO)_{11}\{PPh_2(CH_2)_2Si(OEt)_3\}|$ (25) and $|H_4Ru_4(CO)_{11}\{PPh_2(CH_2)_3Si(OEt)_3\}|$ (26) were made in good yield. Normally clusters such as (25) with a silane ligand do not give a mass spectrum even with a direct probe insert, due to involatility and cluster decomposition on heating. A technique which offers a way around this is fast atom bombardment in which

atoms such as Xe are accelerated using charge-exchange processes (e.g. $Xe^{+\cdot}$ (fast) + Xe (thermal) $\rightarrow$ Xe (fast) + $Xe^{+\cdot}$ (thermal)) and directed at the sample mounted in a suitable media on a metal plate. When they impinge onto the plate their kinetic energy is dissipated in various ways some of which lead to volatilisation and ionisation of the sample. The electric gradient from the plate was arranged in the case of (25) to give positive ions, produced by the bombardment of (25) in the acidic solvent (diamylphenol), directed at the analyser of the mass spectrometer and the positive parent ion, $|HRu_3(CO)_{11}\{PPh_2CH_2CH_2Si(OEt)_3\}|^+$, at 990 a.m.u. (for Ru) was observed (see Figure 4.12).

On reacting (25) and (26) with oxides, yellow powders were obtained which exhibited i.r. spectra in close agreement with those of their homogeneous analogues (see Figures 4.8 and 4.9, respectively).

In order to characterise the supported analogues of (25) - (28) more fully, diffuse reflectance u.v.-visible spectra were run on the SiO_2 supported species (silica has the least background of any of the oxides). As can be seen, (Figures 4.13 and 4.14), there is a fairly close agreement with those obtained for the solution analogues. The spectra, however, do differ in two main points, that is a peak due to silica is seen at the high energy end of the spectrum (< 210 n.m.) and that the cluster peaks for the heterogenerous case in this region are weakened with respect to the solution spectra. This could be due to a lower sensitivity of diffuse reflectance compared to solution u.v.-visible spectroscopy in this region.

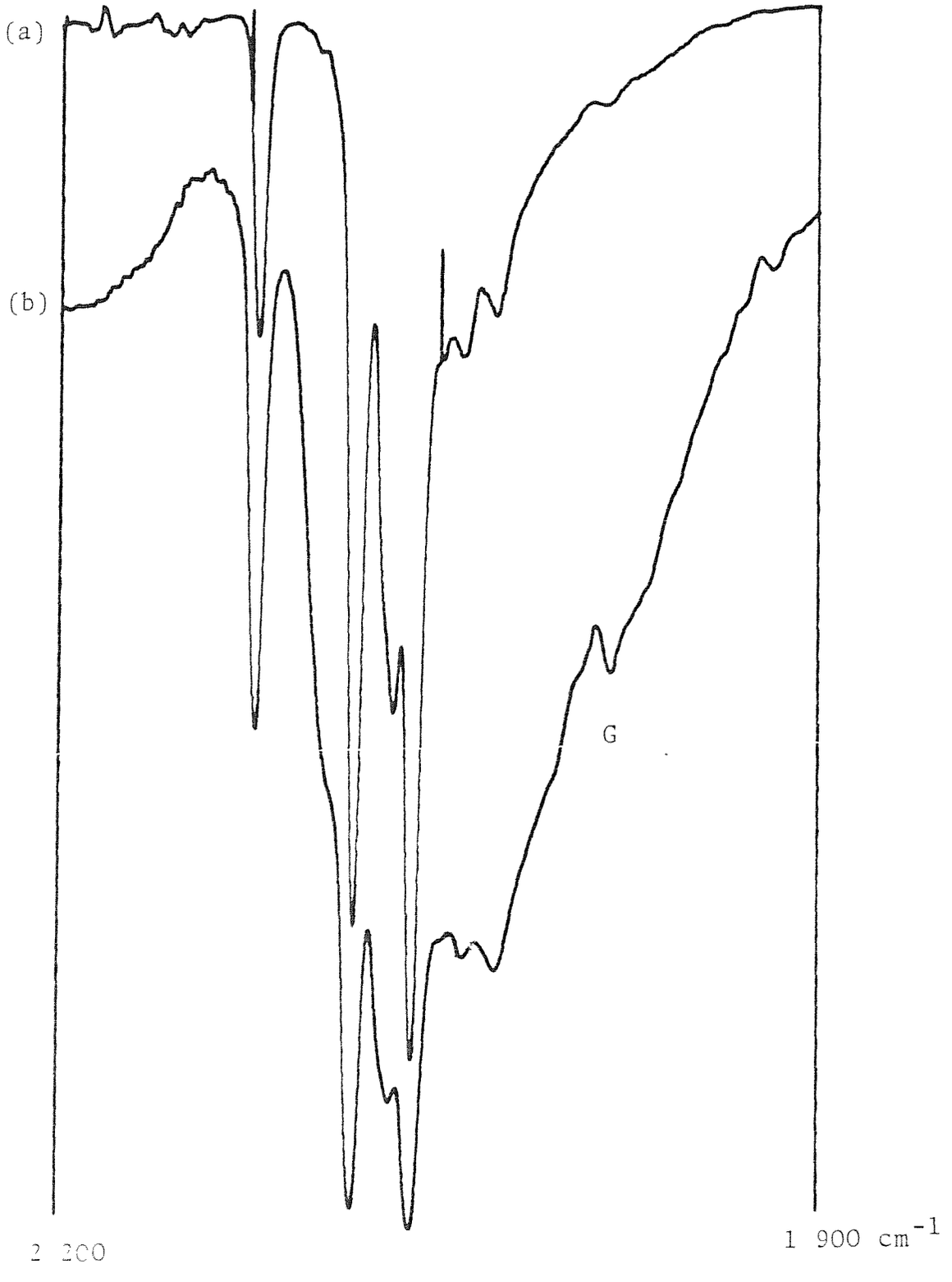

Figure 4.8. I.r. spectra of, (a) $Ru_3(CO)_{11}\{PPh_2(CH_2)_2Si(OEt)_3\}$ (25) in cyclohexane, and (b) Nujol mull of (25) + γ-Al_2O_3. (G = Grating change).

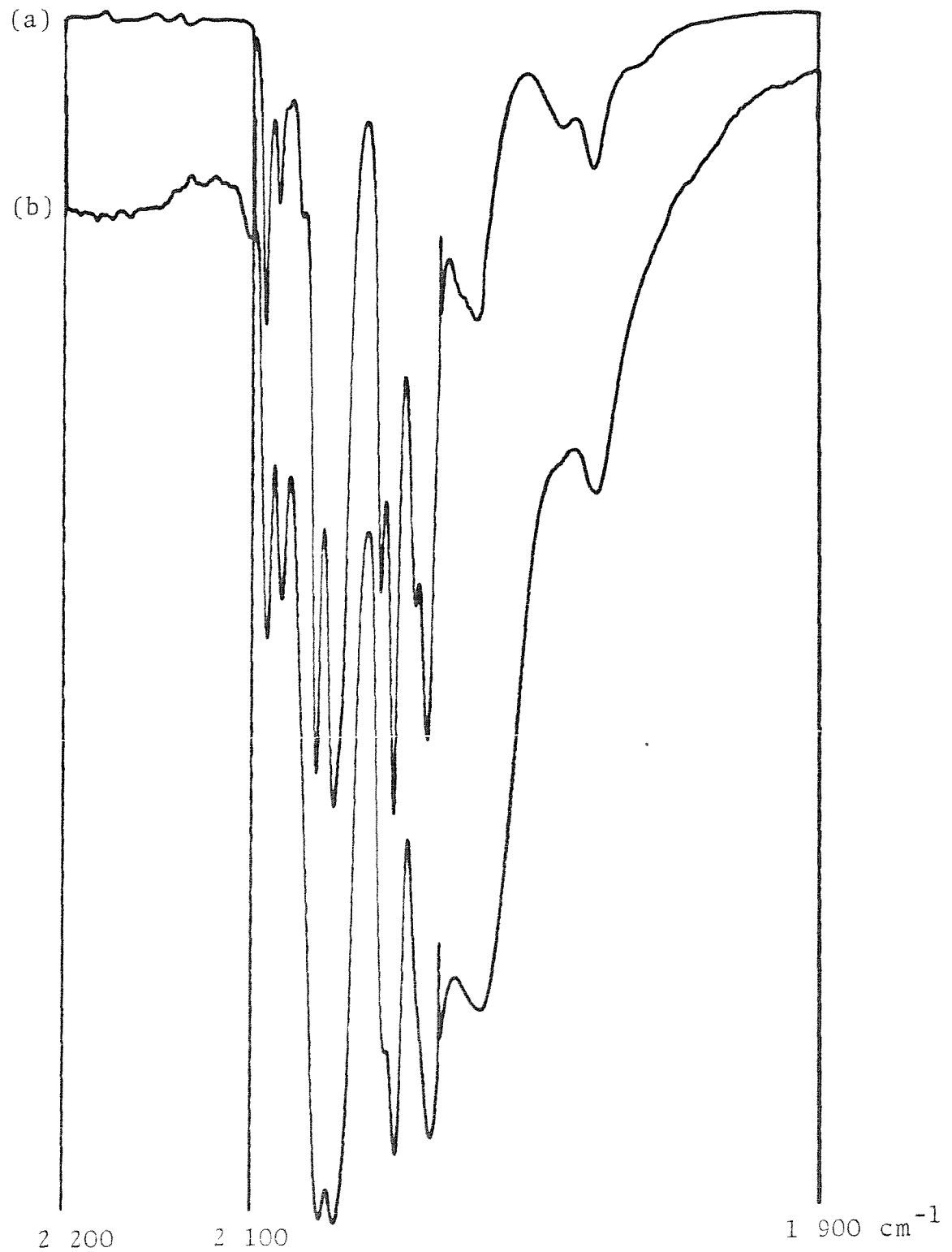

Figure 4.9. I.r. spectra of (a) $[H_4Ru_4(CO)_{11}\{PPh_2(CH_2)_2Si(OEt)_3\}]$ (26) in cyclohexane, and (b) a Nujol mull of (26) + γ-Al_2O_3.

$Ru_3(CO)_{11}\{PPh_2CH_2CH_2Si(OEt)_3\}$

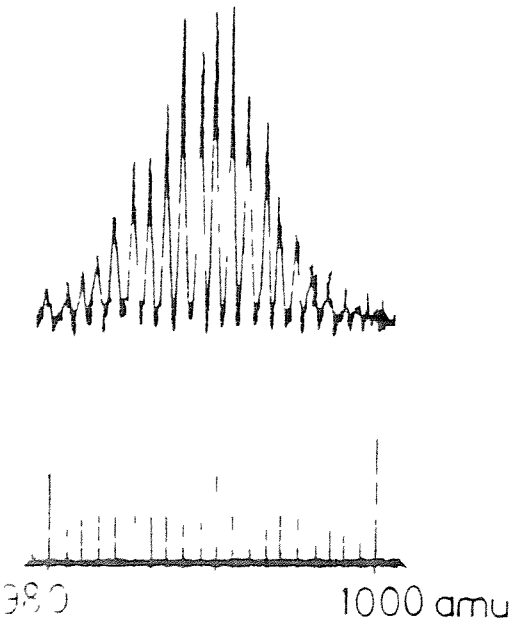

Xe - fab

Figure 4.12

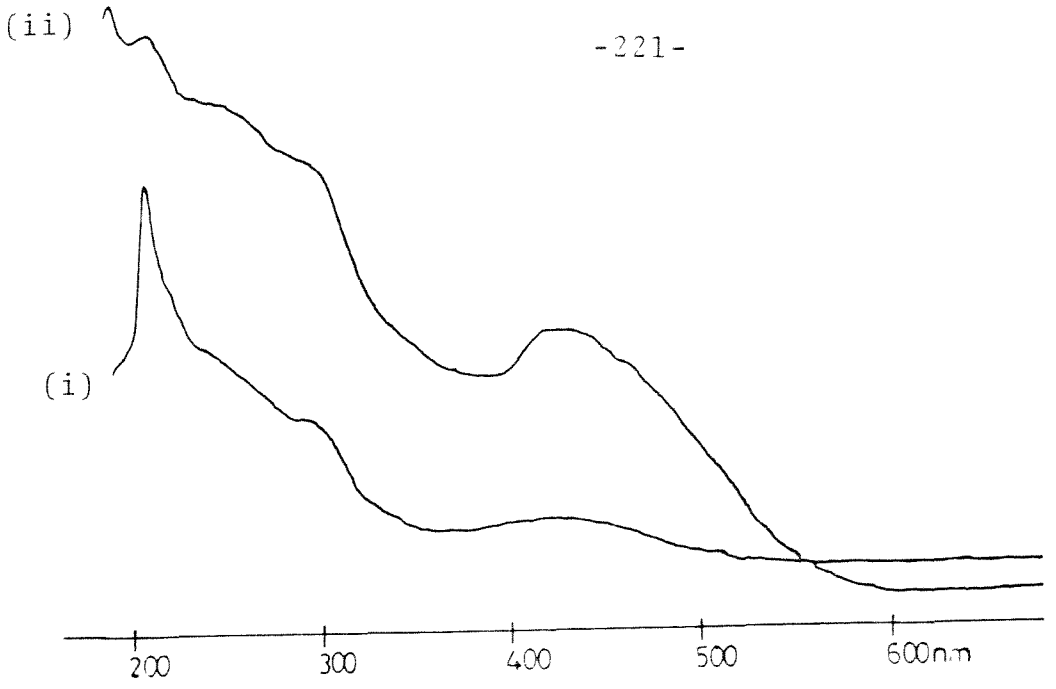

U.v. visible spectra of (i) $[Ru_3(CO)_{11}\{PPh_2(CH_2)_2Si(OEt)_3\}]$ (25) in cyclohexane (solution spectrum, and (ii) (25) on Aerosil 380 (Diffuse reflectance spectrum)

Figure 4.13

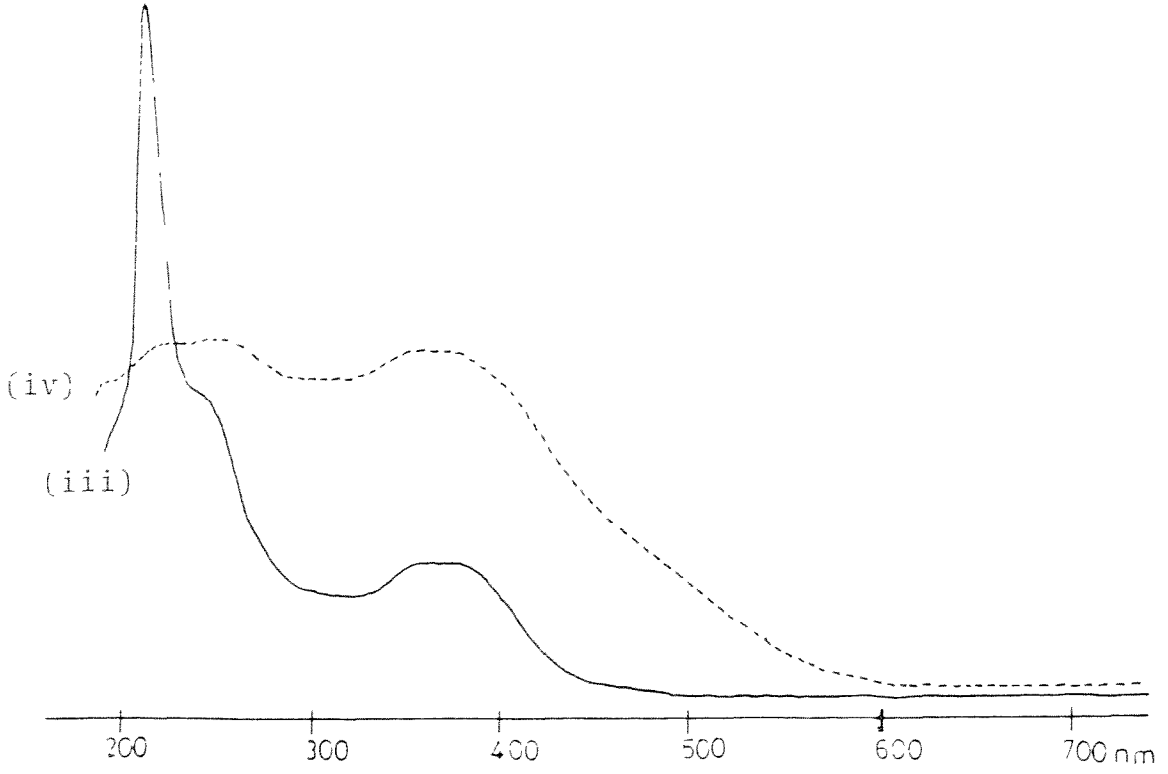

U.v. visible spectra of (iii) $[H_4Ru_4(CO)_{11}\{PPh_2CH_2CH_2Si(OEt)_3\}]$ (26) in cyclohexane, and (iv) (26) on Aerosil 380 (Diffuse reflectance).

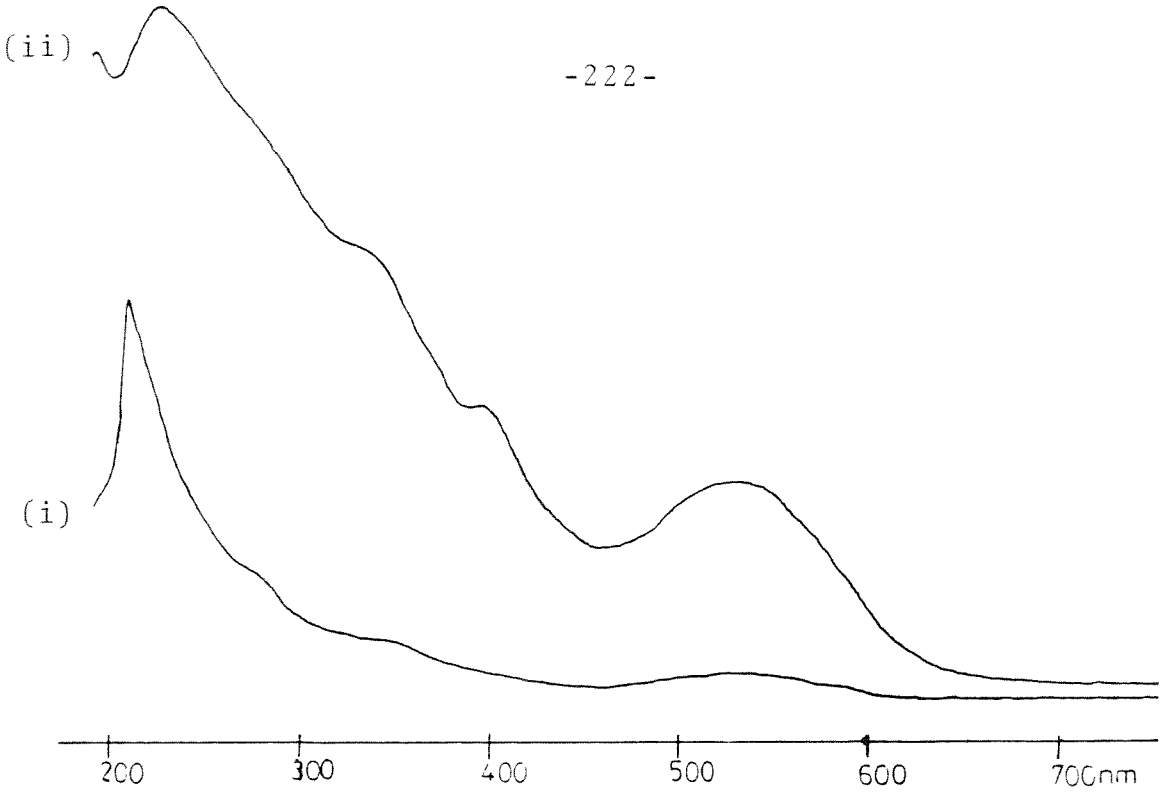

U.v. visible spectra of (i) $[Ru_5C(CO)_{14}\{PPh_2(CH_2)_2Si(OEt)_3\}]$ (27) in cyclohexane, and (ii) (27) on Aerosil 380 (Diffuse reflectance).

Figure 4.14

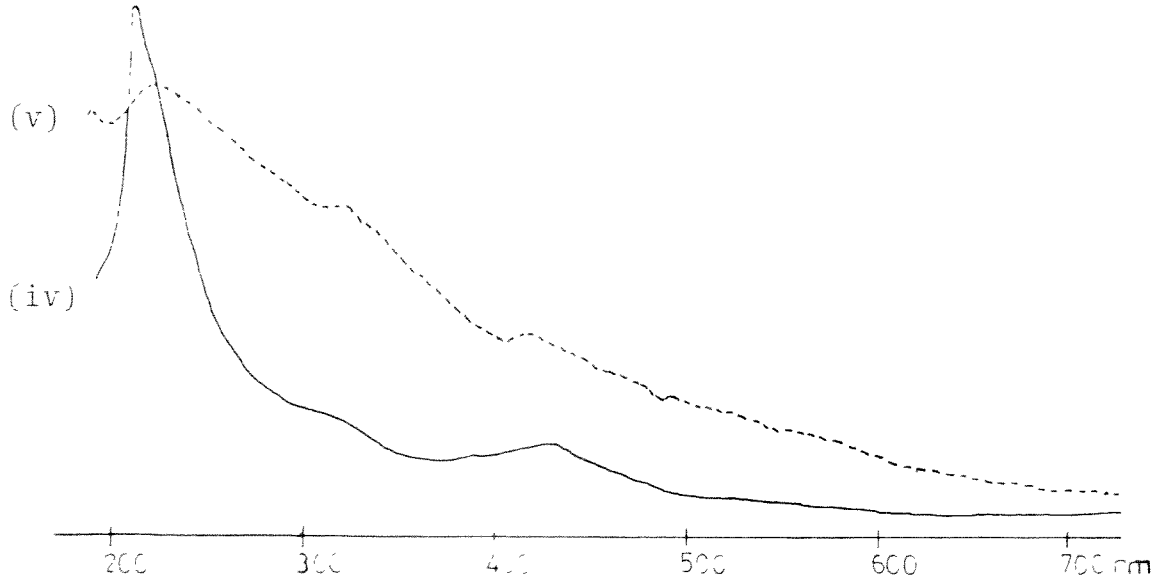

U.v. visible spectra of (iv) $[Ru_6C(CO)_{16}\{PPh_2(CH_2)_2Si(OEt)_3\}]$ (28) in cyclohexane, and (v) (28) on Aerosil 380 (Diffuse reflectance).

Conclusion

As can be seen from the results for amine and isocyanide ligands, the tethering of complexes to oxides via ligands can have complications due to the hydroxyl groups and the acidic and basic sites on the support surface together with possible interactions with the silyl group of the ligand. These caused the amine cluster to change its identity to new unstable clusters which prevented the preparation of the intended bridging and capping clusters. Similarly the desired $|HOs_3(CO)_9(\mu_3\text{-}\eta^2\text{-}HC{=}NR)|$ cluster was unobtainable due to similar reactions which caused a catalysed isomerisation of $|H_2Os_3(CO)_{10}CNR|$ to $|HOs_3(CO)_{10}CN(H)R|$ on anchoring or heating.

The anchoring of the $|Os_3(CO)_{11}CNR|$ cluster was successful but the cluster unfortunately turned out to be inactive towards pentene isomerisation. The anchoring of the alkylidyne tricobalt nonacarbonyl cluster, $|Cl_3SiCCo_3(CO)_9|$ was also successful but unfortunately the -I electronic effect on the oxide transmitted through the apical substituent rendered the clusters inactive towards pentene isomerisation. However, the presence of a CO atmosphere appears to stabilise these clusters and so should make them suitable candidates for hydroformylation catalysis, particularly if the option of modifying the silane with a +I group is used.

The application of flash chromatography and radical anion catalysed substitution reactions to prepare mono-substituted ruthenium silyl phosphine clusters of varying nuclearity (3 → 6) and the subsequent reaction of these with oxides to produce discrete anchored clusters of known structures

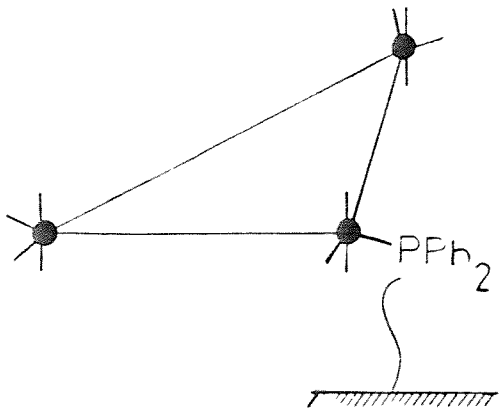

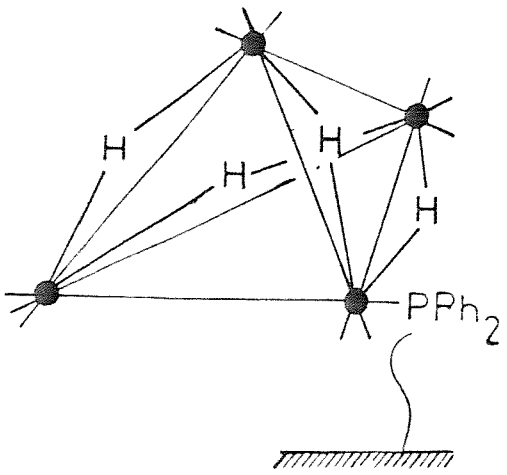

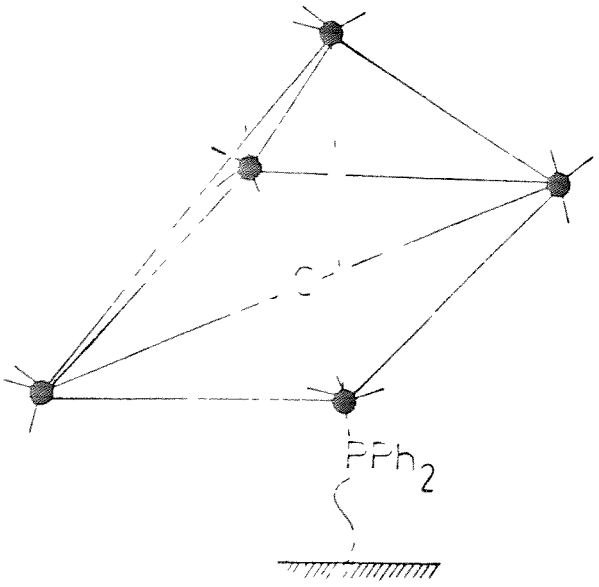

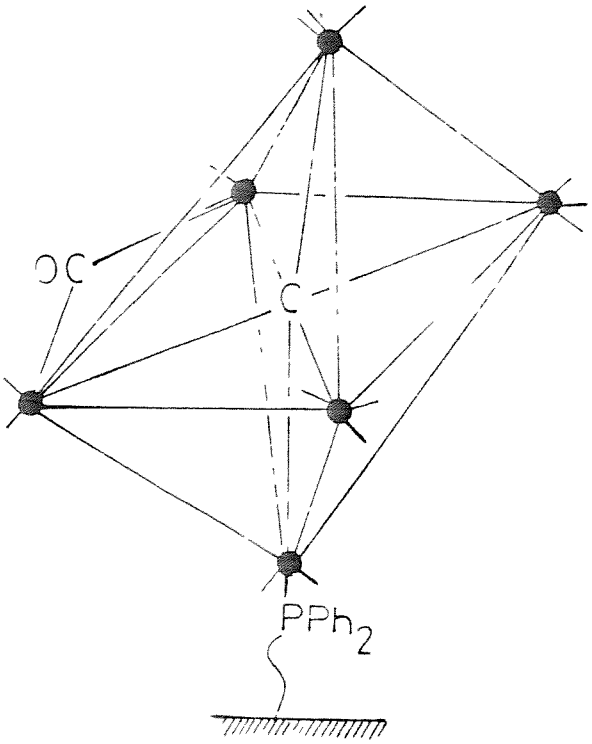

Diagram 4.1.

(e.g. $|Ru_3(CO)_{11}PPh_2R|$,[74] $|Ru_4(H)_4(CO)_{11}PPh_2R|$,[43] $Ru_5C(CO)_{14}$-$PPh_2R|$[79] and $|Ru_6C(CO)_{16}(PPh_2R)|$[63] were R = $(CH_2)_2Si(OEt)_{3-x}$-$(O\text{-}M'O_n)_x$, see diagram 4.1) demonstrates several important points. Most importantly flash chromatography offers a powerful new means of purifying silanated clusters so the anchoring of clusters to surfaces is no longer limited to "clean" reactions and secondly the sodium diphenyl ketyl reaction offers the possibility of expanding ligand anchoring to other systems. For example, $|Ru_3(CO)_{12}|$, $|Fe_3(CO)_{12}|$ and $|H_4Ru_4(CO)_{12}|$ with $CN(CH_2)_3Si(OEt)_3$ should provide fairly straightforward systems. This anchoring specifically of a range of preformed complexes of varying nuclearity should offer the possibility of investigating particle size effects on the chemistry of supported metals but unfortunately time ran out before this could be investigated.

The application of fast atom bombardment offers a new means of characterising these phosphinated silyl clusters. The compound tested, $|Ru_3(CO)_{11}\{PPh_2CH_2CH_2Si(OEt)_3\}|$ is the most unstable of the series and so this technique should be applicable to the others (i.e. $|Ru_4(H)(CO)_{11}P|$, $|Ru_5C(CO)_{14}P|$ and $|Ru_6C(CO)_{16}P|$, P = $PPh_2(CH_2)_2Si(OEt)_3$), and it may find some applications in desorbing supported clusters. Diffuse reflectance u.v.-visible spectroscopy, though on its own it is not powerful enough to characterise a supported cluster has been shown to offer a useful fingerprint confirmation of the supported species.

Experimental

Reactions of $|Os_3(CO)_{12}|$ with NH_2Pr^n.

(i) $|Os_3(CO)_{12}|$ (30 mg) and NH_2Pr^n (3 equivalents) were refluxed in N-octane (100 cm^3) for 3 h, cooled, and the solvent removed under reduced pressure to yield a yellow-brown solid.[2] The individual products were obtained by t.l.c. (eluted with 50 % 40-60 petroleum ether and 50 % diethyl ether). This gave two main yellow bands, the major of which was found to be $|Os_3(CO)_{10}(H)(OCN(H)Pr^n)|$ (R.f. 0.8, 60 % yield) and the other which was incompletely separated from the first contained $|Os_3(CO)_{10}(H)\{N(H)Pr^n\}|$ (R.f. 0.77, 5 % yield).

(ii) $|Os_3(CO)_{12}|$ (30 mg) was stirred overnight in neat amine (1 cm^3).[22] The $|Os_3(CO)_{12}|$ as it reacted slowly dissolved to give a bright yellow solution. This together with one pentane (15 cm^3) washing of the unreacted $|Os_3(CO)_{12}|$ was concentrated under reduced pressure to yield a yellow solid which was purified by t.l.c. to yield $|Os_3(CO)_{10}(H)\{OCN(H)Pr^n\}|$ (80 % yield based on $|Os_3(CO)_{12}|$ consumed).

(iii) $|Os_3(CO)_{12}|$ (50 mg) dissolved in CH_3CN (100 cm^3) had added dropwise a Me_3NO solution (0.1 mg/cm^3, CH_3CN) until the i.r. spectrum of the parent carbonyl has disappeared. The product $|Os_3(CO)_{11}CH_3CN|$ was purified by t.l.c. (R.f. 0.5; eluted with 40 % $MeCl_2$, 60 % light petroleum; 80 % yield). A cyclohexane (50 cm^3) solution of the acetonitrile was stirred overnight with NH_2Pr^n (2 equivalents), then filtered, the solvent removed in vacuo and the yellow solid purified

by t.l.c. to give one pale yellow product $|Os_3(CO)_{10}(H)\{(OCNCH)Pr^n\}|$ (90 % yield based on $|Os_3(CO)_{11}(CH_3CN)|$).

$|Os_3(CO)_{11}(CH_3CN)|$

I.r./cyclohexane: 2 105(w), 2 053(s), 2 041(s), 2 021(m), 2 000(vs), 1 984(sh), and 1 964(m) cm^{-1}.

^1H n.m.r./$CDCl_3$, 31 °C: δ (p.p.m.) 2.75 (s, 3 H, CH_3).

$|Os_3(CO)_{10}(H)\{OCN(H)Pr^n\}|$ (16)

^1H n.m.r./$CDCl_3$, 31 °C: δ (p.p.m.) 5.76 (br, 1 H, N(H)), 3.15 (m, H_a, $NC(H_a)(H_b)$-), 2.86 (m, H_b, $NC(H_a)(H_b)$-), 1.5 (m, 2 H, $NCH_2\underline{CH_2}$-), 0.8 (t, 2 H, CH_3, $^2J_{HH}$ = 7 Hz) and -14.33 (s, 1 H, Os-H-Os).

Mass spectrum: The parent was observed as expected at 943 a.m.u. (for ^{192}Os) followed by peaks corresponding to eleven successive carbonyl losses.

Analysis: calculated C, 17.9 %; H, 1 %; N, 1.5 %

found C, 18.8 %; H, 2 %; N, 1.4 %.

$|Os_3(CO)_{10}(\mu\text{-}H)(\mu\text{-}N(H)Pr^n)|$ (17)

I.r./cyclohexane: 2 105(w), 2 066(vs), 2 052(s), 2 022(s), 2 004(s), 1 990(s), 1 981(w), and 1 976(vw) cm^{-1}.

^1H n.m.r./$CDCl_3$, 30 °C: δ (p.p.m.) 4.54 (br, 1 H, N-H), 3.0 (m, 2 H, $N\text{-}CH_2$), 1.4 (m, 2 H, $NCH_2\underline{CH_2}$), 0.8 (t, 2 H, CH_3, $^2J_{HH}$ = 7 Hz), and -15.0 (d, 1 H, Os-H-Os, J_{NH} = 3 Hz).

Mass spectrum: This compound gave a parent at 915 a.m.u. (for ^{192}Os) followed by a complex fragmentation pattern.

Preparation of $|Os_3(CO)_{10}(H)\{OCN(H)(CH_2)_3Si(OEt)_3\}|$ (18).

This was carried out as in the reaction between $|Os_3(CO)_{12}|$ and NPr^nH_2 (route iii) except t.l.c. was not used in purification. (18) was purified by pumping on (to remove excess ligand, 0.02 mm Hg, 3 days) and then extracting the product with pentane (leaving behind a yellow polymeric material). Removal of the pentane in vacuo yielded a greasy-yellow solid (18) (30 % yield).

I.r./cyclohexane: 2 108(w), 2 067(vs), 2 056(s), 2 023(vs), 2 012(s), 1 994(m), 1 978(w), and 1 949(w) cm^{-1}.

^1H n.m.r./$CDCl_3$, 31 °C: δ (p.p.m.) 5.76 (br, 1 H, N-H), 3.8 (q, 6 H, OCH_2, J_{HH} = 7 Hz), 3.2 (m, H_a, N-(CH_aH_b)-), 1.7 (m, 2 H, NCH_2CH_2), 1.2 (t, 9 H, OCH_2CH_3, J_{HH} = 7 Hz), 0.7 (t, 2 H, $SiCH_2$. J_{HH} = 7 Hz), and -14.28 (s, 1 H, Os-H-Os).

Preparation of aminated silica

Aerosil 380 (10 g, predried) and $NH_2(CH_2)_3Si(OEt)_3$ (3 cm^3) in toluene (100 cm^3) were refluxed with stirring for ten hours. After cooling and filtration the resultant white powder was Soxhlet extracted with diethyl ether (15 h) and dried in vacuo (0.1 mm Hg, 48 h) to yield a free flowing white powder with only a faint amine smell.

I.r./in the aerosil 380 window region.

$NH_2(CH_2)_3Si(OEt)_3$		Disc of aminated silica
Film between KBr discs		(silica background subtracted)
3 371(br,m)	NH_2 stretch	3 370(vbr,m)
3 294(br,m)	NH_2 stretch	3 290(vbr,m)
3 281(br,m)	NH_2 stretch	3 280-2 980(vbr,w)

3 192(br,m)		
2 975(s)	C-H stretch	2 975 broad feature
2 927(s)	C-H stretch	to
2 887(s)	C-H stretch	2 800 (sloping background)
2 764(w)	C-H stretch	
2 737(w)	for O-CH_2 and N-CH_2	
2 633(vw)		2 500
1 886(br,vw)		
1 596(br,m)	NH_2 bend	1 629-1 515(br)
1 483(m)	C-H deformation	1 472(w)
1 444(m)	C-H deformation	1 445(w)
1 391(m)	CH_3 symmetric deformation	1 409(w)
1 367(w)		1 382(w)

Reaction of $|Os_3(CO)_{12}|$ with aminated silica.

This was carried out in the same three ways as the reaction of $|Os_3(CO)_{12}|$ with Pr^nNH_2 except that the work up involved filtration and washing of the surface with CH_2Cl_2 (3 x 20 cm^3) to remove unanchored cluster.

I.r./Nujol mull:

(i) afforded a pale yellow solid (moderate loading), 2 104(vw), 2 090(m), 2 066(m), 2 046(vs), 2 006(s), 1 987(br,s), and 1 915(br,m) cm^{-1}.

(ii) afforded a very pale solid (very low loading), 2 107(vw), 2 086(vw), 2 065(m), 2 052(sh), 2 042(s), 2 018(sh), 2 005(s), 1 984(br,s), 1 968(sh), 1 943(sh,vw), and 1 930(sh,vw) cm^{-1}.

(iii) afforded a pale yellow solid (low loading), 2 107(m), 2 090(w), 2 066(s), 2 053(s), 2 045(s), 2 021(s), 2 011(s), and 2 000-1 950(br,s) cm^{-1}.

Reaction of $|Os_3(CO)_{10}(H)\{OCN(H)(CH_2)_3Si(OEt)_3\}|$ (18) with γ-Al_2O_3.

(18) (5 mg) was stirred with a γ-Al_2O_3 slurry (100 mg, predried, in CH_2Cl_2) for 2 h at r.t. and then filtered, washed (3 x CH_2Cl_2) and dried in vacuo to afford a yellow powder. I.r./Nujol mull (see Figure 4.1): 2 108(vw), 2 089(w), 2 067(m), 2 056(sh), 2 042(s), 2 023(s), 2 010(vs), 1 983(br,s), 1 967(sh), 1 954(sh), 1 940(br,m), and 1 927(br,m) cm^{-1}.

Preparation of tertiarybutyl isocyanide.[23]

Tertiarybutylamine (30 g) had added to it 2 equivalents of $HCO_2C_2H_5$ dropwise (with stirring and cooling by an ice salt bath) over a period of one hour. The mixture was then refluxed for 4 days and distilled under reduced pressure to yield $(CH_3)_3CN(H)C(H)O$ (70 % yield, B.pt. 67 ^{o}C/1.5 mm Hg) as a colourless liquid.

I.r./film between KBr discs.

3 500(br,s) N-H stretch

3 300(br,s) N-H stretch

3 060(m) N-H stretch

2 970(s) C-H stretch

2 920(s) C-H stretch

2 850(s) C-H stretch

2 750(m) C-H stretch

1 615(vs) C=O stretch or N-H bend

1 490(m) C=O stretch

1 425(m) CH_3 deformation

1 410(m) CH_3 deformation

1 340(m) $(CH_3)_3C$ deformation

1 315(m) $(CH_3)_3C$ deformation

^1H n.m.r./$CDCl_3$: δ (p.p.m.) 8.0 (d, 1 H, C(O)-H, J_{H_NH} = 6 Hz), 7.4 (br, 1 H, N-H), and 1.4 (s, 9 H, $C(CH_3)_3$).

Tertiarybutylformanide (30 g) was added dropwise (over 30 minutes) to a stirred solution of P-toluene sulphonyl chloride (50 g) and quinoline (155 g) at 50 - 60 °C under vacuum (0.1 mm Hg). The product distilled off as it was produced and was collected in a liquid nitrogen cooled receiver. Tertiarybutyl isocyanide is a foul smelling colourless liquid which freezes at 0 °C.

I.r./film between KBr discs.

2 960(s) C-H stretch

2 945(w) C-H stretch

2 140(vs) RN≡C stretch

1 470(w) C-H deformation

1 460(w) C-H deformation

1 360(m) $(CH_3)_3C$ deformation

1 235(m)

1 215(m)

^1H n.m.r./$CDCl_3$: δ (p.p.m.) 1.4 (s, 9 H, CH_3).

Preparation of $CN(CH_2)_3Si(OEt)_3$.[31]

$(EtO)_3Si(CH_2)_3NH_2$ was converted into the formamide by repeating the preparation of the tertiarybutylformamide. The silyanated amine took only 3 hours to complete the reaction (the temperature of the reflux increases as the ethylformate is consumed). The product was distilled over under reduced pressure (0.1 mm Hg, 126 °C) as a colourless oil (60 % yield). ^1H n.m.r./$CDCl_3$, 31 °C: δ (p.p.m.) 8.0 (d, 1 H, C(O)(H), H_{H_NH} = 5 Hz), 7.45 (m, 1 H, N-H), 3.8 (=, 6 H, OCH_2, J_{HH} = 7 Hz), 3.5 (m, 2 H, NCH_2), 1.8 (m, 2 H, $NCH_2\underline{CH_2}$), 1.3 (t, 9 H, $OCH_2\underline{CH_3}$, J_{HH} = 7 Hz) and 0.75 (t, 2 H, $SiCH_2$, J_{HH} = 7 Hz).

$(EtO)_3Si(CH_2)_3N(H)C(H)O$ (0.1 mole) had added to it 1.2 equivalents of PPh_3, NEt_3, and CCl_4 all in dichloromethane (100 cm^3). The mixture was refluxed (2.5 h, 65 °C) and the solvent removed under reduced pressure to yield a yellow oil. This was extracted with light petroleum ether (5 x 10 cm^3) and the product was obtained by fractional distillation of this elutant as a colourless foul smelling viscous liquid (10 % overall yield, B.pt. 80 - 90 °C/0.1 mm Hg).
I.r./see later.
^1H n.m.r./$CDCl_3$: δ (p.p.m.) 3.8 (q, 6 H, $O\underline{CH_2}$, J_{HH} = 7 Hz), 3.12 (tt, 2 H, N-CH_2, J_{HH} = 7 Hz, J_{NH} = 2 Hz), 1.8 (m, 2 H, $NCH_2\underline{CH_2}$), 1.3 (t, 9 H, $OCH_2\underline{CH_3}$, J_{HH} = 7 Hz), and 0.75 (t, 2 H, $SiCH_2$, J_{HH} = 8 Hz).

Preparation of isocyanide liganded silica.

$(EtO)_3Si(CH_2)_3NC$ (2 g) and Aerosil 380 (10 g were refluxed

in toluene for 6 h, filtered, Soxhlet extracted (Et_2O, 3 h), and dried in vacuo (0.1 mm Hg, 48 h) to yield a white free flowing powder.

I.r. (see Figure 4.2).

Film of free ligand between KBr discs		disc of liganded silica
2 976(s)	C-H stretch	2 980(m)
2 928(s)	C-H stretch	2 930(m)
2 889(s)	C-H stretch	2 895(m)
2 765(w)	NCH_2 C-H stretch	2 773(w)
2 737(w)	OCH_2 C-H stretch	2 742(w)
	physisorbed NC stretch	2 175(vs)
2 149(vs)	free NC stretch	2 148(vs)
1 484(w)	CH_2 or CH_3 deformations	1 485(w)
1 -47(m)	CH_2 or CH_3 deformations	1 449(w)
1 417(w)		1 413(vw)
1 392(m)	CH_3 symmetrical deformation	1 393(w)
1 367(w)		1 360(w)
1 351(w)		1 340(w)
1 311(w)		

Preparation of $[H_2Os_3(CO)_{10}]$.

This was carried out as in the literature[24] to yield a purple-black solid in 80 - 90 % yield.

I.r./cyclohexane: 2 111(vw), 2 076(vs), 2 063(s), 2 026(vs), 2 011(s), 1 988(m), 1 972(vw), and 1 957(w) cm^{-1}.

^1H n.m.r./$CDCl_3$, 31 °C: δ (p.p.m.) -11.78 (s, 2 H, Os-H-Os).

Mass spectrum: This compound gave a parent, 854 a.m.u. (for ^{192}Os) followed by ten equally spaced peaks corresponding to consecutive carbonyl losses.

Preparation of $|H_2Os_3(CO)_{10}CNBu^t|$.

This was prepared by literature methods[25] to yield it as a yellow powder in 90 - 95 % yield.

I.r./cyclohexane: ν_{NC} = 2 204(w), ν_{CO} = 2 094(m), 2 070(s), 2 067(s), 2 052(s), 2 036(s), 2 023(m), 2 016(m), 2 006(s), 1 992(sh), 1 988(s), and 1 973(m) cm^{-1}.

^1H n.m.r./CD_2Cl_2, variable temperature: δ (p.p.m.)

30 °C: 1.48 (s, 9 H, CH_3) and -14.8 (s, 2 H, Os-H).

0 °C: 1.48 (s, 9 H, CH_3).

-60 °C: 1.48 (s, 9 H, CH_3), the hydride region shows the presence of two isomers in approximate proportions 6:1. The major isomer gave signals -10.21 (d, 1 H, Os-H, J_{HH} = 4 Hz) and -19.77 (d, 1 H, Os-H-Os, J_{HH} = 4 Hz) and the minor isomer gave signals -9.84 (d, 1 H, Os-H, J_{HH} = 4 Hz) and -19.73 (d, 1 H, Os-H-Os, J_{HH} = 4 Hz).

Mass spectrum: This showed a parent at 959 a.m.u. (for ^{192}Os) followed by peaks due to ten successive carbonyl losses. Interestingly no sign of fragmentation of the isocyanide group is observed.

Preparation of $HOs_3(CO)_9(\mu_2\text{-}CN(H)Bu^t)$.

This was prepared according to the literature.[25]

I.r./cyclohexane: 2 098(m), 2 056(vs), 2 047(s), 2 015(vs), 2 000(s), 1 985(s), 1 977(s), and 1 968(sh,m) cm^{-1}.

^{1}H n.m.r./$CDCl_3$, 31 °C: δ (p.p.m.) 1.49 (s, 9 H, CH_3) and -16.95 (s, 1 H, Os-H-Os).

Mass spectrum: The parent was observed at 931 a.m.u. (for ^{192}Os) followed by peaks due to 9 successive carbonyl losses with also a subsidiary pattern due to fragmentation of the isocyanide group.

Preparation of $|H_2Os_3(CO)_{10}\{CN(CH_2)_3Si(OEt)_3\}|$ (19).

Addition of $CN(CH_2)_3Si(OEt)_3$ to $|H_2Os_3(CO)_{10}|$ occurs readily at r.t. as observed[25] for other isocyanides to yield (19).

I.r./cyclohexane: ν_{CN} = 2 221(m), ν_{CO} = 2 099(m), 2 068(s), 2 051(s), 2 031(s), 2 023(m), 2 015(m), 2 005(s), 1 987(br,m), 1 973(m), and 1 924(br,w) cm^{-1}.

^{1}H n.m.r./$CDCl_3$, 0 °C: δ (p.p.m.) 3.98 (t, 2 H, $CN-CH_2$, J_{HH} = 7 Hz), 3.82 (q, 6 H, $O-CH_2$), 1.84 (m, 2 H, $NCH_2\underline{CH_2}$-), 1.22 (t, 9 H, $OCH_2\underline{CH_3}$), 0.75 (t, 2 H, $SiCH_2$), and the hydride region showed the presence of two isomers in proportions 3:1. The major isomer gave signals at -10.14 (d, 1 H, Os-H, J_{HH} = 4 Hz) and -19.77 (d, 1 H, Os-H-Os, J_{HH} = 4 Hz) and the minor at -9.90 (d, 1 H, Os-H) and -19.68 (d, 1 H, Os-H-Os, J_{HH} = 4 Hz).

Preparation of $|HOs_3(CO)_{10}\{CN(H)(CH_2)_3Si(OEt)_3\}|$ (20).

When (19) was heated to 55 °C for 20 minutes it cleanly converted to (20).

I.r./cyclohexane: 2 098(m), 2 055(vs), 2 047(s), 2 015(vs), 2 001(s), 1 986(s), 1 978(s), and 1 969(sh,m) cm^{-1}.

^{1}H n.m.r./$CDCl_3$: δ (p.p.m.) 9.84 (br, 1 H, N-H), 3.9 (q, 6 H, $O\underline{CH_2}$, J_{HH} = 7 Hz and also m, 2 H, NCH_2), 1.9 (m, 2 H, $NCH_2\underline{CH_2}$), 1.22 (t, 9 H, $OCH_2\underline{CH_3}$), 0.8 (t, 2 H, $SiCH_2$) and -16.6 (s, 1 H, Os-H-Os).

Reaction of (19) with oxides.

(19) and the oxide were slurried in CH_2Cl_2 at 0 °C. After 20 minutes - 1 h, all the oxides, after filtering and washing (3 x CH_2Cl_2), had reasonable loadings (except SiO_2). The spectra remained unchanged after refluxing in cyclohexane (2 h, this gave reasonable loadings for SiO_2). The filtrate from this was found to contain ethanol by g.l.c.

I.r./Nujol mull (see Figure 4.3): $M'O_n$ = γ-Al_2O_3, 2 097(m), 2 053(vs), 2 044(s), 2 012(vs), 1 999(br,s), 1 983(br,s), and 1 974(br,s); TiO_2, 2 097(m), 2 053(vs), 2 044(s), 2 013(vs), 1 997(br,s), 1 981(br,s), and 1 973(br,s); SiO_2, 2 099(m), 2 055(vs), 2 047(vs), 2 014(vs), 2 001(br,sh), 1 984(br,s), and 1 976(sh,m); ZnO, 2 097(m), 2 053(vs), 2 044(vs), 2 013(vs), 1 998(br,s), 1 982(br,s), and 1 974(br,s); MgO, 2 096(m), 2 053(vs), 2 043(vs), 2 010(vs), 1 996(br,s), 1 982(br,s), and 1 973(br,s) cm^{-1}.

Reaction of (20) with oxides.

(20) and the oxide were slurried in cyclohexane for 20 - 60 minutes (SiO_2 required refluxing for 2 hours), filtered and washed (3 x CH_2Cl_2).

I.r./Nujol mull: $M'O_n$ =

γ-Al_2O_3, 2 098(m), 2 054(vs), 2 045(s), 2 012(vs), 1 997(br,s), 1 984(br,s), and 1 974(br,s); TiO_2, 2 097(w), 2 052(s), 2 044(w), 2 013(s), 1 997(br,m), 1 986(br,m), and 1 970(br,s); SiO_2, 2 098(m), 2 055(vs), 2 046(vs), 2 014(vs), and 2 000-1 975(vbr,s) cm^{-1}.

Reaction of $|H_2Os_3(CO)_{10}|$ with isocyanide functionalised silica.

A purple solution of $|H_2Os_3(CO)_{10}|$ had added to it small amounts of the oxide until only a faint purple colour remained, after continuing the stirring for 30 minutes, the now yellow solid was recovered by filtration, washed (3 x CH_2Cl_2) and dried in vacuo. Loading from $|H_2Os_3(CO)_{10}|$ consumed = 7 mg/100 mg oxide.

I.r./Nujol mull: 2 098(m), 2 055(s), 2 047(s), 2 015(s), 2 001(s), 1 985(br,s), 1 975(br,s), and 1 960(br,m) cm^{-1}.

Catalysis experiments on homogeneous and heterogeneous analogues of (20).

These were carried out almost exactly as described in Chapter 3. The alterations were the cluster and pentene concentrations which were kept at 4.3 x 10^{-3} and 1 x 10^{-1} M, respectively. The duration of all the experiments was 3 days. See Table 4.1 for results.

Preparation of $Os_3(CO)_{11}CX^tBu|$.

This was prepared according to the literature[26] and after purification by t.l.c. gave a yellow powder (80 % yield).

TABLE 4.1.

Compound	Temp.	Pentene	I.r.	No. of turnovers (per cluster)	Pentene distribution for isomerised pentene cis : trans : 1-pentene
(20)	47 °C	pentene	no change	6	1 : 2.8 : -
		cis-pent-ene	no change	0.8	- : 3 : 1
		trans-pent-2-ene	no change	0.5	all 1-pentene
	80 °C	pent-1-ene	no change	7	1 : 2.5 : -
		cis-pent-2-ene	no change	12	- : 5 : 1
		trans-pent-2-ene	no change	1	all 1-pentene
((20) + γ-Al_2O_3)	47 °C	pent-1-ene	no change	3	1 : 2.5 : -
		cis-pent-2-ene	no change	5	- : 7 : 1
		trans-pent-2-ene	no change	0	
	80 °C	pent-1-ene	slight decomposition to	1	1 : 2.5 : -
		cis-pent-2-ene	give two new bands in	0	
		trans-pent-2-ene	all cases at ~ 110(br)	0	
			and 1 935(br) cm^{-1}.		

I.r./cyclohexane: ν_{CN} = 2 188(br,w), and 2 180(sh,vw), ν_{CO} = 2 160(m), 2 052(s), 2 040(s), 2 020(m), 2 005(m), and 1 980(br,m) cm^{-1}.

^1H n.m.r./$CDCl_3$, 31 °C: δ (p.p.m.) 1.58 (s, 9 H, CH_3).

Mass spectrum: This spectrum exhibited a parent at 955 a.m.u. (for ^{192}Os) followed by eleven peaks due to successive carbon monoxide losses.

Preparation of $|Os_3(CO)_{11}\{CN(CH_2)_3Si(OEt)_3\}|$ (21).

This was prepared in the same way as $|Os_3(CO)_{11}CNBu^t|$, that is $|Os_3(CO)_{11}NCMe|$ was reacted with the isocyanide.[26] However, as t.l.c. could not be used to purify (21) it was purified by taking it up in a small quantity of cold pentane (-40 °C). In doing this about 20 - 30 % of the compound had to be sacrificed with the impurities.

I.r./cyclohexane: ν_{CN} = 2 220(br,w) and 2 199(br,w), ν_{CO} = 2 102(m), 2 068(m), 2 055(s), 2 040(vs), 2 035(m), 2 023(m), 2 016(w), 2 006(s), 2 002(w), 1 990(m), and 1 956(vw) cm^{-1}.

^1H n.m.r./$CDCl_3$, 31 °C: δ (p.p.m.) 4.0 (m, 2 H, N-CH_2), 3.85 (q, 6 H, O-CH_2), 1.9 (m, 2 H, $NCH_2\underline{CH_2}$), 1.24 (t, 9 H, $OCH_2\underline{CH_3}$), and 0.8 (t?, 2 H, $SiCH_2$).

Reaction of (21) with surfaces.

A solution of (21) was added to a slurry of the oxide and stirred for 5 days. It was then filtered, washed (3 x CH_2Cl_2) and dried in vacuo to yield a yellow powder.

I.r./Nujol mull (see Figure 4.4): $M'O_n$ =

γ-Al_2O_3, 2 212(br,w), 2 102(m), 2 068(m), 2 055(s), 2 043(s), 2 036(m), 2 024(m), 2 016(w), and 2 010-1 940(br,s); TiO_2, 2 210(br,w), 2 103(m), 2 067(m), 2 055(s), 2 042(s), 2 036(m), 2 022(m), 2 016(vw), and 2 010-1 950(vbr,s); SiO_2, 2 213(br,vw), 2 101(w), 2 066(w), 2 054(m), 2 040(s), 2 036(w), and 2 120-1 940(br,s) cm^{-1}.

Reaction of $|Os_3(CO)_{11}CH_3CN|$ with isocyanide functionalised silica.

A solution of excess $|Os_3(CO)_{11}CH_3CN|$ (25 mg) was stirred overnight with a slurry of the oxide (100 mg) in CH_2Cl_2, filtered, washed (3 x CH_2Cl_2) and dried *in vacuo* to yield a pale yellow powder.

I.r./Nujol mull: 2 217(br,vw), 2 200(br,vw), 2 102(w), 2 067(w), 2 055(w), 2 039(s), 2 034(w), 2 023(br,m), 2 016(sh), and 2 000-1 950(vbr,s) cm^{-1}.

Preparation of cobalt nonacarbonyl clusters.

These were carried out according to the literature, $|HCCo_3(CO)_9|$,[27] $|Et_3SiCCo_3(CO)_9|$ (22) (Et_3SiH made from EtMgBr and Cl_3SiH), $|Cl_3SiCCo_3(CO)_9|$ (23) and $|(HO)_3SiCCo_3(CO)_9|$ (24).[59]

$|HCCo_3(CO)_9|$.

I.r./cyclohexane: 2 108(w), 2 057(s), 2 042(s), and 2 014(w) cm^{-1}.

^1H n.m.r./$CDCl_3$: δ (p.p.m.) 12 (br, 1 H, C-H).

Mass spectrum: This gave a parent at 442 a.m.u. followed by peaks due to 9 stepwise carbonyl losses.

$|Et_3SiCCo_3(CO)_9|$ (22).

I.r./cyclohexane: 2 101(m), 2 052(vs), 2 039(s), 2 019(m), and 2 004(vw) cm^{-1}.

^1H n.m.r./$CDCl_3$: δ (p.p.m.) 1.2 (br, 9 H, CH_3) and 0.2 (br, 6 H, CH_2).

Mass spectrum: This gave a parent at 556 a.m.u. followed by a pattern demonstrating 9 stepwise carbonyl losses together with fragmentation of the alkyl groups.

$|Cl_3SiCCo_3(CO)_9|$ (23).

I.r./CH_2Cl_2: 2 107(w), 2 058(vs), and 2 041(m) cm^{-1}.

Mass spectrum: Parent at 574 a.m.u.

$|(HO)_3SiCCo_3(CO)_9|$ (24).

I.r./CH_2Cl_2: 2 107(w), 2 059(vs), and 2 042(m) cm^{-1}.

^1H n.m.r./$CDCl_3$: δ (p.p.m.) 2.15 (s, 3 H, SiOH).

Mass spectrum: Parent at 514 a.m.u.

Reaction of (23) with oxides.

In a typical reaction, (23) (5 mg) in CH_2Cl_2 (25 cm^3) was added to a slurry of the surface (100 mg) and stirred at r.t. for 30 minutes (silica required 4 days at r.t. or one hour at reflux under carbon monoxide to obtain a reasonable loading). It was then filtered, washed (Soxhlet extracted, Et_2O, 2 h, under CO) and dried *in vacuo* to afford a purple solid.

I.r./Nujol mull (see Figure 4.5): $M'O_n$ =

SiO_2, 2 109(w), 2 060(m), and 2 043(s); γ-Al_2O_3, 2 105(w), 2 056(vs), and 2 041(s); MgO, 2 106(vw), 2 056(s), and

2 038(m); TiO_2, 2 106(w), 2 056(s), and 2 040(vs); ZnO, 2 106(w), 2 055(s), and 2 044(s); SnO_2, 2 104(w), 2 054(s), and 2 040(s) cm^{-1}.

Catalysis experiments on $|RCCo_3(CO)_9|$.

These were carried out as described in Chapter 3, see Table 4.2 for results.

Preparation of $PPh_2(CH_2)_2Si(OEt)_3$.[28]

A solution of PPh_2H (10 g) and $(EtO)_3SiCHCH_2$ (15 g, 1.5 equivalents) in n-pentane (50 cm^3) was irradiated for 3 days with a 125W Hg lamp (glass filter). The cloudy solution was distilled under reduced pressure to yield as a major product $PPh_2CH_2CH_2Si(OEt)_3$ (70 % yield, 14.2 g) a viscous colourless liquid which freezes on cooling.

I.r.: See later.

^1H n.m.r./$CDCl_3$: δ (p.p.m.) 7.3 (m, 10 H, Ph), 3.8 (q, 6 H, OCH_2), 2.1 (m, 2 H, PCH_2), 1.2 (t, 9 H, CH_3), and 0.7 (m, 2 H, $SiCH_2$).

Mass spectrum: This gave a parent at 376 a.m.u.

Preparation of phosphinated silica[29] and alumina.

$PPh_2(CH_2)_2Si(OEt)_3$ (1 g) was stirred with a sample of the oxide (5 g) in refluxing toluene, while the ethanol-toluene azeotrope was collected using a Dean and Stark apparatus. The oxide was recovered after 6 h by filtration, then Soxhlet extracted for 5 h (Et_2O) and dried in vacuo to give a white free-flowing powder.

TABLE 4.2.

R	Temp.	time	Pentene	i.r. result	G.l.c. result
Cl_3Si	47-48 °C	48 h	pent-1-ene	no change	no catalysis
	47-48 °C	48 h	cis-pent-2-ene	no change	no catalysis
	47-48 °C	48 h	trans-pent-2-ene	no change	no catalysis
	78-80 °C	72 h	pent-1-ene	changed to a 2 peak pattern. Peaks at 2 069(w) and 2 038(w) cm^{-1}.	no catalysis
	78-80 °C	72 h	cis-pent-2-ene	Very slight change, new shoulders at 2 069(sh) and 2 037(sh) cm^{-1}.	no catalysis
	78-80 °C	72 h	trans-pent-2-ene	Extra peaks at 2 069 and 2 037 cm^{-1}.	no catalysis
Et_3Si	47-48 °C	72 h	pent-1-ene	Extra peaks at 2 068(vw) and 2 014(vw)	10 turnovers to trans-pent-2-ene only.
			cis-pent-2-ene	Peaks at 2 068(vw) and 2 014(vw)	no catalysis
			trans-pent-2-ene	no change	no catalysis
H	47-48 °C	72 h	pent-1-ene	no change	isomerisation and polymerisation.
			cis-pent-2-ene	no change	2-3 turnovers (isomerisation (isomerisation)
			trans-pent-2-ene	no change	isomerisation and polymerisation.

I.r. Film of free ligand		Disc of Phosphinated silica (SiO_2 backgound ignored).
3 404(br,vw)		
3 071(m)		3 068
3 054(m)		
2 974(s)	C-H stretch	2 981
2 926(s)	C-H stretch	2 935
2 887(s)	C-H stretch	
1 587(w)	C-H stretch aromatic	1 595
1 572(vw)	C-H stretch aromatic	
1 482(s)	C-H stretch atomatic	1 487
1 435(s)	C-H stretch aromatic	1 440
1 411(w)	P-Ph stretch	1 411
1 391(s) cm^{-1}		

Reaction of $[Ru_4(H_4)(CO)_{12}]$ with phosphinated oxides.

(i) thermal method

A suspension of the oxide was refluxed in a solution of $[Ru_4(H_4)(CO)_{12}]$ (1P:2Ru_4) in light petroleum (40 - 60 ^oC B.pt) for 4 hours. The orange-brown solid was filtered off, washed (3 x CH_2Cl_2) and dried in vacuo.

I.r./Nujol mull (see Figure 4.6): MO_n = SiO_2, 2 092(vw), 2 084(sh,s), 2 054(br,vs), 2 028(s), 2 015(s), and 1 997(vs); γ-Al_2O_3, 2 092(w), 2 084(s), 2 054(br,s), 2 030(s), 2 012(s), and 1 995(vbr,s) cm^{-1}.

(ii) photochemical method

A slurry of the oxide was stirred in a n-pentane solution of $|Ru_4(H_4)(CO)_{12}|$ ($1P:2Ru_4$) and irradiated with 125W mercury lamp with a pyrex filter. The reaction was monitored by removing aliquots of the solid and recording the i.r. spectra as Nujol mulls. Irradiation for 35 minutes was required to afford relatively strong ν_{CO} absorptions.

I.r./Nujol mull (see Figure 4.6): $M'O_n$ = SiO_2, 2 092(w), 2 083(w), 2 062(sh), 2 049(br,vs), 2 024(s), 2 003(m), and 1 990(br,m); γ-Al_2O_3, 2 092(w), 2 082(w), 2 049(br,vs), 2 026(s), 2 002(m), and 1 987(br) cm^{-1}.

These yellow powders darkened over a period of two weeks at r.t. and eventually gave spectra similar to those obtained by the thermal method.

Reaction of $|Ru_3(CO)_{12}|$ with $PPh_2(CH_2)_2Si(OEt)_3$.

$|Ru_3(CO)_{12}|$ (4×10^{-4} mole) and $PPh_2(CH_2)_2Si(OEt)_3$ (4×10^{-4} mole) were dissolved in dry tetrahydrofuran and sodium benzophenone ketyl (1×10^{-3} molar in t.h.f.) was added dropwise until no further reaction on addition occurred (30 seconds between additions). The solvent was removed under reduced pressure and the red solid taken up in light petroleum ether and applied to a flash chromatography column. On eluting with solvents of gradually increasing polarity, first unreacted $|Ru_3(CO)_{12}|$ and then $Ru_3(CO)_{11}PPh_2(CH_2)_2Si(OEt)_3$ (25) was obtained. Drying in vacuo overnight caused crystallisation of the dark orange solid (25) (70 % yield based on $Ru_3(CO)_{12}$ consumed).

I.r./cyclohexane: 2 094(m), 2 043(s), 2 023(s), 2 013(vs), 1 993(m), and 1 984(m) cm^{-1}.

^{1}H n.m.r./$CDCl_3$, 31 °C: δ (p.p.m.) 7.4 (m, 10 H, Ph), 3.75 (q, 6 H, OCH_2), 2.5 (m, 2 H, P-CH_2), 1.2 (t, 9 H, CH_3), and 0.49 (m, 2 H, $SiCH_2$).

^{31}P n.m.r./CH_2Cl_2: 34.11 p.p.m.

Analysis: calculated C, 38.8 %; H, 3.0 %.

found C, 40.0 %; H, 3.3 %.

u.v./cyclohexane: 268(s), 250(sh), 300(sh), and 420(w) n.m.

Preparation of $|H_4Ru_4(CO)_{11}\{PPh_2(CH_2)_2Si(OEt)_3\}|$ (26).

A sample of $|H_4Ru_4(CO)_{12}|$ was reacted and separated in the same way as $|Ru_3(CO)_{12}|$ and $PPh_2(CH_2)_2Si(OEt)_3$. This gave a yellow crystalline solid (26) (60 % yield based on $|H_4Ru_4(CO)_{12}|$ consumed).

I.r./cyclohexane: 2 092(m), 2 086(m), 2 065(s), 2 055(s), 2 030(s), 2 023(a), 2 012(sh), 2 005(s), 1 989(sh,m), 1 967(w), 1 960(m), and 1 947(vw) cm^{-1}.

^{1}H n.m.r./$CDCl_3$, 31 °C: δ (p.p.m.) 7.4 (m, 10 H, Ph), 3.78 (q, 6 H, OCH_2), 2.55 (m, 2 H, PCH_2), 1.9 (q, 9 H, CH_3), 0.6 (m, 2 H, $SiCH_2$) and -17.40 (d, 4 H, Ru-H-Ru, J_{PH} = 3 Hz).

^{31}P n.m.r./CH_2Cl_2: 37.24 p.p.m.

Analysis: calculated C, 38.6 %; H, 3.4 %.

found C, 37.7 %; H, 3.2 %.

u.v./cyclohexane: 210(sh), 240(m), 300(sh), and 370(m) n.m.

Preparation of $|Ru_5C(CO)_{14}\{PPh_2(CH_2)_2Si(OEt)_3\}|$ (27).

A well stirred dilute CH_2Cl_2 solution of $|Ru_5(CO)_{15}|$ was cooled to -40 °C and the i.r. monitored continuously by means of a flow cell. The phosphine also in a cooled dilute CH_2Cl_2 solution was added dropwise (5-15 seconds between additions) until the parent carbonyl had almost wholly been consumed. The solvent was then removed under reduced pressure and the product purified by flash chromatography. This yielded a purple black solid (27) (80 % yield).

I.r./cyclohexane: 2 086(m), 2 054(vs), 2 044(s), 2 023(vs), 2 014(s), 1 996(br,m), 1 980(w), and 1 963(br,w) cm^{-1}.

^1H n.m.r./$CDCl_3$, 31 °C: δ (p.p.m.) 7.3 (m, 10 H, Ph), 3.7 (q, 6 H, OCH_2), 2.5 (m, 2 H, PCH_2), 1.2 (t, 9 H, CH_3), and 0.4 (m, 2 H, $SiCH_2$).

^{31}P n.m.r./CH_2Cl_2: 39.5 p.p.m.

Analysis: calculated C, 32.6 %; H, 2.3 %.

found C, 33.3 %; H, 3.0 %.

u.v./cyclohexane: 208(s), 270(sh), 340(sh), 400(sh), and 530(m) n.m.

Preparation of $Ru_6C(CO)_{16}\{PPh_2(CH_2)_2Si(OEt)_3\}$ (28)

A stirred solution of $Ru_6C(CO)_{17}$ in CH_2Cl_2 (0 °C) had added to it one equivalent of the phosphine. After 24 h at r.t. the solvent was removed under reduced pressure and the product purified by flash chromatography. This gave (28) as a dark brown solid (80 % yield).

I.r./cyclohexane: 2 082(m), 2 053(s), 2 044(s), 2 030(vs), 2 017(sh), 2 002(w), 1 981(br,m), and 1 840(br,w) cm^{-1}.

^{1}H n.m.r./$CDCl_3$, 31 °C: δ (p.p.m.) 7.4 (m, 10 H, Ph), 3.75 (q, 6 H, OCH_2), 2.55 (m, 2 H, PCH_2), 1.2 (t, 9 H, CH_3), and 0.49 (m, 2 H, $SiCH_2$).

^{31}P n.m.r./CH_2Cl_2) 43.2 p.p.m.

u.v./cyclohexane: 210(vs), 310(sh), 420(sh), and 520(sh) n.m.

Reaction of $|Ru_5C(CO)_{15}|$ with phosphinated alumina.

An excess of $|Ru_5C(CO)_{15}|$ was added to a cooled slurry of the oxide (-40 - -50 °C) in CH_2Cl_2 and stirred for two hours. It was then filtered, washed (3 x CH_2Cl_2) and dried in vacuo. This yielded a purple solid.

I.r./Nujol mull (see Figure 4.7): 2 084(m), 2 067(m), 2 053(s), 2 040(s), 2 020(s), 2 010(s), 1 998(sh), 1 988(sh), 1 977(sh), 1 958(br,w), and 1 891(br,w) cm^{-1}.

Reaction of the phosphinated clusters (25) - (28) with oxides.

These were interacted with slurries of the oxides in cyclohexane or CH_2Cl_2. After stirring at r.t. for 4 days under a stabilising CO atmosphere, the excess cluster was removed by filtration and washing (3 x CH_2Cl_2) the oxide. This yielded, in the cases of (25) and (26), bright yellow (27) purple, and (28) red brown powders.

I.r./Nujol mulls:

(25) + $M'O_n$ = (see Figure 4.8).

SiO_2, 2 094(m), 2 045(s), 2 023(sh), and 2 011(s); γ-Al_2O_3,

2 094(m), 2 056(sh), 2 043(s), 2 023(s), 2 012(s), and 1 989(br,s); TiO_2, 2 094(m), 2 043(s), 2 023(s), 2 012(s), 1 993(m), and 1 984(m); MgO, 2 094(m), 2 056(sh), 2 043(s), 2 023(s), 2 012(s), 1 992(m), and 1 984(m) cm^{-1}.

(26) + $M'O_n$ = (see Figure 4.9).

SiO_2, 2 093(m), 2 086(m), 2 063(sh), 2 056(s), 2 025(s), 2 012(sh), 2 005(s), 1 990(sh), and 1 959(sh); γ-Al_2O_3, 2 092(m), 2 084(m), 2 064(s), 2 055(s), 2 029(sh), 2 023(s), 2 004(s), 1 989(s), and 1 959(m); TiO_2, 2 092(m), 2 084(m), 2 064(s), 2 055(s), 2 028(sh), 2 022(s), 2 011(sh), 2 003(s), 1 988(m), and 1 960(w); MgO, 2 092(m), 2 085(m), 2 064(s), 2 055(s), 2 025(sh), 2 022(s), 2 012(sh), 2 003(s), 1 989(s), and 1 959(m) cm^{-1}.

(27) + $M'O_n$ - (see Figure 4.10).

SiO_2, 2 087(w), 2 056(m), 2 043(m), 2 023(m), and 2 014(m); γ-Al_2O_3, 2 086(m), 2 055(s), 2 042(s), 2 021(s), 2 013(s), and 1 988(m); TiO_2, 2 086(m), 2 055(s), 2 042(s), 2 015(br,s), 1 999(sh), 1 988(sh), and 1 960(sh); MgO, 2 086(m), 2 055(s), 2 042(s), 2 021(sh), 2 014(s), 1 987(m), and 1 961(sh) cm^{-1}.

(28) + $M'O_n$ = (see Figure 4.11).

SiO_2, 2 083(m), 2 L54(s), 2 043(sh), 2 030(vs), 2 017(sh), 1 984(br,m), and 1 840(br,m); γ-Al_2O_3, 2 082(m), 2 053(s), 2 043(s), 2 029(vs), 1 980(br,s), and 1 835(br,m); TiO_2, 2 082(m), 2 052(s), 2 043(s), 2 029(vs), 2 016(sh), 2 000(w), 1 981(br,s), and 1 839(br,w); MgO, 2 082(m), 2 053(s), 2 043(s), 2 029(vs), 2 014(w), 2 001(w), 1 980(br,m), and 1 840(br,w) cm^{-1}.

u.v.-visible (diffuse reflectance) (see Figures 4.13 and 4.14) (__) + $M'O_n(SiO_2)$ =

(25), 424, 376, 288(sh), 244(sh), and 208; (26), 364, 248, and 216; (27), 530, 396(sh), 336(sh), and 220; (28), 520, 420, 308(sh), and 210 n.m.

References for Chapter 4.

1. G.R. Crooks, B.F.G. Johnson, J. Lewis, and I.G. Williams, J.Chem.Soc.(A), (1969), 797.

2. K.A. Azam, C.C. Yin, and A.J. Deeming, J.Chem.Soc.,Dalton Trans., (1978), 1201.

3. R. Mason, Pure and Applied Chem., (1973), 33, 513; R. Mason and D.M.P. Mingos, J.Organomet.Chem., (1973), 50, 53.

4. C. Choo Yin and A.J. Deeming, J.Chem.Soc.,Dalton Trans., (1974), 1013.

5. Y.C. Lin, C.B. Knoblez, and H.D. Kaesz, J.Am.Chem.Soc., (1981), 103, 1216.

6. F. Iwasaki, M.J. Mays, P.R. Raithby, P.L. Taylor, and P.J. Wheatley, J.Organomet.Chem., (1981), 213, 185.

7. A.J. Deeming and M. Underhill, J.Organomet.Chem., (1972), 42, C60.

8. H.D. Kaesz, J.Organomet.Chem., (1981), 213, C41.

9. J.S. Field, R.J. Haines, and D.N. Smit, J.Organomet.Chem., (1982), 224, C49.

10. M.J. Mays and D. Gavens, J.Organomet.Chem., (1977), 124, C37, and ibid, (1979), 177, 443.

11. J.A. Osborn and G.G. Stanley, Angew.Chem.,Int.Ed.Engl., (1980), 19, 1025.

12. R.D. Adams and N.M. Golembeski , J.Am.Chem.Soc., (1979), 101, 2579.

13. J. Evans, Chem.Soc.Rev., (1981), 10, 159.

14. A.S. Listysn, V.L. Kuznetsov, and Y.I. Yermankov, React.Kinet.Catal.Lett., (1980), 14, 445.

15. B.H. Robinson and W.S. Tham, J.Organomet.Chem., (1969),16,45.

16. T.W. Matheson, B.H. Robinson, and W.S. Tham, J.Chem.Soc.(A), (1971), 1457

17. B.H. Robinson and J.L. Spencer, J.Chem.Soc.(A), (1971), 2045.

18. C.U. Pittmann, G.M. Wileman, W.D. Wilson, and R.C. Ryan, Angew.Chem.,Int.Ed.Engl., (1980), 19, 478.

19. M. Ichikawa, J.Chem.Soc.,Chem.Commun., (1978), 566.

20. M.I. Bruce, D.C. Relioe, J.G. Matisons, B.K. Nickolson, P.H. Rieger, and M.L. Williams, J.Chem.Soc.,Chem.Commun., (1982), 442.

21. W.C. Still, M. Kahn, and A. Mitra, J.Organomet.Chem., (1978), 43, 2923.

22. A.J. Arce, and A.J. Deeming, J.Chem.Soc.,Chem.Commun., (1980), 1102.

23. J. Casanova, E.R. Schuster, and N.D. Werner, J.Chem.Soc., (1963), 4280.

24. S.A.R. Knox, J.W. Koeske, M.A. Andrews, and H.D. Kaesz, J.Am.Chem.Soc., (1975), 97, 3942.

25. R.D. Adams and N.M. Galenbeski, J.Am.Chem.Soc., (1978), 100, 4622.

26. B.F.G. Johnson, J. Lewis, and D.A. Pippard, J.Chem.Soc., Dalton Trans., (1981), 407.

27. D. Seyferth, J.E. Hallgren, and P.L.K. Hunb, J.Organomet.Chem., (1973), 50, 265.

28. H. Niebergall, Makromal,Chem., (1962), 52, 218.

29. K.G. Allun, R.D. Hancock, I.V. Howell, S. McKenzie, R.C. Pitkethly, and P.J. Robinson, J.Organomet.Chem., (1975), 87, 203.

30. R. Pierantozzi, K.J. McQuade, B.C. Gates, M. Wolf, H. Knözinger, and W. Ruhmann, J.Am.Chem.Soc., (1979), 101, 5436.

31. B.C. Mc.Kusick and M.E. Hermes, Org.Synth., (1961), 41, 14; R. Appel, R. Kleinstuck, and K.D. Ziehn, Angew.Chem., Int.Ed.Engl., (1971), 10, 132.

32. A. Gauter, Ann.Chem., (1867), 142, 289.

33. A.W. Hoffman, An.Chem., (1867), 144, 114.

34. "Isonitrile Chemistry", Ed. I. Ugi, Academic Press (1971), New York and London.

35. M.K. Kemp, J.Phys.Chem., (1967), 71, 765.

36. "High Resolution Nuclear Magnetic Resonance Spectroscopy", Vol. 2, page 1040, J.W. Emsley, J. Feeney, and L.H. Suttcliffe, Pergamon Press, Oxford (1966).

37. J.A.S. Howell and M. Berry, J.Chem.Soc.,Chem.Commun., (1980), 1039.

38. W.D. Horrocks and R.H. Mann, Spectrochim.Acta, (1963), 19, 1375.

39. P. von R. Schleyer and Allerhand, J.Am.Chem.Soc., (1962), 84, 1322; ibid, (1963), 85, 866.

40. K.K. Joshi, C.S. Mills, P.L. Pauson, B.W. Shaw, and W.H. Stubbs, J.Chem.Soc.,Chem.Commun., (1965), 181.

41. F.A. Cotton and F. Zingales, J.Am.Chem.Soc., (1961), 83, 351.

42. M.J. Mays and P.D. Gavens, J.Chem.Soc.,Dalton Trans., (1980), 911.

43. R. Bau and R.D. Wilson, J.Am.Chem.Soc., (1976), 98, 4687.

44. M.J. Mays and P.D. Gavens, J.Chem.Soc.,Dalton Trans., (1980), 911.

45. G. Süss Fink, Z.Naturforsch, (1980), 35B, 354.

46. D. Seyferth, Adv.Organomet.Chem., (1976), 14, 98.

47. C.H. Bamford, C.G. Eastmond, and W.R. Maltman, J.Chem.Soc.,Fataday, (1964), 60, 1432.

48. G. Pályi, F. Baumgartner, and I. Czasik, J.Organomet.Chem., (1973), 49, C35.

49. D. Seyferth and J.E. Hallgren, J.Organomet.Chem., (1973), 49, C41.

50. N. Sakamoto, T. Kitamura, and T. Joh, Chem.Lett., (1973), 583.

51. G.A. Olah, E.B. Baker, J.C. Evans, W.S. Tolgyesi, J.S. McIntyre, and I.J. Bastien, J.Am.Chem.Soc., (1964), 86, 1360.

52. T. Komijo, T. Kitamura, N. Sakamoto, and T. Joh, J.Organomet.Chem., (1973), 54, 265.

53. P.A. Elder and B.H. Robinson, J.Organomet.Chem., (1972), 36, C45.

54. W. Andreas, Z. Lazlo, and H. Gattfried, Chem.Ber., (1982), 4, 1286.

55. W. Hieber and W. Hübel, Z.Elektrochem., (1953), 57, 235.

56. Th. Kruck and W. Lang, Chem.Ber., (1965), 98, 3060.

57. Th. Kruck and A. Prosch, Z.Anorg.Allg.Chem., (1969), 371, 1.

58. R.C. Ryan, C.U. Pittman, and J.P.O. Connor, J.Am.Chem.Soc., (1977), 99, 1988.

59. D. Seyferth, C.N. Rudie, and M.O. Nestle, J.Organomet.Chem., (1979), 178, 227.

60. Z. Otero-Schipper, J. Lieto, and B.C. Gates, J.Catal. (1980), 63, 175.

61. S.C. Brown and J. Evans, J.Chem.Soc.,Chem.Commun., (1978), 1063.

62. S.C. Brown and J. Evans, J.Organomet.Chem., (1980), 194, C53.

63. S.C. Brown, J. Evans, and M. Webster, J.Chem.Soc.,Dalton Trans., (1981), 2263.

64. R. Pierantozzi, K.J. McQuade, B.C. Gates, M. Wolf, H. Knözinger, and W. Ruhmann, J.Am.Chem.Soc., (1979), 101, 5436.

65. F.R. Hartley and P.N. Vezey, Ad.Organomet.Chem., (1977), 15, 189.

66. "Structure of Metallic Catalysts", J.R. Anderson, Academic Press, (1975), New York, London, San Francisco.

67. S.C. Brown, Personal communication.

68. M.I. Bruce, G. Shaw, and F.G.A. Stone, J.Chem.Soc.,Dalton Trans., (1972), 2094.

69. A.J. Deeming, B.F.G. Johnson, and J. Lewis, J.Chem.Soc.(A), (1970), 897.

70. R.D. Wilson, S.M. Wu, R.A. Love, and R. Bau, Inorg.Chem., (1978), 17, 1271.

71. G. Ciani, L. Carlaschelli, M. Manassero, and U. Sartorelli, J.Organomet.Chem., (1977), 129, C25.

72. G.F. Stuntz and J.R. Shapley, J.Am.Chem.Soc., (1977), 99, 607, and references therein.

73. R.E. Benfield, B.F.G. Johnson, P.R. Raithby, and G.M. Sheldrick, Acta.Crystallogr., (1978), B34, 666.

74. E.J. Forbes, N. Goodhand, D.L. Jones, and A.T. Hamor, J.Organomet.Chem., (1979), 182, 143.

75. G. Raper and W.S. McDonald, J.Chem.Soc.(A), (1971), 3430.

76. A. Poe and M.V. Twigg, J.Chem.Soc.,Dalton Trans., (1974), 1860.

77. G.A. Vaglio and M. Valle, Inorg.Chim.Acta, (1978), 30, 161.

78. J. Lewis and B.F.G. Johnson, Pure and Appl.Chem., (1982), 54, 97.

79. B.F.G. Johnson, J. Lewis, J.N. Nicholls, and M. McPartlin, J.Chem.Soc.,Chem.Commun., (1981), 415.

80. B.F.G. Johnson, J. Lewis, P.R. Raithby, G.J. Will, M. McPartlin, and W.J.H. Nelson, J.Organomet.Chem., (1980), 185, C17.

81. G.A. Vaglio and M. Valle, Inorg.Chim.Acta, (1978), 30, 161.

82. J.I. Graff and M.S. Wrighton, J.Am.Chem.Soc., (1980), 102, 2133.

CHAPTER 5

Some Aspects of the Chemistry of Clusters with Bidentate Phosphine Ligands.

The impetus for this investigation into the reactions of clusters of varying geometries with polydentate phosphine ligands was partly provided by the work described in previous chapters. One of the principle problems encountered in the anchoring of clusters was their increased instability in the oxide environment. Attempts to overcome this with bridging and capping ligands met with limited success due to oxide interactions with either the ligand or the cluster, which, in general, caused an increased tendency towards fragmentation. This activity was caused by either acid/base sensitivity in the ligand (e.g. the formamide linkage in $|Os_3(CO)_{10}(H)(OCNCH)R|$ which can behave like its organic counterpart[1]) or poor design/fitting of the cap/bridge. For example, the sulphur cap in $|HOs_3(CO)_9(\mu_3\text{-}SR)|$ comprises of a 3e 3 centre bond to two osmium atoms and a dative bond to the third and as a result allows reaction with the oxide to produce a species thought to be $|HOs_3(CO)_9(\mu_2\text{-}SR)(O_{oxide})|$.

A possible way around this problem could be to use polydentate ligands which are capable of individually co-ordinating to each metal atom strongly with the same fluxionality, such as polydentate phosphine ligands. These, despite their air sensitivity, do offer the advantage of forming highly stable cluster phosphine bonds which are rarely cleaved and then only under forcing conditions.[2] These ligands have been shown to stabilise clusters towards fragmentation (e.g. $|HC(PPh_2)_3Rh_4(CO)_9|$[3]) and to act as templates for cluster production (e.g. $|HC(PPh_2)_3Ni_5(CO)_9|$[4]); though experiments with them on ruthenium clusters have shown that low yields are commonly

obtained (e.g. $|Ru_3(CO)_9(PBu_2)_3SiMe|$, 16 %,[5] and $|Ru_3(CO)_9(PPh_2)_3PH|$, < 10 %,[6]) and the compounds fo not display the postulated increase in stability (e.g. $|H_4Ru_4(CO)_9(PPh_2)_3PH|$ which decomposes at 60 °C). The reason for this may be poor fitting of the ligand, and in order to explore this a systematic study of the binding of four bidentate phosphines of general formula $PPh_2(CH_2)_nPPh_2$ with different chain lengths (n = 1 - 4) to ruthenium clusters of nuclearity three to six was carried out.

^{31}P n.m.r. has been shown to be a valuable tool in characterising mononuclear complexes;[7] however, so far its potential for clusters has not been fully explored. One effect of use - if it applies to clusters - is Δ_R, this is a ring size dependent contribution to the observed ^{31}P n.m.r. shift,[8] which would provide valuable structural information about clusters substituted with polydentate phosphines.

Another possible use of ^{31}P n.m.r. is in the characterising of heterogeneous species. ^{31}P n.m.r. magic angle spinning[22,36] studies on oxide attached phosphine ligands and mononuclear complexes[9] have demonstrated the applicability of this technique to phosphine anchored clusters, where it should be particularly valuable in characterising systems containing more than one species. At present the main technique used is comparative i.r. spectroscopy, but with mixed systems its use in quantifying and identifying the species present is severely limited due to the large number of overlapping carbonyl bands present. In order to evaluate the applicability of ^{31}P n.m.r. in characterising clusters both homogeneously

and heterogeneously, and to see if Δ_R effects exist, a series of monodentate phosphine substituted clusters were also prepared.

One of the speculated principle advantages of anchored clusters over conventional metallic catalysts is their ability to perform specific catalysis by virtue of their discrete structures, like mononuclear complex catalysts. For example,[10] $|Rh^{I}Cl(-)Diop|$ has been shown to be an active chiral hydrosilation catalyst, both homogeneously and on polymer supports. The anchored version is produced by anchoring (-)Diop (see Diagram 5.1). This is produced by condensing a precursor of (-)Diop with a supported aldehyde obtained by dimethylsulphoxide (DMSO) oxidation of the chlorinated polymer. This method of anchoring should also be applicable to oxide supports, assuming an anchored aldehyde can be produced and the oxide does not interfere with acetal formation. To investigate this possibility the reactions of (-)Diop with clusters were investigated together with the feasibility of producing anchored (-)Diop on oxides.

(a) Ruthenium clusters with monodentate phosphine ligands.

The reaction of ruthenium carbonyl with monodentate phosphines has been studied in depth.[28-32] The postulated mechanisms for the benzophenone and thermal reactions have been mentioned in the preceeding chapter. The crystal structure of $|Ru_3(CO)_{11}PPh_3|$ shows[32] that the phosphine occupies on equatorial site as is expected on steric rather than electronic grounds. Unlike $|Fe_3(CO)_{11}PPh_3|$[33] but like

ANCHORED CHIRAL HYDROSILATION

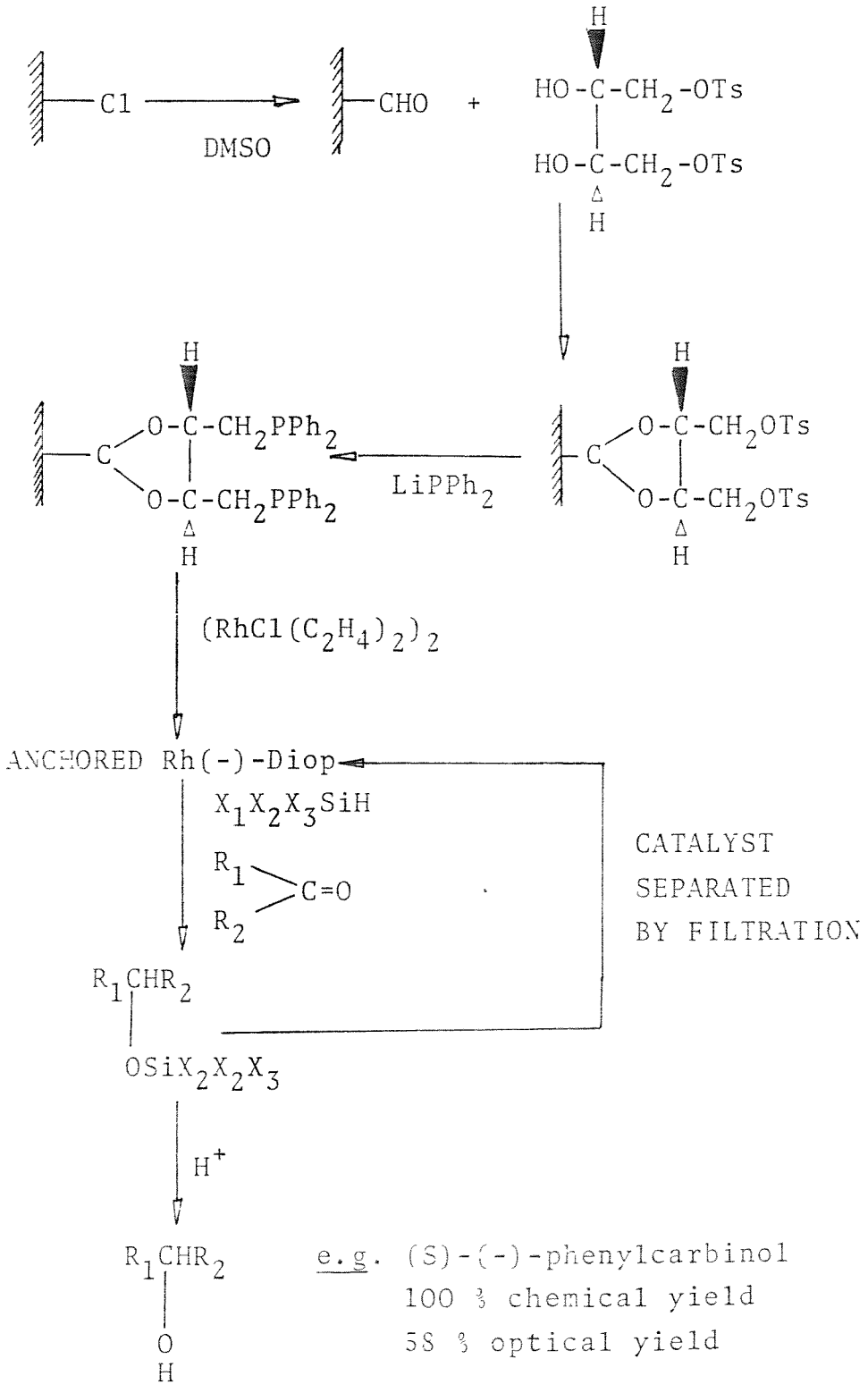

Diagram 5.1.

$|Os_3(CO)_{11}P(OMe)_3|$[34] and $|Ru_3(CO)_{11}PPh_3|$ it possesses no bridging carbonyls and this is probably a consequence of the greater size of the Ru_3 and Os_3 triangles. A ^{13}C n.m.r. study on $|Os_3(CO)_{12-n}(PEt_3)_n|$ (n = 1, 2 and 3) has shown that the phosphines occupy equatorial sites in solution (see Diagram 5.2) with the phosphines disposed to obtain minimal steric interactions.

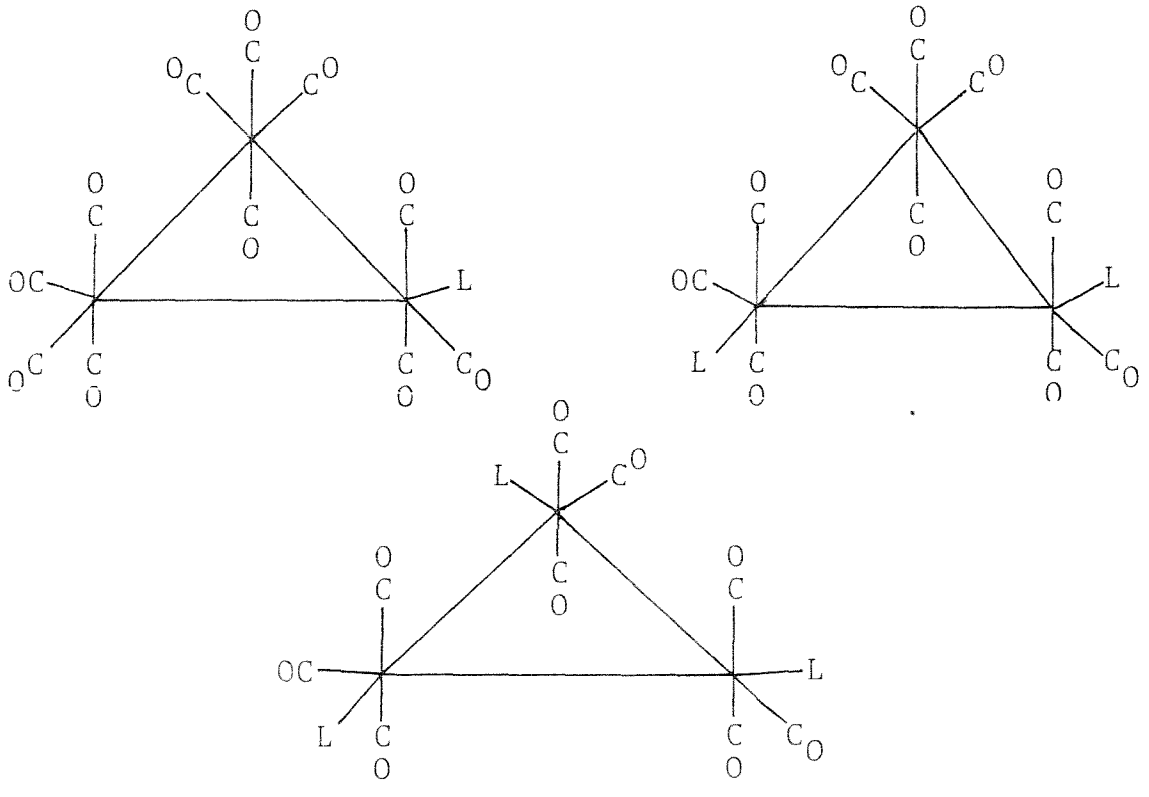

Diagram 5.2.

The structures of the substituted ruthenium clusters are thought to be identical to their osmium counterparts because of the similarity of their carbonyl fingerprints in the i.r. The ^{31}P n.m.r. confirms this by displaying the predicted spectra. That is, single peaks for the mono and tri-substituted

derivatives and two peaks of equal intensity for the di-substituted compounds. Interestingly, $|Os_3(CO)_{10}(PEt_3)_2|$ at 30 - 40 °C shows only one peak in the ^{31}P n.m.r. because of an exchange process which produces a plane of symmetry between the two phosphinated osmium atoms (probably a $Os(CO)_3PR_3$ unit rotation). The reason why this is not observed for the ruthenium analogues, $|Ru_3(CO)_{10}(PPh_2R)_2|$, could be as a result of the greater cone angles of the phosphines employed (e.g. PEt_3 = 132°, PPh_2Me = 136°), or electronic differences between the two clusters.

As previously observed, the stretching frequency of the CO bands decreases as the degree of substitution increases. This is in accord with the phosphines employed being poorer π acceptors than the replaced carbonyls. For example, the frequency of the totally symmetric stretch for the carbonyls is $|Ru_3(CO)_{12}|$ occurs at 2 117 cm^{-1} (obtained from the Raman spectrum of a single crystal, as this mode is i.r. inactive) whereas the highest frequency bands in $|Ru_3(CO)_{12-n}(PPh_2Me)_n|$ are: n = 1, 2 097; n = 2, 2 073; n = 3, 2 047 cm^{-1}. The ^1H n.m.r. spectra also show this effect of increasing electron density on the cluster as n increases. That is, as n increases the alkyl groups on the phosphine experience an increased shielding because the increased electron density on the cluster inhibits the donation of the electrons by the phosphine. For example, for $|Ru_3(CO)_{12-n}(PPh_2Me)_n|$ where n = 1, 2 and 3 the methyl doublet is observed at δ 2.18, 2.14 and 2.1, respectively, however, this effect, though it is also seen for

the other derivatives, does not extend significantly along the alkyl chain (e.g. in $|Ru_3(CO)_{12-n}(PPh_2Bu^n)_n|$ the methyl resonance occurs at n = 1, 0.9; n = 2, 0.85; and n = 3, 0.9 δ). Surprisingly, the predicted increased shielding is not observed in the ^{31}P n.m.r. (e.g. for $|Ru_3(CO)_{12-n}(PPh_2Me)_n|$ the signals occur at: n = 1, 14.9; n = 2, 14.33 (average); and n = 3, 15.76 p.p.m.). The reason for this discrepancy is not obvious but it appears to be general for all the derivatives.

The reaction of $|H_4Ru_4(CO)_{12}|$ with phosphines has been reported[2] and the products, $|H_4Ru_4(CO)_{12-n}(PR_3)_n|$ (n = 1, 2, 3 and 4), shown to involve substitution at different ruthenium centres.[37] The solid state structures of $|H_4Ru_4(CO)_{11}P(OMe)_3|$[38] and $|H_4Ru_4(CO)_{10}(PPh_3)_2|$[39] have been determined and show a distorted tetrahedral, "D_{2d}" core of ruthenium atoms with four long Ru — Ru and two short Ru — Ru distances. The ^1H n.m.r. of these complexes[37] show that the hydrides in solution are fluxional. The ^1H n.m.r. spectra of $|H_4Ru_4(CO)_{12-n}(P(OMe)_3)_n|$ (n = 1-4), showed that only one time averaged isomer existed for each value of n, as the hydride signals displayed simple coupling patterns. However, the ^1H n.m.r. results for $|H_4Ru_4(CO)_{12-n}(PPh_2R)_n|$ (n = 2 and 3), indicate the presence of isomers or inequivalent phosphines on the n.m.r. time scale, as the hydride signals were either broad (n = 2) or complex multiplets (n = 3). The ^{31}P n.m.r. spectra confirmed this with for n = 2 and 3, two signals being observed with approximate abundances of 2:1.

In the case of n = 2, this is probably because the greater

cone angle[8] of PPh_2R (PPh_2Me = 136°, PPh_2Et = 140 °C) compared with $P(OMe)_3$ (107°) causes slowing down of the interconversion of the two possible solution isomers (see Diagram 5.3, carbonyls and hydrides omitted for clarity) sufficiently for them to be resolved on the n.m.r. time scale (e.g. cooling of $|H_4Ru_4(CO)_{10}(PPhMe)_2|$ caused the broad hydride signal to be resolved into a complex multiplet). The possibility of the two isomers differing in the positions of the bridging hydrides cannot be ruled out, but it appears to be unlikely as no change was seen in the ^1H n.m.r. spectrum for $|H_4Ru_4(CO)_8(P(OMe)_3)_4|$ on cooling to -100 °C.[37] Variable temperature ^{13}C n.m.r. studies on these compounds should resolve this problem. The proportions of these two isomers appears to be independent of the R group in the phosphine PPh_2R, but this is not unexpected as the cone angles do not vary significantly as the alkyl chain length is increased (e.g. PEt_3, PPr_3 and PBu_3 all have the same cone angle of 132°).

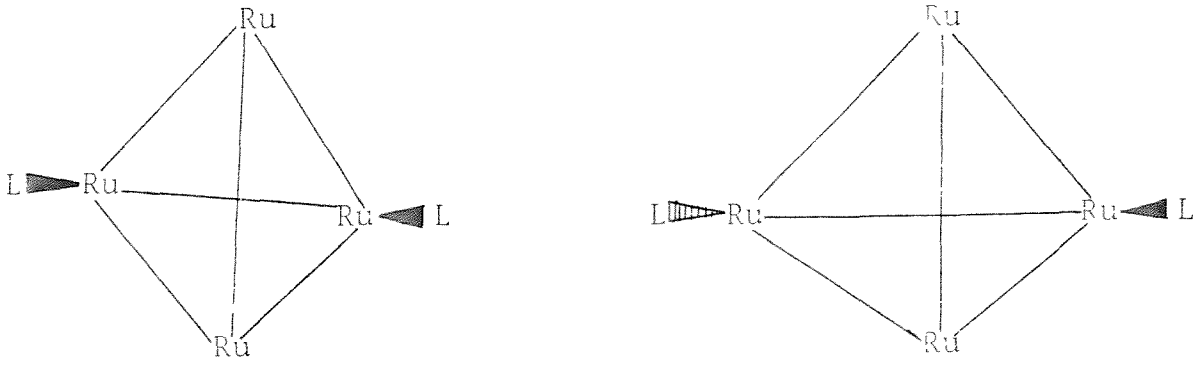

Symmetry D_{2d} C_1

Diagram 5.3.

For n = 3, ^{31}P n.m.r. indicates that there are either two isomers or two phosphine environments present. A molecular model indicated that the latter possibly was the most likely, with one phosphine occupying a different environment from the other two. A way to visualise this is to consider each phosphine as sitting asymmetrically on a face: the justification for this being that the $M(CO)_3$ or $M(CO)_2L$ units are staggered (from the crystal structures[38,39]) with respect to the M --M edges of the cluster (see Diagram 5.4). In the case of n = 3, two of the phosphines possess a vacant face adjacent to them whereas the other phosphines nearest vacant face is <u>trans</u> to it (see Diagram 5.5). Again the presence of isomers due to the hydrides cannot be ruled out, without a ^{13}C n.m.r. study. The reason why this is not observed for the $P(OMe)_3$ analogue is again probably due to

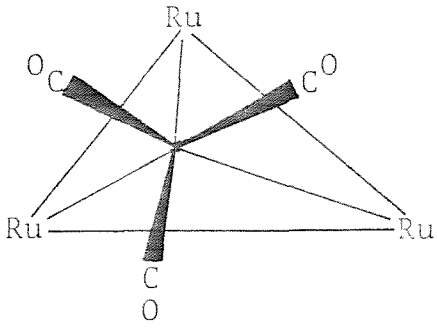

Diagram 5.4.

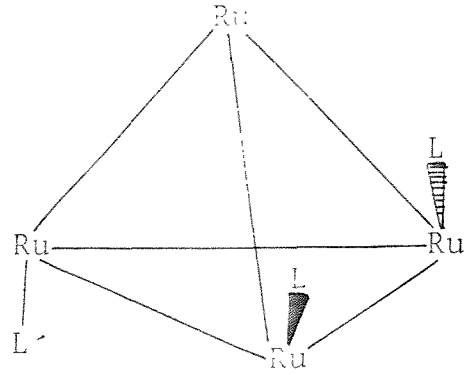

Diagram 5.5.

its smaller cone angle allowing a facile exchange process causing equivalence of the phosphines. Such a process would involve a facile rotation of the $M(CO)_2L$ groups.

The i.r. spectra of $|H_4Ru_4(CO)_{12-n}(PPh_2R)_n|$ (n = 1, 2, and 3) again show the trend of decreasing the CO stretching frequency as the degree of substitution increases. For example, the highest frequency CO bands for $|H_4Ru_4(CO)_{12-n}(PPh_2Me)_n|$ are n = 0, 2 109 (Raman); n = 1, 2 094; n = 2, 2 076; and n = 3, 2 061 cm^{-1}. Also again the protons on the alkyl group carbon adjacent to the phosphorus show an upfield shift as n increases. For example, in $|H_4Ru_4(CO)_{12-n}(PPh_2Et)_n|$ the position of the quintet is n = 1, 2.56; n = 2.4, (average); and n = 3, 1.9 (average) δ. The average position of the hydride signal, however, shows an opposite trend (e.g. $|H_4Ru_4(CO)_{12-n}(PPh_2Et)_n|$ n = 0, -17.77; n = 1, -17.42; n = 2, -17.05; and n = 3,-16.66 δ as the "peak" moves downfield by increment of approximately δ 0.4 with each successive addition).

The reaction and structure of the two major products from the $|Ru_5C(CO)_{15}|$ with PPh_3 have been reported.[40] Both the mono and disubstituted products involve replacement of the basal CO ligands of the square pyramidal cluster. In the disubstituted compound $|Ru_5C(CO)_{13}(PPh_3)_2|$, the two phosphines are thought to occupy trans positions below the square face and supporting evidence for this is provided by the crystal structure of $Ru_5C(CO)_{13}DPPB$ (isomer 2, see later, Figures 5.7, 5.8, pages 315 and 316). This compound also possesses a similar i.r. spectrum to the disubstituted product. The mechanism of the reaction of $Ru_5C(CO)_{15}$ with phosphines

has been discussed in the preceeding chapter. The same trends in the carbonyl and ^{1}H n.m.r. spectra as seen for Ru_3 and Ru_4 clusters are observed. The ^{31}P n.m.r. shift also shifts unambiguously to lower values from the mono to di-substituted derivatives.

The reaction of $|Ru_6C(CO)_{17}|$ with phosphines together with a crystal structure ($|Ru_6C(CO)_{16}PPh_2Et|$) have been reported.[42,43] The disubstituted derivative is thought to exist as a mixture of cis and trans isomers with for L = $P(OMe)_3$, the cis isomer predominating.[56] This is in part confirmed by the ^{31}P n.m.r. results which show two unequal peaks which vary in relative intensity as R is changed. For example, when R = Me 4:1, Et 7:1 and for R = Pr^n and Bu^n the minor up field peak is probably hidden by the major peak. This decrease in abundance of the minor peak as the cone angle increases indicates that it is probably the cis isomer. The work of S.C. Brown[56] indicated that the cis-isomer predominates for $P(OMe)_3$. This is in accord with the product distribution being determined by electronic factors (favouring a cis product, possibly by a M --M bond cleavage mechanism, facilitated by the adjacent phosphine) and steric factors (predominating as the cone size increases $P(OMe)_3$ << PPh_2Me < PPh_2Et, PPh_2Pr^n and PPh_2Bu^n). The i.r., ^{1}H n.m.r. and ^{31}P n.m.r. results again show the same trends as observed for Ru_3, Ru_4 and Ru_5 clusters. That is, as n increases ν_{CO} decreases and the ^{31}P and ^{1}H n.m.r. peaks move upfield. The ^{31}P n.m.r. spectrum of $Ru_6C(CO)_{13}(PPh_2Et)_4|$ shows only a

single peak and so indicates that this compound exists as only one isomer containing all the substituted ruthenium atoms in a plane (see Diagram 5.6), and that the $M(CO)_2L$ apices

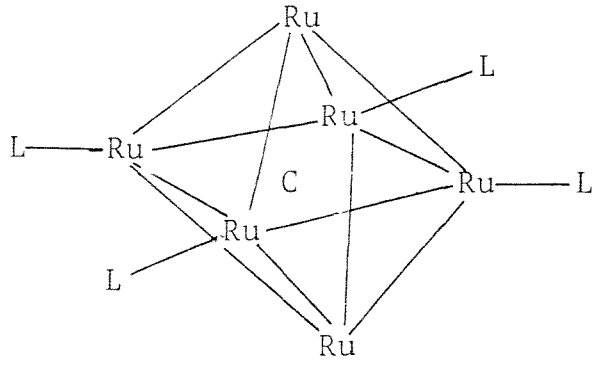

Diagram 5.6.

are probably fluxional to cause all the phosphines to become equivalent.

Analysis of the ^{31}P n.m.r. shifts for the monosubstituted clusters demonstrates at least four contributing factors to the observed shift. The results in Table 5.1 can be simplified in several ways. Firstly, subtraction of the shift of the PPh_2Me substituted cluster should remove all cluster effects (see Table 5.2) and leave effects caused by differences in the ligands. As can be seen, the discrepancies are mostly caused by differences in the free ligands initial shift (ΔL, compared to PPh_2Me). Subtraction from Table 5.2 of these differences (ΔL) of the free ligand from free PPh_2Me should leave effects caused by differences in the R on co-ordination (see Table 5.3). As can be seen these effects are small but show a dependence on both the ligand and cluster, as would be expected, if the differeences are due to an interaction between

R and the cluster. The most important contribution to the final ^{31}P n.m.r. shift is that caused by co-ordination to the cluster. This itself can be subdivided into 3 main factors that is the nature of the metal (i.e. ruthenium(0) rather than Ru^{2+} or Fe^{3+}, so this term should be the same for all the clusters considered), the change in the C — P — C angles on co-ordination (i.e. angle opening causes a downfield shift) and a new term not seen for mononuclear complexes, the cluster nuclearity/geometry.

Subtraction of the ^{31}P n.m.r. shifts for the triruthenium subtracted clusters from other clusters substituted with the same ligand should remove shifts caused by the nature of the metal and possibly ligand effects (i.e. angle opening or closing on co-ordination) and leave effects caused by the differences between the clusters (see Table 5.4 for the results of this subtraction).

The assumption that the change in the C — P — C angles upon co-ordination is the same across this series of clusters, is supported by their crystal structures and the small dependence of the ^{31}P n.m.r. shifts on R (as in PPh_2R, see Table 5.3) and therefore steric size of the phosphines. This leaves as the only remaining variables which cannot be separated because of the small number of systems studied, cluster size and geometry.

To summarise, the position of the observed ^{31}P n.m.r. signal for a monosubstituted cluster is given by a combination of four main factors. These are, the initial position of the

free ligand (determined by electronic and steric factors), the nature of the metal, the change in the C --P —C angles on co-ordination and the cluster nuclearity/geometry.

The ^{31}P n.m.r. shifts for the disubstituted clusters (see Table 5.5) can be treated in a similar manner. Again, subtraction of the PPh_2Me substituted cluster from the raw results illustrates the effect the shift of the free ligand has on the final value. Interestingly, this appears not to be additive; that is, the ^{31}P n.m.r. shifts are not significantly larger than for the monosubstituted clusters (see Tables 5.6 and 5.2). Also subtraction of ΔL from the results in Table 5.6 illustrates the R group is again interacting with the cluster and possibly the other phosphine (see Table 5.7). Subtraction of the disubstituted Ru_3 cluster from the analogous higher nuclearity clusters again demonstrates the effect of cluster size/geometry on the ^{31}P n.m.r. shift (see Table 5.8).

On comparing the results for the disubstituted clusters to those of the monosubstituted clusters, there is a general small shift upfield (see Table 5.9, Δ shift = disubstituted - monosubstituted) on going from the mono to disubstituted cluster, which is in accord with the cluster becoming more electron rich and so accepting less electron density from the phosphine.

Although the data for trisubstituted clusters is limited, the results suggest the existence of cluster size/geometry, and free ligand effects on the final observed ^{31}P n.m.r. peak positions, similar to those seen for mono and disubstituted clusters (see Table 5.10).

TABLE 5.1

^{31}P n.m.r. shifts of the monosubstituted clusters

Nuclearity				
Ru_3	Ru_4	Ru_5	Ru_6	Ligand
36.03				PPh_3 +6.00
14.90	19.45	20.61	26.00	PPh_2Me -26.38
30.60	33.17	36.69	39.90	PPh_2Et -11.45
27.14	29.85	33.68	37.60	PPh_2Pr^n -16.58
27.44	30.45	34.20	38.14	PPh_2Bu^n -16.13
34.11	37.24	39.50	43.20	$PPh_2(CH_2)_2Si(OEt)_3$ -8.90

TABLE 5.2.

^{31}P n.m.r. shifts minus the shift of the PPh_2Me substituted cluster.

Ru_3	Ru_4	Ru_5	Ru_6	ΔL	L
0	0	0	0	0	PPh_2Me
15.70	13.72	16.08	13.90	14.92	PPh_2Et
12.24	10.40	13.07	11.60	9.80	PPh_2Pr^n
12.54	11.0	13.59	12.16	10.25	PPh_2Bu^n
19.21	17.79	18.89	17.20	17.48	$PPh_2(CH_2)_2Si(OEt)_3$

TABLE 5.3.

^{31}P n.m.r. shifts minus the shift of the PPh_2Me substituted cluster minus, ΔL, the difference in the shift of the free ligand from free PPh_2Me.

Nuclearity					
Ru_3	Ru_4	Ru_5	Ru_6		Ligand
0	0	0	0	0	PPh_2Me
0.77	-1.21	1.15	-1.03	0	PPh_2Et
2.44	0.60	3.27	1.80	0	PPh_2Pr^n
2.29	0.75	3.34	1.89	0	PPh_2Bu^n
1.73	0.31	1.41	-0.28	0	$PPh_2(CH_2)_2Si(OEt)_3$

TABLE 5.4.

^{31}P n.m.r. shifts minus the shift of the Ru_3 cluster substituted with the same ligand.

Nuclearity				
Ru_3	Ru_4	Ru_5	Ru_6	Ligand
0	4.55	5.71	11.10	PPh_2Me
0	2.57	6.09	9.30	PPh_2Et
0	2.71	6.54	10.46	PPh_2Pr^n
0	3.01	6.76	10.70	PPh_2Bu^n
0	3.13	5.39	9.09	$PPh_2(CH_2)_2Si(OEt)_3$

TABLE 5.5.

^{31}P n.m.r. shifts for disubstituted clusters

Nuclearity				
Ru_3(average)	Ru_4(average)	Ru_5	Ru_6	Ligand
14.33	18.65	19.90	25.30	PPh_2Me
30.25	33.02	34.50	39.40	PPh_2Et
26.39	29.85	31.87	37.24	PPh_2Pr^n
26.61	30.40	32.13	37.84	PPh_2Bu^n

TABLE 5.6

^{31}P n.m.r. shifts minus the shift of the PPh_2Me substituted Cluster

Nuclearity					
Ru_3(average)	Ru_4(average)	Ru_5	Ru_6	ΔL	Ligand
0	0	0	0	0	PPh_2Me
15.92	14.37	14.60	14.10	14.92	PPh_2Et
12.06	11.20	11.97	11.94	9.80	PPh_2Pr^n
12.28	11.75	12.22	12.54	10.25	PPh_2Bu^n

TABLE 5.7

^{31}P n.m.r. shifts minus the shift of the PPh_2Me substituted cluster minus ΔL.

Nuclearity					
Ru_3(average)	Ru_4(average)	Ru_5	Ru_6	ΔL	Ligand
0	0	0	0	0	PPh_2Me
1.00	-0.55	-0.32	-0.82	0	PPh_2Et
2.26	1.40	2.17	2.14	0	PPh_2Pr^n
2.03	1.50	1.97	2.29	0	PPh_2Bu^n

TABLE 5.8.

^{31}P n.m.r. shifts minus the average shift of the Ru_3 cluster disubstituted with the same ligand.

Nuclearity			
Ru_4(average)	Ru_5	Ru_6	Ligand
4.32	5.57	10.97	PPh_2Me
2.77	4.25	9.15	PPh_2Et
3.46	5.48	10.85	PPh_2Pr^n
3.79	5.51	11.25	PPh_2Bu^n

TABLE 5.9.

The difference in the ^{31}P shifts of the mono- and disubstituted clusters.

Nuclearity				
Ru_3	Ru_4	Ru_5	Ru_6	Ligand
-0.57	-0.80	-0.71	-0.70	PPh_2Me
-0.35	-0.15	-2.19	-0.50	PPh_2Et
-0.75	0.00	-1.81	-0.40	PPh_2Pr^n
-0.83	-0.05	-2.08	-0.30	PPh_2Bu^n

TABLE 5.10.

^{31}P n.m.r. shifts for trisubstituted clusters

Ru_3	Ru_4	L
15.76	17.87	PPh_2Me
31.51	34.20	PPh_2Et
28.10		PPh_2Pr^n
28.32		PPh_2Bu^n

(b) $|Ru_3(CO)_{12}|$ with Polydentate phosphines.

The reaction of $|Ru_3(CO)_{12}|$ with tridentate phosphines, such as $HC(PPh_2)_3$,[6] $CH_3C(CH_2PPh_2)_3$[44] and $MeSi(PBu^n)_3$,[5] has been only marginally successful, since the yields of the required products, $|Ru_3(CO)_9(\mu_3\text{-}P_3R')|$ have been low in general. The importance of tailoring the capping phosphine to the cluster is demonstrated by the reaction of $CH_3C(CH_2PPh_2)_3$(TDPME) with $|Ru_3(CO)_{12}|$ during which only mononuclear products such as $|Ru(CO)_2$TDPME$|$ were obtained despite there being an excess of $|Ru_3(CO)_{12}|$ present. The reactions of $|Ru_3(CO)_{12}|$ with $HC(PPh_2)_3$ and $MeSi(PBu^n)_3$ were more successful as the desired products were obtained, though only in low yields (typically in less than 15 % yield), together with numerous side products, e.g. $|Ru_3(CO)_{10}\{\mu_2\text{-}(PPh_2)C(PPh_2)(H)\}|$ (one phosphine unattached).

In order to investigate the tailoring of capping tridentate phosphines to $|Ru_3(CO)_{12}|$ it was found to be more convenient to experiment with the readily accessible bidentate phosphines, $PPh_2(CH_2)_nPPh_2$ (where n = 1, DPPM; n = 2, DPPE; n = 3, DPPP, n = 4, DPPB). The i.r. spectra of the compounds with the general formula $|Ru_3(CO)_{10}(\mu_2\text{-}(PPh_2)_2(CH_2)_n)|$ (see Figure 5.1) indicate the possible existence of 3 distinct structures: a DPPM structure, a DPPE and DPPP structure, and a DPPB and (-)-Diop structure ((-)-Diop = (-)2,3,-o-isopropylidene-2,3-dihydroxy-1,4,bisdiphenylphosphinobutane).

A recent single crystal structure determination on $|Ru_3(CO)_{10}$DPPE$|$[45] has shown that the bidentate phosphine ligand assumes an equatorial edge bridging mode with both phosphines

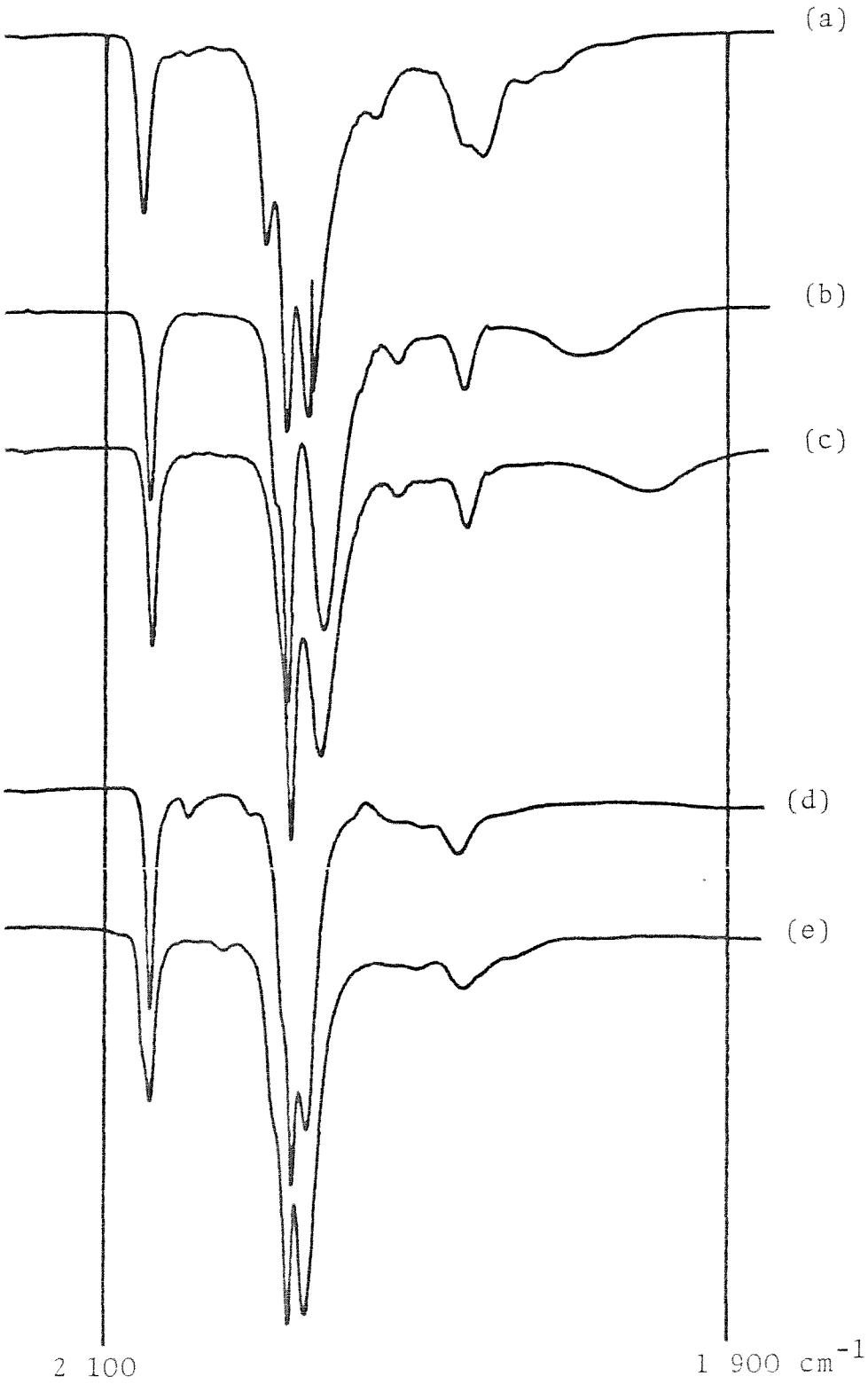

Figure 5.1. I.r. spectra in cyclohexane of (a) $[Ru_3(CO)_{10}DPPM]$ (b) $Ru_3(CO)_{10}DPPE]$, (c) $[Ru_3(CO)_{10}DPPP$, (d) $[Ru_3(CO)_{10}DPPB]$, and (e) $[Ru_3(CO)_{10}(-)$-Diop$]$.

occupying sites the same side of an Ru --Ru edge. The structure of $|Ru_3(CO)_{10}DPPM|$[46] has been shown to be effectively the same by a variable temperature ^{13}C n.m.r. study. A possible explanation as to why their i.r. spectra are so different is that, the different bite size and steric requirements of the two ligands cause different perturbations to the ligand anticubooctahedron.

The crystal structure of $|Ru_3(CO)_{10}DPPE|$ demonstrates that the Ru_3 triangle size is virtually unaffected by the substitution (average Ru --Ru distance, $Ru_3(CO)_{12}$ = 2.851 Å and $|Ru_3(CO)_{10}DPPE|$ = 2.853 Å). This is surprising, as phosphine substitution usually causes a lengthening of Ru —Ru bonds (e.g. $|Ru_3(CO)_{11}PPh_3|$ average Ru —Ru distance = 2.88 Å) due to a combination of both electronic and steric factors. In addition to this, a crystal structure determination on the analogous compound $|Ru_3(CO)_{10}${1,2-bis(dimethylarsino)tetrafluorocyclobut-1-ene}| has shown that this ligand also bridges an edge equatorially but the bridged edge is nearly 0.06 Å longer than the others. This is probably a consequence of the different bite of this biarsine ligand compared to the DPPE ligand (which must have a restraining effect on the size of the Ru_3 triangle).

The solid state structure of $|Ru_3(CO)_{10}DPPE|$, compared with $|Ru_3(CO)_{12}|$ shows large distortions (14 - 20°) in the positions of the equatorial and axial carbonyl ligands caused by accommodating the bridging DPPE ligand. The differences in the i.r. spectra of the DPPE and DPPM adducts are probably

due to these distortions. Interestingly, not only does the DPPM adduct form more readily (by thermal reaction) but it is also more thermally stable than the DPPE adduct. Hence, the DPPM ligand appears to have a more appropriate shape/bite for bridging a Ru — Ru edge.

The ^{31}P n.m.r. spectra of both $|Ru_3(CO)_{10}DPPM|$ and $|Ru_3(CO)_{10}DPPE|$ at 31 ^{o}C are sharp singlets indicating that either both phosphorus atoms are equivalent or they are made equivalent by a fluxional process. Further evidence for fluxionality is obtained from the ^{1}H n.m.r. spectra. In the case of $|Ru_3(CO)_{10}DPPM|$ the methylene is observed as a sharp triplet signal at 31 ^{o}C, which broadens on cooling. This indicates that the methylene protons are rapidly exchanging, probably by a flipping process similar to that known for cyclopentane (see diagram 5.7).

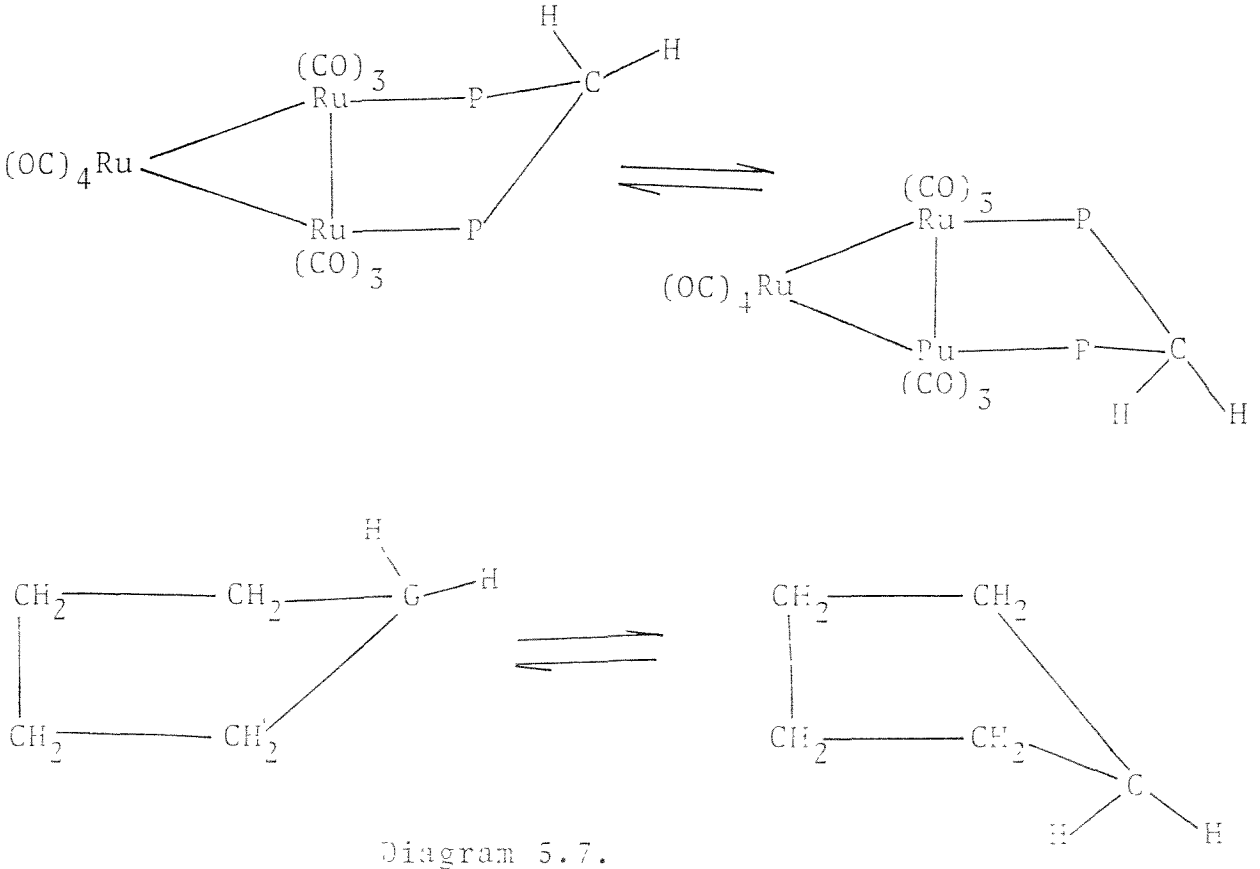

Diagram 5.7.

This analogy with organic cycloalkanes could also explain why the $|Ru_3(CO)_{10}DPPE|$ adduct is distorted, that is the six-membered bidentate phosphine ring is trying to adopt a conformation of minimum strain like the chair conformation of cyclohexane. This effect has been previously observed by Cotton and co-workers[48] for compounds of the type $|Mo_2Br_4(dppe)_2|$ and $|MoX_4(arphos)_2|$ (X = Cl or Br, arphos = $PPh_2CH_2CH_2AsPh_2$). These have very similar spectroscopic properties and a crystal structure has been carried out on $|Mo_2Br_4(arphos)_2|$. This demonstrated that both the ligands assume a bridging mode, with the two approximately square $|MoBr_2(PAS)|$ sets rotated from a completely eclipsed configuration by about 30 ^{o}C. The driving force for this twist appears to be the two fused $(AsPh_2CH_2CH_2PPh_2)_2Mo_2$ 6-membered rings which both adopt chair conformations. This twist causes about 0.5 of the δ bond to be broken and the band order (from the crystal structure) to be about 3.5 instead of 4.

The recent crystal structure of $|Ru_3(CO)_8(DPPM)_2|$[58], in which both DPPM ligands equatorially bridge different edges of the cluster, provides support for the postulated structure of $|Ru_3(CO)_{10}(DPPM)|$. This compound, like $|Ru_3(CO)_{10}DPPM$, displays a sharp triplet at 31 ^{o}C in the methylene region of the ^{1}H n.m.r. spectrum and two sharp signals of equal intensity at 31 ^{o}C in the ^{31}P n.m.r. spectrum. Therefore, the mechanism of interchange of the methylene hydrogens must not involve a change in the mode of bonding of the ligand (see Diagram 5.6, carbonyl and phenyl ligands omitted for clarity), but rather

the flipping motion proposed for the monosubstituted cluster.

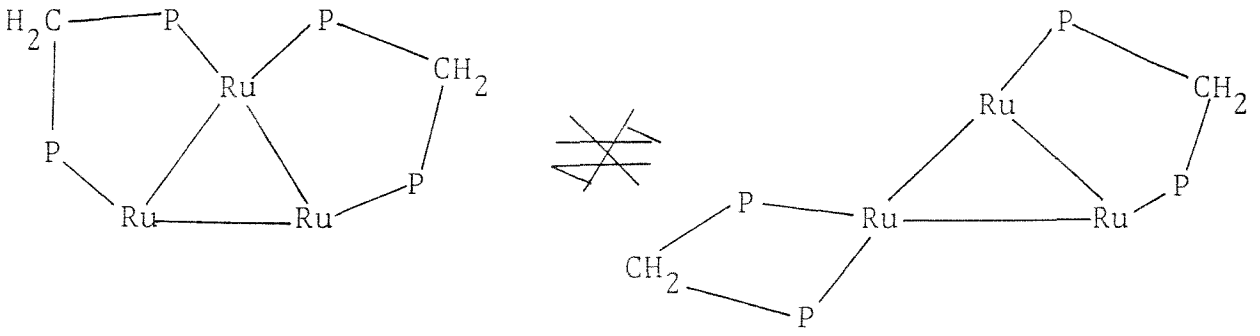

Diagram 5.8.

The similarity of the i.r. spectra of $|Ru_3(CO)_{10}DPPB|$ and $|Ru_3(CO)_{10}\{(-)\text{-Diop}\}|$ indicate that both have similar structures (see Figure 5.1). The ^1H and ^{31}P n.m.r. spectra suggest that the two phosphines occupy identical environments, though fluxionality cannot be ruled out. An attempted single crystal study on $|Ru_3(CO)_{10}\{(-)\text{-Diop}\}|$ during my period of study was unsuccessful due to decomposition of the sample. However, new crystals[57] have subsequently been obtained and their structure solved.

The crystals for the X-ray diffraction study were obtained from a CH_2Cl_2/pentane solvent mixture, and the completed structure showed the partial inclusion of CH_2Cl_2 into a hole in the crystal (random occupancy of about 33 %). Despite this source of disorder the final R value obtained was 0.05 . The structure of the $|Ru_3(CO)_{10}\{(-)\text{-Diop}\}|$ molecule is related to that found for $|Ru_3(CO)_{10}DPPE|$, in that the phosphine also bridges an edge equatorially (see Figures 5.2 and 5.3, and Table 5.11). The differences in the i.r. carbonyl spectra of

the DPPE and (-)-Diop adducts are presumably due to the different distortions seen in the two clusters.

Interestingly, the absolute configuration for the (-)-Diop ligand was obtained from the X-ray study, as there proved to be two possible mirror image solutions. When the left hand side configuration for the ligand was used (see Diagram 5.9), the R value fell to a lower value (0.05 rather than 0.10), and hence showed that this is the absolute configuration of the (-)-Diop ligand.

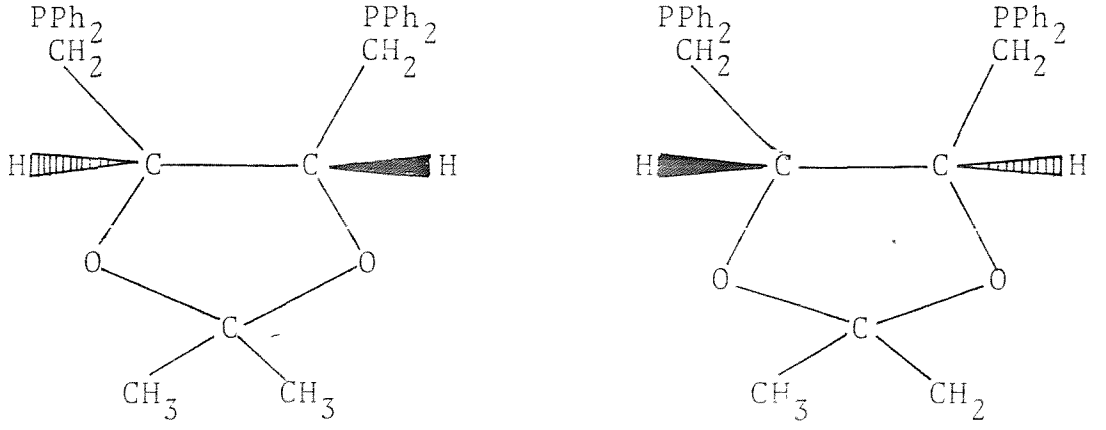

Diagram 5.9.

This chirality in the ligand induces an asymmetry in the "$Ru_3(CO)_{10}$" cluster fragment. The rigid ketal ring in the middle of the bidentate phosphines alkyl chain backbone, with its specific trans stereochemistry, causes the ligand to straddle the Ru — Ru edge asymmetrically. For example, Figure 5.3 shows that one PPh_2CH_2- unit occurs above and one below the plane of the Ru_3 triangle. This, together with the resulting preferred orientation of the rest of the phosphine

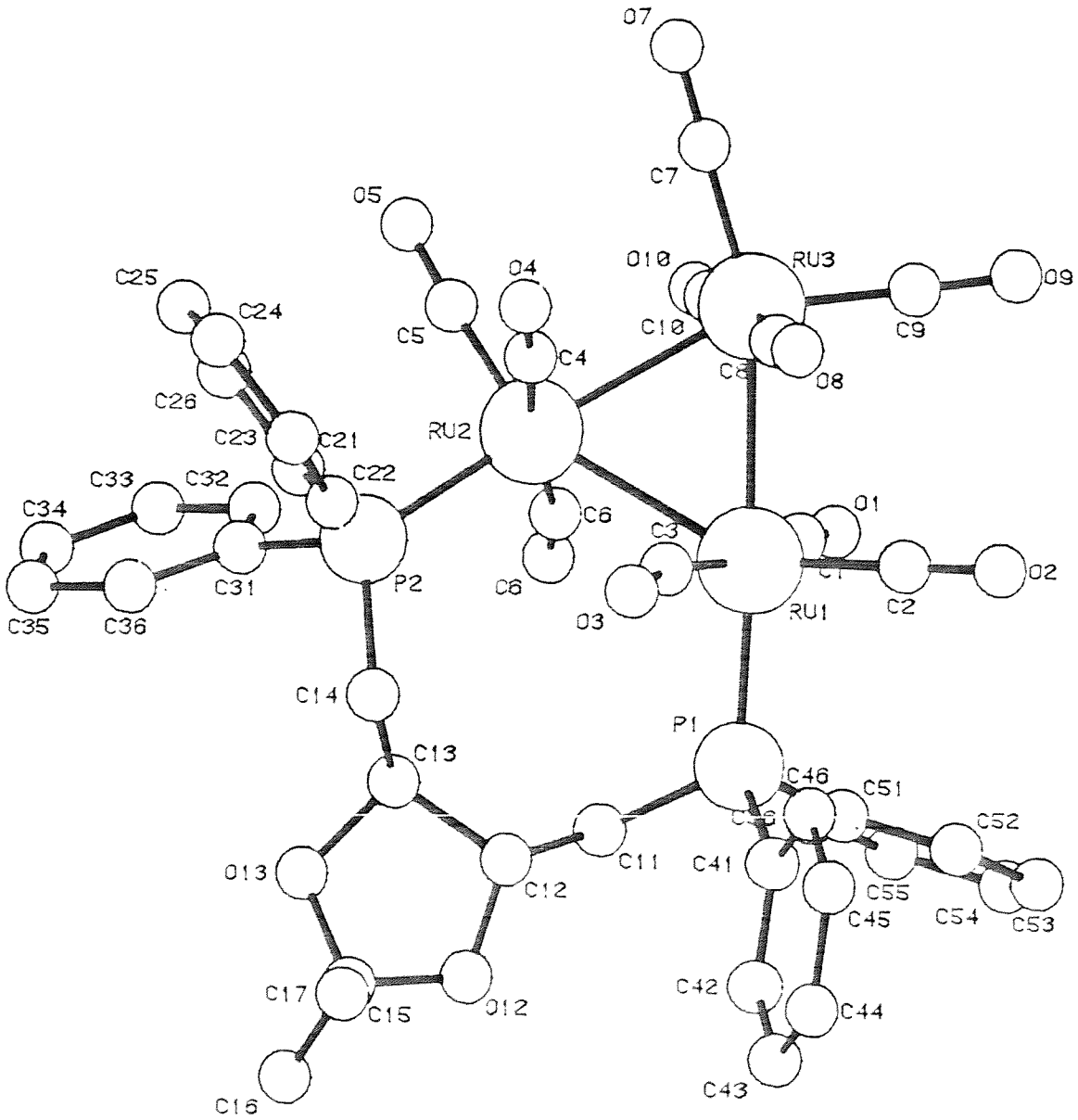

Figure 5.2. The solid state structure of $[Ru_3(CO)_{10}\{(-)\text{-Diop}\}.xCH_2Cl_2]$ viewed from above the ruthenium triangle.

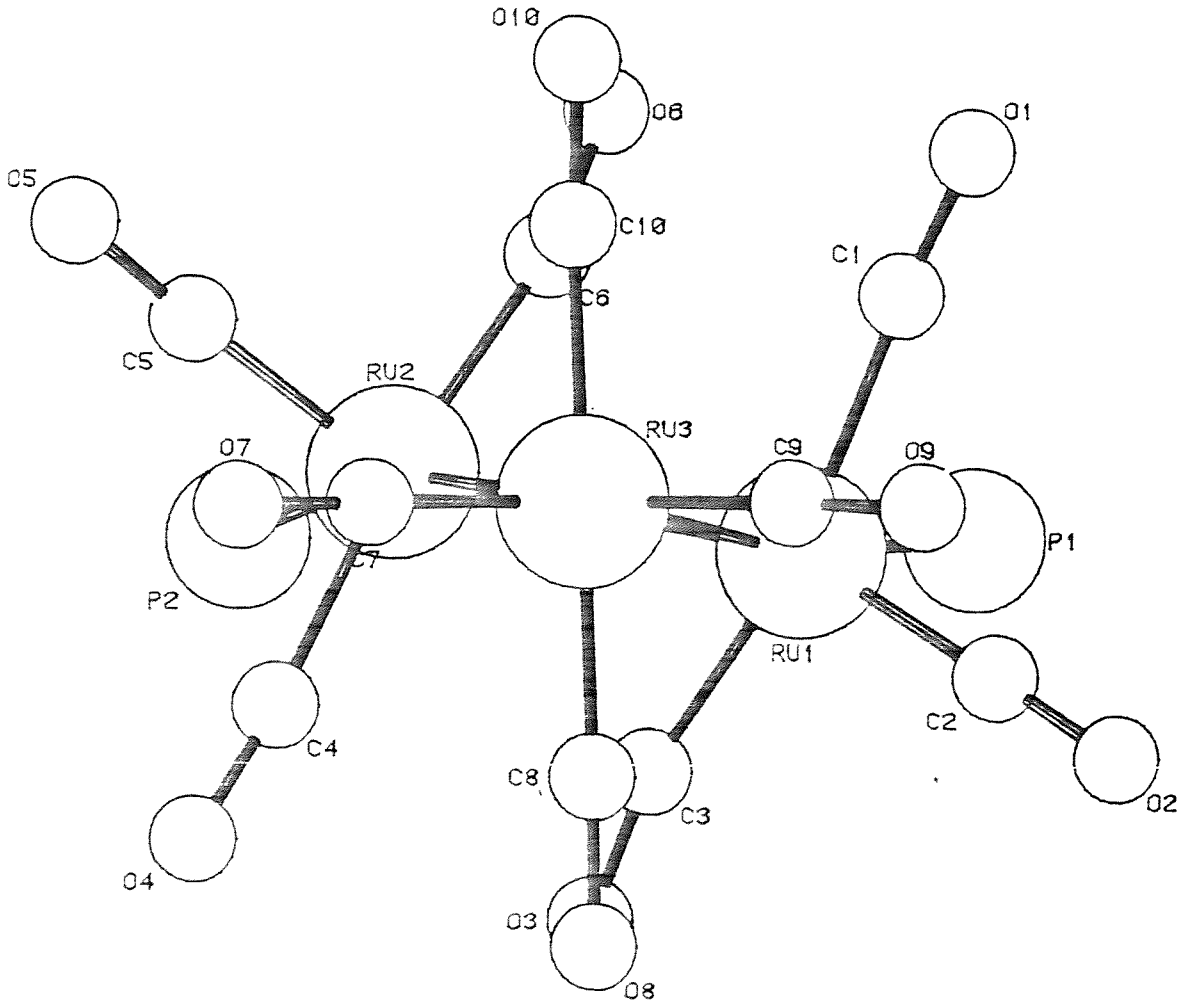

Figure 5.3. The crystal structure of $\{Ru_3(CO)_{10}\{(-)\text{-Diop}\}.x\text{-}CH_2Cl_2\}$ viewed in the Ru_3 plane with the phenyl groups and alkyl backbone of the (-)-Diop ligand omitted for clarity.

TABLE 5.11.

Selected bond lengths and angles for

$|Ru_3(CO)_{10}\{(-)\text{-Diop}\}.x\ CH_2Cl_2|$.

Bond lengths (in Å, standard deviations in brackets).

Ru(1) - Ru(2)	2.888 (.001)
Ru(1) - Ru(3)	2.836 (.002)
Ru(2) - Ru(3)	2.845 (.002)
Ru(1) - P(1)	2.328 (.003)
Ru(2) - P(2)	2.337 (.004)

average Ru — C = 1.8982

average C — O (for carbonyls) = 1.1556

Non-bonded distances.

Ru(1) - C(6)	2.819 (.015)
Ru(2) - C(3)	2.756 (.015)
P(1) - P(2)	5.094 (.004)

Bond angles (in degrees)

Ru(1) - Ru(2) - Ru(3)	59.3 (.0)
Ru(2) - Ru(1) - Ru(3)	59.6 (.0)
Ru(1) - Ru(3) - Ru(2)	61.1 (.0)
Ru(2) - Ru(1) - P(1)	117.2 (.1)
Ru(1) - Ru(2) - P(2)	116.7 (.1)
Ru(1) - C(3) - O(3)	166.6 (1.4)
Ru(2) - C(o) - O(6)	167.0 (1.3)

TABLE 5.11 (Continued).

Torsion angles

Ru(3) - Ru(1) - Ru(2) - P(2)	-163.27
Ru(3) - Ru(2) - Ru(1) - P(1)	-170.48

Angles between normals to planes

Ru(1) - Ru(2) - Ru(3)/C(8) - Ru(3) - C(10)	78.60
Ru(1) - Ru(2) - Ru(3)/C(7) - Ru(3) - C(9)	10.88
C(8) - Ru(3) - C(10)/C(7) - Ru(3) - C(9)	67.85
C(1) - Ru(1) - C(3)/C(4) - Ru(2) - C(6)	31.83

ligand causes the two $Ru(CO)_3$ units to partially rotate to minimise the interactions. In addition to this the Ru — Ru edge bridged by the phosphine is abnormally long (2.888 Å compared to 2.851 Å in $|Ru_3(CO)_{12}|$) and the other two edges are shorter than that seen for $|Ru_3(CO)_{12}|$ (see Table 5.11, Ru(1) - Ru(3) = 2.836, and Ru(2) - Ru(3) = 2.845 Å). This lengthening of the bridged edge is presumably caused by accommodating the ligand, which causes the $Ru(CO)_3$ groups to partially rotate. A consequence of this is that two carbonyls ($C_{(6)}O_{(6)}$ and $C_{(3)}O_{(3)}$) appear to have a weak semi-bridging character, as the oxygens are swept back from the weakly co-ordinated metal (angles Ru(2) - $C_{(6)}$ - $O_{(6)}$ and Ru(1) - $C_{(3)}$ - $O_{(3)}$ = 166 - 167 °C, compared to 180 °C typically observed for terminal carbonyl ligands). It is interesting to speculate that the partial rotation of the $Ru(CO)_3$ units (caused by accommodating the (-)-Diop ligand) causes partial breakage of the Ru — Ru bond and this is offset by the weakly semi-bridging carbonyls and increased Ru — Ru bonding to the unique Ru atom.

The induction of the chirality of the ligand into the structure of the cluster is evident in this X-ray. The importance of this lies in chiral catalysis where the optical induction in the products depends on the interaction of the substrates with the catalyst. The catalyst can be made chiral by either asymmetry in the ligand envelope (e.g. compounds $ML'L''L'''L''''$ are potentially chiral) or by induced asymmetry caused by interaction with a comparatively distant chiral centre

as in this case. This interaction with the chiral ligand in $|Ru_3(CO)_{10}\{(-)\text{-Diop}\}|$ (see Figures 5.2 and 5.3) extends beyond the immediately co-ordinated metal atoms. For example, the unique $Ru(CO)_4$ unit is partially rotated so as to minimise the interaction with carbonyls $C_{(4)}O_{(4)}$, $C_{(5)}O_{(5)}$, $C_{(2)}O_{(2)}$, and $C_{(1)}O_{(1)}$ which are pushed back by the straddling phosphine.

As the alkyl chain length between the two phosphines increases, the proportion of the products involving the linking of two or more clusters increases. This is presumably because after one end of the phosphine becomes attached the likelihood of the unattached end colliding with the adjacent ruthenium centre decreases as the chain length increases. For DPPB and (-)-Diop the chain length is sufficiently long to allow the synthesis of reasonable amounts of $|\{Ru_3(CO)_{11}\}_2(\text{bidentate-phosphine})|$, particularly under conditions of high concentration and a large excess of $|Ru_3(CO)_{12}|$. These compounds were identified by comparative i.r. spectroscopy (with mono-substituted Ru_3 clusters such as $|Ru_3(CO)_{11}PPh_2Me|$) and ^{31}P n.m.r. (which shows both phosphines as equivalent). The benzophenone ketyl catalysed reaction, because of its mechanism (see preceeding chapter), allows the preparation of moderate yields of these clusters, even if they have short chains (e.g. $|\{Ru_3(CO)_{11}\}_2DPPE|$[45] can be obtained in yields over 50 %) and these may be of future interest in producing new higher nuclearity clusters.

Another possible aspect of interest with these clusters may be their ability to co-ordinate dioxygen. For example,

both $|Ru_3O(CO)_6(DPPM)_2|$ and $|Ru_3O(CO)_6(dpam)_2|$ (dpam = bis-diphenylarsinomethane) contain a μ_3-oxygen atom and are produced by interacting the disubstituted clusters with molecular oxygen.[50]

(c) $|H_4Ru_4(CO)_{12}|$ with bidentate phosphines.

The reaction of $|H_4Ru_4(CO)_{12}|$ with bidentate phosphines proceeds, with gentle heating or sodium benzophenone ketyl catalysis, to give as the main products, cluster compounds of the general formulae $|H_4Ru_4(CO)_{10}(P--P)|$ (P — P = Bidentate Phosphine ligand).

The structure of two isomers of $|H_4Ru_4(CO)_{10}(DPPE)|$ have been reported.[51,52] These differ in the mode of co-ordination of the DPPE ligand which can either bridge an edge or chelate to one ruthenium atom. The latter is the thermally stable form with the bridged isomer, produced by Me_3NO assisted phosphine substitution, converting slowly at r.t. to the corner co-ordinated isomer. Obviously the Me_3NO oxidation of the second carbonyl occurs at the least substituted ruthenium atom, presumably on steric grounds.

The structures of the compounds, $|H_4Ru_4(CO)_{10}(P — P)|$, were identified by comparing their i.r. spectra with those of the known isomers of $|H_4Ru_4(CO)_{10}DPPE|$ (see Figure 5.4). For example, the structure of $|H_4Ru_4(CO)_{10}DPPB$ appears to be a mixture of both the edge and corner isomers from the the i.r., ^{31}P n.m.r. and ^{1}H n.m.r. spectra. The preference of a ligand in these cluster/ligand systems for a particular geometry is

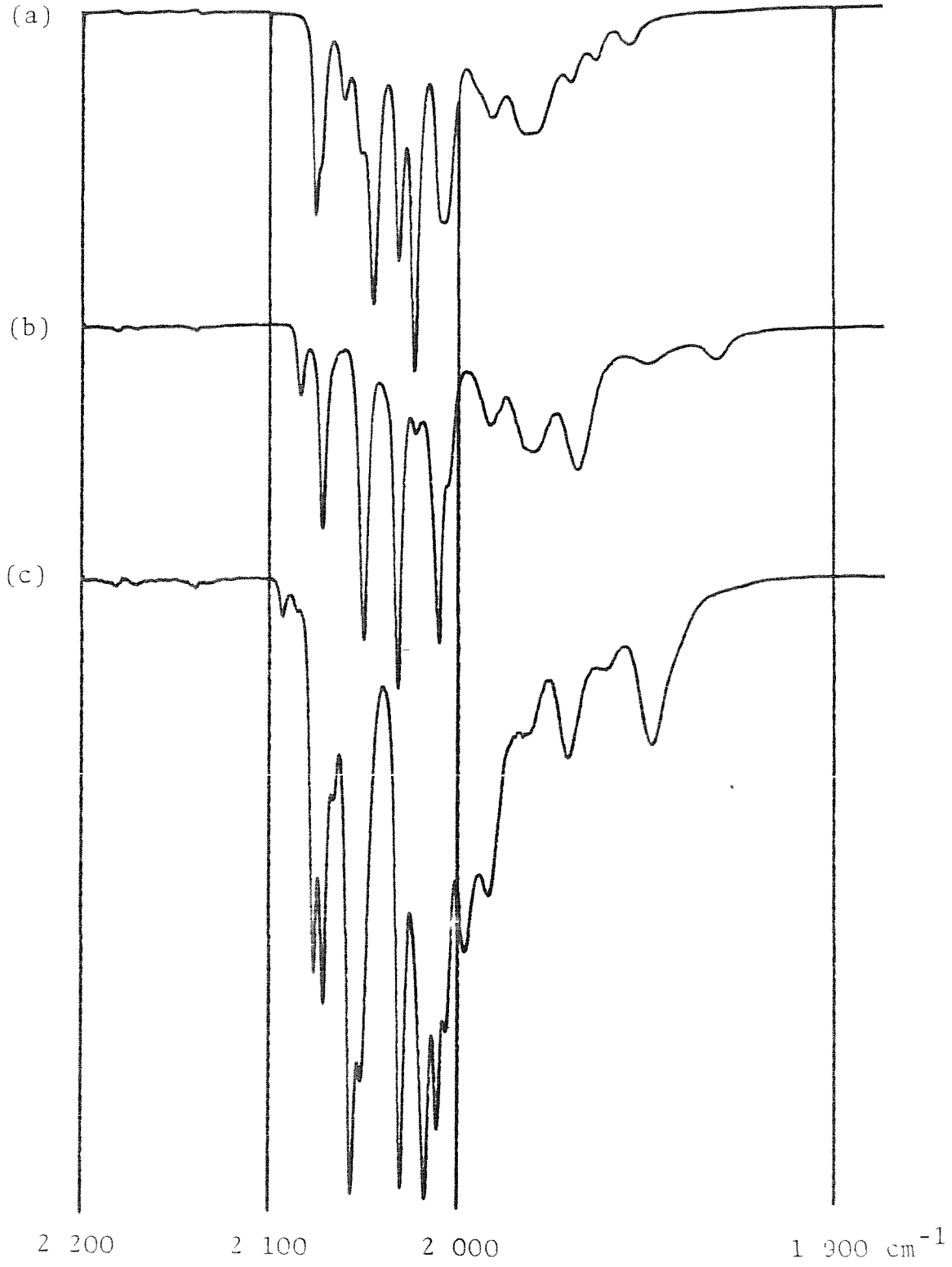

Figure 5.4. I.r. spectra in cyclohexane of
(a) $H_4Ru_4(CO)_{10}$DPPE (corner isomer)
(b) $H_4Ru_4(CO)_{10}$DPPM (bridging isomer)
and (c) $H_4Ru_4(CO)_{10}$DPPB both isomers.

controlled by a balance of thermodynamic and kinetic factors. For example, in $|H_4Ru_4(CO)_{10}DPPE|$ the edge bridging isomer is formed kinetically by the Me_3NO assisted substitution but thermodynamically the corner isomer is the most stable. For DPPM and DPPP the thermodynamic balance is in favour of the edge bridging isomer. Possible explanations for this change in mode of bonding are: that DPPM prefers to form a five membered ring (edge bridging) to a four membered ring (corner co-ordinating) on ring strain grounds; that DPPE prefers to form a five membered ring on a corner rather than a six membered ring bridging an edge, in which it cannot obtain a low ring strain chair conformation because of the stereochemistry of the bonding (the two phosphorus and co-ordinated ruthenium atoms are confined to a plane); and, that DPPP prefers an edge bridging mode for probably the same reason. In the case of DPPB the increase in the ring size probably accounts for the occurrence of both isomers. The proportions of the two isomers of the complex containing DPPB does not change upon standing. This indicates that they are equally stable thermodynamically which is probably a consequence of the greater flexibility of the long alkyl chain separating the two phosphines.

Interestingly, the sodium benzophenone ketyl catalysed reaction was found in all cases to produce the thermodynamically stable isomer. This was illustrated by the reactions of DPPM, DPPE, DPPP and DPPB which gave the same isomer distribution for $H_4Ru_4(CO)_{10}(P--P)|$, by both the thermal and ketyl assisted substitution routes. This preference for the radical reaction to give the most stable isomer is hard to explain as this is

not necessarily the kinetic product. For example, when the ring size is small (less than six membered) and one end of the phosphine becomes attached, the unattached end is held in a favourable position to complete the ring. However, when the ring size increases to above six this advantage is lost and it becomes favourable to form the smallest ring. For example, the DPPB ligand can form either seven or eight membered rings and on ring size considerations one would expect DPPB to form kinetically a seven membered ring (corner co-ordinating mode) in preference to an eight membered edge bridging ring. However, the radical catalysed reaction produces only the thermodynamic ratio of the isomers.

This decrease in the favourability of forming rings as their size increases is manifested in the lowering of the yields of $|H_4Ru_4(CO)_{10}(P-P)|$ from DPPE to DPPB, together with an increase in side products, such as $|\{H_4Ru_4(CO)_{11}\}_2$(-)-Diop|, which involve the linking of two or more clusters.

From its i.r. spectra, the compound $|H_4Ru_4(CO)_{10}\{$(-)-Diop$\}|$, like $|H_4Ru_4(CO)_{10}$DPPB|, exists as a mixture of corner and bridging isomers but owing to problems in purification this compound could not be obtained in the pure state and so confirmation of this by ^{31}P and ^{1}H n.m.r. was not possible. One point worth mentioning during the discussion of the structure of these clusters is that no evidence was found to suggest the separate existence of a bridging isomer in which the phosphorus atoms are disposed trans- across the Ru — Ru edge (see Diagram 5.10) rather than cis- as in '$H_4Ru_4(CO)_{10}$DPPE'.

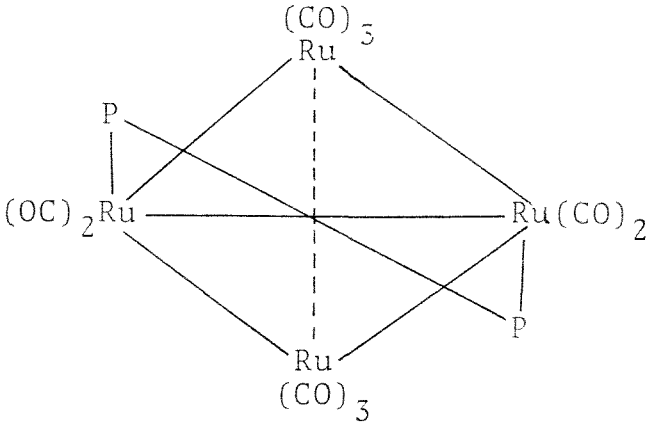

Diagram 5.10.

$[H_4Ru_4(CO)_{10}DPPM]$ was investigated more closely spectroscopically. The ^{13}C n.m.r. spectra (see Figure 5.5) of this compound show the presence of several fluxional processes. These can be interpreted with the aid of the ^{1}H n.m.r. spectra. At 60 ^{o}C all the carbonyls and hydrides are equivalent. On cooling the carbonyl exchange process slows first (coalescence occurs at 40 ^{o}C in the ^{13}C n.m.r.), the hydride exchange process only slows down to the ^{1}H n.m.r. time scale by -50 ^{o}C. At 0 ^{o}C localised carbonyl exchange is occurring and gives rise to a 3 line pattern of relative intensities 3:4:3. This is probably caused by two separate processes, two rotations on the two unsubstituted ruthenium atoms causing the two peaks of intensity 3 and an exchange process causing equivalence of the carbonyls on the phosphine substituted ruthenium atoms. The mechanism causing the equivalence of the carbonyls on the phosphine substituted ruthenium atoms can be inferred from the ^{1}H n.m.r. spectra.

The variable temperature ^{1}H n.m.r., thought unsuccessful in "freezing out" the hydrides (due to poor solubility in the

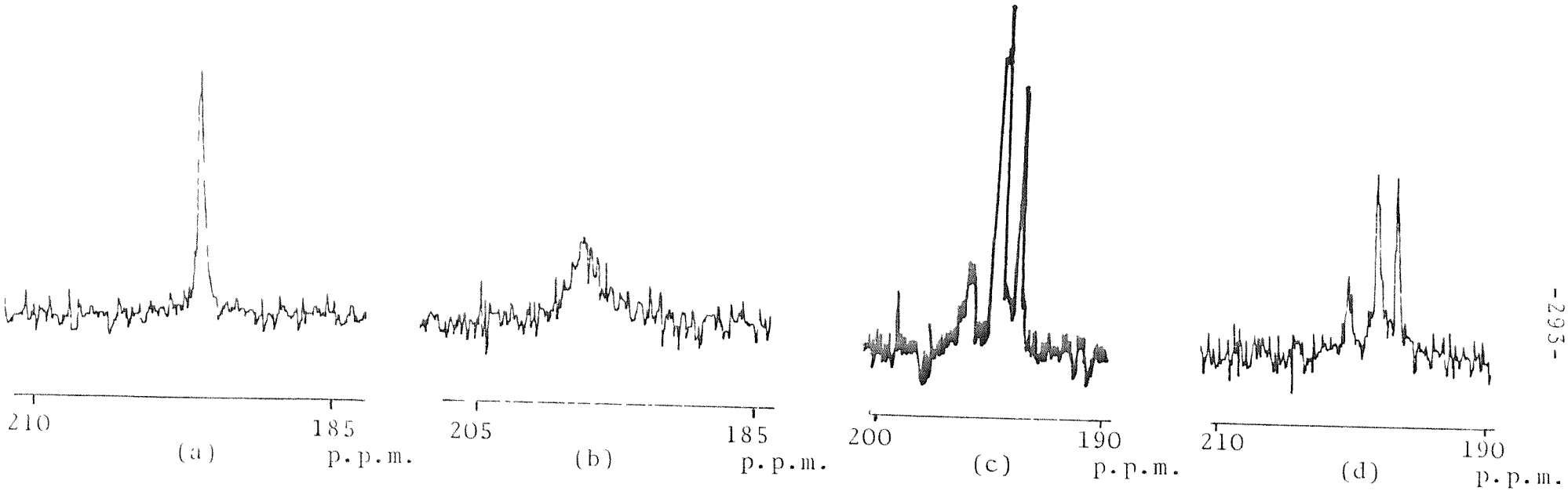

Figure 5.5. ^{13}C n.m.r. spectra of $[H_4Ru_4(CO)_{10}DPPM]$ in either d^8-toluene (80 °C — 21 °C) or CD_2Cl_2/CF_2ClH (0 - -114 °C) at (a) 60 °C, (b) 21 °C, (c) 0 °C, and (d) -30 °C.

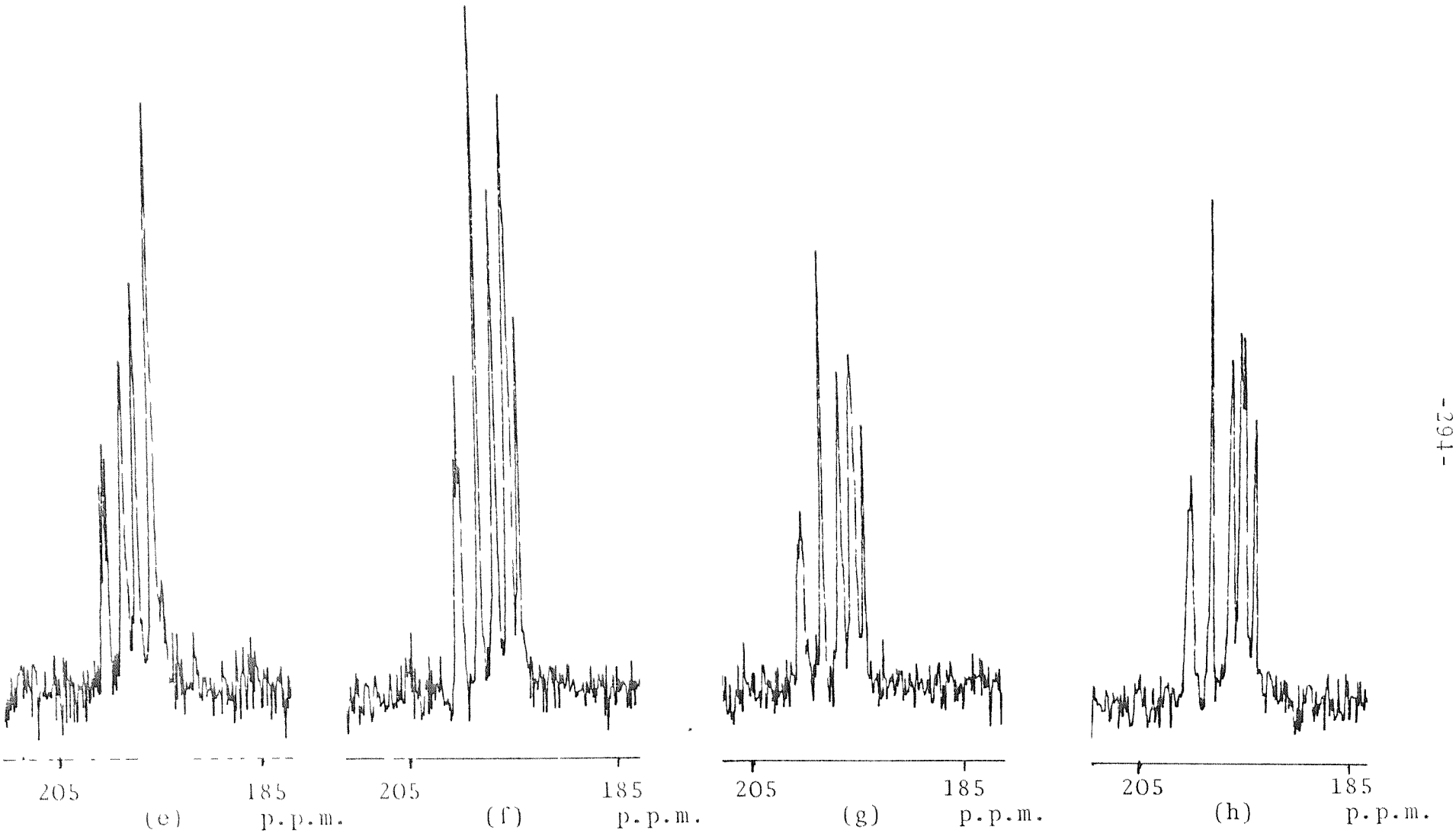

Figure 5.5. (Continued). (e) -50 °C, (f) -74 °C, (g) -84 °C, and (h) -104 °C.

solvents employed at these temperatures), does demonstrate the presence of two fluxional processes affecting the methylene protons. The higher temperature process causes interconversion of the methylene protons. This could occur by the conversion of the edge-bridge into a corner-bridge and then back after rotation or by a rocking motion on the substituted ruthenium centres (see Diagram 5.11). As this methylene proton interconversion process "ceases" on the n.m.r. time scale at 45 ^{o}C neither mechanism can be eliminated, though the edge-corner mechanism would explain how all the carbonyls become equivalent. The conversion of the edge-bridge DPPE isomer[51] to the corner isomer provides a precedent for such a mechanism, but has too high an energy barrier to make this an observable process in the n.m.r.

As the methylene proton interconversion process is not occurring rapidly at 0 ^{o}C, the carbonyl exchange process giving rise to the four equivalent carbonyls on the phosphine substituted rutheniums must not involve a change in the mode of co-ordination of the phosphine. For example, if the edge-corner fluxionality occurred the methylene protons would also be made equivalent at the same time. A possible mechanism, which has also been proposed for $[Ru_3(CO)_{10}(DPM)]$,[46] involves the conversion of terminal carbonyls into bridging carbonyls on the phosphine bridged edge (see Diagram 5.12), though a localised polytopial exchange cannot be ruled out.

The high temperature fluxional process interconverting the methylene protons (discussed earlier) ceases to be rapid at 45 ^{o}C and on cooling to 31 ^{o}C the ^{1}H n.m.r. signal sharpens

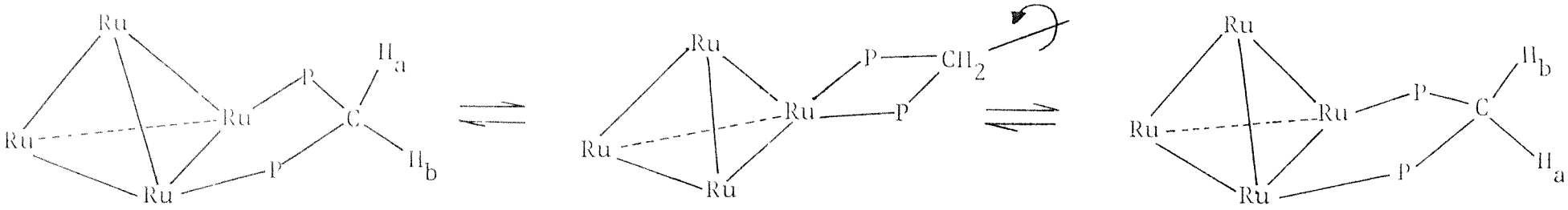

Edge-corner mechanism

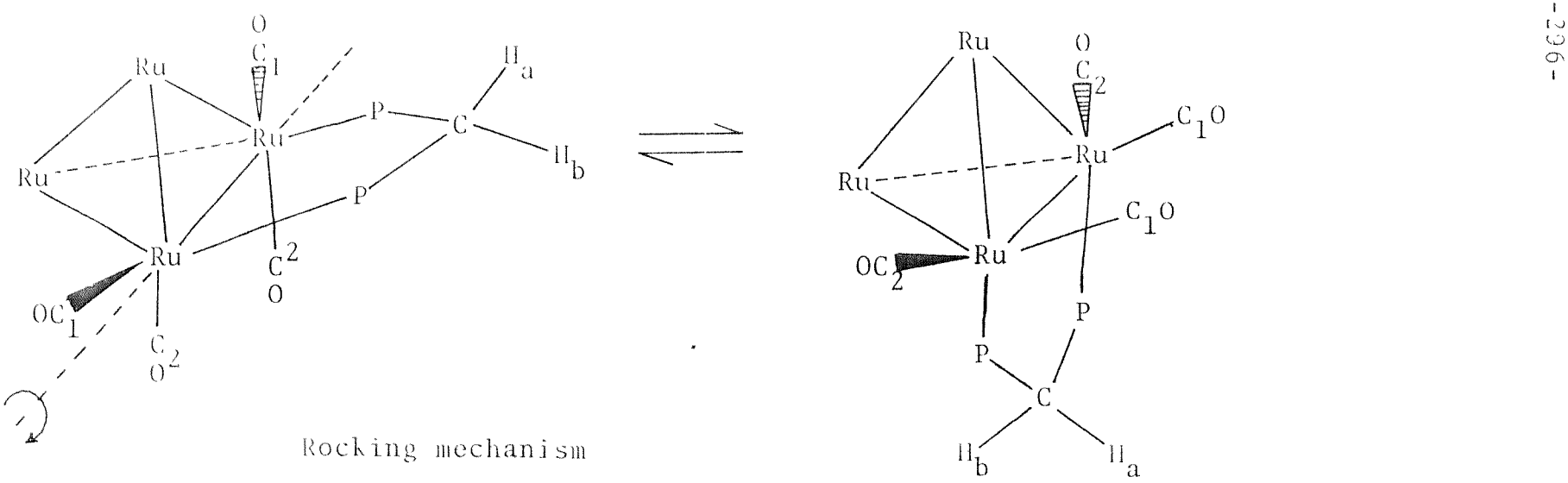

Rocking mechanism

Diagram 5.11.

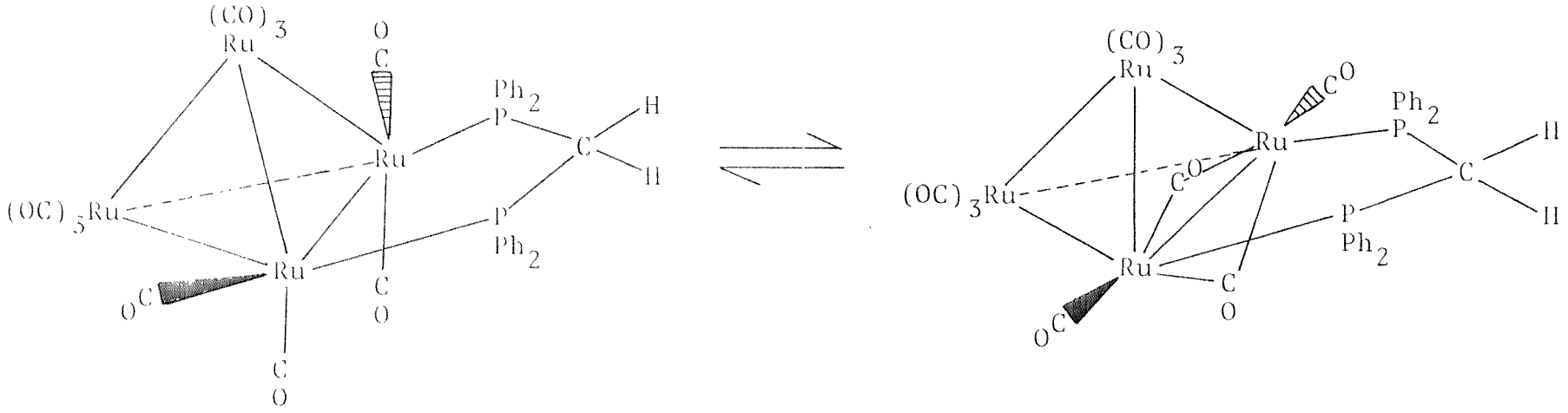

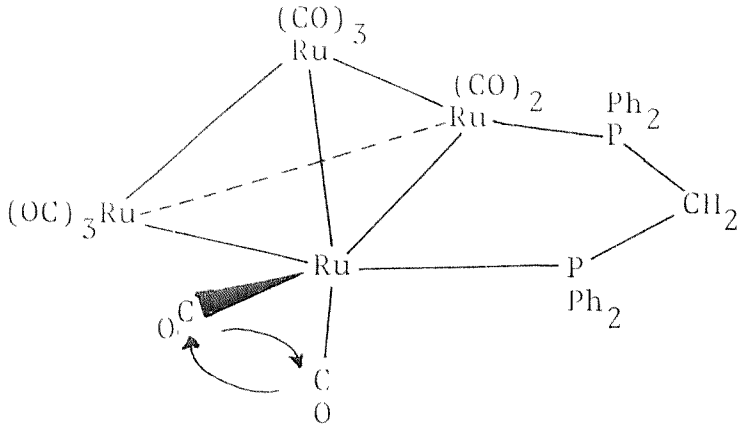

localised polytopial exchange

Diagram 5.12.

to a multiplet consisting of an overlapping pair of triplet of doublets. This is because each of the two protons are in different environments (i.e. towards or away from the cluster) and so each give rise to a triplet (coupling to two phosphorus atoms) of doublets (coupling to the each other). On cooling further this multiplet first broadens (-20 ^{o}C) and then sharpens again (-50 ^{o}C). This change could be due to the slowing down of carbonyl exchange process on the phosphine substituted ruthenium atoms but this is probably not the case as the pattern of the multiplet at -50 ^{o}C is different from that obtained at -30 ^{o}C. An explanation of this is that this broadening and sharpening of the methylene proton signals represents a slowing down of the flipping motion of the five membered ring (a similar motion has been proposed for $|Ru_3(CO)_{10}DPPM|$,[46] Diagram 5.13).

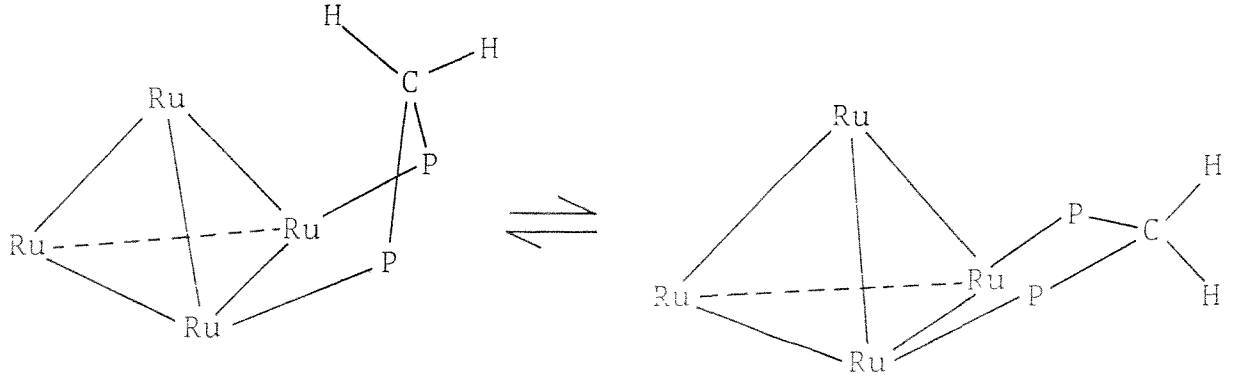

isomer a isomer b

Diagram 5.13.

The ^{13}C n.m.r. spectrum at -50 ^{o}C, shows a splitting of the peak assigned to the carbonyls on the phosphine substituted ruthenium atoms. This could be due to a "freezing" out of

the postulated terminal-bridging exchange process (see Diagram 5.12). Another spectral change that occurs on cooling to -50 ^{o}C in the ^{13}C n.m.r. spectra is that the downfield peak of intensity three shows phosphine or hydride coupling to give a triplet. Phosphine coupling can be ruled out as one would expect to observe it also at higher temperatures, particularly below 45 ^{o}C when the phosphine movement is frozen out. The observation of hydride coupling to only this $Ru(CO)_3$ unit can be explained in terms of localised freezing out of only the two hydrides about Ru(3), (see Diagram 5.14). This would also explain why the hydride signal at these temperatures is broad. A similar behaviour to this has been observed for $|H_4Ru_4(CO)_{10}DPPE|$, where the crystal structure incidentally shows structure (i).[52]

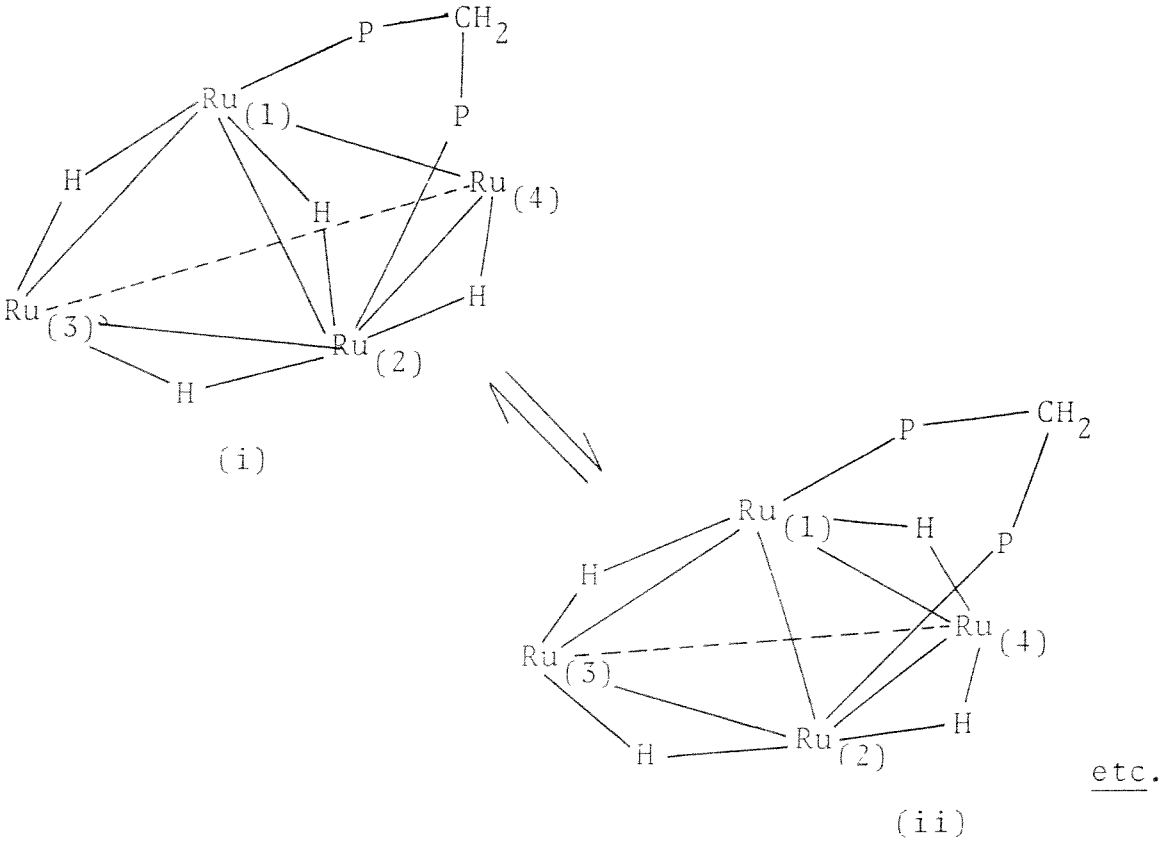

Diagram 5.14.

Further cooling of the ^{13}C n.m.r. samples causes further changes in the n.m.r. spectra. The rotation of the carbonyls on Ru(4) slows down and the peak of intensity 3 splits into two, of relative intensities 2:1 (one towards the phosphine and two away). The rotation of the carbonyls on Ru(4) is more restricted than for Ru(3) as the phosphine is directed towards Ru(4). The peak of intensity 2 (for the carbonyls on Ru(4)) on further cooling sharpens enough to display a slight splitting into a doublet which can be explained in terms of the hydrides becoming frozen as in structure (i). This splitting is presumably not observed for the other peaks due to solvent broadening and the strong angle dependence[35] of $^{2}J_{HC}$ (this would also explain why $^{2}J_{PC}$ is not observed).

(d) $|Ru_5C(CO)_{15}|$ with bidentate phosphines.

The reaction of $|Ru_5C(CO)_{15}|$ with bidentate phosphines (P — P) proceeds rapidly under mild conditions to give as the main product, cluster compounds of the general formulae $|Ru_5C(CO)_{13}(P — P)|$, and since under gentle conditions phosphine substitution occurs only at basal and not apical ruthenium atoms,[40] only 6 main co-ordination modes are likely to occur (see Diagram 5.15), two corner co-ordinating and three edge bridging differing in the occupation of equatorial or axial sites by the phosphine and one diagonally bridging mode. Of these only (a), (b) and (f) have been observed during this study.

The compound $|Ru_5C(CO)_{13}DPPM|$ in solution exists as an equilibrium mixture of (b) (major) and (a) (minor), ((a):(b) =

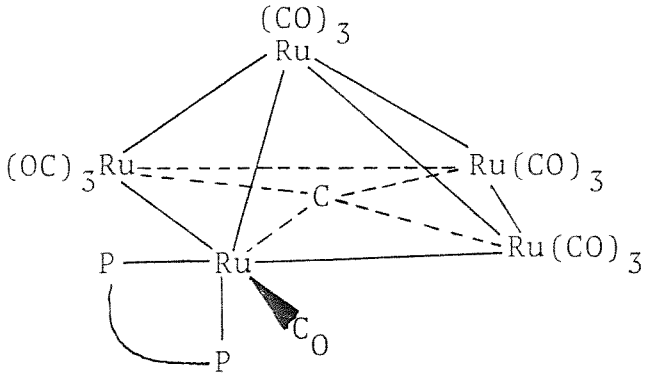

(a)

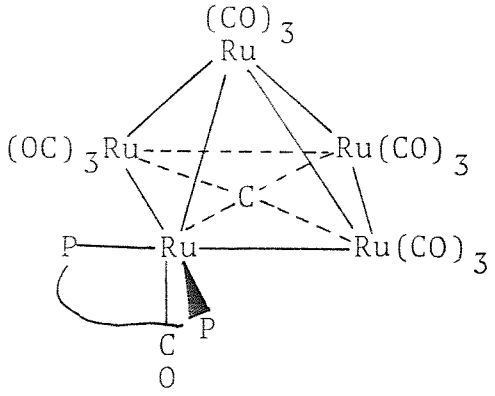

(b)

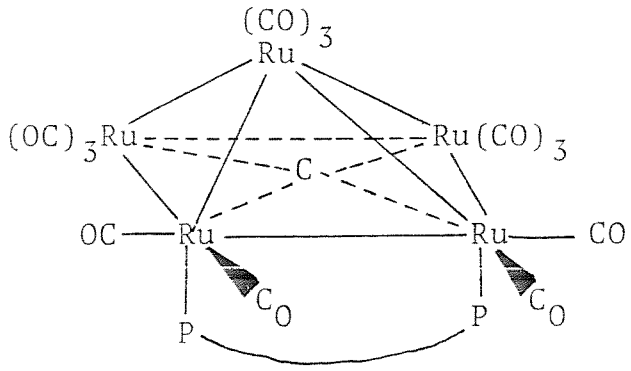

(c)

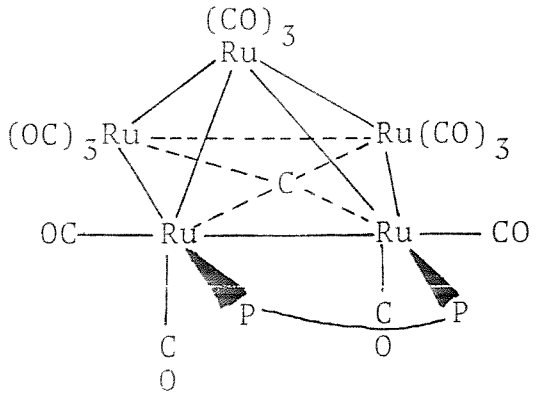

(d)

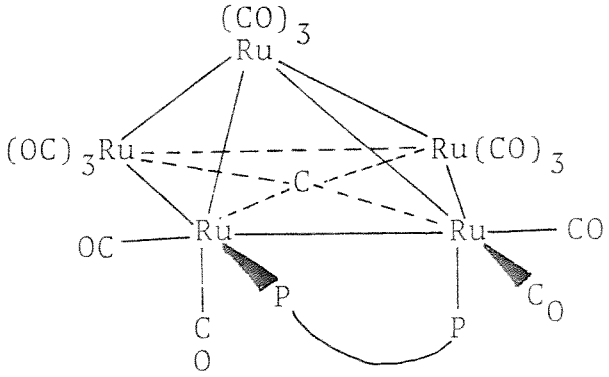

(e)

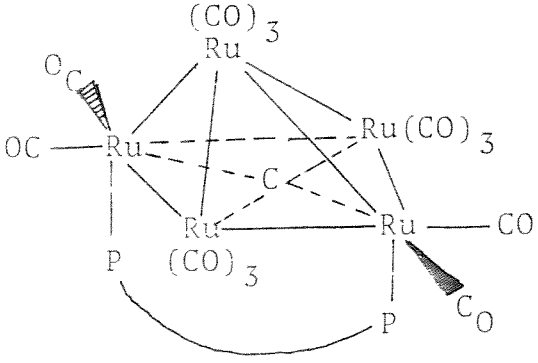

(f)

Diagram 5.15.

1:10, see Diagram 5.15). The evidence for this comes principally from the ^{31}P n.m.r. which shows a sharp singlet at r.t. but on cooling to -90 ^{o}C this broadens, splits and sharpens into a 3 signal pattern. The two weaker signals of equal intensity can be assigned to structure (a) (since it has inequivalent phosphorus atoms). The strong signal similarly can be assigned to structure (b) which possesses equivalent phosphorus atoms. Some supporting evidence for this comes from its variable temperature ^{13}C n.m.r. spectra (see Figure 5.6). At 60 ^{o}C only a singlet is observed as all the carbonyls are exchanging positions; on cooling this exchange slows down and by 21 ^{o}C localised exchange occurs on the n.m.r. time scale, with the carbonyls on the axial ruthenium atom appearing to have a separate exchange process to those on the basal ruthenium atoms (this has also been observed for $[Ru_5C(CO)_{15}]$). These two processes at 21 ^{o}C give rise to two singlets, one of relative intensity 3 due to the carbonyls on the axial ruthenium atom (made equivalent presumably by a rotation) and one of intensity 10 due to the carbonyls on the basal ruthenium atoms. The mechanism of the latter process is unclear but the complexity of the changes which occur on cooling indicate that at least two separate processes occur which together cause equivalence of these ten carbonyls. On cooling to 0 ^{o}C this peak broadens and then splits into 3 peaks of relative intensities 2:2:6. An explanation for this is that, as the phosphine rotation "ceases" at about -40 ^{o}C (see the ^{31}P n.m.r. and ^{1}H n.m.r. spectra, the rotation of the two basal $Ru(CO)_3$ groups adjacent to the phosphine substituted ruthenium atoms

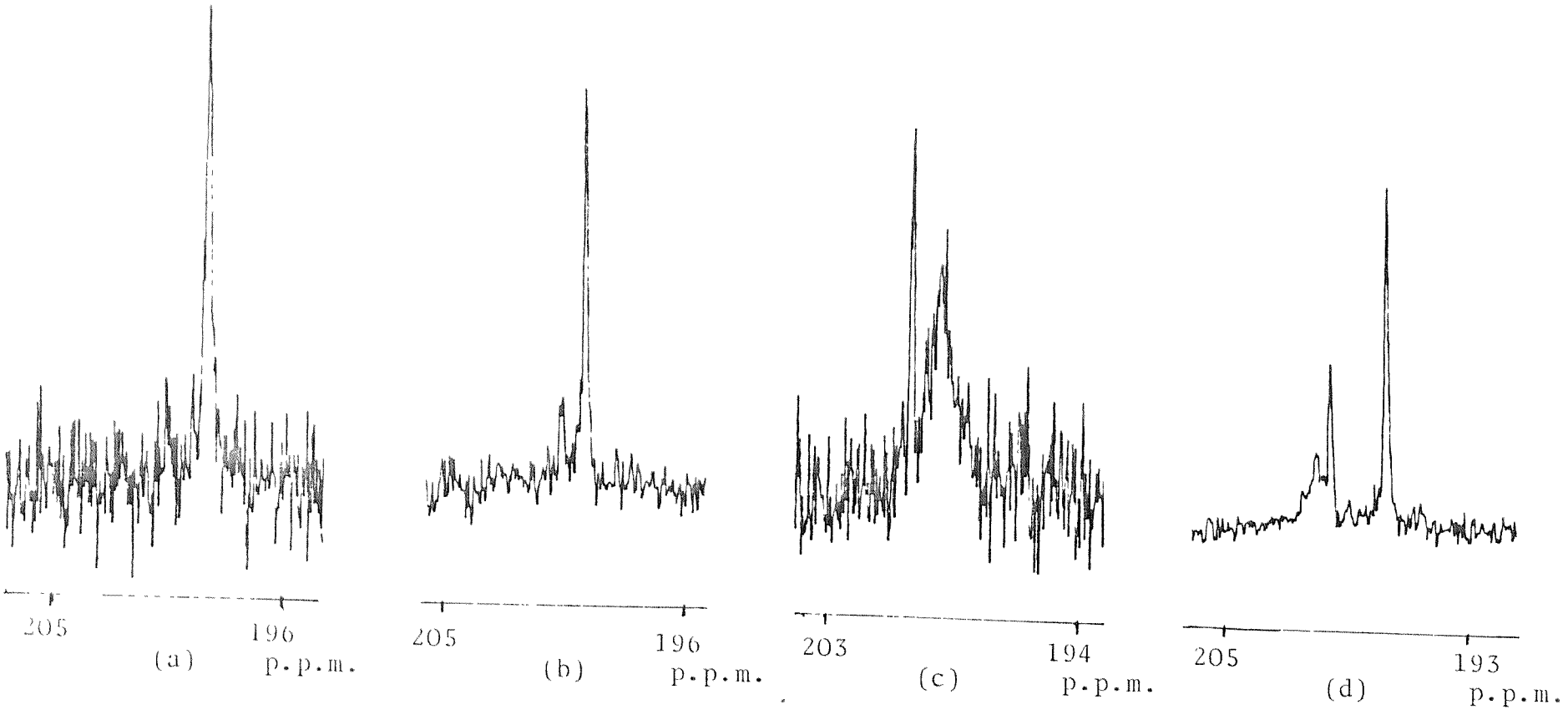

Figure 5.6. ^{13}C n.m.r. spectra of $|Ru_5C(CO)_{13}DPPM|$ in d^8-toluene (60 °C - 0 °C), CD_2Cl_2 (30—-60 °C) and $CD_2Cl_2/CFCl_2H$ (0 - -121 °C) at (a) 60 °C, (b) 30 °C, (c) 0 °C, and (d) -40 °C.

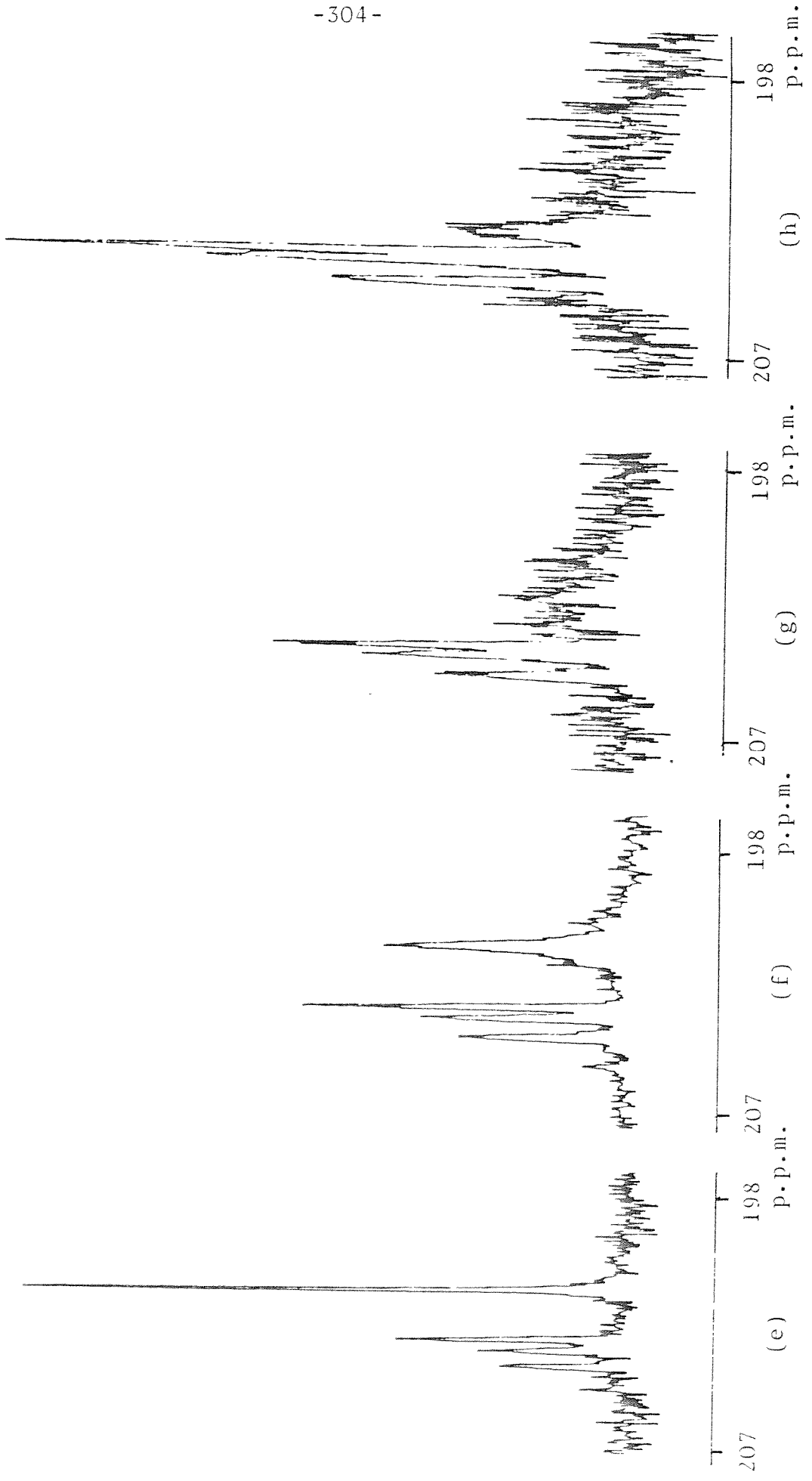

Figure 5.6. (Continued). (e) -60 °C, (f) -107 °C, (g) -117 °C, and (h) -125 °C.

ceases, presumably on steric grounds, and this should give rise to two pairs of equivalent equatorial carbonyls (see Diagram 5.16, C_1O and C_2O) which would explain the two signals of intensity 2. As the carbonyl on the phosphine substituted Ru atom is not seen a rapid exchange of the axial carbonyls (see Diagram 5.16, C_3O) on the basal ruthenium atoms must occur and this coupled with the rotation of the trans $Ru(CO)_3$ unit to the phosphine substituted ruthenium atom would explain the equivalence of these 6 carbonyls. Upon cooling further this peak due to 6 carbonyls broadens but by -125 °C (the lowest temperature obtainable on the n.m.r. machine) it is not frozen out. Interestingly the peak assigned to the carbonyls on the axial ruthenium does not broaden by -125 °C, and this is what one would expect from the similarity of the two possible carbonyl sites.

The ^1H n.m.r. spectra of $|Ru_5C(CO)_{13}DPPM|$ demonstrate the importance of the rotation of the phosphine substituted ruthenium unit in interconverting the two isomers and also the methylene protons in the DPPM ligand. For example, at 45 °C a triplet is seen because the rapid rotation interconverts the two otherwise inequivalent methylene protons, whereas at -60 °C when this process is slow on the n.m.r. time scale the two protons are inequivalent.

The solid state structure of $|H_2Ru_5C(CO)_{13}DPPE$ has been determined by X-ray diffraction[41] and shows that it exists as structure (a) (see Diagram 5.15); however, this work suggests that $|Ru_5C(CO)_{13}DPPE|$ exists solely in solution as structure (b). A main piece of evidence for this arises from

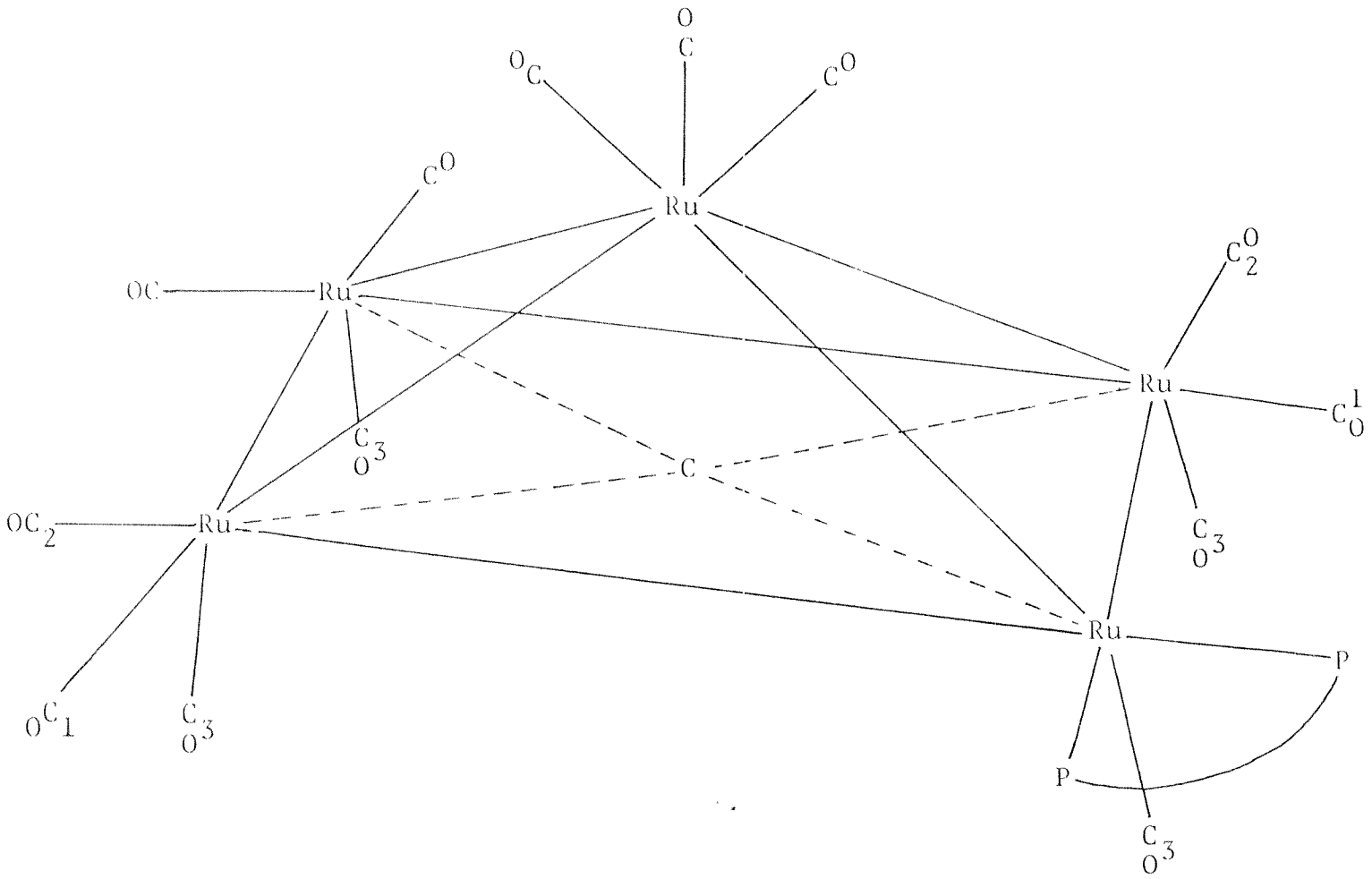

Diagram 5.16.

comparing its i.r. spectrum with that of $|Ru_5C(CO)_{13}DPPM|$. Since $|Ru_5C(CO)_{13}DPPM|$ exists in solution as mostly structure (b) with traces of structure (a) (as suggested by the ^{31}P n.m.r. spectra), its i.r. spectrum should show a ν_{CO} pattern indicative of (b) with small impurity peaks due to (a). However, the i.r. spectrum of $|Ru_5C(CO)_{13}DPPE|$ agrees only with the major peaks in the spectrum of the DPPM adduct (see Figure 5.7) and so must have predominantly structure (b) (like the DPPM adduct) in solution.

The ^{13}C n.m.r. spectra of $|Ru_5C(CO)_{13}DPPE|$ (see Figure 5.8) shows that this molecule possesses a plane of symmetry at low temperatures and so suggests that it possesses structure (b), but rapid rotation of the Ru(phosphine)CO unit cannot be ruled out. At high temperatures all the carbonyls are made equivalent by exchange processes and a sharp singlet is seen (103 ^{o}C); upon cooling this broadens and splits into a two peak pattern of relative areas 3:10 and like in the DPPM adduct these can be assigned to the carbonyls on the axial ruthenium and those on the basal ruthenium atoms, respectively. Also, similarly to the DPPM case, the band due to the axial ruthenium atom carbonyls remains sharp to the lowest temperatures studied, while the other band broadens.

This slowing of the exchange of carbonyls between the different sites on the basal ruthenium atoms occurs in stages (similarly to the DPPM adduct) and so indicates that several dynamic processes are occurring within the molecule. The first process to slow causes a broadening of the peak (at 197 p.p.m., -32 ^{o}C) to give two broad bands of approximate areas

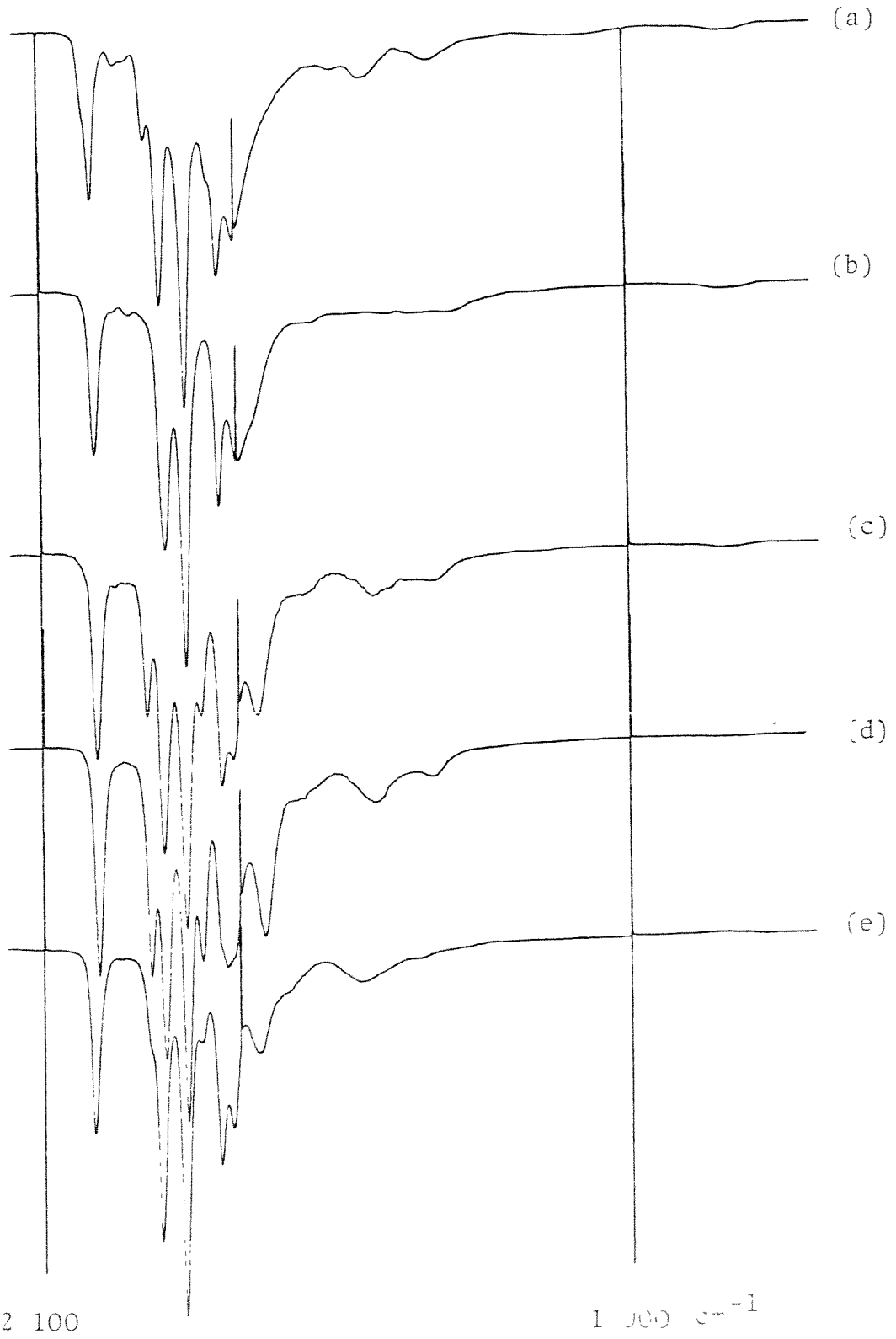

Figure 5.7. I.r. spectra in cyclohexane of the corner co-ordinating adducts, $[Ru_5C(CO)_{13}(DPPR)]$, where R = (a) DPPM, (b) DPPE, (c) DPPP, (d) DPPB, and (e) (-)-Diop.

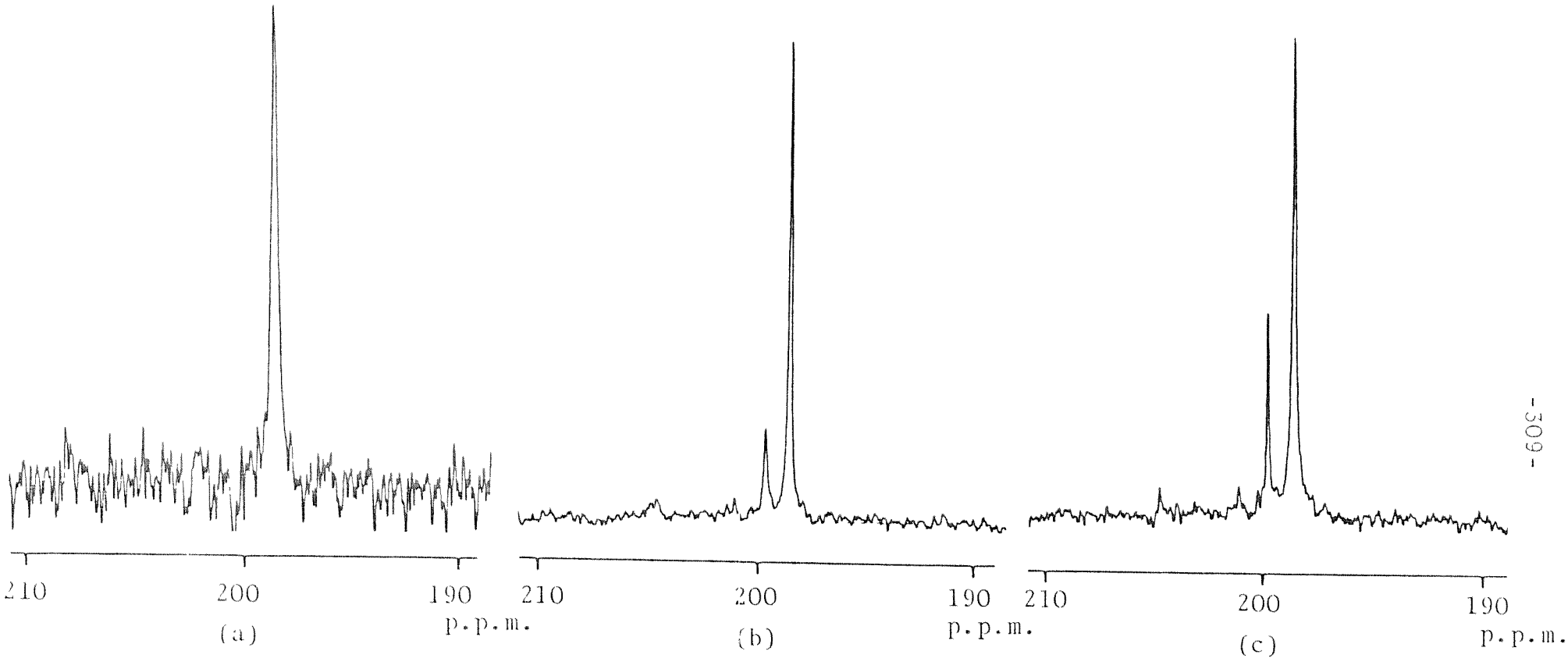

Figure 5.8. ^{13}C n.m.r. spectra of $[Ru_5C(CO)_{13}DPPE]$ in d^8-toluene (103 - 25 ^oC) and $CD_2Cl_2/CDCl_2H$ (-17 - -115 ^oC) at (a) 103 ^oC, (b) 61 ^oC, (c) 34 ^oC.

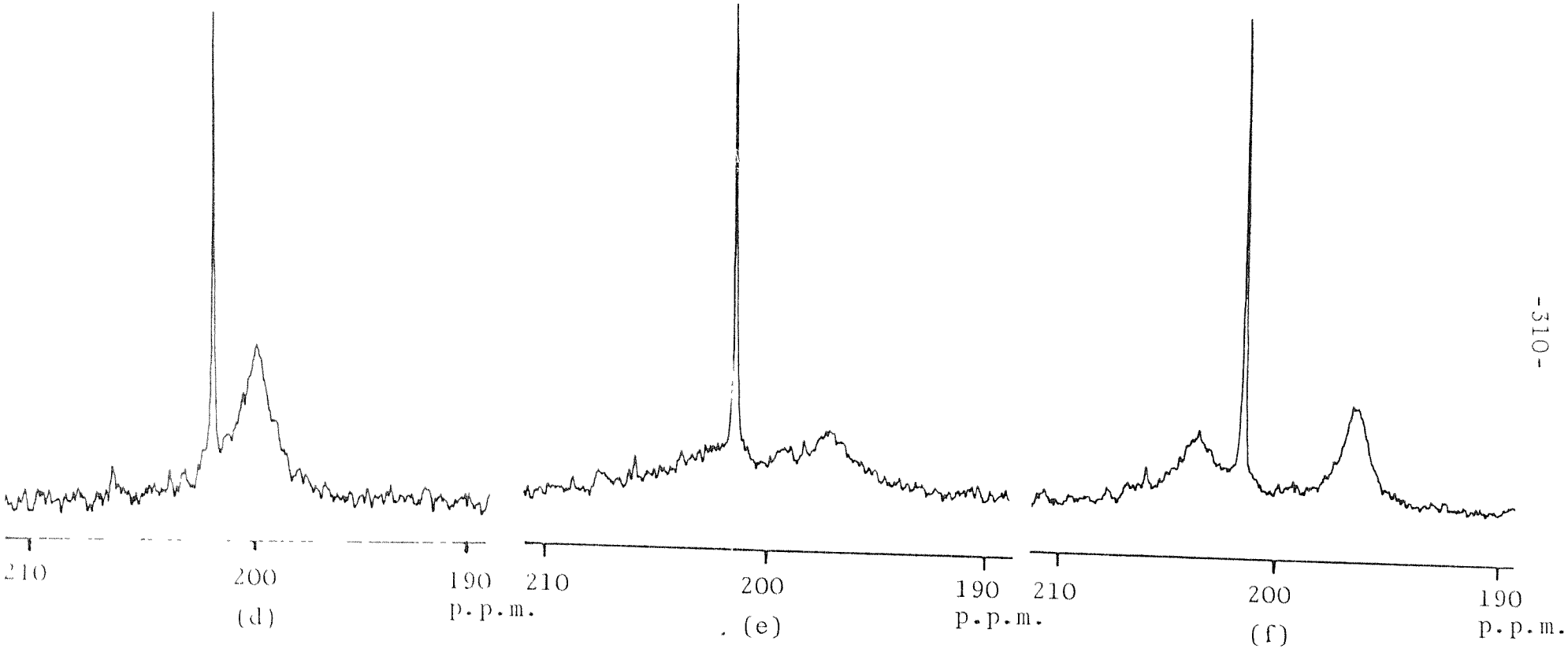

Figure 5.8 (Continued). (d) -17 °C, (e) -32 °C, (f) -48 °C.

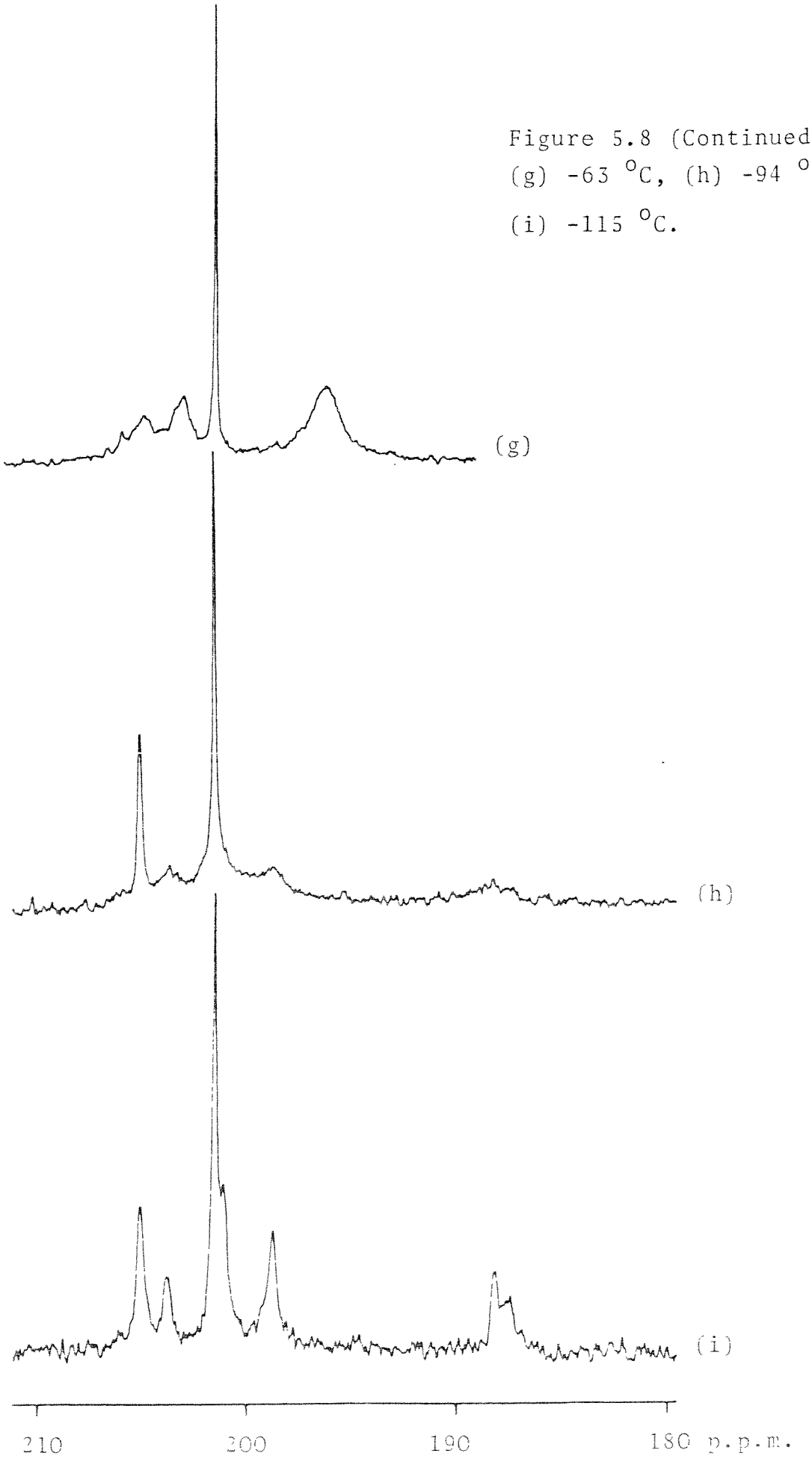

Figure 5.8 (Continued).
(g) -63 °C, (h) -94 °C,
(i) -115 °C.

4:6 (peaks at 203.5 and 196.5 p.p.m., respectively at -48 °C) these could be assigned to the axial and equatorial carbonyls respectively, but in reality the situation appears to be more complex with an intermediate peak being produced on further cooling (at -83 °C and -73 °C) which on further cooling broadens (at -94 °C) and meanwhile a new peak becomes evident (≈ 205 p.p.m.) corresponding to two equivalent carbonyls. Upon cooling further the other exchange processes slow down and the other basal carbonyls "freeze out" to give a pattern of relative areas 2:1:3:2:2:1, indicative of a plane of symmetry existing in the molecule with the phosphine occupying two equatorial sites. Unfortunately, as a result one cannot tell whether or not the rotation of the Ru(phosphine)CO unit has ceased. Incidentally, in the spectrum at -115 °C the peak at ∿ 187 p.p.m. appears to be of area 2 but its integral is 1, so the small peak on the side is possibly a result of noise in the spectrum. The ^{31}P n.m.r. spectra (40 °C - -90 °C) like the ^{13}C n.m.r. spectra support the claim that $|Ru_5C(CO)_{15}DPPE|$ exists in solution as predominately structure (b) with two equivalent phosphines, though rotation of the Ru(CO)phosphine unit again cannot be ruled out.

Initially when $Ru_5C(CO)_{15}$ is reacted with DPPP, a new compound, with an i.r. spectrum similar to the disubstituted compounds $Ru_5C(CO)_{15}(PPh_2R)_2$ is formed. This on standing converts to a mixture of compounds mainly of structures (a) and (b) (its i.r. spectrum is very similar to $|Ru_5C(CO)_{15}DPPM|$) with some of the initial compound (thought to have structure (f),

see Diagram 5.15). The ^{31}P n.m.r. spectra demonstrates the existence of (f) and (a) + (b) in equilibrium proportions of 1:5. On cooling no evidence is observed in the spectra for a slowing down of the exchange of (a)$\rightleftharpoons$(b) but this could be because this compound exists mainly as isomer (b).

The opposite type of behaviour is observed for DPPB, which initially produces a mixture containing mainly (a) and (b) with some (f), which on standing converts into wholly (f). This complex exhibits one $^{31}P-\{^{1}H\}$ resonance and the ^{13}C n.m.r. spectrum is consistent with both phosphines occupying equivalent sites on the basal ruthenium atoms. Its i.r. spectrum (see Figure 5.9) is similar to that obtained for compounds of the general formulae, $|Ru_5C(CO)_{13}(PPh_2R)_2|$.

This similarity was confirmed by a single crystal X-ray diffraction study, crystal data: $C_{42}H_{28}O_{13}P_2Ru_5$, monoclinic, space group $P2_1/n$, a = 10.650(8), b = 17.440(3), c = 23.889(4) Å, β = 96.67(4)°, Z = 4, U = 4 406.7 Å^3, μ(Mo-K_α) = 17.4 cm^{-1}. The data were collected using an Enraf Nonius CAD-4 diffractometer which gave 4 077 unique reflections $|F > 2.5\sigma(F)|$. The structure was solved by direct methods to locate the Ru_5 cluster and subsequent structure factor and electron density calculations located the remaining non-hydrogen atoms. Least squares refinement (237 parameters) gave R = 0.049.

The molecular structure (see Figures 5.10, 5.11, and Table 5.12) is derived from that of the parent $|Ru_5C(CO)_{15}|$, with the phosphorus atoms occupying axial positions on trans ruthenium atoms of the ruthenium square face. Although the phosphorus atoms are crystallographically distinct,

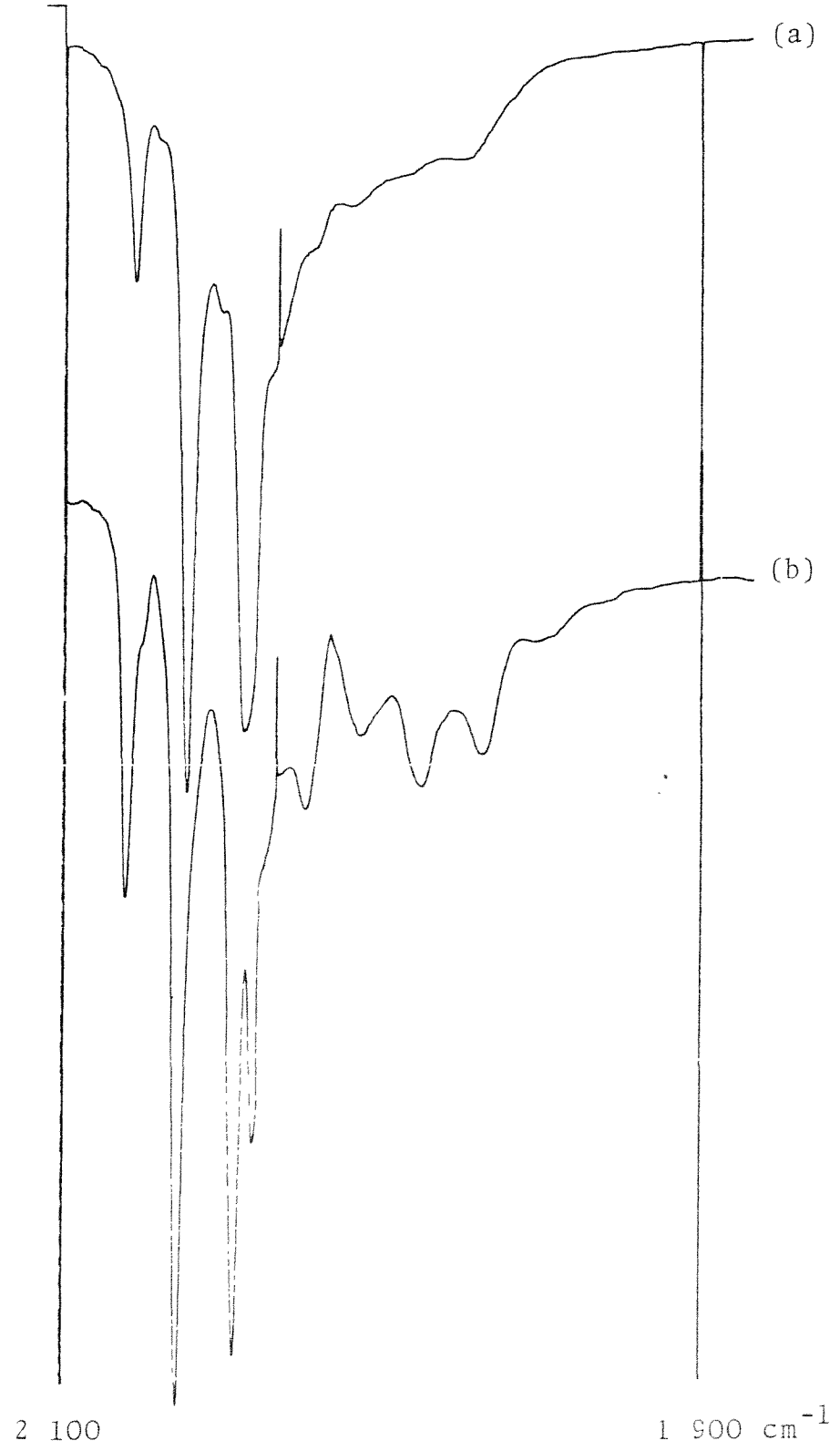

Figure 5.9. I.r. spectra of (a) $[Ru_5C(CO)_{15}(PPh_2Et)_2]$ and (b) $[Ru_5C(CO)_{13}$DPPB (diagonally co-ordinating form) in cyclohexane.

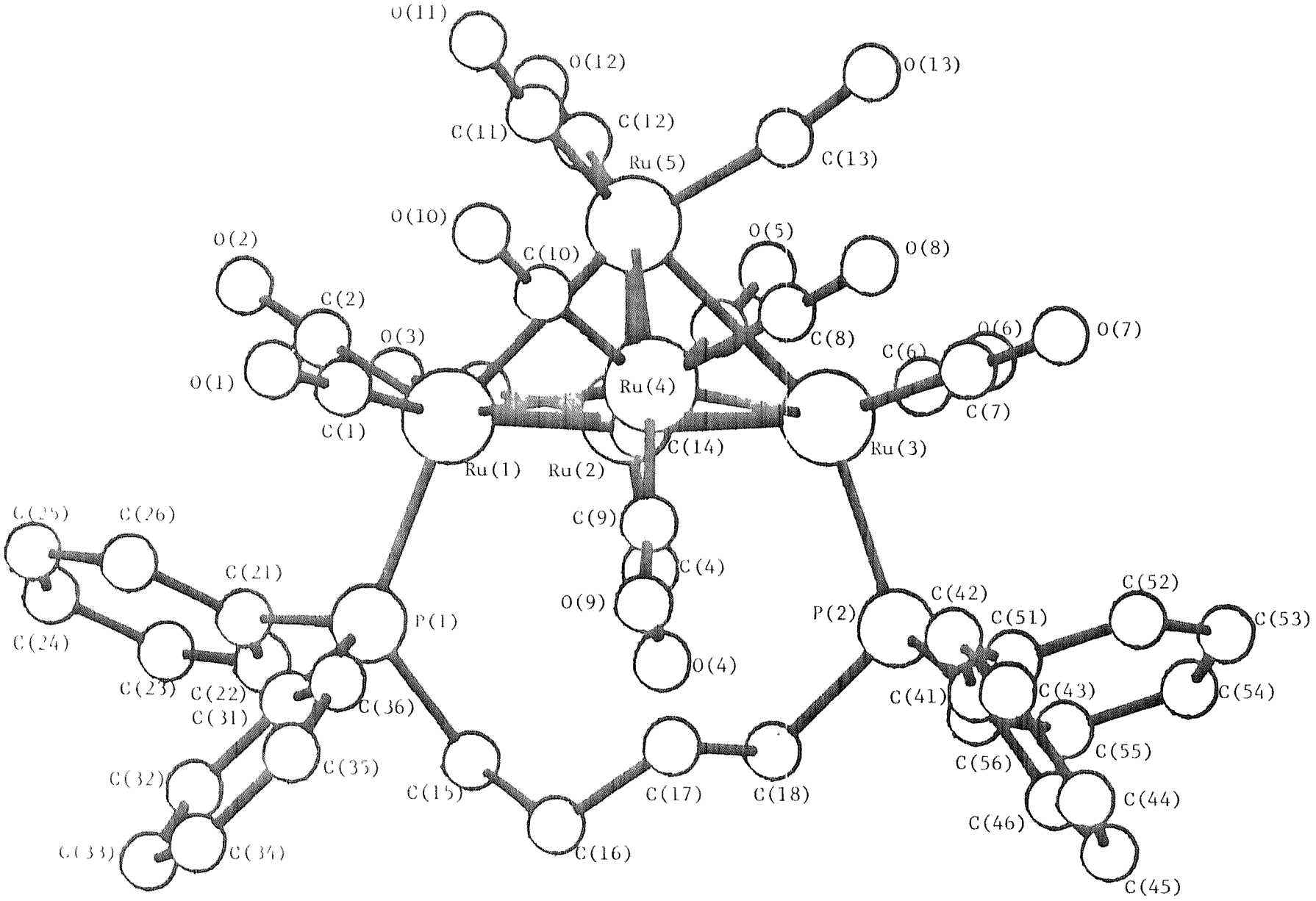

Figure 5.10. Molecular structure of $|Ru_5C(CO)_{15}(DPPB)|$

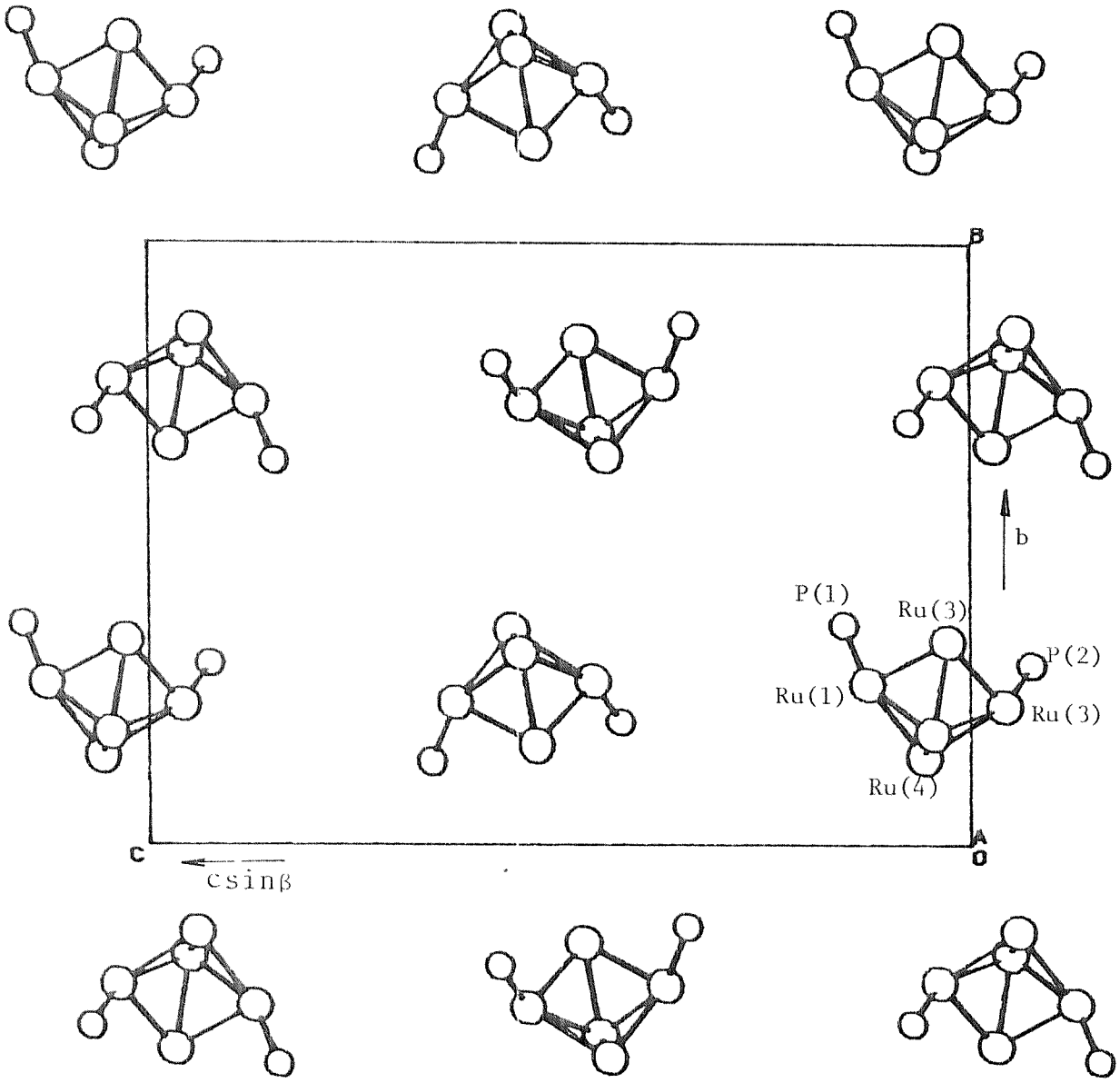

Figure 5.11. Contents of the unit cell viewed from +a excluding all C and O atoms for clarity.

TABLE 5.12.

Selected bond lengths (Å) and angles (degrees) for $|Ru_5C(CO)_{13}(PPh_2(CH_2)_4PPh_2)|$ with estimated standard deviations in parentheses.

(a) distances

Ru(1) - Ru(2)	2.873(1)
Ru(1) - Ru(4)	2.891(1)
Ru(1) - Ru(5)	2.847(1)
Ru(2) - Ru(3)	2.837(1)
Ru(2) - Ru(5)	2.778(1)
Ru(3) - Ru(4)	2.894(1)
Ru(3) - Ru(5)	2.881(1)
Ru(4) - Ru(5)	2.760(1)
Ru(1) - P(1)	2.367(3)
Ru(3) - P(2)	2.337(3)

Central carbide

Ru(1) - C(14)	2.024(9)
Ru(2) - C(14)	2.073(9)
Ru(3) - C(14)	2.002(9)
Ru(4) - C(14)	2.064(9)
Ru(5) - C(14)	2.163(9)
P(1) - C(15)	1.868(10)
P(1) - C(21)	1.835(6)
P(1) - C(31)	1.839(5)
P(2) - C(18)	1.843(10)
P(2) - C(41)	1.828(5)
P(2) - C(51)	1.830(5)

Terminal CO distances

C - O(min)	1.155(12)
C - O(max)	1.196(19)
C - O(mean)	1.169

TABLE 5.12. (Continued).

Phosphines alkyl chain.

C(15) - C(16)	1.521(14)
C(16) - C(17)	1.520(14)
C(17) - C(18)	1.521(13)

distance of carbide (C(14)) below Ru(1), Ru(2), Ru(3) and Ru(4) plane = 0.21.

(b) Bond angles

Ru(1) - Ru(2) - Ru(3)	89.5(1)
Ru(1) - Ru(2) - Ru(5)	60.5(1)
Ru(3) - Ru(2) - Ru(5)	61.7(1)
Ru(2) - Ru(3) - Ru(4)	91.2(1)
Ru(2) - Ru(3) - Ru(5)	58.1(1)
Ru(1) - Ru(4) - Ru(5)	60.4(1)
Ru(3) - Ru(4) - Ru(1)	88.0(1)
Ru(3) - Ru(4) - Ru(5)	61.2(1)
Ru(4) - Ru(3) - Ru(5)	57.1(1)
Ru(4) - Ru(1) - Ru(2)	90.5(1)
Ru(4) - Ru(1) - Ru(5)	57.5(1)
Ru(5) - Ru(1) - Ru(2)	58.5(1)
Ru(1) - Ru(5) - Ru(2)	61.0(1)
Ru(1) - Ru(5) - Ru(3)	89.1(1)
Ru(1) - Ru(5) - Ru(4)	62.1(1)
Ru(2) - Ru(5) - Ru(3)	60.1(1)
Ru(2) - Ru(5) - Ru(4)	95.4(1)
Ru(3) - Ru(5) - Ru(4)	61.7(1)
P(1) - Ru(1) - Ru(2)	99.1(1)
P(1) - Ru(1) - Ru(4)	116.9(1)
P(1) - Ru(1) - Ru(5)	154.5(1)
P(2) - Ru(3) - Ru(2)	103.4(1)
P(2) - Ru(3) - Ru(4)	107.1(1)
P(2) - Ru(3) - Ru(5)	152.1(1)

TABLE 5.12. (Continued)

Ru(1) - C(14) - Ru(3)	172.8(5)
Ru(1) - C(14) - Ru(5)	85.6(3)
Ru(2) - C(14) - Ru(4)	163.4(5)
Ru(2) - C(14) - Ru(5)	81.9(3)
Ru(3) - C(14) - Ru(5)	87.4(3)
Ru(4) - C(14) - Ru(5)	81.5(3)
R - C - O(max)	176.6(1)
(min)	171.2(1.5)
(mean)	175.2
Ru(1) - P(1) - C(15)	122.4(4)
Ru(1) - P(1) - C(21)	108.8(3)
Ru(1) - P(1) - C(31)	118.9(2)
Ru(3) - P(2) - C(18)	116.3(3)
Ru(3) - P(2) - C(41)	119.3(2)
Ru(3) - P(2) - C(51)	111.9(2)
C(15) - P(1) - C(21)	102.5(4)
C(15) - P(1) - C(31)	99.1(4)
C(21)- P(1) - C(51)	102.4(3)
C(18) - P(2) - C(41)	100.9(3)
C(18) - P(2) - C(51)	104.5(4)
C(41) - P(2) - C(51)	102.0(3)
P(1) - C(15) - C(16)	118.6(8)
C(15) - C(16) - C(17)	115.0(9)
C(16) - C(17) - C(18)	112.4(8)
C(17) - C(18) - P(2)	113.1(7)

they would be expected to be equivalent in solution, as observed by ^{31}P n.m.r. The binding of the phosphine, to non-adjacent metal atoms is noteworthy and the bite of this particular ligand is appropriate to achieve this. The mean Ru(apical) —Ru(basal) —P angle (153.5°) is 10° less than the corresponding Ru(apical) —Ru(basal) —C(carbonyl) angle (164°). The strapping phosphine causes the ML_3 units in the base to the square pyramid to tilt in this relatively small distortion. Interestingly, for DPPP this strapping conformation is the kinetic product but not the thermodynamic product (presumably because of the shorter chain length) of the reaction whereas for DPPB, the DPPM structure is the kinetic product (presumably due to the unfavourability of producing a larger ring).

The importance of the alkyl chain flexibility on the pattern of substitution of $[Ru_5C(CO)_{15}]$ with bidentate ligands is demonstrated by the reaction of the (-)-Diop ligand. This ligand contains, in the middle of the 4-membered alkyl chain separating the two phosphorus atoms, a trans ring junction to a five membered ketal ring which should restrict the flexibility of the alkyl chain. This is manifested in the reaction of (-)-Diop which behaves like DPPP (3 membered alkyl chain) rather than DPPB (4 membered alkyl chain like (-)-Diop). That is (-)-Diop, similar to DPPP, initially forms structure (f) which on standing converts to a mixture of isomers (a) and (b) (see Diagram 5.15). The evidence for this comes from its (i) i.r. spectrum - which resembles initially that of the DPPB adduct, and on standing in solution converts to one resembling the DPPM

adduct; (ii) ^{1}H n.m.r. spectrum - which for the final product mixture shows only two main $P\underline{CH}_2$ environments of equal abundance; (iii) ^{31}P spectrum - which shows initially a single peak (at 23.19 p.p.m.) which on standing decreases, concomitant with the growth of two peaks of equal intensity (at 29.30 and 19.68 p.p.m.).

Since the final i.r. spectrum of this compound, $|Ru_5C(CO)_{13}$-{(-)-Diop}|, resembles closely that of the DPPM adduct, (see Figure 5.7), it is reasonable to assume that it occurs mostly as isomer (b) (see Diagram 5.15) in cyclohexane solution. However, both the ^{31}P and ^{1}H n.m.r. spectra indicate that the two phosphines are inequivalent and hence suggest that this compound has predominantly structure (a) in CH_2Cl_2 or $CDCl_3$ solution, and also rigid on the n.m.r. time scale. An explanation for this is that the compound has predominantly structure (b) in all the solvents but the two phosphines are made inequivalent due to the chirality of the ligand. That is the trans-ring junction in the alkyl backbone forces the methylene groups adjacent to the phosphines to occur above and below the plane of the square base of the cluster (a similar straddling effect has been seen for $'Ru_3(CO)_{10}$-{(-)-Diop}, see Figures 5.2 and 5.3). This coupled with the structure being rigid on the n.m.r. time scale explains why the phosphines and the adjacent methylenes are inequivalent (see Diagram 5.17).

As was seen for Ru_3 and Ru_4 clusters the abundance of products involving the linking of two or more clusters increases as the chain length increases. For example, a major side

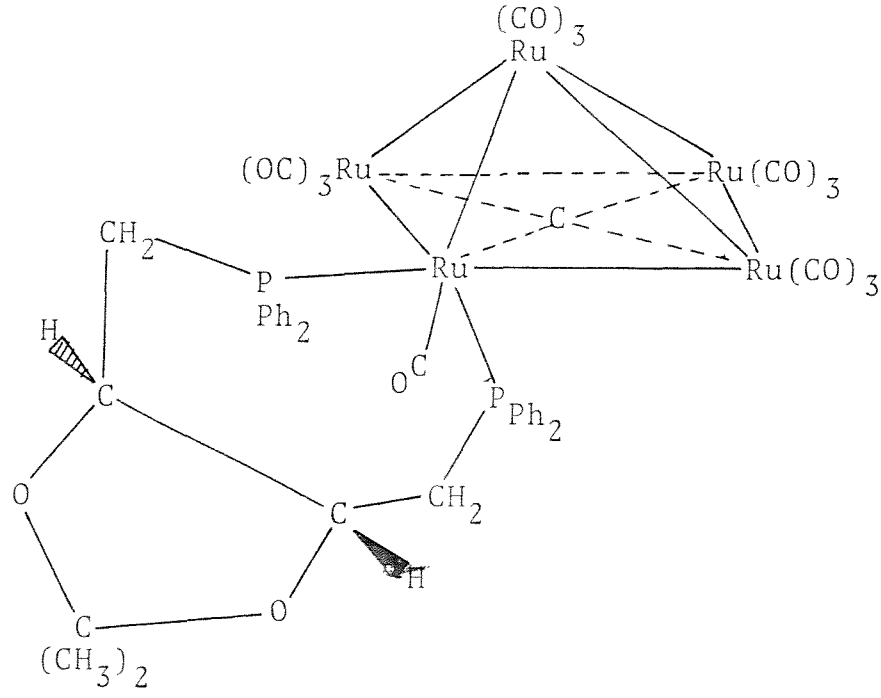

Diagram 5.17.

product from the reaction of DPPB or (-)-Diop with $|Ru_5C(CO)_{15}|$ is $|\{Ru_5C(CO)_{14}\}_2(P-P)|$ (where P — P = DPPB or (-)-Diop) and this displays an i.r. spectrum similar to the mono-substituted $|Ru_5C(CO)_{14}PPh_2R|$ clusters (see Figure 5.12). Confirmation that both ends of the phosphines were attached was obtained by a successful analyses and ^{31}P n.m.r. spectra which showed that both phosphorus atoms were equivalent.

The reaction of DPPM with $|Ru_5C(CO)_{15}|$ gave $|Ru_5C(CO)_{11}(DPPM)_2|$ as well as $|Ru_5C(CO)_{13}DPPM|$, the yield of which could be increased to over 90 % by reacting an excess of DPPM with the cluster overnight. The ^1H, ^{31}P and ^{13}C n.m.r. spectra indicate that this molecule probably has structure (g), though structure (h) cannot be eliminated (see Diagram 5.18). The low temperature ^{13}C n.m.r. spectrum from -116 ^oC - -46 ^oC

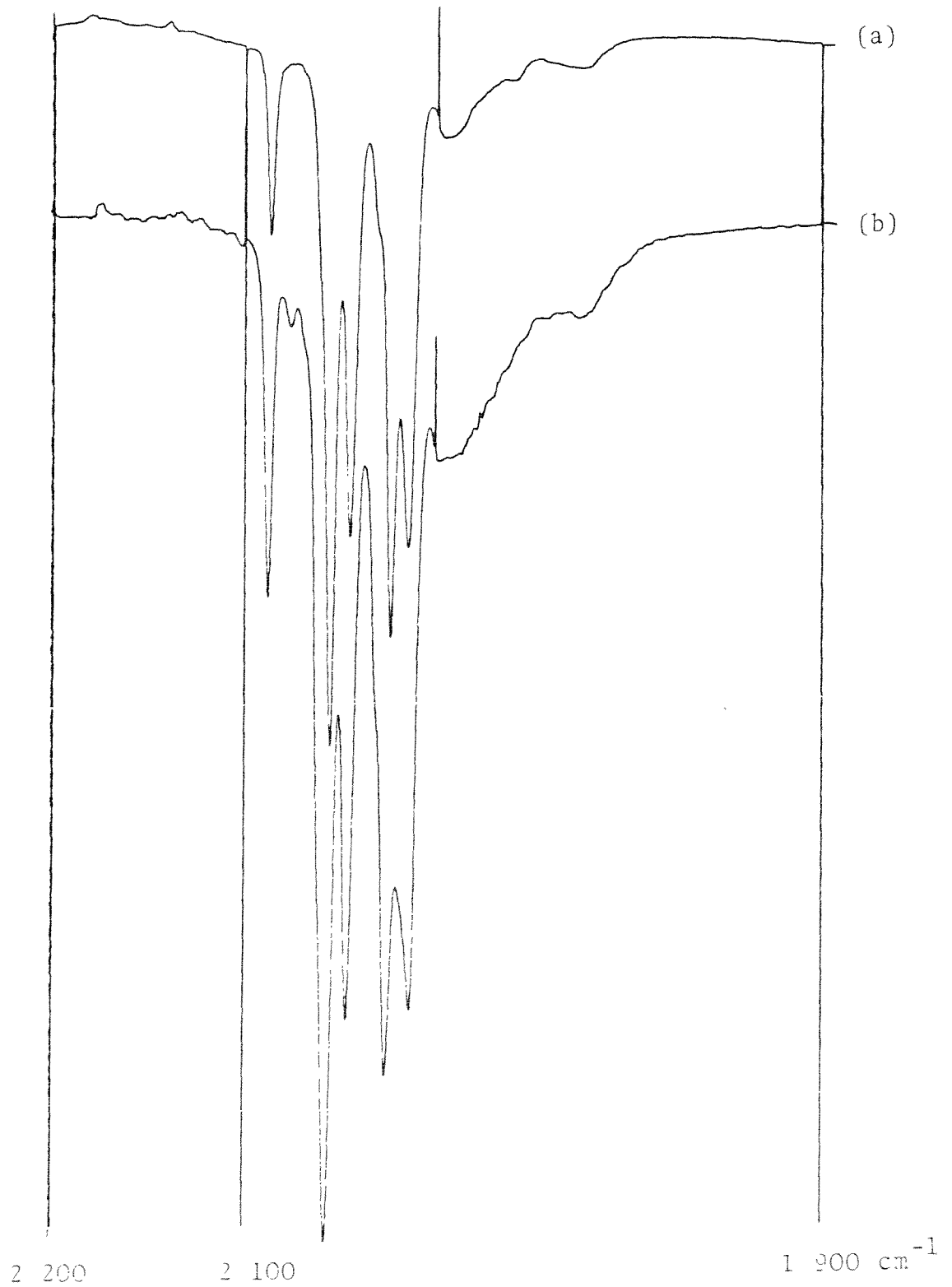

Figure 5.12. I.r. spectra of (a) $[Ru_5C(CO)_{14}PPh_2Et]$ and (b) $[(Ru_5C(CO)_{14})_2DPPB]$, in cyclohexane.

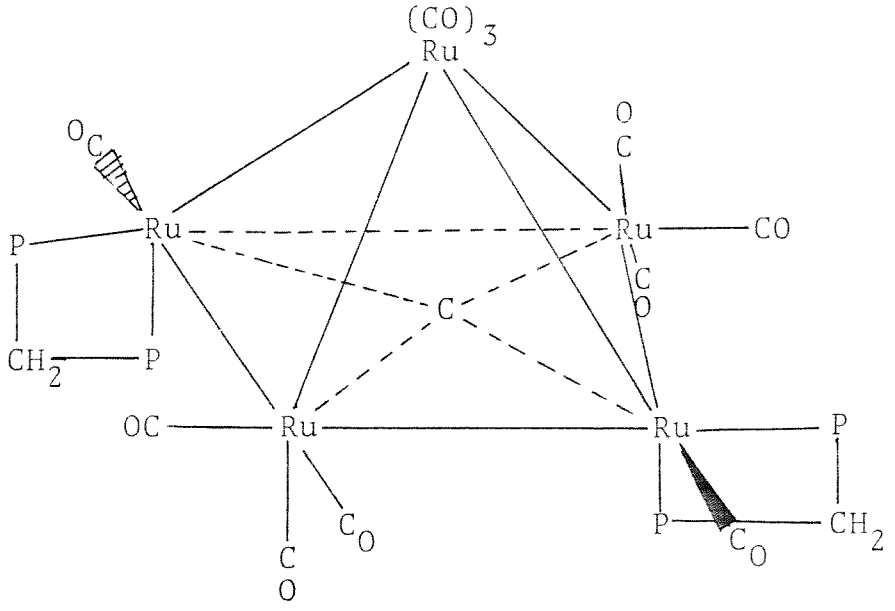

(g)

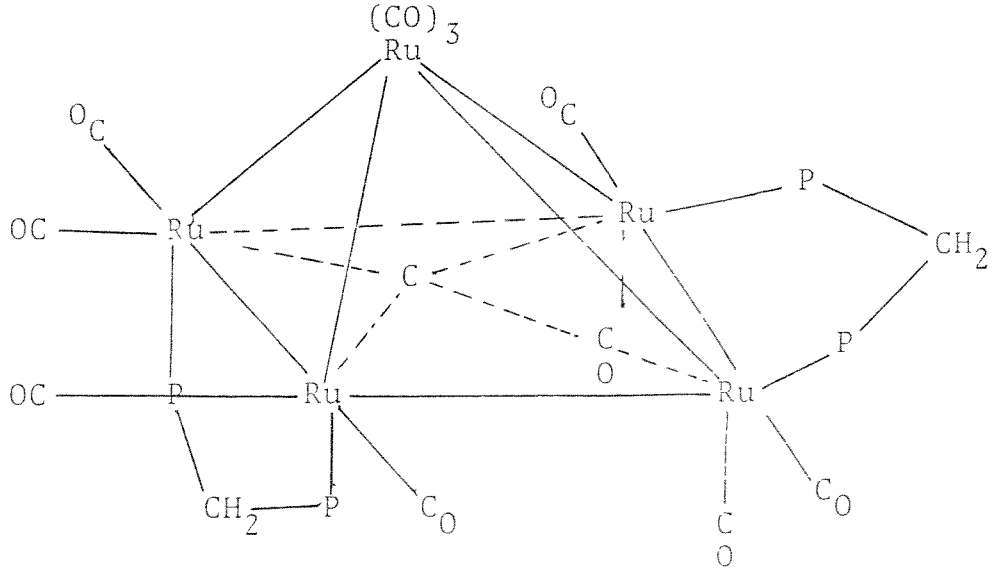

(h)

Diagran 5.18.

effectively does not change and consists of a 5 band pattern of relative intensities 2:3:2:2:2, which indicates the existence of either a plane of symmetry (e.g.structure (h)) or a two-fold axis of symmetry (e.g. structure (g)). The peak of intensity 3, in the light of what occurs as the sample is warmed, can be assigned to the carbonyls on the axial ruthenium atom. On warming, the bands of intensity 2 broaden unevenly and coalesce to produce two bands of intensity 4 by 85 ^{o}C, presumably caused by two unknown equilibrating processes. The existence of a carbonyl band of intensity 2 shifted a fair distance downfield from the other peaks in the low temperature spectra indicates that probably only two carbonyls are on the ruthenium substituted by the DPPM ligands, i.e. the structure is probably option (g). The ^{31}P n.m.r. spectra indicate the existence of an equilibrating process between the two phosphine environments seen in the low temperature spectrum. This could occur in option (g) by a rotation of the two Ru(CO)(phosphine) units, and in option (h) by a rocking process for the phosphines moving them from axial to equatorial sites together with a semi-rotation of the two carbonyls. This latter process would explain the occurrence of the two bands of intensity 4 in the high temperature spectrum but not the uneven sharpening of these two peaks.

A possible explanation of this uneven broadening and different positions of the two bands is that they are due to localised exchange of only axial or equatorial carbonyls which have different activation energies. Such a process is not possible for structure (h) as the process of exchange of the

two phosphine environments would necessarily exchange the axial and equatorial carbonyls. This is not the case for (g), if the exchange process requires the formation of intermediates with axial bridging carbonyls it will also require rotation of Ru(CO)(DPPM) units since the $Ru(CO)_3$ units are isolated by the phosphine which occupies both axial and equatorial sites. This would also cause equivalence, when fast enough, between the equatorial carbonyls since this motion would generate two time-averaged planes of symmetry bisecting the cluster along the two $Ru_{basal}-Ru_{axial}-Ru_{basal}$ planes.

The ^1H n.m.r. spectra of $|Ru_5C(CO)_{11}(DPPM)_2|$ confirms that a Ru(CO)(phosphine) unit rotation occurs above -65 ^oC with the two sets of signals for the different types of methylene protons broadening and coalescing by -10 ^oC, though a high temperature limiting spectrum was not obtained (i.e. a triplet), because of cluster decomposition on heating.

(e) $|Ru_6C(CO)_{17}|$ clusters with bidentate phosphines.

The attempted reaction of $|Ru_6C(CO)_{17}|$ with $HC(PPh_2)_3$ to produce $|Ru_6C(CO)_{14}\{\mu_3\text{-}(PPh_2)_3CH\}|$ was unsuccessful under a variety of conditions. This result demonstrates again the need to study the effect of chain length on the mode of co-ordination of polydentate phosphines. The reaction of $|Rh_6C(CO)_{16}|$ with bidentate phosphines has been reported,[53] to give clusters of the general formulae $|Rh_6(CO)_{14}(P\text{ --}P)|$ (where (P — P) = DPPE and DPPB) with two different structures. In the DPPB adduct the phosphorus atoms are thought to co-ordinate to adjacent Rh atoms and in the DPPE adduct one phosphorus atom co-ordinates to a Rh atom and the other to a face bridging carbonyl.

$|Ru_6C(CO)_{17}|$ reacts under mild conditions (r.t., CH_2Cl_2 solution, overnight) with bidentate phosphines to give in moderate to high yields clusters of the general formulae $|Ru_6C(CO)_{15}(P\text{ --}P)|$ (where P — P = bidentate phosphine). Air stable crystals of the first member of this series $|Ru_6C(CO)_{15}$-DPPM| were obtained from a cyclohexane/CH_2Cl_2 diffusion and subjected to an X-ray diffraction study. Crystal data - $C_{41}H_{22}O_{15}P_2Ru_6$, Monoclinic C centred, space group C2/c, a = 14.116(4), b = 18.132(4), c = 35.665(4), β = 101.04(2)°, Z = 8, U = 8 959.6 Å^3, μ(Mo-K_α) = 17.4 cm^{-1}. The data was collected using an Enraf Nonius CAD-4 diffractometer which gave 5 261 unique reflections $|F > 2.5\sigma(F)|$ which were used in the structure determination. A Patterson function clearly indicated the presence of a Ru_6 cluster from the Ru — Ru vectors around the origin. Multan-80 was used to determine the

position of the cluster in the unit cell. The four E-maps with the highest CFOM values were examined and of these the one with the highest CFOM gave the correct solution (which agreed with the Patterson map). Subsequent difference electron density synthesis rapidly located the remaining atoms. Least squares refinement of isotopic atoms reduced the R value to 0.082. The Ru and P atoms were made anisotropic and rigid phenyl groups were introduced (C — C = 1.395 Å, C — H = 1.08 Å) and the model converged to R = 0.0516 (R_w = 0.0569, 250 parameters).

This single crystal study demonstrated that the phosphine bridges a Ru — Ru edge (see Table 5.13, and Figure 5.13). Imperfect tailoring of the ligand to the cluster is evident in the torsional and bond angles in the ligand which show an asymmetry in its mode of co-ordination, though the possibility that this is due to packing effects in the crystal cannot be ruled out. The other members of this series $|Ru_6C(CO)_{15}\{P — P\}|$ (where P — P = DPPE, DPPP, DPPB, (-)-Diop) are thought to have similar structures because of the strong similarities in their ν_{CO} fingerprint patterns to $|Ru_6C(CO)_{15}DPPM|$ (see Figure 5.14). However, there is a gradual change in the fingerprint pattern as the chain length increases. That is new lower frequency bands appear and become resolved (bands at 1 995 and 1 900 cm^{-1}) and a new bridging band (1 865 cm^{-1}) appears. These results suggest the appearance of a new isomer but the ^{31}P n.m.r. spectra show only sharp singlets at 31 °C. However, on cooling of these samples to -85 °C these singlets broaden (e.g. 5 Hz at 31 °C, and at -85 °C, DPPM 200 Hz, DPPE 100 Hz and DPPB

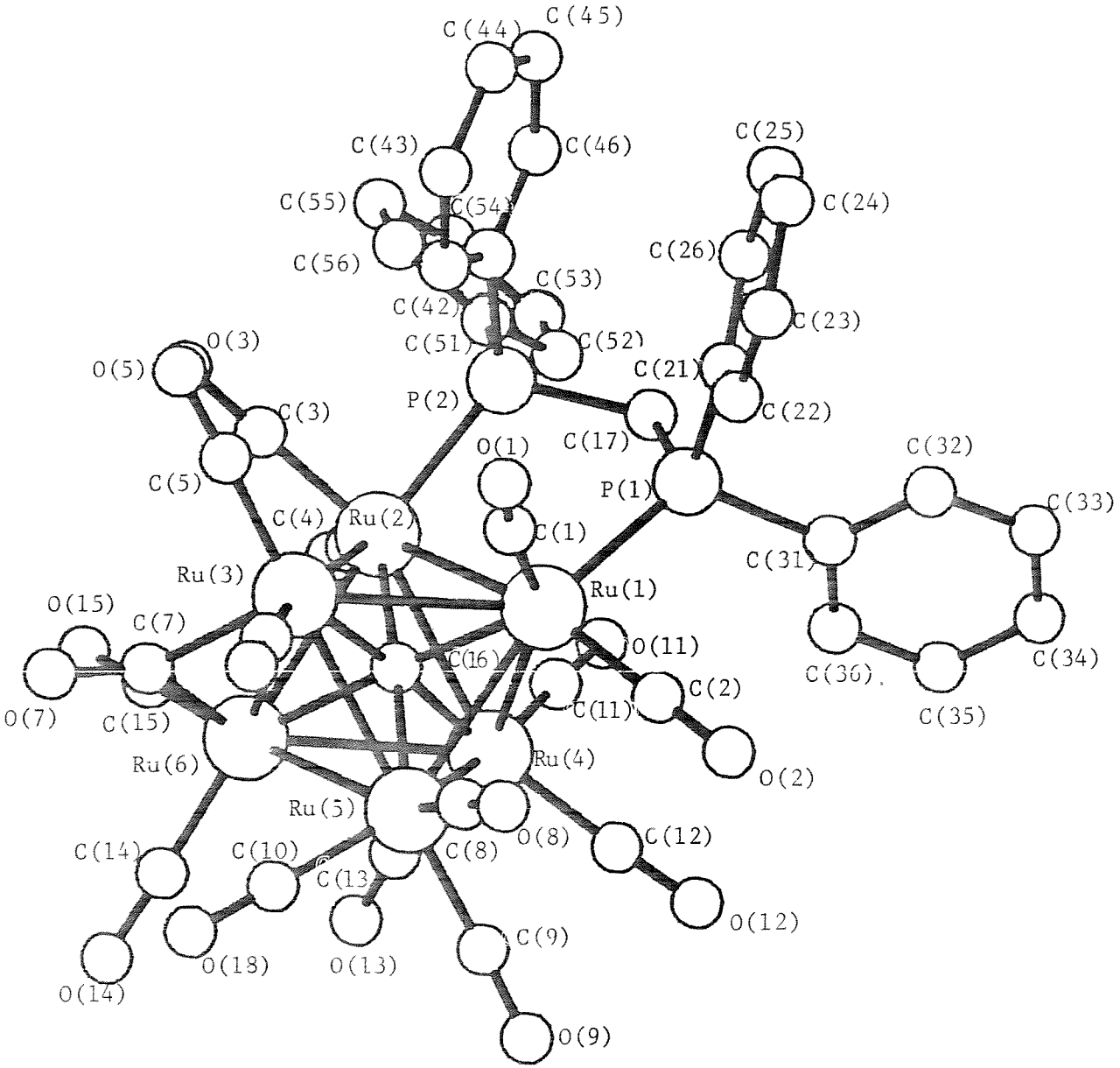

Figure 5.13 The solid state structure of $[Ru_6C(CO)_{15}(\mu\text{-DPPM})$. Hydrogen atoms omitted for clarity.

TABLE 5.13.

Selected bond lengths (Å) and angles (degrees for $|Ru_6C(CO)_{15}$-$(PPh_2CH_2PPh_2)$ with estimated standard deviations in parentheses.

(a) distances.

Ru(1) - Ru(2)	2.986(1)
Ru(1) - Ru(3)	2.975(1)
Ru(1) - Ru(4)	2.874(1)
Ru(1) - Ru(5)	2.897(1)
Ru(2) - Ru(3)	2.936(1)
Ru(2) - Ru(5)	2.900(1)
Ru(2) - Ru(6)	2.870(1)
Ru(3) - Ru(4)	2.857(1)
Ru(3) - Ru(6)	2.838(1)
Ru(4) - Ru(5)	2.903(1)
Ru(4) - Ru(6)	2.898(1)
Ru(5) - Ru(6)	2.938(1)
Ru(1) - P(1)	2.345(3)
Ru(2) - P(2)	2.328(3)
Central carbide	
Ru(1) - C(16)	2.038(10)
Ru(2) - C(16)	2.021(10)
Ru(3) - C(16)	2.048(10)
Ru(4) - C(16)	2.074(10)
Ru(5) - C(16)	2.063(10)
Ru(6) - C(16)	2.093(10)
P(1) - C(21)	1.822(7)
P(1) - C(31)	1.840(7)
P(1) - C(17)	1.843(11)
P(2) - C(41)	1.819(7)
P(2) - C(51)	1.825(7)
P(2) - C(17)	1.822(11)

TABLE 5.13 (Continued).

Terminal CO			
Ru - C(min)	1.832(14)	C - O(min)	1.150(18)
Ru - C(max)	1.927(14)	C - O(max)	1.188(17)
Ru - C(mean)	1.862	C - O(mean)	1.169
Bridging			
Ru(3) - C(7)	2.051(13)	C(7) - O(7)	1.191(15)
Ru(6) - C(7)	2.062(13)		

C — C = 1.395* C — H = 1.08*

(* = constrained during refinement).

(b) Angles

Ru - Ru - Ru on triangular faces (24)

max	62.5°	(1)
min	58.4°	(1)
|idealised	= 60.0°|	

Ru - Ru - Ru on square sections (12)

max	91.4	(1)
min	88.7	(1)
|idealised	= 90.0°|	

Ru(1) - P(1) - C(21)	116.1(3)
Ru(1) - P(1) - C(31)	118.5(3)
Ru(1) - P(1) - C(17)	111.2(4)
Ru(2) - P(2) - C(41)	119.1(3)
Ru(2) - P(2) - C(51)	111.9(3)
Ru(2) - P(2) - C(17)	114.3(4)
P(1) - C(17) - P(2)	112.1(6)

Terminal CO's

Ru - C - O	max	179(1)
	min	168(1)
	mean	176

Bridging CO

Ru(3) - C(7) - Ru(6)	87.3(5)
Ru(3) - C(7) - O(7)	135.1(1.1)
Ru(6) - C(7) - O(7)	137.5(1.1)

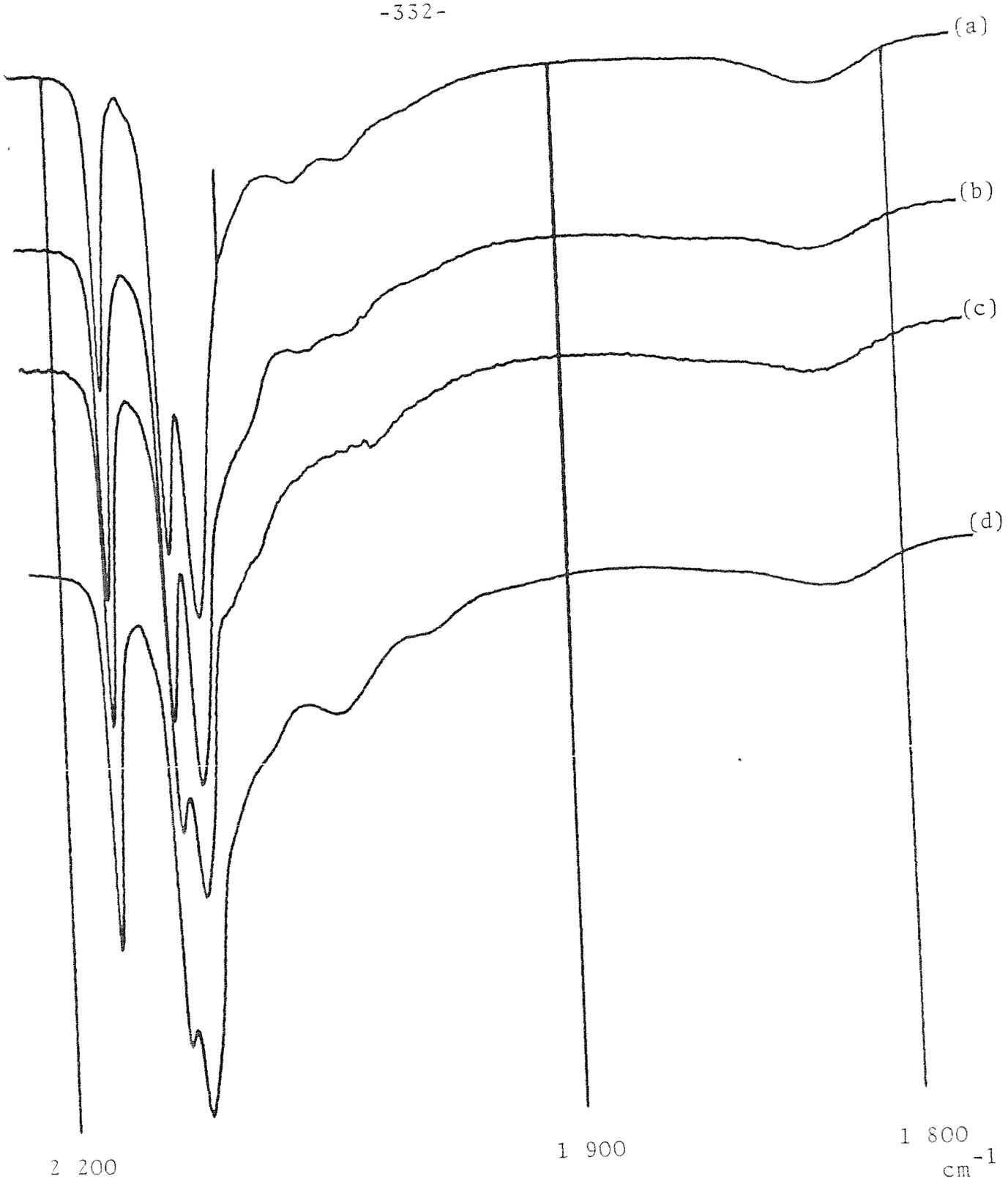

Figure 5.14 The carbonyl fingerprints of compounds of the general formulae $Ru_6C(CO)_{15}(P-P)$ in CH_2Cl_2, where (P — P) is (a) DPPM, (b) DPPE, (c) DPPP, and (d) DPPB.

coalescence) and in one case, DPPP, there is a partially resolved splitting of the peak into an unequal pair of peaks. An insight into what is happening was gained from a variable temperature ^{13}C n.m.r. study on $|Ru_6C(CO)_{15}DPPM|$.

In the case of $|Ru_6C(CO)_{15}DPPM|$ one would expect from the X-ray structure determination the phosphines to be inequivalent and the signal due to the methylene protons to be two triplets of doublets. However, at r.t. and down to -80 ^{o}C this signal is only a triplet and hence indicates that the protons are exchanging environments. There are three possible processes for this (see Diagram 5.19). The first two mechanisms involving the change of position of co-ordination of the phosphine on the octahedron can be ruled out in the light of the ^{13}C n.m.r. spectra. At 25 ^{o}C the ^{13}C n.m.r. spectrum displays a singlet with all the carbonyls exchanging, possibly caused by the bridging carbonyl migrating over the whole of the metal cluster. On cooling first coalescence occurs (-46 ^{o}C), and then localised exchange is evident (-66 ^{o}C) with carbonyls dividing into two sets. One set corresponding to 4 carbonyls are assigned to those on the phosphine substituted ruthenium atoms by virtue of its upfield position (194 p.p.m.). The other set downfield ($\sim$ 205 p.p.m.) are attributed to the remaining 11 carbonyls on the unsubstituted ruthenium atoms. Since the four carbonyls on the substituted ruthenium atoms are distinct at -66 ^{o}C and the methylene protons' signal is still a sharp triplet at -66 ^{o}C mechanisms (i) and (ii) can be ruled out as these should cause equivalence of all the

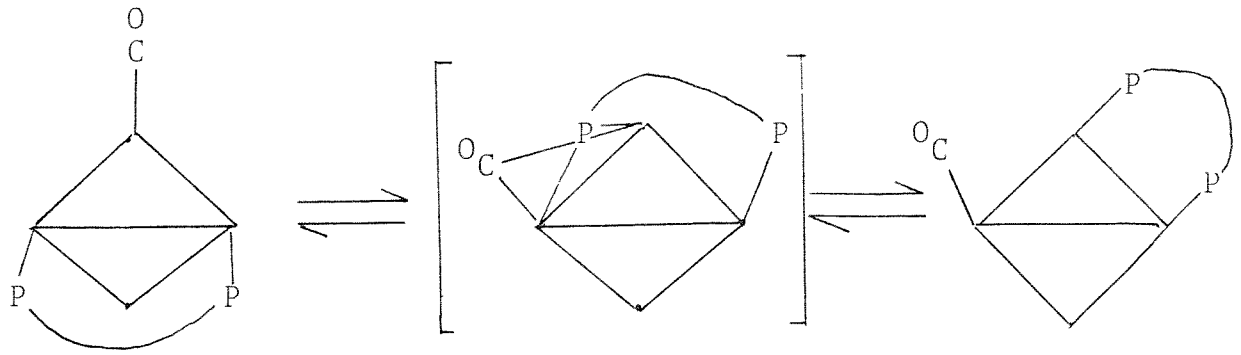

(i) Phosphine walking mechanism

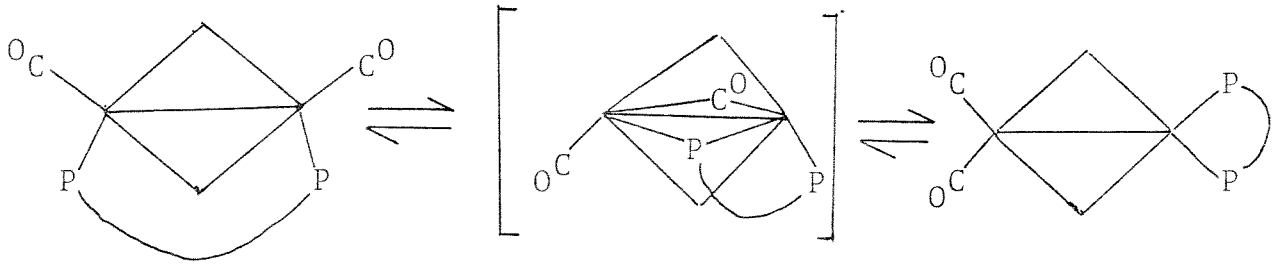

(ii) Bridge-corner mechanism

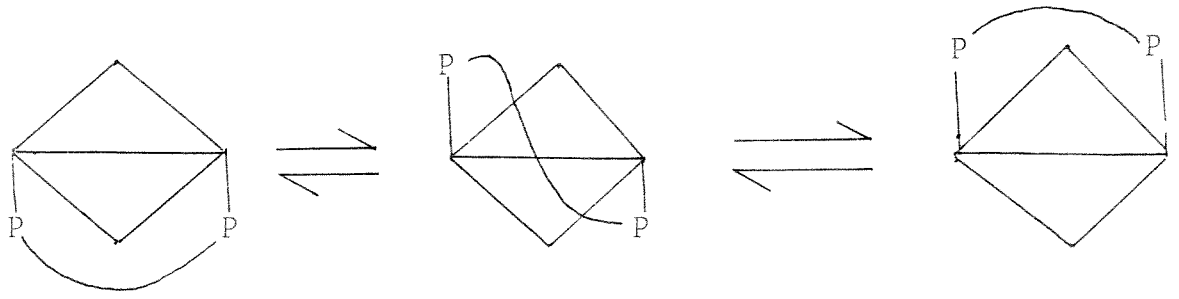

isomer a isomer b

(iii) $Ru(CO)_2P$ partial rotation mechanism

Diagram 5.19.

carbonyls. Mechanism (iii) would not explain why the four carbonyls are equivalent because the $Ru(CO)_2P$ unit rock would not interchange the two distinct carbonyls. Further evidence for another exchange process occurring on these $Ru(CO)_2P$ units is provided by the fact that this peak remains sharp down to -116 °C while the ^{31}P n.m.r. signal is broad by -85 °C, so the process interconverting the two isomers (seen for the DPPP adduct) must not be responsible for this equivalence. A possible process that would cause this has been proposed for $|Ru_3(CO)_{10}DPPM|$ and involves the exchange of carbonyls between the $Ru(CO)_2P$ units by the formation of a doubly bridging carbonyl intermediate on the phosphine bridged edge.

On cooling further the signal due to the carbonyls on the unsubstituted ruthenium atoms broadens and starts to resolve the localised exchange within the $Ru(CO)_3$ units, but due to limitations with the solvent the low temperature limiting spectrum was unobtainable. Interestingly, at no temperature was a bridging carbonyl observed as one would expect if it is involved in the exchange between the different $Ru(CO)_3$ and $Ru(CO)_2P$ units.

The yields of the products $|Ru_6C(CO)_{15}(P—P)|$ decrease when longer chain length phosphines are employed which is in common with the observations for Ru_3, Ru_4 and Ru_5 clusters. Again as the yields of the desired products decrease there is an increase in the proportion of products involving the linking of two or more clusters. For example, the compounds $|\{Ru_6C(CO)_{16}\}_2(P—P)|$ (P — P = (-)-Diop or DPPB) could be obtained in high yields (up to 70 %) using high cluster

concentration, low reaction temperature and excess cluster with respect to the phosphine.

(F) Ring parameters, do they exist?

One of the basic problems of the organometallic chemist is the determination of the structure and stereochemistry of complex molecules. Shaw and co-workers[7] have pointed out that there is a good linear correlation between the chemical shift of a tertiary phosphine, δ_F, and the change in the chemical shift upon co-ordination to a metal Δ. From the relationship $\Delta = A\delta_F + B$, co-ordination shifts of phosphines can usually be predicted, for a given complex, once enough analogues are known for calculation of the constants A and B. This relationship, however, failed for compounds involving metalated phosphines, and chelating phosphines. This was overcome by the introduction of a new term, Δ_R the ring contribution[8].

Δ_R is equal to the co-ordination shift of a chelated phosphine complex minus the co-ordination shift of an equivalent phosphorus in a non-chelated analogue. The co-ordination shift Δ is equal to the change between the chemical shift of a free (non-co-ordinated) phosphine ligand δ_F, and the observed chemical shift of the phosphorus atom under study δ_P, (in p.p.m. relative to H_3PO_4 with deshielded values being given a positive sign), i.e.

$$\Delta_R = \Delta_{chelate}(\delta_P - \delta_F) - \Delta_{non\text{-}chelate}(\delta_P - \delta_F)$$

The value of Δ_R varies with the ring size, for 4 membered rings it is large and negative, for 5 membered rings it is large

and positive, for 6 membered rings it is small and negative, and for larger rings it is near zero. Only one example of its use in the structural determination of clusters exists in the literature, that is for the two isomers of $|H_4Ru_4(CO)_{10}DPPE|$.[51,52] So, in order to explore this more fully, the ^{31}P n.m.r. spectra were investigated for chelate clusters and their closest non-chelate analogues. For example, to investigate ring parameters with DPPM, DPPE, DPPP and DPPB, PPh_2R was used, where R = Me, Et, Pr^n and Bu^n, respectively. Thus to measure the ring parameter for $|Ru_5C(CO)_{13}DPPM|$, $|Ru_5C(CO)_{13}(PPh_2Me)_2|$ was prepared and both their ^{31}P n.m.r. spectra run and the results inserted into the equation, e.g.

^{31}P n.m.r. shifts: DPPM = -22.70, PPh_2Me = -26.38,

$Ru_5C(CO)_{13}DPPM$ = +14.97. $Ru_5C(CO)_{13}(PPh_2Me)_2$ = +19.90 (average).

$$\Delta_R = (14.97 - (-22.70) - (19.90 - (-26.38)) = -8.61.$$

The ring contributions for the other bidentate phosphine substituted clusters were calculated similarly. For clusters, such as $|Ru_3(CO)_{10}(PPh_2R)_2|$ and $H_4Ru_4(CO)_{10}(PPh_2R)_2$, where the phosphorus atoms are either inequivalent or two isomers exist, a weighted average of ^{31}P n.m.r. peak positions was used in the calculation. The results of these calculations are shown in Table 5.14. These results demonstrate that either there is no ring size dependent contribution to the ^{31}P n.m.r. shift of the chelate clusters or that the model non-chelate compounds used were not suitable analogues. This unsuitability of the non-chelate cluster compounds is probably a consequence of the

Table 5.14.

Calculated ^{31}P n.m.r. ring parameters Δ_R.

Ring Size	Compound	Δ_R
4	$\|Ru_5C(CO)_{13}DPPM\|$	-8.61
5	$\|Ru_3(CO)_{10}DPPM\|$	-3.38
	$\|H_4Ru_4(CO)_{10}DPPM\|$	-11.27
	$\|Ru_6C(CO)_{15}DPPM\|$	-8.28
	$\|H_4Ru_4(CO)_{10}DPPE\|$ (corner)	+33.63
	$\|Ru_5C(CO)_{13}DPPE\|$	+5.97
	$\|HC(PPh_2)_3Ru_3(CO)_9\|$	+15.11
	$\|HC(PPh_2)_3Ru_4(H)_4(CO)_9\|$	+0.92
6	$\|Ru_3(CO)_{10}DPPE\|$	+10.82
	$\|H_4Ru_4(CO)_{10}DPPE\|$ (edge)	+1.30
	$\|Ru_6C(CO)_{15}DPPE\|$	+1.53
	$\|Ru_5C(CO)_{13}DPPP\|$ (major)	+9.27
7	$\|Ru_3(CO)_{10}DPPP\|$	+2.13
	$\|H_4Ru_4(CO)_{10}DPPP\|$	+0.40
	$\|Ru_6C(CO)_{15}DPPP\|$	+12.45
8	$\|Ru_3(CO)_{10}DPPB\|$	-2.64
	$\|Ru_6C(CO)_{15}DPPB\|$	-2.07

sensitivity of the observed ^{31}P n.m.r. shift on the geometry of the substitution. For example, in $|Ru_5C(CO)_{13}DPPM|$ two isomers exist which differ only in the stereochemistry of the phosphine, which chelates to one basal atom, however, each isomer possesses distinct ^{31}P n.m.r. signals (e.g. major isomer = 17.05 p.p.m., minor isomer = 14.07 and 12.85 p.p.m.).

A possible way around this problem, could be to use as model compounds, compounds which contain chelating phosphines which can form large rings (e.g. DPPB can form either 7 or 8 membered rings) and so have a negligible ring contribution to their observed ^{31}P n.m.r. shift. This approach, however, is of limited value as the length of the alkyl chain separating the phosphorus atoms often strongly affects the mode of substitution. For example, $|Ru_5C(CO)_{13}(P\,—\,P)|$ displays three different modes of substitution as the chain length varies. In the one case, where the mode of substitution is insensitive to this, $|Ru_3(CO)_{10}(P\,—\,P)|$, calculation of the ring parameters using $|Ru_3(CO)_{10}(DPPB)|$ as the model "non-chelate" analogue, still does not give meaningful ring parameters (e.g. the values obtained where: DPPM, -2.77; DPPE, 12.42, and DPPP, 5.00). A possible explanation for this is that the longer Ru —Ru bond length, compared to the C —C bond length, causes a change in the expected conformations of the rings, and since any change in the angle of the substituents on the phosphorus causes a shift in the ^{31}P n.m.r. signal, the expected ring parameters should be different for rings containing Ru —Ru bonds. Indeed, this change in the ^{31}P n.m.r. shift to high field when structural constraints require small CPC angles[55] (e.g. the chemical shift of $P(OMe)_3$ = -141.7 p.p.m., < OPO =

100.1°; and P_4 = +450 p.p.m., < PPP = 60 °C) has been advanced as a partial explanation for the occurrence of ring size dependent contributions to the ^{31}P n.m.r. shift of chelate mononuclear compounds. A possible use of this is that if the Δ_R values for clusters can be accurately evaluated, the deviation from the ideal value for a given ring size will reflect on the suitability of the phosphine for that mode of chelation.

Despite this failure to predict Δ_R values for chelate clusters, these results demonstrate that the ^{31}P n.m.r. shift is highly sensitive to both the geometry and nuclearity of the cluster. This suggests that ^{31}P magic angle spinning n.m.r.[22,36], should be a powerful tool in identifying anchored clusters provided that the model homogeneous compounds are available.

(g) The specific anchoring of a chiral cluster.

The anchoring of the chiral (-)-Diop ligand onto aldehyde containing resins has been reported. This was achieved by condensing hydrolysed (-)-Diop with an anchored aldehyde (produced by dimethylsulphoxide oxidation of the chlorinated resin) to generate an anchoring acetal link (see Diagram 5.1). An attempt was made to expand this approach to oxides, first an anchored alkyl chloride was prepared by reacting $(MeO)_3Si(CH_2)_3Cl$ with silica and γ-alumina, and then dimethylsulphoxide oxidation was attempted. Unfortunately, during this step extensive leaching of the anchored ligand occurred, which precluded the obtaining of a reasonable loading of (-)-Diop.

This problem was overcome by preparing an acetal with silane anchoring functionality (see Diagram 5.20). Two routes for

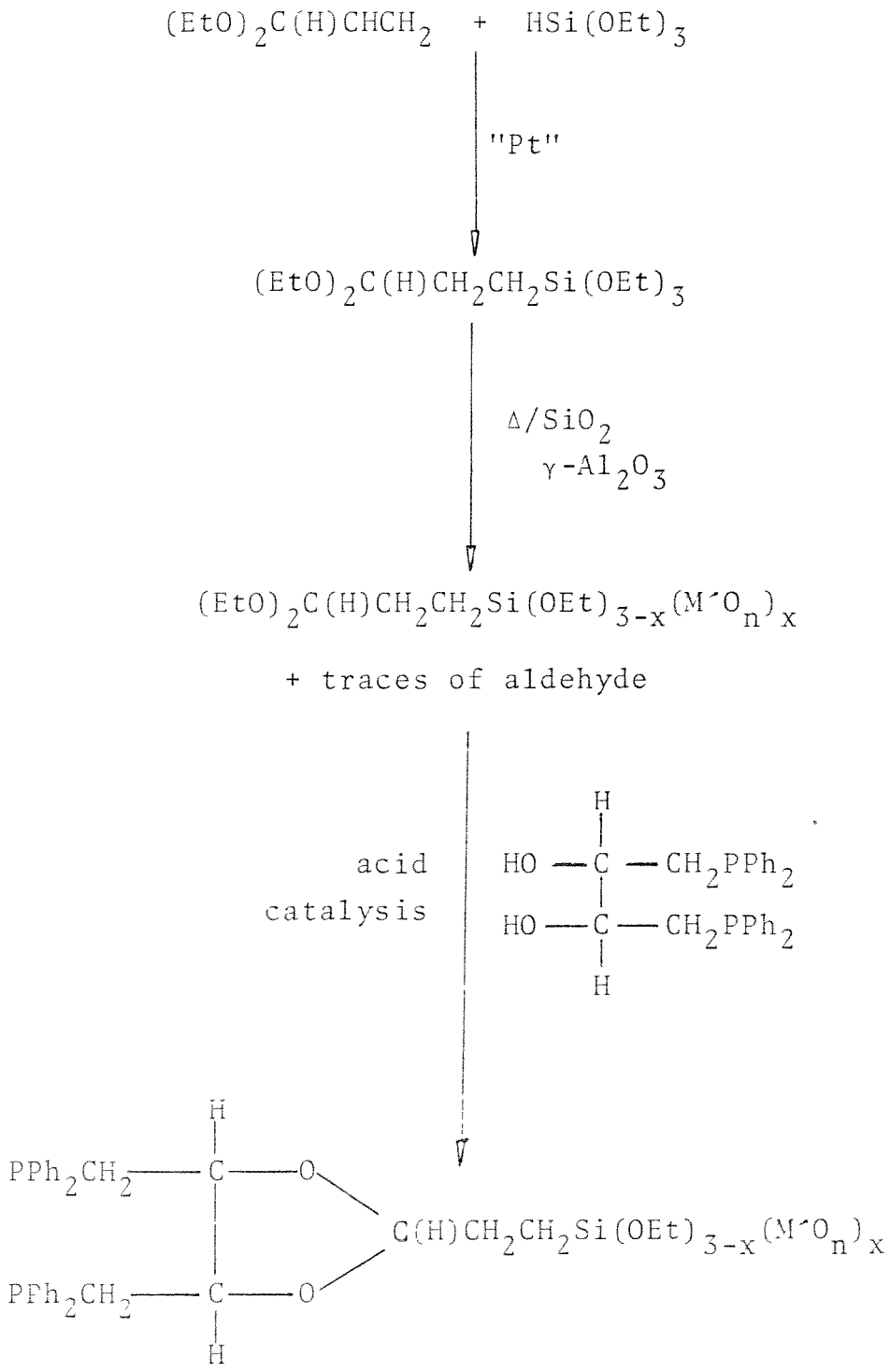
(EtO)2C(H)CHCH2 + HSi(OEt)3
"Pt"
(EtO)2C(H)CH2CH2Si(OEt)3
Δ/SiO2
γ-Al2O3
(EtO)2C(H)CH2CH2Si(OEt)3-x(M'On)x
+ traces of aldehyde
acid
catalysis
HO — C — CH2PPh2
HO — C — CH2PPh2
PPh2CH2 — C — O
PPh2CH2 — C — O
C(H)CH2CH2Si(OEt)3-x(M'On)x

Diagram 5.20

preparing anchored diop containing clusters were evaluated. The first approach used was to prepare the anchored acetal (identical conditions were used to those employed for $(MeO)_3Si-(CH_2)_3Cl$) and then by using acid catalysis, condense it with hydrolysed (-)-Diop. Thought this route appeared to be successful, control of the degree of substitution of the cluster during anchoring was lacking. For example, when $|Ru_6C(CO)_{17}|$ was reacted with anchored (-)-Diop on silica, the cluster was anchored, but not in the required fashion. That is, from the i.r. spectra, several products could be discerned besides the planned product $|Ru_6C(CO)_{15}$"(-)-Diop"|, such as $|Ru_6C(CO)_{16}P|$. The occurrence of this $|Ru_6C(CO)_{16}P|$, in higher yields than was observed for solution reactions under similar circumstances (approximately one equivalent of the anchored bidentate phosphine was stirred with the cluster overnight in CH_2Cl_2) suggest that partial oxidation of the phosphine ligand may have occurred during the anchoring. This oxide induced oxidation of phosphine ligands during anchoring has been observed previously.

An alternative synthesis which overcomes these problems is to prepare and purify the (-)-Diop substituted homogeneous cluster (e.g. $|Ru_6C(CO)_{15}\{(-)\text{-Diop}\}|$) and condense it with the silane containing acetal, and then react this with oxides. This was found to be preferable to reacting the Diop substituted clusters directly with anchored acetal, during which extensive cluster decomposition occurred. Thus anchored $Ru_6C(CO)_{15}$-"(-)-Diop" was prepared as shown in Diagram 5.21 (see also Figure 5.16). Unfortunately, samples prepared by this route proved to have a poor resistance to leaching presumably due to

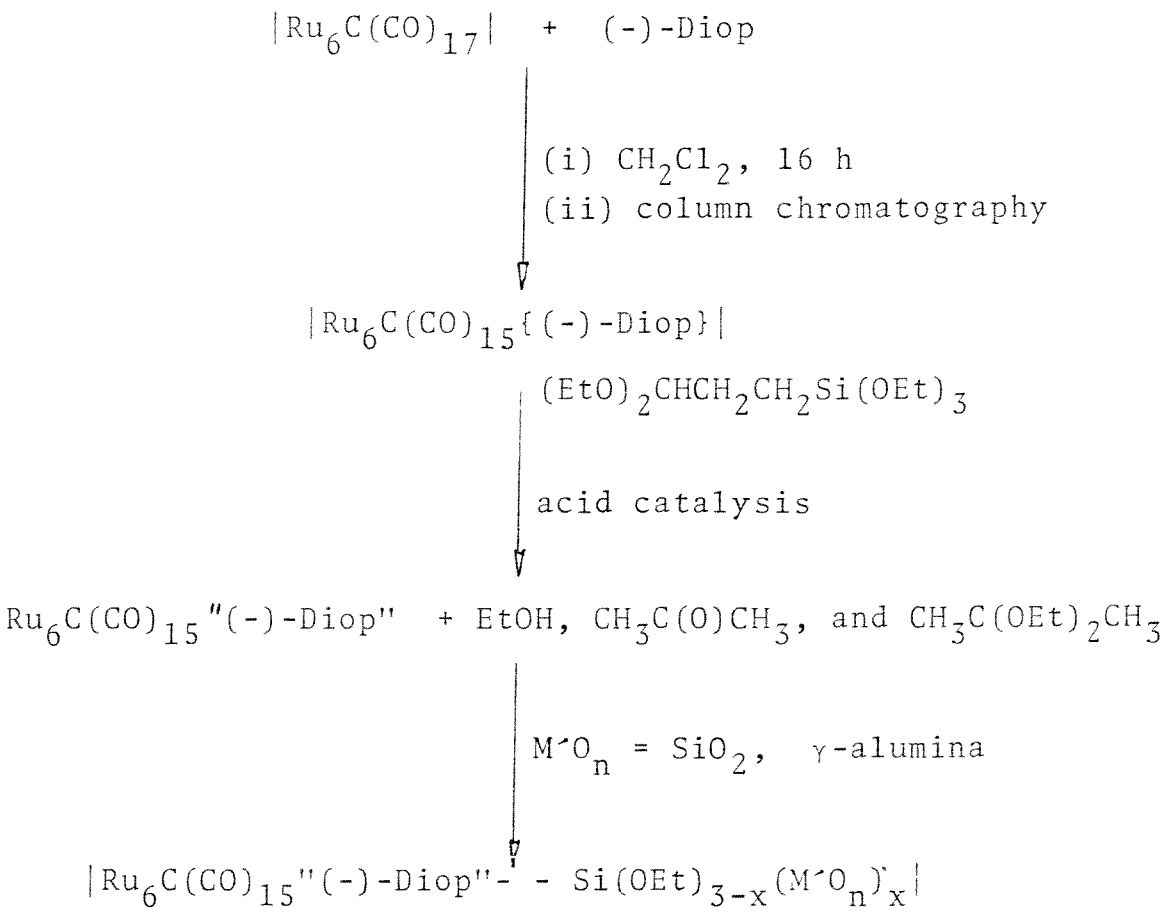
|Ru6C(CO)17| + (-)-Diop
(i) CH2Cl2, 16 h
(ii) column chromatography
|Ru6C(CO)15{(-)-Diop}|
(EtO)2CHCH2CH2Si(OEt)3
acid catalysis
Ru6C(CO)15"(-)-Diop" + EtOH, CH3C(O)CH3, and CH3C(OEt)2CH3
M'On = SiO2, γ-alumina
|Ru6C(CO)15"(-)-Diop"- - Si(OEt)3-x(M'On)x|

Diagram 5.21.

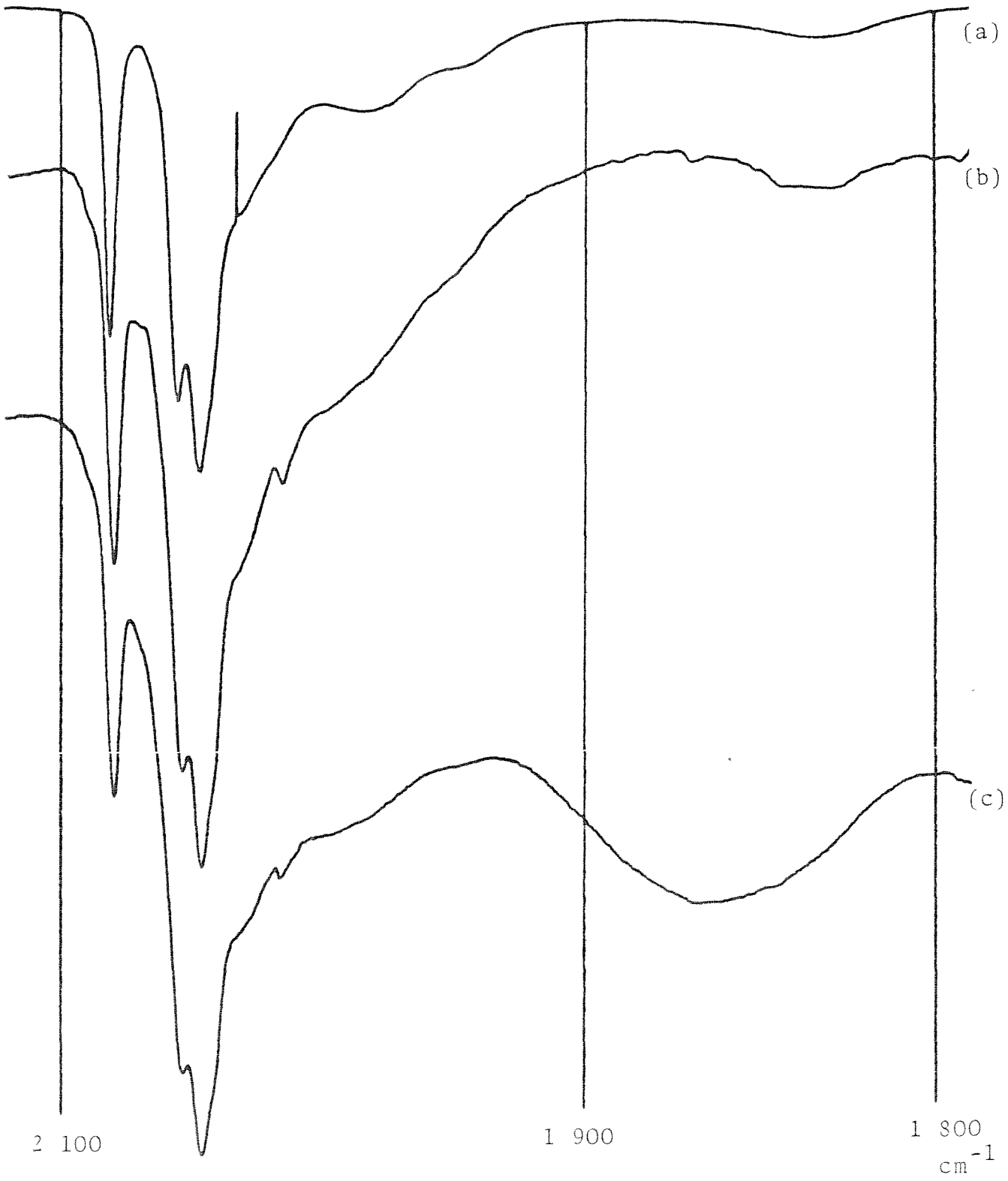

Figure 5.16. I.r. spectra of (a) $[Ru_6C(CO)_{15}(-)\text{-Diop}]$ in CH_2Cl_2, (b) $[Ru_6C(CO)_{15}"(-)\text{-Diop}"]$ anchored onto silica with the silica background subtracted out, and (c) spectrum (b) before subtraction (Nujol mull).

the oxide environment catalysing the hydrolysis of the acetal link.

Conclusion.

The reaction of ruthenium clusters of nuclearities 3 - 6 with monodentate phosphines PPh_2R yielded the known substitution products, i.e. $|Ru_3(CO)_{12-x}(PPh_2R)_x|$ (x = 1 - 3), $|H_4Ru_4(CO)_{12-x}(PPh_2R)_x|$ (x = 1 - 4), $|Ru_5C(CO)_{15-x}(PPh_2R)_x|$ (x = 1 and 2) and $|Ru_6C(CO)_{17-x}(PPh_2R)_x|$ (x = 1 - 4). Analysis of these compounds spectroscopically showed in general as the degree of substitution increased, the CO stretching frequency decreased and the degree of shielding of the alkyl groups on the phosphine increased, as one would expect with phosphines being poorer π acceptors than the replaced carbonyls.

Interestingly, the phosphines in $|Ru_3(CO)_{10}(PPh_2R)_2|$ were found to be rigid at 31 °C on the n.m.r. time scale, unlike the osmium analogue $|Os_3(CO)_{10}(PEt_3)_2|$. This is presumably due to a combination of the smaller Ru_3 ring size, and the larger cone angles of the phosphines employed. Unlike the compounds $|H_4Ru_4(CO)_{12-n}(P(OMe)_3)_n|$ (n = 1 - 4) in which only one isomer was found to exist for each n on the n.m.r. time scale, the compounds $|H_4Ru_4(CO)_{12-n}(PPh_2R)_n|$ (n = 2,3) were found to have either two isomers (n = 2) or inequivalent phosphines (n = 3). This is probably a reflection of the larger cone angles of phosphines (PPh_2R) compared to trimethylphosphite. Two isomers were found to occur for $|Ru_6C(CO)_{15}(PPh_2R)_2|$, as reported for $|Ru_6C(CO)_{15}(P(OMe)_3)_2|$, and as R changed the product distribution changed. S.C. Brown reported

that the cis-isomer predominates for $P(OMe)_3$. The abundance of the minor upfield peak decreased as R changed from Me to Et and this is in accord with the minor isomer for phosphines PPh_2R being the cis-isomer and this again indicates the importance of cone angles in determining the geometry of the substitution of clusters.

Analysis of the ^{31}P n.m.r. shifts of these clusters showed the existence of contributions due to the free ligands initial shift, nature of the metal, change in the C — P — C angles on co-ordination, and a new term not observed for mononuclear complexes, a cluster nuclearity/geometry contribution (which increases as the nuclearity of the cluster increases).

The reaction of ruthenium clusters of nuclearities 3 - 6 with bidentate phosphines of varying chain length yielded several novel geometries. In the case of Ru_3 clusters, $|Ru_3(CO)_{10}(P-P)|$, 3 co-ordination modes were observed, a DPPM, a DPPE and DPPP, and a DPPB and (-)-Diop mode. The structures of all the adducts have been shown to involve a bridging phosphine occupying two cis equatorial positions. The differences in the i.r. spectra of these compounds (see Figure 5.1) are probably a result of distortions in the carbonyl envelope caused by accommodating the different bidentate phosphines.

Only two isomers were observed for the compounds, $|H_4Ru_4(CO)_{10}(P-P)|$. These have been previously observed for $H_4Ru_4(CO)_{10}DPPE$[1], and involve the phosphine either bridging an edge or co-ordinating to a corner. DPPM and DPPP both form the edge bridging compound thermally whereas DPPE forms the corner co-ordinated compound. A reason for this could be the

driving force in 6 membered rings to achieve boat and chair conformations (to relieve ring strain) and this is impossible for an edge-bridging ligand as the two phosphines and two edge ruthenium atoms, because of bonding considerations, have to be in a single plane. The DPPB adduct displays both isomers and there appears to be no preference for either mode possibly because the alkyl backbone is sufficiently flexible to avoid ring strain.

Three different phosphine co-ordination arrangements have been observed for $|Ru_5C(CO)_{13}(PPh_2(CH_2)_nPPh_2)|$. The identity of the kinetically and thermodynamically favoured form is a function of the phosphine chain length. A summary of the isomerisation processes of the five $|Ru_5C(CO)_{13}(P—P)|$ derivatives is presented in Diagram 5.22. There is no evidence for an edge bridging co-ordination mode d. A single crystal X-ray study on isomer a of $|Ru_5C(CO)_{13}$DPPB| was carried out and confirmed the diagonal bridging mode of the phosphine on the square face of the cluster. Interestingly, (-)-Diop acts like DPPP rather than DPPB which has the same alkyl chain length and this is a reflection of the restriction in the flexibility of the chain caused by the ketal ring.

The general structure of the compounds '$Ru_6C(CO)_{15}(P—P)$' was found by a single crystal X-ray structure determination on the first member of the series, '$Ru_6C(CO)_{15}$DPPM', to involve an edge bridging mode with both phosphines co-ordinated to adjacent ruthenium atoms. In order to explain the gradual variation in the i.r. spectra as the chain length increased, cis and trans orientations of the phosphines had to be proposed (see Diagram 5.19'). Supporting evidence for this was obtained by a ^1H and

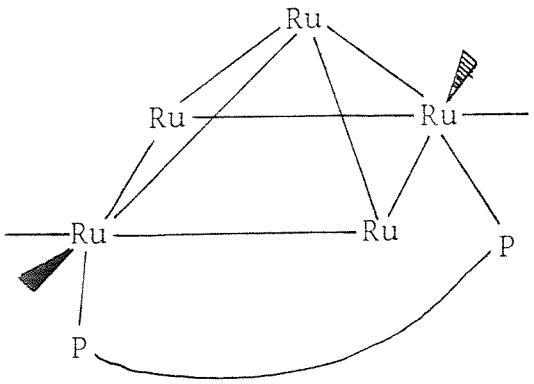

a

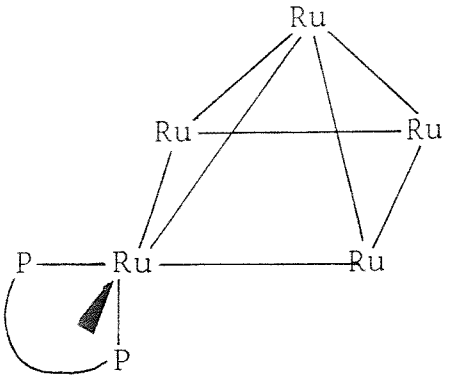

b

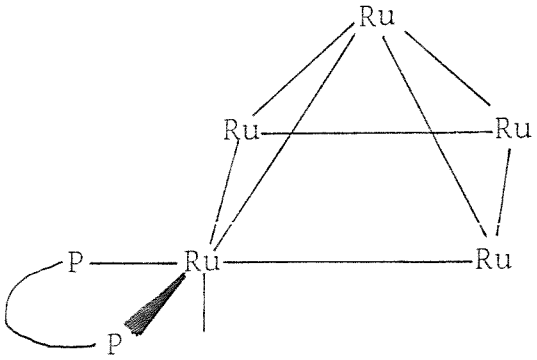

c

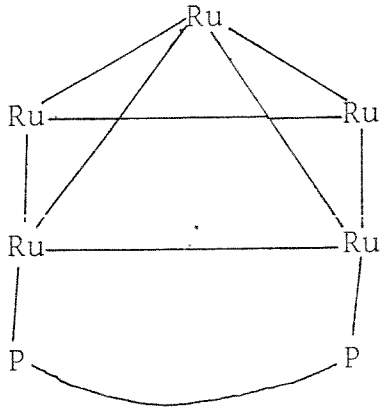

d

Ligand	Isomerisation
DPPM	c ⇌ b
DPPE	c ⟵ b
DPPP	a → b ⇌ c
DPPB	b ⇌ c — a
(-)-Diop	a → b ⟶ c

Diagram 5.22

^{13}C n.m.r. study on $|Ru_6C(CO)_{15}DPPM|$ in addition to low temperature ^{31}P n.m.r. spectra of the other adducts.

The Δ_R, ring parameters, were calculated for these chelate clusters but the model compounds used proved to be poor models for the chelate clusters and as a result no trend was obvious. The failure of this, however, did demonstrate the sensitivity of the ^{31}P n.m.r. shift to the cluster geometry.

Anchored Diop was prepared and though it was suitable for anchoring clusters the lack of specificity, demonstrated by the product distribution obtained for $|Ru_6C(CO)_{17}|$, was undesirable. This was subsequently overcome by a route which allowed the initial preparation and purification of the (-)-Diop substituted cluster homogeneously before anchoring it by exchanging the ketal for an acetal containing a $Si(OEt)_3$ functionality.

Experimental

All the i.r. spectra were run in cyclohexane, the ^{1}H n.m.r. in $CDCl_3$ (31 ^{o}C, and measured in δ (p.p.m.)) and ^{31}P n.m.r. in CH_2Cl_2 (31 ^{o}C, and measured in p.p.m. relative to 85 % H_3PO_4) except where mentioned otherwise.

The ^{13}C n.m.r. spectra were all recorded with the aid of $Cr(acac)_3$ as a spin relaxant and with the exceptions of $HC(PPh_2)_3$ and $|Ru_5C(CO)_{13}DPPB|$ were on ^{13}CO enriched samples prepared from the corresponding ^{13}CO enriched clusters.

Preparation of alkyldiphenylphosphines PPh_2R.

These were prepared by two main routes. The diphenylethylphosphine was prepared by a Grignard reaction (ethylmagnesium bromide with chlorodiphenylphosphine[11]) and the others were prepared by the action of lithium diphenyl phosphide on the corresponding alkyl bromide.[12] All the products were purified by distillation in vacuo which gave as products colourless viscous oils (typically in yields of approximately 80 %).

PPh_2Me

B.Pt. 115 - 118 ^{o}C/0.2 mm Hg (literature[13] 108 - 110/1.5 mm Hg). ^{1}H n.m.r./δ(p.p.m.): 7.4 (m, 10 H, Ph) and 1.8 (d, 3 H, J_{PH} = 7 Hz) ^{31}P n.m.r.: -26.38 p.p.m. (literature 28.0[14] and 28.1[15] in $CDCl_3$). m.s. This gave a parent ion at 200.062 a.m.u. followed by a complex fragmentation pattern dominated by P — C cleavage processes. For example, the table below shows all the peaks of intensity more than 7 % of the base peak.

Measured mass in a.m.u.	% intensity of base peak	assignment
200.06	100.0	$CH_3PPh_2^+$
199.05	22.4	$CH_2PPh_2^+$
185.04	54.4	PPh_2^+
184.03	10.2	$P(Ph)(C_6H_4)^+$
183.02	65.7	$P(C_{12}H_8)^+$
107.01	9.3	PPh^+
100.04	7.0	$CH_3PPh_2^{2+}$
91.05	22.4	$PhCH_2^+$
78.05	11.0	$C_6H_6^+$
77.04	24.1	$C_6H_5^+$
51.03	12.2	
31.99	16.9	PH^+

PPh_2Et

B.Pt. 125 - 130 °C/0.5 mm Hg (literature, 108 - 111 °C/0.3 mm Hg,[14] 114 - 116 °C/0.3 mm Hg[15] and 112 - 116 °C/0.1 mm Hg[16]).
^1H n.m.r./δ(p.p.m.): -7.15 (m, 10 H, Ph), 2.0 (m, 2 H, CH_2) and 1.05 (dt, 3 H, CH_3, J_{PH} = 20 Hz, J_{HH} = 7 Hz).
^{31}P n.m.r.: -11.45 p.p.m. (literature -13.5[14] and -12.5[15] in $CDCl_3$)
m.s. This gave a parent ion at 214.08 a.m.u. and similar fragmentation pattern to the methyl analogue.

PPh_2Pr^n

B.Pt. 120 - 130 °C/0.1 mm Hg (literature 138 °C/1 mm Hg[11])
^1H n.m.r./δ(p.p.m.): 7.3 (m, 10 H, Ph), 2.0 (td, 2 H, PCH_2, J_{PH} = 3 Hz, J_{HH} = 7 Hz), 1.5 (m, 2 H, $PCH_2\underline{CH_2}$) and 1.0 (t(distorted), 3 H, CH_3).

^{31}P n.m.r.: -16.58 p.p.m. (literature -17.6[17])

m.s. This gave a parent ion at 228.09 a.m.u. followed by a similar fragmentation to the methyl analogue.

PPh_2Bu^n

B.Pt. 150 - 160 °C/0.2 mm Hg (literature 117 - 120 °C/0.3 mm Hg[18], 140 °C/0.45 mm Hg[19] and 114 - 115/0.15 mm Hg[20])

^1H n.m.r./δ(p.p.m.): 7.3 (m, 10 H, Ph), 2.05 (t(distorted), 2 H, PCH_2), 1.4 (m, 4 H, $PCH_2(\underline{CH_2})_2CH_3$) and 0.9 (t(distorted), 3 H, CH_3).

^{31}P n.m.r.: -16.13 p.p.m. (literature -17.1[21]).

m.s. This compound gave a parent ion at 242.10 a.m.u., but unlike the methyl analogue, alkyl chain fragmentation dominates the fragmentation pattern (e.g. the base peak at 199.00 a.m.u. can be assigned to $CH_2PPh_2^+$).

Preparation of bidentate phosphines $PPh_2(CH_2)_nPPh_2$

These were carried out according to the reported preparation[12] of DPPM (n = 1) and DPPE (n = 2) by varying the alkyl halide reacted with the lithium diphenylphosphide. The phosphines for n = 3 DPPP and n = 4 DPPB are also white powders like DPPM and DPPE.

DPPM

^1H n.m.r./δ(p.p.m.): 7.55 (m, 20 H, Ph), and 3.05 (t, 3 H, CH_2, J_{PH} = 2 Hz).

^{31}P n.m.r.: -22.70 p.p.m. (literature -23.6[14]).

m.s. This sample gave a fragmentation identical to that reported in the literature (parent ion at 384.12 a.m.u.).

DPPE

^{1}H n.m.r./δ(p.p.m.): 7.3 (m, 20 H, Ph), and 2.05 (t, 4 H, CH_2).

^{31}P n.m.r.: -12.12 p.p.m. (literature -13.2[22]).

m.s. This compound gave a parent ion at 398.12 a.m.u. followed by a similar fragmentation pattern to DPPM.

DPPP

^{1}H n.m.r./δ(p.p.m.): 7.35 (m, 20 H, Ph), 2.2 (m, 4 H, P-CH_2) and 1.6 (m, 2 H, $PCH_2\underline{CH_2}$).

^{31}P n.m.r.: -16.90 p.p.m.

m.s. A parent ion (412.16 a.m.u.) was observed followed by a complex fragmentation pattern similar to that observed for DPPM but with a very low abundance of PPh_3^+. Obviously this must be due to the greater separation of the two PPh_2 units in DPPP compared with DPPM and DPPE.

DPPB

^{1}H n.m.r./ (p.p.m.): 7.35 (m, 10 H, Ph), 2.0 (m, 4 H, PCH_2) and 1.55 (m, 4 H, $PCH_2\underline{CH_2}$).

^{31}P n.m.r.: -16.00 p.p.m.

m.s. This gave a similar mass spectrum to the DPPP (parent ion observed at 426.19 a.m.u.) but with no PPh_3^+ in the fragmentation pattern.

Preparation of $HC(PPh_2)_3$

This white powder was prepared in 70 % yield by a literature preparation.[23]

^{1}H n.m.r./ (p.p.m.): 7.17 (m, 30 H, Ph) and 4.15 (br, 1 H, C-H).

^{13}C n.m.r./$CDCl_3$: δ (p.p.m.) 135 (m, 6 C, P-C_{phenyl}), 134 (m,

12 C, C_{ortho}), 131 (m, 6 C, C_{para}), 127 (m, 12 C, C_{meta}) and 25.3 (q, 1 C, C-H, J_{PC} = 45 Hz).

^{31}P n.m.r.: -9.70 p.p.m.

m.s. A parent ion (383.21 a.m.u.) was observed followed by PPh_3^+, $CH_2PPh_2^+$, $P(C_{12}H_8)^+$ as the most important ions in a complex fragmentation pattern.

Preparation of (-)2,3,-O-isopropylidene-2,3,-dihydroxy-1,4,-bisdiphenyl phosphinobutane or (-)-Diop.

This was prepared according to the literature by converting Lg-tartaric acid to a dimethyl-2,3-o-isopropylidene-Lg-tartrate[24] and then reducing it to 2,3,-O-isopropylidene-Lg-threitol[25] and then tosylating it to 1,4,-ditosyl-2,3-o-isopropylidene-Lg-theitol[24] which on reaction with $LiPPh_2$ gave (-)-Diop (see Diagram 5.23).

^1H n.m.r./δ(p.p.m.): 7.35 (m, 20 H, Ph), 3.92 (q(distorted), 2 H, C-H, J_{HH} = 5 Hz, J_{PH} = 2 Hz and 6 Hz), 2.39 (m, 4 H, CH_2, J_{HH} = 5 Hz, J_{PH} = 3 Hz) and 1.36 (s, 6 H, CH_3).

^{31}P n.m.r.: -22.50 p.p.m.

m.s. This exhibited a very weak parent ion (499.20 a.m.u.) and a fragmentation pattern similar to that obtained with DPPB.

Preparation of $|Ru_3(CO)_{11}L|$ and $|Ru_3(CO)_{10}L_2|$ (L = PPh_3, PPh_2Me, PPh_2Et, PPh_2Pr^n and PPh_2Bu^n).

The most convient method found was to prepare both simultaneously, as the two products could be easily separated and purified by flash chromatography. In general, a solution of sodium benzophenone ketyl (0.025 M in t.h.f.) was added drop-

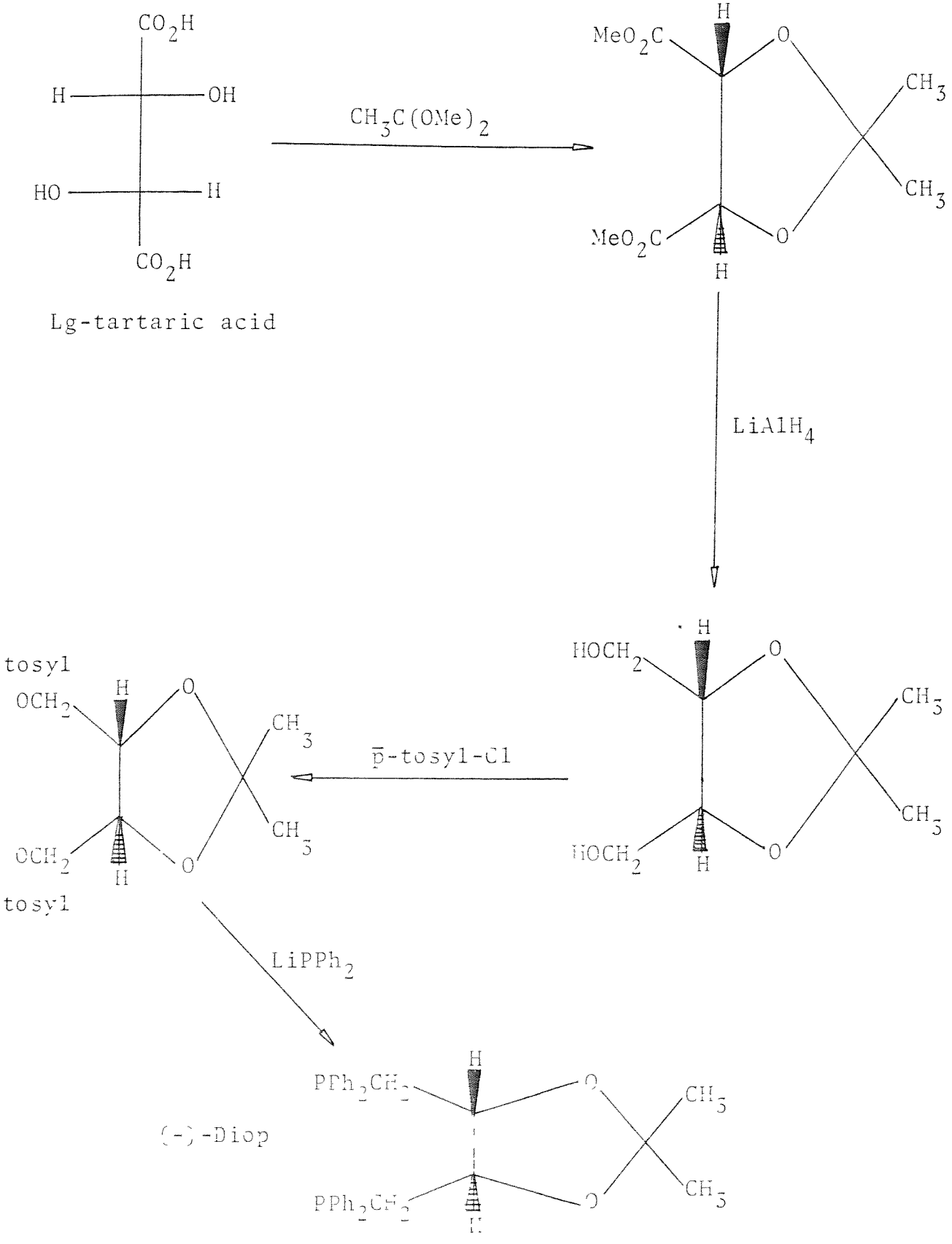
CO2H
H
OH
HO
H
CO2H
Lg-tartaric acid
CH3C(OMe)2
MeO2C
H
O
CH3
CH3
MeO2C
O
H
LiAlH4
HOCH2
H
O
CH3
CH3
HOCH2
H
O
p-tosyl-Cl
tosyl
OCH2
H
O
CH3
CH3
OCH2
H
O
tosyl
LiPPh2
PPh2CH2
H
O
CH3
CH3
PPh2CH2
O
H
(-)-Diop

Diagram 5.23.

-wise to a solution of $|Ru_3(CO)_{12}|$ (50 mg) and the phosphine 1.5 equivalents) in 40 cm^3 dry t.h.f., until no further reaction was detected by i.r. spectroscopy. The solvent was removed under reduced pressure and the residue applied to a flash chromatography column. The most convenient method of application found was to add a small amount of column material to the solution before removing the solvent; the resulting orange powder could then be poured directly onto the column and then eluted with solvents of gradually increasing polarity. This yielded first unreacted $|Ru_3(CO)_{12}|$, then $|Ru_3(CO)_{11}L|$ and finally $|Ru_3(CO)_{10}L_2|$. The yields of the orange-red crystalline mono- and di-substituted derivatives were generally 70 - 90 % of the expected maximum values.

$|Ru_3(CO)_{11}PPh_3|$

I.r.: 2 098(m), 2 047(vs), 2 032(m), 2 025(m), 2 016(vs), 1 998(m), 1 987(m) and 1 963(w) cm^{-1}.

^1H n.m.r./δ(p.p.m.): 7.5 (m, 15 H, Ph).

^{31}P n.m.r.: 36.03 p.p.m.

Analysis: calculated C, 39.9 %; H, 1.7 %

found C, 40.1 %; H, 1.6 %.

$|Ru_3(CO)_{11}PPh_2Me|$

I.r.: 2 097(m), 2 045(s), 2 028(s), 2 014(s), 2 001(m), 1 995(m), 1 985(m) and 1 961(w) cm^{-1}.

^1H n.m.r./δ(p.p.m.): 7.5 (m, 10 H, Ph) and 2.18 (d, 3 H, CH_3, J_{PH} = 9 Hz).

^{31}P n.m.r.: 14.90 p.p.m.

Analysis: calculated C, 35.5 %; H, 1.6 %.

found C, 35.7 %; H, 1.7 %.

$|Ru_3(CO)_{10}(PPh_2Me)_2|$

I.r.: 2 073(w), 2 020(vs), 1 998(br,s), 1 986(sh) and 1 974(sh) cm^{-1}.

^1H n.m.r./δ(p.p.m.): 7.44 (m, 20 H, Ph) and 2.14 (d, 6 H, CH_3, J_{PH} = 9 Hz)

^{31}P n.m.r.: 14.93 and 13.72 p.p.m.

Analysis: calculated C, 43.9 %; H, 2.6 %

found C, 44.2 %; H, 2.8 %.

$|Ru_3(CO)_{11}PPh_2Et)|$

I.r.: 2 097(m), 2 045(s), 2 030(sh), 2 024(m), 2 015(vs), 1 986(m) and 1 960(w) cm^{-1}.

^1H n.m.r./δ(p.p.m.): 7.6 (m, 10 H, Ph), 2.5 (quintet, 2 H, CH_2, J_{HH} = 7 Hz, J_{PH} = 7 Hz) and 0.92 (dt, 3 H, CH_3, J_{HH} = 7 Hz, J_{PH} = 20 Hz).

^{31}P n.m.r.: 30.60 p.p.m.

$|Ru_3(CO)_{10}(PPh_2Et)_2|$

I.r.: 2 074(m), 2 064(w), 2 019(s), 1 998(br,vs), 1 987(sh) and 1 977(sh) cm^{-1}.

^1H n.m.r./δ(p.p.m.): 7.5 (m, 20 H, Ph), 2.46 (quintet, 4 H, CH_2, $J_{HH} = J_{PH}$ = 7 Hz) and 0.92 (dt, 6 H, CH_3, J_{HH} = 7 Hz, and J_{PH} = 20 Hz).

^{31}P n.m.r.: 31.70 and 28.80 p.p.m.

$|Ru_3(CO)_{11}PPh_2Pr^n|$

I.r.: 2 097(m), 2 046(s), 2 030(sh), 2 024(m), 2 015(vs), 2 000(w), 1 995(m), 1 986(m), and 1 959(w) cm^{-1}.

^1H n.m.r./δ(p.p.m.): 7.45 (m, 10 H, Ph), 2.4 (q(distorted), 2 H, P-CH_2), 1.3 (m, 2 H, $PCH_2\underline{CH_2}$) and 0.98 (t(distorted), 3 H, CH_3).

^{31}P n.m.r.: 27.14 p.p.m.

$|Ru_3(CO)_{10}(PPh_2Pr^n)_2|$

I.r.: 2 073(m), 2 019(s), 1 997(vs), 1 987(sh) and 1 977(sh) cm^{-1}.

^1H n.m.r./δ(p.p.m.): 7.4 (m, 20 H, Ph), 2.38 (m, 4 H, PCH_2), 1.3 (m, 4 H, $P\underline{CH_2}CH_3$) and 0.98 (t(distorted), 6 H, CH_3).

^{31}P n.m.r.: 26.99 and 25.78 p.p.m.

$|Ru_3(CO)_{11}(PPh_2Bu^n)|$

I.r.: 2 097(m), 2 045(s), 2 030(sh), 2 024(m), 2 014(vs), 2 000(w), 1 995(m), 1 986(m) and 1 959(w) cm^{-1}.

^1H n.m.r./δ(p.p.m.): 7.45 (m, 10 H, Ph), 2.5 (q(distorted), 2 H, PCH_2), 1.3 (m, 4 H, $PCH_2(\underline{CH_2})_2CH_3$) and 0.9 (t, 3 H, CH_3, J_{HH} = 6 Hz).

^{31}P n.m.r.: 27.44 p.p.m.

$|Ru_3(CO)_{10}(PPh_2Bu^n)_2|$

I.r.: 2 073(m), 2 060(w), 2 045(w), 2 018(s), 1 997(br,s), 1 987(sh), 1 977(sh) and 1 960(sh) cm^{-1}.

^1H n.m.r./δ(p.p.m.): 7.4 (m, 20 H, Ph), 2.45 (m, 4 H, PCH_2), 1.3 (m, 8 H, $PCH_2(\underline{CH_2})_2(CH_3)$ and 0.85 (t, 6 H, CH_3, J_{HH} = 7 Hz).

^{31}P n.m.r.: 27.29 and 25.93 p.p.m.

Preparation of $|Ru_3(CO)_9L_3|$

In general $|Ru_3(CO)_{12}|$ (50 mg) was refluxed overnight in n-pentane (100 cm^3) with 3.1 equivalents of the phosphine, cooled and the solvent removed under reduced pressure, after adding a small amount of "flash silica". The purple powder was added to the column and eluted with solvents of increasing polarity until the violet fraction came across. Removal of solvent in vacuo gave a 80 - 90 % yield of a dark violet crystalline solid.

$|Ru_3(CO)_9(PPh_2Me)_3|$

I.r.: 2 047(m), 1 975(vbr,vs) and 1 949(m) cm^{-1}.

^1H n.m.r./δ(p.p.m.): 7.35 (m, 30 H, Ph), and 2.1 (d, 9 H, CH_3, J_{PH} = 10 Hz)

^{31}P n.m.r.: 15.76 p.p.m.

$|Ru_3(CO)_9(PPh_2Et)_3|$

I.r.: 2 045(m), 2 017(w), 1 975(vbr,vs) and 1 940(w) cm^{-1}.

^1H n.m.r./δ(p.p.m.): 7.35 (m, 30 H, Ph), 2.48 (quintet, 6 H, CH_2, $J_{PH} = J_{HH}$ = 8 Hz) and 0.9 (dt, 9 H, CH_3, J_{HH} = 7 Hz, J_{PH} = 20 Hz).

^{31}P n.m.r.: 31.51 p.p.m.

Analysis: calculated C, 52.1 %; H, 4.3 %;
found C, 52.2 %; H, 4.4%.

$|Ru_3(CO)_9(PPh_2Pr^n)_3|$

I.r.: 2 045(w), 1 970(vbr,vs) and 1 940(m) cm^{-1}.

^1H n.m.r./δ(p.p.m.): 7.35 (m, 30 H, Ph), 2.35 (m, 6 H, PCH_2), 1.25 (m, 6 H, $PCH_2\underline{CH_2}CH_3$) and 0.98 (m, 9 H, CH_3).

^{31}P n.m.r.: 28.10 p.p.m.

$|Ru_3(CO)_9(PPh_2Bu^n)_3|$

I.r.: 2 042(w), 1 970(vbr,vs) and 1 946(m) cm^{-1}.

^1H n.m.r./δ(p.p.m.): 7.4 (m, 30 H, Ph), 2.41 (m, 6 H, $P-CH_2$), 1.15 (m, 12 H, $PCH_2(\underline{CH_2})_2CH_3$) and 0.93 (t, 9 H, CH_3, J_{HH} = 7 Hz).

^{31}P n.m.r.: 28.34 p.p.m.

Preparation of $|H_4Ru_4(CO)_{12-n}(L)_n|$ (n = 1 and 2).

These were prepared in the same way as $|Ru_3(CO)_{11}L|$ and $|Ru_3(CO)_{10}L_2|$ except that $Ru_3(CO)_{12}$ was replaced by $|H_4Ru_4(CO)_{12}|$ and the yields of the yellow orange products were lower - about 60 % of the expected maximum values.

$|H_4Ru_4(CO)_{11}(PPh_2Me)|$

I.r.: 2 094(m), 2 088(m), 2 067(s), 2 058(s), 2 032(s), 2 026(s), 2 008(s), 1 990(m), 1 969(m) and 1 964(m) cm^{-1}.

^1H n.m.r./δ(p.p.m.): 7.5 (m, 10 H, Ph), 2.13 (d, 3 H, CH_3, J_{PH} = 9 Hz) and -17.42 (d, 4 H, Ru-H-Ru, J_{PH} = 3 Hz).

^{31}P n.m.r.: 19.45 p.p.m.

Analysis: calculated C, 31.4%; H, 1.9 %

found C, 32.0 %; H, 2.4 %.

$|H_4Ru_4(CO)_{10}(PPh_2Me)_2|$

I.r.: 2 076(s), 2 036(s), 2 029(w), 2 018(s), 2 009(s), 1 996(s), 1 969(w) and 1 951(m) cm^{-1}.

^1H n.m.r./δ(p.p.m.): 7.5 (m, 20 H, Ph), 2.2 (br, ≈ 2 H, CH_3), 2.02 (d, ≈ 4 H, CH_3, J_{PH} = 8 Hz) and -18.09 (br, 4 H, Ru-H-Ru).

^{31}P n.m.r.: 19.32 (major) and 17.32 (minor) p.p.m.
(major:minor ≈ 2:1).

Analysis: calculated C, 39.7 %; H, 2.8 %
found C, 39.8 %; H, 2.7 %.

$|H_4Ru_4(CO)_{11}(PPh_2Et)|$

I.r.: 2 095(m), 2 088(w), 2 067(s), 2 058(s), 2 033(m), 2 026(s), 2 008(s), 1 995(m), 1 990(sh), 1 970(w) and 1 962(m) cm^{-1}.

1H n.m.r./δ(p.p.m.): 7.45 (m, 10 H, Ph), 2.56 (quintet, 2 H, CH_2, $J_{PH} \approx J_{HH}$ = 7 Hz), 1.06 (dt, 3 H, CH_3, J_{HH} = 7 Hz and J_{PH} = 20 Hz), and -17.42 (d, 4 H, Ru-H-Ru, J_{PH} = 3 Hz).
^{31}P n.m.r.: 33.17 p.p.m.

$|H_4Ru_4(CO)_{10}(PPh_2Et)_2|$

I.r.: 2 077(m), 2 057(s), 2 029(m), 2 018(s), 2 008(m), 1 996(m), 1 970(w) and 1 949(w) cm^{-1}.

^1H n.m.r./δ(p.p.m.): 7.4 (m, 20 H, Ph), 2.4 (m, ≈ 4 H, CH_2), 1.0 (m, 3 H, CH_3) and -17.05 (br, 4 H, Ru-H-Ru).
^{31}P n.m.r.: 33.77 (mahor) and 31.51 (minor) p.p.m.
(major:minor ≈ 2:1)

$|H_4Ru_4(CO)_{11}(PPh_2Pr^n)|$

I.r.: 2 094(m), 2 087(m), 2 067(s), 2 058(s), 2 033(m), 2 026(s), 2 008(s), 1 989(m), 1 970(w) and 1 962(m) cm^{-1}.

^1H n.m.r./δ(p.p.m.): 7.5 (m, 10 H, Ph), 2.42 (q(distorted), 2 H, PCH_2), 1.4 (m, 2 H, $PCH_2\underline{CH_2}CH_3$), 0.9 (t(distorted), 3 H, CH_3) and -17.42 (d, 4 H, Ru-H-Ru, J_{PH} = 2 Hz).
^{31}P n.m.r.: 20.35 p.p.m.

$H_4Ru_4(CO)_{10}(PPh_2Pr^n)_2$

I.r.: 2 076(m), 2 056(s), 2 029(m), 2 017(s), 2 009(m), 1 996(m), 1 970(m) and 1 949(w) cm^{-1}.

^1H n.m.r./δ(p.p.m.): 7.4 (m, 20 H, Ph), 2.3 (m, 4 H, P-CH_2), 1.4 (m, 4 H, $PCH_2\underline{CH}_2CH_3$), 0.9 (t(distorted), 6 H, CH_3) and -17.05 (br, 4 H, Ru-H-Ru).

^{31}P n.m.r.: 30.75 (major) and 28.04 (minor) p.p.m. (major:minor = 2:1).

$H_4Ru_4(CO)_{11}(PPh_2Bu^n)$

I.r.: 2 095(m), 2 088(w), 2 067(s), 2 058(s), 2 033(m), 2 025(s), 2 008(s), 1 989(m), 1 970(w) and 1 962(m) cm^{-1}.

^1H n.m.r./δ(p.p.m.): 7.5 (m, 10 H, Ph), 2.44 (m, 2 H, P-CH_2), 1.3 (m, 4 H, $PCH_2(\underline{CH}_2)_2CH_3$), 0.89 (t, 2 H. CH_3, J_{HH} = 6 Hz) and -17.42 (d, 4 H, Ru-H-Ru, J_{PH} = 3 Hz).

^{31}P n.m.r.: 30.45 p.p.m.

$H_4Ru_4(CO)_{10}(PPh_2Bu^n)_2$

I.r.: 2 076(s), 2 056(vs), 2 029(s), 2 017(vs), 2 009(s), 1 995(s), 1 985(sh), 1 970(m) and 1 949(m) cm^{-1}.

^1H n.m.r./δ(p.p.m.): 7.4 (m, 20 H, Ph), 2.38 (m, 4 H, P-CH_3), 1.35 (m, 8 H, $PCH_2(\underline{CH}_2)_2CH_3$), 0.84 (m, 6 H, CH_3) and -17.04 (br, 4 H, Ru-H-Ru).

^{31}P n.m.r.: 31.36 (major) and 28.49 (minor) p.p.m. (major:minor ≈ 2:1)

Preparation of $H_4Ru_4(CO)_9L_3$

The reaction of $H_4Ru_4(CO)_{12}$ with PPh_2R, under the same

conditions as used for preparing $|Ru_3(CO)_9(PPh_2R)_3|$, typically gave, after flash chromatography, 60 - 70 % yields of these yellow products.

$|H_4Ru_4(CO)_9(PPh_2Me)_3|$

I.r.: 2 061(m), 2 024(s), 2 002(m), 1 990(m), 1 962(m) and 1 941(w) cm^{-1}.

^1H n.m.r./δ(p.p.m.): 7.35 (m, 30 H, Ph), 1.9 (two uneven doublets, 9 H, CH_3, J_{PH} = 9 Hz in both) and -16.7 (m, 4 H, Ru-H-Ru).

^{31}P n.m.r.: 18.54 (major) and 16.53 (minor) p.p.m. (major:minor ≈ 2:1)

$|H_4Ru_4(CO)_9(PPh_2Et)_3|$

I.r.: 2 060(m), 2 022(s), 2 003(m), 1 988(m), 1 961(m) and 1 940(w) cm^{-1}.

^1H n.m.r./δ(p.p.m.): 7.35 (m, 30 H, Ph), 2.3 ("quintet", ≈ 4 H, PCH_2, $J_{HH} \approx J_{PH}$ = 6 Hz) also 1.9 ("quintet", ≈ 2 H, PCH_2, $J_{HH} \approx J_{PH}$ = 6 Hz), 2.1 - 0.4 (two uneven overlapping dt, 9 H, CH_3) and -16.6 (m, 4 H, Ru-H-Ru).

^{31}P n.m.r.: 36.02 (major) and 30.55 (minor) p.p.m. (major:minor ≈ 2:1)

Preparation of $|Ru_5C(CO)_{14}L$

A solution of $Ru_5C(CO)_{15}$ (25 mg) in CH_2Cl_2 (50 cm^3) was cooled to -40 °C and its i.r. spectrum continuously monitored by means of a flow cell as the phosphine in CH_2Cl_2 (10 cm^3) was slowly added. The reaction was stopped when the i.r. of the

starting material was absent. The solvent was removed in vacuo and the residue purified by flash chromatography to yield the product as a red-purple crystalline solid in about 90 % yield.

$[Ru_5C(CO)_{14}(PPh_2Me)]$

I.r.: 2 088(w), 2 056(vs), 2 046(s), 2 024(s), 2 017(s), 1 997(w), 1 983(w) and 1 965(sh) cm^{-1}.

^1H n.m.r./δ(p.p.m.): 7.4 (m, 10 H, Ph) and 2.2 (d, 3 H, CH_3, J_{PH} = 9 Hz).

^{31}P n.m.r.: 20.61 p.p.m.

$[Ru_5C(CO)_{14}(PPh_2Et)]$

I.r.: 2 088(m), 2 056(s), 2 046(s), 2 025(s), 2 016(s), 1 998(m), 1 982(w) and 1 963(w) cm^{-1}.

^1H n.m.r./δ(p.p.m.): 7.4 (m, 10 H, Ph), 2.5 ("quintet", 2 H, P-CH_2, $J_{HH} \simeq J_{PH}$ = 7 Hz), 1.86 (dt, 3 H, CH_3, J_{HH} = 7 Hz, J_{PH} = 20 Hz).

^{31}P n.m.r.: 36.69 p.p.m.

$[Ru_5C(CO)_{14}(PPh_2Pr^n)]$

I.r.: 2 088(m), 2 056(s), 2 046(s), 2 025(s), 2 016(s), 1 998(m), 1 983(w) and 1 965(w) cm^{-1}.

^1H n.m.r./δ(p.p.m.): 7.39 (m, 10 H, Ph), 2.4 (m, 2 H, P-CH_2), 1.3 (m, 2 H, $PCH_2\underline{CH_2}CH_3$) and 0.94 (t(distorted), 3 H, CH_3).

^{31}P n.m.r.: 33.85 p.p.m.

Analysis: calculated C, 31.7 %; H, 1.5 %

found C, 31.8 %; H, 1.6 %.

$|Ru_5C(CO)_{14}(PPh_2Bu^n)|$

I.r.: 2 088(m), 2 056(s), 2 046(s), 2 025(s), 2 015(s), 1 996(m), 1 983(sh) and 1 963(w) cm^{-1}.

^1H n.m.r./δ(p.p.m.): 7.37 (m, 10 H, Ph), 2.42 (q(distorted), 2 H, P-CH_2), 1.4 (m, 4 H, $PCH_2(\underline{CH_2})_2CH_3$) and 0.83 (t, 3 H, CH_3, J_{HH} = 7 Hz).

^{31}P n.m.r.: 34.20 p.p.m.

Preparation of $|Ru_5C(CO)_{13}L_2|$

A solution of $|Ru_5C(CO)_{15}|$ (25 mg, CH_2Cl_2 50 cm^3) was monitored continuously by i.r., by using a flow cell, while the phosphine was added. The reaction was stopped when a pure spectrum of the disubstituted derivative was obtained. After removal of solvent in vacuo and purification of the residue by flash chromatography, the dark purple crystalline products were typically obtained in almost quantitative yields.

$|Ru_5C(CO)_{13}(PPh_2Me)_2|$

I.r.: 2 070(w), 2 044(vs), 2 028(m), 2 018(s), 2 012(s), 2 000(sh), 1 994(sh), 1 984(vbr,m) and 1 973(vbr,m) cm^{-1}.

^1H n.m.r./δ(p.p.m.): 7.4 (m, 20 H, Ph) and 2.18 (d, 6 H, CH_3, J_{PH} = 8 Hz).

^{31}P n.m.r.: 19.90 p.p.m.

Analysis Calculated C, 37.5 %; H, 2.0 %
found C, 38.2 %; H, 2.2 %.

$|Ru_5C(CO)_{13}(PPh_2Et)_2|$

I.r.: 2 069(m), 2 045(vs), 2 016(s), 2 012(s), 2 002(sh), 1 992(w) and 1 970(vbr,w) cm^{-1}.

^{1}H n.m.r./δ(p.p.m.): 7.44 (m, 20 H, Ph), 2.25 ("quintet", 4 H, CH_2, $J_{HH} \approx J_{PH}$ = 7 Hz) and 1.8 (dt, 6 H, CH_3, J_{HH} = 7 Hz, J_{PH} = 20 Hz).
^{31}P n.m.r.: 34.50 p.p.m.

$|Ru_5C(CO)_{13}(PPh_2Pr^n)_2|$

I.r.: 2 068(m), 2 043(vs), 2 016(s), 2 002(sh), 1 993(sh), 1 984(sh) and 1 959(vbr,w) cm^{-1}.
^{1}H n.m.r./δ(p.p.m.): 7.45 (m, 20 H, Ph), 2.3 (m, 4 H, P-CH_2), 1.3 (m, 4 H, P-$CH_2\underline{CH_2}CH_3$) and 0.86 (t(distorted), 6 H, CH_3).
^{31}P n.m.r.: 31.87 p.p.m.

$|Ru_5C(CO)_{13}(PPh_2Bu^n)_2|$

I.r.: 2 068(m), 2 043(vs), 2 016(s), 2 012(sh), 2 002(sh) and 1 960(vbr,w) cm^{-1}.
^{1}H n.m.r./δ(p.p.m.): 7.44 (m, 20 H, Ph), 2.34 (m, 4 H, P-CH_2), 1.3 (m, 8 H, $PCH_2(\underline{CH_2})_2CH_3$) and 0.8 (t(distorted), 6 H, CH_3).
^{31}P n.m.r.: 32.12 p.p.m.

All the reactions with $|Ru_5C(CO)_{15}|$ were carried out in a flow cell because the occurrence of $|Ru_3(CO)_{12}|$ (produced in variable proportions during its synthesis) as an impurity, made accurate calculation of the amount of phosphine required impossible.

Preparation of $|Ru_6C(CO)_{16}L|$

An equimolar quantity of L was added to a solution of $|Ru_6C(CO)_{17}|$ (30 mg, CH_2Cl_2 30 cm^3), cooled to 0 °C. After an immediate darkening in colour, the solution was left stirring overnight at r.t. Removal of the solvent in vacuo and

purification of the residue by flash chromatography gave $|Ru_6C(CO)_{16}L|$ as a red-brown crystalline solid (typically 80 % yield).

$|Ru_6C(CO)_{16}(PPh_2Me)|$

I.r.: 2 085(m), 2 056(m), 2 046(s), 2 032(vs), 2 020(m), 2 006(m), 1 982(m), 1 967(w), 1 956(w) and 1 837(vbr,w) cm^{-1}.

^1H n.m.r./δ(p.p.m.): 7.44 (m, 10 H, Ph) and 2.34 (d, 3 H, CH_3, J_{PH} = 8 Hz).

^{31}P n.m.r.: 26.00 p.p.m.

$|Ru_6C(CO)_{16}(PPh_2Et)|$

I.r.: 2 084(m), 2 056(s), 2 046(s), 2 032(vs), 2 020(m), 2 001(m), 1 983(br,m) and 1 846(vbr,w) cm^{-1}.

^1H n.m.r./δ(p.p.m.): 7.44 (m, 10 H, Ph), 2.58 (quintet, 2 H, PCH_2, $J_{HH} \simeq J_{PH}$ = 6.5 Hz) and 1.08 (dt, 3 H, CH_3, J_{HH} = 7 Hz and J_{PH} = 19 Hz).

^{31}P n.m.r.: 39.90 p.p.m.

$|Ru_6C(CO)_{16}(PPh_2Pr^n)|$

I.r.: 2 084(m), 2 056(s), 2 046(s), 2 032 vs), 2 020(m), 2 003(w), 1 983(m), 1 970(sh) and 1 847(br,w) cm^{-1}.

^1H n.m.r. δ(p.p.m.): 7.44 (m, 10 H, Ph), 2.5 (q(distorted), 2 H, $P-CH_2$), 1.4 (m, 2 H, $PCH_2\underline{CH_2}CH_3$) and 1.0 (t(distorted), 3 H, CH_3).

^{31}P n.m.r.: 37.60 p.p.m.

$|Ru_6C(CO)_{16}(PPh_2Bu^n)|$

I.r.: 2 084(m), 2 055(s), 2 046(s), 2 032(vs), 2 019(m), 2 003(w), 1 982(m), 1 967(w) and 1 839(vbr,w) cm^{-1}.

^1H n.m.r./δ(p.p.m.): 7.44 (m, 10 H, Ph), 2.5 (m, 2 H, P-CH_2), 1.38 (m, 4 H, $PCH_2(\underline{CH_2})(CH_3)$ and 0.88 (m, 3 H, CH_3).

^{31}P n.m.r.: 38.14 p.p.m.

Analysis calculated C, 30.3 %; H, 1.5 %

found C, 30.5 %; H, 1.5 %.

Preparation of $|Ru_6C(CO)_{15}L_2|$

$|Ru_6C(CO)_{17}|$ (25 mg) and L (2.1 equivalents) were heated in refluxing cyclohexane for 3 hours during which time the solution turned dark brown. After removing the solvent in vacuo and flash chromatographing the residue, $|Ru_6C(CO)_{15}L_2|$ a dark red-brown solid was obtained in about 70 % yield.

$|Ru_6C(CO)_{15}(PPh_2Me)_2|$

I.r.: 2 065(m), 2 029(s), 2 017(vs), 1 994(m), 1 981(m), 1 972(m), 1 953(w), 1 861(br,w) and 1 838(br,w) cm^{-1}.

^1H n.m.r./δ(p.p.m.): 7.4 (m, 20 H, Ph), 2.28 (d(minor isomer), CH_3, J_{HP} = 9 Hz) and 2.23 (d(major isomer), CH_3, J_{HP} = 9 Hz), (major:minor ≈ 3:1).

^{31}P n.m.r.: 25.30 (major) and 24.30 (minor) p.p.m. (major:minor ≈ 4:1)

Analysis calculated C, 35 %; H, 1.8 %

found C, 36 %; H, 2.2 %.

$[Ru_6C(CO)_{15}(PPh_2Et)_2]$

I.r.: 2 065(m), 2 028(s), 2 015(vs), 1 990(m), 1 980(m), 1 970(sh), 1 950(w), 1 857(br,w) and 1 838(br,w) cm^{-1}.

^1H n.m.r./δ(p.p.m.: 7.44 (m, 20 H, Ph), 2.46 (quintet, 4 H, CH_2) and 0.99 (dt, 6 H, CH_3).

^{31}P n.m.r.: 39.40 (major) and 39.60 (minor) p.p.m. (major:minor ≈ 7:1)

$[Ru_6C(CO)_{15}(PPh_2Pr^n)_2]$

I.r.: 2 064(m), 2 028(s), 2 014(vs), 2 003(w), 1 995(m), 1 980(m), 1 973(sh), 1 950(w), 1 857(br,w) and 1 837(br,w) cm^{-1}.

^1H n.m.r./δ(p.p.m.): 7.44 (m, 20 H, Ph), 2.39 (m, 4 H, P-CH_2), 1.4 (m, 4 H, $PCH_2\underline{CH_2}CH_3$) and 0.9 (m, 6 H, CH_3).

^{31}P n.m.r.: 37.24 p.p.m.

$[Ru_6C(CO)_{15}(PPh_2Bu^n)_2]$

I.r.: 2 064(m), 2 028(s), 2 014(vs), 2 003(w), 1 994(m), 1 979(m), 1 960(sh), 1 950(w), 1 857(br,w) and 1 857(br,w) cm^{-1}.

^1H n.m.r./δ(p.p.m.): 7.44 (m, 20 H, Ph), 2.38 (m, 4 H, P-CH_2), 1.35 (m, 8 H, $PCH_2(\underline{CH_2})_2CH_3$) and 0.85 (m, 6 H, CH_3).

^{31}P n.m.r.: 37.84 p.p.m.

Preparation of $Ru_6C(CO)_{13}(PPh_2Et)_4$

$Ru_6C(CO)_{17}$ (25 mg) was stirred overnight with a large excess of PPh_2Et (10 equivalents) in CH_2Cl_2 (30 cm^3). Removal of the solvent *in vacuo* and separation of the residue by flash

chromatography gave $|Ru_6C(CO)_{13}(PPh_2Et)_4|$ as a brown powder in 50 % yield.

I.r.: 2 044(m), 2 006(vw), 1 969(s) and 1 946(m) cm^{-1}.

^1H n.m.r./δ(p.p.m.): 7.35 (m, 40 H, Ph), 2.48 (quintet, 8 H, CH_2) and 0.9 (dt, 12 H, CH_3).

^{31}P n.m.r.: 31.10 p.p.m.

Preparation of $|Ru_3(CO)_{10}(PPh_2(CH_2)_nPPh_2)|$

The highest yield route to $|Ru_3(CO)_{10}DPPM|$ (n = 1) and $|Ru_3(CO)_{10}DPPE|$ (n = 2) was found to be to reflux overnight a solution of $|Ru_3(CO)_{12}|$ (50 mg) and phosphine (1.1 equivalents) in n-pentane (100 cm^3). This gave typically 60 - 70 % yields of these orange-red crystalline products after removing the solvent in vacuo and isolating the products by flash chromatography. When this preparation was repeated for other phosphines with a longer chain lengths, the yields dramatically decreased, with for DPPB (n = 4) the products involving the linking of 2 or more clusters predominating. In these cases the benzophenone reaction (as used for $Ru_3(CO)_{12}|$ and PPh_2R) gave more satisfactory yields (typically 30 - 50 %).

$|Ru_3(CO)_{10}DPPM$

I.r.: 2 083(s), 2 062(w), 2 023(s), 2 013(vs), 2 002(vs), 1 985(m), 1 960(m) and 1 950(m) cm^{-1}.

^1H n.m.r./δ(p.p.m.): 7.4 (m, 20 H, Ph) and 4.3 (t, 2 H, CH_2, J_{PH} = 10 Hz).

^{31}P n.m.r.: 14.63 p.p.m.

Analysis calculated C, 43 %; H, 2.3 %

found C, 43.5 %; H, 2.5

$[Ru_3(CO)_{10}(DPPE)]$

I.r.: 2 080(s), 2 045(w), 2 013(vs), 1 998(vs), 1 980(m), 1 964(m) and 1 937(br,w) cm^{-1}.

^1H n.m.r./δ(p.p.m.): 7.5 (m, 20 H, Ph) and 2.2 (m, 4 H, CH_2).

^{31}P n.m.r.: 40.40 p.p.m.

Analysis: calculated C, 54.4%; H, 3.2 %

found C, 55.0%; H, 3.1 %.

$[Ru_3(CO)_{10}(DPPP)]$

I.r.: 2 079(s), 2 044(w), 2 011(vs), 1 999(vs), 1 980(m), 1 964(m) and 1 921(br,m) cm^{-1}.

^1H n.m.r./δ(p.p.m.): 7.44 (m, 20 H, Ph), 2.6 (q, 4 H, P-CH_2, $J_{HH} \approx J_{PH}$ = 6 Hz) and 1.5 (m, 2 H, $PCH_2\underline{CH_2}$).

^{31}P n.m.r.: 28.20 p.p.m.

$[Ru_3(CO)_{10}(DPPB)]$

I.r.: 2 080(s), 2 062(w), 2 032(w), 2 011(vs), 2 004(vs), 1 980(w), 1 996(m) and 1 900(vbr,w) cm^{-1}.

^1H n.m.r./δ(p.p.m.): 7.5 (m, 20 H, Ph), 2.5 (q, 4 H, P-CH_2, $J_{HH} \approx J_{PH}$ = 7 Hz) and 1.1 (m, 4 H, $PCH_2\underline{CH_2}$).

^{31}P n.m.r.: 24.10 p.p.m.

$Ru_3(CO)_8(DPPM)_2$. Orange-red crystalline solid.

I.r.: 2 061(m), 2 045(w), 1 992(m), 1 974(s), 1 967(s), 1 945(m), 1 928(w), 1 910(w) and 1 894(br,w) cm^{-1}.

^1H n.m.r./δ(p.p.m.): 7.2 (m, 40 H, Ph) and 4.06 (t, 4 H, CH_2, J_{PH} = 10 Hz).

^{31}P n.m.r.: 21.86, 21.11, 18.39, 17.79 p.p.m.

Analysis calculated C, 53.3 %; H, 3.0 %

found C, 53.0 %; H, 3.0 %.

$|\{Ru_3(CO)_{11}\}_2DPPE|$

I.r.: 2 097(m), 2 047(s), 2 029(s), 2 028(sh) and 2 017(br,vs) cm^{-1}.

^1H n.m.r./δ(p.p.m.): 7.5 (m, 20 H, Ph) and 2.1 (m, 4 H, CH_2).

Reaction of $|Ru_3(CO)_{12}|$ with (-)-Diop.

A solution of one equivalent of $|Ru_3(CO)_{12}|$ and (-)-Diop in t.h.f. was reacted with sodium benzophenone ketyl, as described for $|Ru_3(CO)_{12}|$ with monodentate ligands, earlier. This yielded two main orange-red crystalline products, $|\{Ru_3(CO)_{11}\}_2$-(-)-Diop| (30 %) and $|Ru_3(CO)_{10}$((-)-Diop)| (40 - 50 % based on $Ru_3(CO)_{12}$ consumed).

$|\{Ru_3(CO)_{11}\}_2\{(-)\text{-Diop}\}|$

I.r.: 2 097(m), 2 046(s), 2 025(sh), 2 015(vs) and 1 990(sh) cm^{-1}.

^1H n.m.r./δ(p.p.m.): 7.4 (m, 20 H, Ph), 3.5 (t(broad), 2 H, C(H)O-, J_{PH} = 8 Hz), 2.3 (m, 4 H, P-CH_2) and 1.42 (s, 6 H, CH_3).

^{31}P n.m.r.: 25.0C p.p.m.

$Ru_3(CO)_{10}\{(-)\text{-Diop}\}$

I.r.: 2 080(m), 2 045 w), 2 013(vs), 2 005(vs), 1 976(w), 1 954(m) and 1 893(vbr,w) cm^{-1}.

^1H n.m.r./δ(p.p.m.): 7.4 (m, 20 H, Ph), 3.8 (m, 2 H, C(H -O-, J_{PH} = 10 Hz), 2.8 (m, 4 H, PCH_2, very complex pattern) and 1.42 (s, 6 H, CH_3).

^{31}P n.m.r.: 13.81 p.p.m.

Preparation of $|H_4Ru_4(CO)_{10}(P—P)|$

Both the benzophenone ketyl catalysed and thermal reactions (under the same conditions used for the preparation of $|Ru_5(CO)_{10}\{(PPh_2)_2(CH_2)_n\}|$) gave similar yields after separation of the products by flash chromatography.

$|H_4Ru_4(CO)_{10}(DPPM)|$

I.r.: 2 085(w), 2 073(s), 2 052(s), 2 034(s), 2 024(m), 2 012(s), 1 993(m), 1 981(m), 1 969(s), 1 952(s) and 1 933(w) cm^{-1}.

^1H n.m.r./ (p.p.m.), $CDCl_3$ 45 - 50 °C, d^8-toluene 45 - 70 °C.

60 °C: 7.3 (m, 20 H, Ph), 3.78 (t, 2 H, CH_2, J_{PH} = 10 Hz) and -16.38 (t, 4 H, Ru-H-Ru, J_{PH} = 3 Hz).

45 °C: 7.3 (m, 20 H, Ph), 3.78 (br, 2 H, CH_2) and -16.38 (t, 4 H, Ru-H-Ru).

31 °C: 7.3 (m, 20 H, Ph), 3.8 (m, 2 H, CH_2) and -16.38 (t, 4 H, Ru-H-Ru).

-20 °C: 7.3 (m, 20 H, Ph), 3.8 (br, 2 H, CH_2) and -16.39 (br, 4 H, Ru-H-Ru).

-50 °C: 7.3 (m, 20 H, Ph), 4.0 (m, 1 H, CH_a), 3.4 (m, 1 H, CH_b) and -16.3 (vbr, 4 H, Ru-H-Ru).

^{13}C n.m.r./ (p.p.m.), d^8-toluene 80 - -21 °C, CD_2Cl_2/CF_2ClH 0 - 114 °C.

Temperature	Position	No. of carbonyls	
60 °C	194.88	10	all carbonyls
40 °C	broad		exchanging slowing
21 °C	no signal		coalescence
0 °C	197.88 (br)	3	
	195.73 (t)	4	J_{HP} or J_{HC} = 4 Hz
	194.24 (t)	3	J_{HP} or J_{HC} = 3 Hz
-50 °C	198.35 (t)	3	J_{HP} or J_{HC} = 6 Hz
	196.72	2	
	195.66	2	
	194.35	3	
-74 °C	198.56 (t)	3	J_{HP} or J_{HC} = 6 Hz
	196.88	2	
	195.57	2	
	194.51	2	
	193.62	1	
-84 °C	198.76 (t)	3	J_{HP} or J_{HC} = 5 Hz
	196.98	2	
	195.55	2	
	194.60	2	
	193.61	1	
-104 °C	198.84 (t)	3	J_{HP} or J_{HC} = 6 Hz
	197.10	2	
	195.47	2	
	194.55 (d)	2	J_{HC} or J_{PC} = 4 Hz
	193.54	1	

^{31}P n.m.r.: 11.73 p.p.m.

Analysis calculated C, 39.1 %; H, 2.4 %

found C, 38.9 %; H, 2.5 %.

$|H_4Ru_4(CO)_{10}DPPE|$ (corner chelating isomer)

I.r.: 2 076(s), 2 061(w), 2 046(s), 2 033(s), 2 024(s), 2 009(s), 1 992(w), 1 982(m), 1 971(w), 1 964(w) and 1 956(w) cm^{-1}.

^1H n.m.r./δ(p.p.m.), $CDCl_3$, -50 °C: 7.44 (m, 20 H, Ph), 2.2 (m, 4 H, CH_2), -19.2 (t, 1 H, Ru-H-Ru), -16.5 (s, 1 H, Ru-H-Ru), -16.1 (dd, 1 H, Ru-H-Ru) and -14.8 (dd, 1 H, Ru-H-Ru).

^{31}P n.m.r.: 66.73 p.p.m.

$|H_4Ru_4(CO)_{10}DPPP|$

I.r.: 2 073(s), 2 052(s), 2 032(s), 2 012(s), 2 003(w), 1 991(m), 1 981(m), 1 971(m) and 1 951(m) cm^{-1}.

^1H n.m.r./δ(p.p.m.): 7.44 (m, 20 H, Ph), 2.45 (m, 4 H, PCH_2), 1.6 (m, 2 H, $PCH_2\underline{CH_2}$) and -17.14 (br, 4 H, Ru-H-Ru).

^{31}P n.m.r.: 30.83 p.p.m.

$|H_4Ru_4(CO)_{10}DPPB|$

I.r.: 2 078(s), 2 073(s), 2 058(s), 2 054(s), 2 032(s), 2 019(s), 2 013(s), 2 009(s), 1 999(s), 1 993(s), 1 972(m), 1 963(w) and 1 950(m) cm^{-1}.

^1H n.m.r./δ(p.p.m.): 7.4 (m, 20 H, Ph), 2.6 (m, 4 H, PCH_2), 1.5 (m, 4 H, $PCH_2\underline{CH_2}$) and -16.73, -17.47 (br, 4 H, Ru-H-Ru, two isomers of abundances 2:1, respectively).

^{31}P n.m.r.: 33.32 (minor) and 23.52 (major) p.p.m. (major:minor ≈ 3:1)

$(H_4Ru_4(CO)_{11})_2$(-)-Diop

I.r.: 2 095(s), 2 083 (m), 2 081(w), 2 060 (s), 2 057(s), 2 027(s), 2 009(s), 1 991(w) and 1 957(m) cm^{-1}.

^{1}H n.m.r./δ(p.p.m.): 7.45 (m, 20 H, Ph), 3.64 (m, 2 H, C(H)-O-, J_{PH} = 9 Hz), 2.35 (m, 4 H, PCH_2), 1.29 (s, 6 H, CH_3) and -17.45 (d, 8 H, Ru-H-Ru, J_{PH} = 4 Hz).
^{31}P n.m.r.: 26.75 p.p.m.

$|H_4Ru_4(CO)_{10}$(-)-Diop|

I.r.: 2 079(m), 2 075(m), 2 060(s), 2 056(sh), 2 033(s), 2 020(vs), 2 015(s), 2 009(m), 2 001(m), 1 985(w), 1 975(w) and 1 952(br,m) cm^{-1}.

Preparation of ^{13}CO enriched $|Ru_5C(CO)_{15}|$

A solution of $|Ru_5C(CO)_{15}|$ (100 mg, 30 cm^3 CH_2Cl_2) was stirred overnight at 40 °C under a partial pressure of ^{13}CO (quantity calculated for about 35 % enrichment). The red product was purified by flash chromatography from two side products ($|Ru_3(CO)_{12}|$ and $|Ru_6C(CO)_{17}|$).
^{13}C n.m.r./δ(p.p.m.), d^8-toluene, 103 - 25 °C, CD_2Cl_2/CH_2Cl_2 -48 - -115 °C.

103 - -48 °C	191.45	12 basal carbonyls
	196.70	3 axial carbonyls
-73 °C	191.45	signal broadening
	196.70	sharp
-115 °C	195.2	very broad
	198.55	sharp

Preparation of $|Ru_5C(CO)_{15}$(P -- P)|

An equimolar quantity of the bidentate ligand was added to a cooled solution (-20 °C) of $|Ru_5C(CO)_{15}|$. After 15 minutes the reaction was allowed to warm to r.t. and stirred for 3 hours. The solvent was removed in vacuo and the residue worked up by

flash chromatography. The yields decreased as the chain length increased, e.g. $|Ru_5C(CO)_{13}(P—P)|$, DPPM 80 %, DPPE 80 %, DPPP 60 % and DPPB 30 %. However, the yields of the DPPP and DPPB derivatives could be increased by heating the solution to 50 °C, increasing the dilution, and adding all the phosphine at once.

$|Ru_5C(CO)_{13}DPPM|$

I.r.: 2 074(m), 2 062(w), 2 047(m), 2 039(s), 2 027(s), 2 016(sh), 2 010(s), 2 002(s), 1 968(w) and 1 951(w) cm^{-1}.

^1H n.m.r./δ(p.p.m.), $CDCl_3$, 45 — -50 °C; CD_2Cl_2 30 — -98 °C.

+45 °C: 7.3 (m, 20 H, Ph) and 4.66 (t, 2 H, CH_2, J_{PH} = 11 Hz).

+30 °C: 7.3 (m, 20 H, Ph) and 4.66 (br, 2 H, CH_2).

+10 °C: 7.3 (m, 20 H, Ph) and 4.60 (vbr, 2 H, CH_2).

-10 °C: 7.3 (m, 20 H, Ph).

-40 °C: 7.3 (m, 20 H, Ph), 5.2 (vbr, 1 H, CH_a) and 4.0 (vbr, 1 H, CH_b).

160 °C: 7.3 (m, 20 H,)h), 5.2 (m, 1 H, CH_a) and 4.0 (m, 1 H, CH_b).

-90 °C: no improvement in quality.

^{13}C n.m.r./δ(p.p.m.), d^8-toluene, 60 - 0 °C, CD_2Cl_2, 30 — -60 °C, $CD_2Cl_2/CFCl_2H$ 0 — -121 °C (see Figure 5.6).

Temperature	Position	No. of carbonyls	
60 °C	199.30 (s)	13	
40 °C	199.15 (br)	13	
21 °C	200.88	3	carbonyls on axial Ru
	199.12	10	carbonyls on basal Ru's
0 °C	201.49	3	
	199.15 (br)	10	

-40 °C	203.09 (br)		
	201.81	3	
	196.92		
-60 °C	204.51		
	203.01		
	202.02	3	
	201.88		
-90 °C	204.51		
	203.01		
	202.20	3	
	201.88 (br)		
-107 °C	204.77		
	203.16		
	202.30		
	197.35 (vbr)		
-117 °C	203.27		
	202.61		
	202.45	3	
	197		broad featrue
-119 °C	203.27		
	202.61	3	
	202.45		
	197		coalescence

-125 °C The three remaining bands are unchanged and new features are starting to appear.

^{31}P n.m.r./δ(p.p.m.), 31 → -90 °C,

31 °C	14.97 (s, 2 P, DPPM)
17 °C	14.97 (s, 2 P, 10 Hz peak width)
-40 °C	14.40 (s, 2 P, 60 Hz peak width)
-80 °C	12.85 and 14.07 (minor isomers)
	16.87 (major isomer, 100 Hz wide)

-90 °C 12.85 and 14.07 (minor isomer)
17.05 (major isomer, 20 Hz wide)
(major:minor = 9.5:1)

Analysis calculated C, 46.2%; H, 2.8 %
found C, 45.5 %; H, 3.6 %.

$|Ru_5C(CO)_{13}DPPE|$

I.r.: 2 073(m), 2 056(w), 2 038(s), 2 027(vs), 2 010(s), 2 001(m) and 1 947(br,w) cm^{-1}.

^1H n.m.r./δ(p.p.m.): 7.5 (m, 20 H, Ph) and 2.3 (m, 4 H, CH_2).

^{13}C n.m.r./δ(p.p.m.), d^8-toluene 103 - 25 °C; $CD_2Cl_2/CFHCl_2$, -17 — -115 °C (see Figure 5.8).

Temperature	Position	No. of carbonyls	
103 °C	198.81	13	all carbonyls exchanging
94 °C	198.62 (br)	13	localised exchange occurring
84 °C	198.58		basal carbonyls exchanging
	199.7 (sh)		
75 °C	198.58		
	199.7 (br)		
48 °C	198.58		
	199.7 (br) sharper)		
25 °C	198.58	10	
	199.75	3	axial carbonyls exchanging
-17 °C	199.5 (br)		localised exchange about basal Ru atoms
	201.50	3	

-32 °C	∿ 197.3 (vbr)		
	201.5	3	
-48 °C	196.5 (br)		
	201.5	3	
	203.5 (br)		
-63 °C	196.2		
	201.5	3	
	202.9		
	204.9		
-73 °C	197.1 (vbr)		
	201.5	3	
	202.9		
	205.1		
-83 °C	198.2		
	201.46	3	
	202.6		
	205.08		
-94 °C	188		
	198		
	201.44	3	
	203.6		
	205.02		
-105 °C	188.03	1	
	198.6 (br)	2	
	201.44	3	
	203.8		
	205.02		
-115 °C	187.2 }	1	J_{PC} ?
	187.9 }		
	198.6	2	
	200.95	2	
	201.42	3	
	203.08	1	
	204.97	2	

^{31}P n.m.r.: +39.80 p.p.m. (no change observed in peak width from 40 — -90 °C).

Analysis calculated C, 38.1 %; H, 2.5 %

found C, 37.7 %; H, 2.0 %.

$|Ru_5C(CO)_{13}DPPP|$

When freshly made this compound was wholly isomer (i) but on standing a solution of it converted to predominantly isomer (ii) (within a couple of hours).

Isomer (i)

I.r.: 2 070(m), 2 046(s), 2 020(s), 2 011(s), 1 993(m), 1 981(m), 1 966(m), 1 952(m) and 1 939(w) cm^{-1}.

Isomer (ii)

I.r.: 2 073(s), 2 047(s), 2 039(s), 2 028(vs), 2 020(s), 2 009(s), 2 004(m), 1 996(m), 1 966(w) and 1 952(w) cm^{-1}.

^1H n.m.r./δ(p.p.m.): 7.5 (m, 2 0 H, Ph), 2.2 (m, 4 H, $P-CH_2$) and 1.5 (m, 2 H, $PCH_2\underline{CH_2}$).

^{31}P n.m.r./δ(p.p.m.), 30 — -90 °C, no change was observed in the two peak spectra: 40.37 (isomer ii) and 33.39 (isomer i) (isomer ii:isomer i ≈ 5:1).

$|Ru_5C(CO)_{15}DPPB|$

When this compound was freshly made, it consisted of mainly isomer (ii) with traces of isomer (i) which upon standing in solution converted into wholly isomer (i).

Isomer (ii)

I.r.: 2 073(s), 2 046(s), 2 039(s), 2 028(s), 2 020(s), 2 007(s), 1 994(s), 1 966(m) and 1 951(w) cm^{-1}.

Isomer (i)

I.r.: 2 071(m), 2 046(s), 2 020(s), 2 012(s), 1 994(m), 1 981(m), 1 966(m), 1 952(m) and 1 939(w) cm^{-1}.

^{1}H n.m.r./δ(p.p.m.): 7.5 (m, 20 H, Ph), 2.18 (m, 4 H, PCH_2) and 0.98 (m, 2 H, $PCH_2\underline{CH_2}$).

^{13}C n.m.r./δ(p.p.m.), natural abundance, CD_2Cl_2, 31 °C, carbonyls: 201.2 (s, 3 carbonyls, apical ruthenium carbonyls), 199.05 (s, 10 carbonyls, carbonyls on basal ruthenium atoms); phenyl ring carbons: 132.7 (d, 12 C, Ph, J_{PC} = 8 Hz), 131.4 (d, 12 C, Ph, J_{PC} = 10 Hz), 129.1 ("t", 18 C, Ph, J_{PC} = 7 Hz), alkyl chain carbons: 32.5 (d, 2 C, PCH_2, J_{PC} = 9 Hz) and 23.3 ("d", 2 C, $PCH_2\underline{CH_2}$).

^{31}P n.m.r.: 34.06 p.p.m.

Analysis: calculated C, 38.6 %; H, 2.1 %

found C, 39.0 %; H, 2.1 %.

$[\underline{Ru_5C(CO)_{11}(DPPM)_2}]$

I.r./CH_2Cl_2: 2 025(m), 1 998(s), 1 987(m), 1 969(m), 1 960(sh), and 1 940(w) cm^{-1}.

^{1}H n.m.r./ (p.p.m.), CD_2Cl_2, 30 — -85 °C:

30 °C: 7.3 (m, 40 H, Ph) and 4.4 - 3.7 (br, 4 H, CH_2).

0 °C: 7.3 (m, 40 H, Ph) and 4.0 (br, 4 H, CH_2).

-10 °C: 7.3 (m, 40 H, Ph) and 4.0 (vbr, 4 H, CH_2).

-20 °C: as above.

-45 °C: 7.3 (m, 40 H, Ph) and 4.0 (br, 4 H, CH_2).

-65 °C: 7.3 (m, 40 H, Ph) and 4.0, 3.4 (br, 4 H, 2 H each, CH_a and CH_b).

-85 °C, -90 °C, solvent broadening obscuring any improvement in the methylene protons signals.

^{13}C n.m.r./δ(p.p.m.), d^8-toluene, 85 - 23 °C, $CD_2Cl_2/CFHCl_2$, -3 - -116 °C:

Temperature	Position	No of carbonyls	
85 °C	204.88	3	
	203.09	4	
	201.17	4	
65 °C	204.89	3	
	203.11	4	
	201.1	4	broadening
52 °C	204.90	3	
	203.1	4	broadening
	201.2	4	broadening
37 °C	204.84	3	
	203.1	4	broadening
	201.1	4	broad
23 °C	204.92	3	
	203.2	4	no longer sharp
	201		broad
-3 °C	206.24	3	
-26 °C	206.15	3	
	205.5 (br)		
	203.6 (br)		
	198.5 (br)		
-46 °C	206.26	3	
	206.03	2	
	205.57	2	
	203.50	2	
	198.25	2	

-116 °C	206.26	3	peak slightly broadened
	206.3	2	
	205.57	2	
	203.50	2	
	198.25	2	

^{31}P n.m.r./δ(p.p.m.), 80 - 0 °C, $(CH_2Cl)_2$; 0 — -90 °C, CH_2Cl_2:

80 °C 10 p.p.m. (80 Hz width

70 °C 10 p.p.m. (200 Hz width)

50 °C ∿ 10 p.p.m. unresolved doublet (400 Hz width

40 °C ∿ 10 p.p.m. unresolved doublet (600 Hz width)

0 °C ∿ 10 p.p.m. unresolved doublet (1071 Hz width, 13.2 p.p.m. across)

-40 °C peaks at 3.61 and 17.21 p.p.m. (peak width 100 Hz)

-65 °C peaks at 3.56 and 17.26 p.p.m. (peak width 20 Hz)

-90 °C peaks at 3.52 and 17.30 p.p.m. (peak width 10 Hz)

Analysis: calculated C, 46.2 %; H, 2.8 %

found C, 45.5 %; H, 3.5 %.

$[(Ru_5C(CO)_{14})_2DPPB]$

I.r.: 2 089(m), 2 058(s), 2 047(s), 2 024(s), 2 013(sh), 1 998(sh) and 1 956(sh) cm^{-1}.

^1H n.m.r./δ(p.p.m.), CD_2Cl_2: 7.4 (m, 20 H, Ph), 2.2 (m, 4 H, PCH_2) and 0.9 (m, 4 H, $PCH_2\underline{CH_2}^-$).

Analysis: calculated C, 31.0 %; H, 1.2 %

found C, 30.9 %; H, 1.3 %.

Reaction of $Ru_5C(CO)_{15}$ with (-)-Diop.

An equimolar quantity of (-)-Diop was aded to a heated cyclohexane solution of $Ru_5C(CO)_{15}$ (50 °C, 50 cm^3, 200 mg).

After an immediate darkening of the red solution, the reaction was stirred for a further 30 minutes. The solvent was removed in vacuo and the residue applied to a flash chromatography column. Upon elution with solvents of gradually increasing polarity, first unreacted $|Ru_5C(CO)_{15}|$, then $|\{Ru_5C(CO)_{14}\}_2(-)\text{-Diop}|$ (40 %) and finally $|Ru_5C(CO)_{13}\{(-)\text{-Diop}\}|$ (50 % yield based on $|Ru_5C(CO)_{15}|$ consumed), were obtained.

$|\{Ru_5C(CO)_{14}\}_2(-)\text{-Diop}|$

I.r. (see Figure 5.7): 2 088(m), 2 057(vs), 2 047(s), 2 026(s), 2 015(s), 2 000(m), 1 990(m) and 1 963(w) cm^{-1}.

^1H n.m.r./δ(p.p.m.): 7.35 (m, 20 H, Ph), 3.4 (t, 2 H, -OC(H)-, J_{HH} = 7 Hz), 2.4 (m, 4 H, PCH_2) and 1.44 (s, 6 H, CH_3).

^{31}P n.m.r.: 26.75 p.p.m.

Analysis: calculated C, 31.5 %; H, 1.38 %
found C, 31.6 %; H, 1.4 %.

$|Ru_5C(CO)_{13}\{(-)\text{-Diop}\}|$

I.r.: 2 075(m), 2 047(sh), 2 029(vs), 2 011(vs), 2 012(m), 2 005(m), 1 996(w) and 1 970(br,w) cm^{-1}.

^1H n.m.r./δ(p.p.m.: 7.4 (m, 20 H, Ph), 4.12 (quintet(distorted), 1 H, -OC(H_a)-), 3.6 (quintet(distorted), 1 H, -OC(H_b)-), 2.8 and 2.2 (complex m, 4 H, PCH_2, CH_2 groups inequivalent) and 1.43 (s, 6 H, CH_3).

^{31}P n.m.r.: initially 23.19 p.p.m., finally 29.30 and 19.68 p.p.m.

Analysis: calculated C, 39.06 %; H, 2.31 %
found C, 39.3 %; H, 2.3 %.

Preparation of $|Ru_6C(CO)_{15}(P-P)|$

An equimolar quantity of the phosphine was added to a CH_2Cl_2 solution of $|Ru_6C(CO)_{17}|$ and stirred overnight. After removing the solvent in vacuo the residue was purified by flash chromatography. Again the yields of the longer chain derivatives could be increased by increasing the dilution and heating the reaction mixture.

$|Ru_6C(CO)_{15}DPPM|$

I.r./CH_2Cl_2: 2 073(s), 2 036(vs), 2 019(vs), 1 979(m), 1 965(m), 1 946(w) and 1 823(br,m) cm^{-1}.

^1H n.m.r./δ(p.p.m.), CD_2Cl_2: 7.35 (m, 20 H, Ph) and 4.98 (t, 2 H, CH_2, J_{PH} = 12 Hz). This spectrum remained unchanged down to -50 °C. Unfortunately, temperatures below this were unattainable due to solubility problems.

^{13}C n.m.r./δ(p.p.m.), CD_2Cl_2, 0 - 30 °C; $CHFCl_2/CH_2Cl_2$, 0 - -115 °C:

Temperature	Position		No. of carbonyls
25 °C	202.08	(s)	15
-46 °C	202.9	(vbr)	
-66 °C	205.5	(br)	
	195.2	(vbr)	
-86 °C	205.52		
	196.27		
	194.56	(s)	4
-96 °C	205.7		
	194.50	(s)	4

-106 °C	206.76	(br)	
	205.7	(br)	
	194.45	(s)	4
-115 °C	204.33	(br)	
	201.99	(br)	
	197.09	(br)	
	194.78	(br)	
	194.71	(br)	
	194.37		4

^{31}P n.m.r./31 — -85 °C: 31 °C, 20.70 p.p.m. (5 Hz peak width; -85 °C, ~ 20.70 p.p.m. (200 Hz peak width).

Analysis: calculated C, 34.5 %; H, 1.55 %

found C, 34.9 %; H, 1.6 %.

$[Ru_6C(CO)_{15}DPPE]$

I.r./CH_2Cl_2: 2 073(s), 2 036(vs), 2 020(vs), 1 995(sh), 1 978(m), 1 963(m), 1 945(w), 1 858(br,w) and 1 826(br,m) cm^{-1}.

^1H n.m.r./δ(p.p.m.): 7.4 (m, 20 H, Ph) and 2.4 (m, 4 H, CH_2).

^{31}P n.m.r.; 31 °C, 40.26 p.p.m. (5 Hz width); -85 °C, ~ 40.00 p.p.m. (100 Hz width).

$Ru_6C(CO)_{15}DPPP$

I.r./CH_2Cl_2: 2 072(s), 2 033(vs), 2 020(vs), 1 997(sh), 1 990(sh), 1 961(br,m), 1 856(br,w) and 1 825(br,m) cm^{-1}.

^1H n.m.r./δ(p.p.m.): 7.5 (m, 20 H, Ph), 2.5 (q(distorted), 4 H, PCH_2, J_{PH} = 10 Hz) and 1.6 (m, 2 H, $PCH_2\underline{CH_2}$).

^{31}P n.m.r.: 31 °C, 49.36 p.p.m. (5 Hz width); -85 °C, two unequal peaks 48.10 and 50.60 p.p.m. (only partially resolved).

$[Ru_6C(CO)_{15}DPPB]$

I.r./CH_2Cl_2: 2 077(s), 2 055(sh), 2 045(sh), 2 030(m), 2 005(br,vs), 1 957(br,m), 1 899(br,w) and 1 859 - 1 828(br,w) cm^{-1}.

^1H n.m.r./δ(p.p.m.), CD_2Cl_2: 7.4 (m, 20 H, Ph), 2.45 (q(distorted), 4 H, PCH_2) and 1.1 (m, 4 H, $PCH_2\underline{CH_2}$).

^{31}P n.m.r.: 31 °C, 35.90 p.p.m. (7 H width); -85 °C coalescence.

Analysis: calculated C, 36.1 %; H, 1.9 %

found C, 36.5 %; H, 1.7 %.

$[\{Ru_6C(CO)_{16}\}_2DPPB]$

I.r./CH_2Cl_2: 2 077(s), 2 055(sh), 2 045(sh), 2 030(m), 2 005(br,vs), 1 957(br,m), 1 899(br,w) and 1 859 - 1 828(br,w) cm^{-1}.

^1H n.m.r./δ(p.p.m.), CD_2Cl_2: 7.4 (m, 20 H, Ph), 2.3 (m, 4 H, PCH_2) and 0.89 (m, 4 H, $PCH_2\underline{CH_2}$).

^{31}P n.m.r.: 24.01 p.p.m.

Analysis: calculated C, 29.1 %; H, 1.1 %

found C, 30.0 %; H, 1.2 %.

$[Ru_6C(CO)_{15}((-)\text{-Diop})]$

I.r./CH_2Cl_2: 2 073(s), 2 034(sh), 2 022(vs), 2 000(sh), 1 965(m), 1 930(sh) and 1 836(br,w) cm^{-1}.

1H n.m.r./δ(p.p.m.): 7.4 (m, 20 H, Ph), 3.9 (m, 2 H, -OCC(H)-), 2.9 (m, 4 H, PCH_2) and 1.5 (s, 6 H, CH_3).

^{31}P n.m.r.: 40.40 p.p.m.

Analysis: calculated C, 36.71 %; H, 2.0 %

found C, 36.0 %; H, 2.3 %.

$[\{Ru_6C(CO)_{15}\}_2((-)\text{-Diop})]$

I.r./CH_2Cl_2: 2 077(s), 2 055(m), 2 045(m), 2 029(m), 2005(br,vs), 1 957(br,m), 1 898(br,w) and 1 860 - 1 825(br,w) cm^{-1}.

^1H n.m.r./CD_2Cl_2: Unsatisfactory spectrum due to low solubility.

Analysis: calculated C, 29.65 %; H, 1.22 %

found C, 29.3 %; H, 1.3 %.

Preparation of anchored (-)-Diop containing clusters.

Route (i)

(i) Anchoring of $(MeO)_3Si(CH_2)_3Cl$.

A sample of dried Aerosil 380 (150 °C, vacuum 20 h, 10 g) slurried in toluene (200 cm^3), had added $(MeO)_3Si(CH_2)_3Cl$ (2.5 g) and was refluxed for 48 h while the methanol/toluene azeotrope was removed by a Dean and Stark apparatus. After cooling the solid was filtered off, washed (CH_2Cl_2, 6 x 50 cm^3) and dried in vacuo (48 h). In order to improve the resistance of the sample to leaching and to minimise oxide interaction in the following steps, the solid was slurried in CH_2Cl_2 (100 cm^3) and treated with $SiMe_3Cl$. After 24 h reflux, HCl evolution had ceased, and the sample was recovered by filtration, washed with methanol (3 x 50 cm^3) and CH_2Cl_2 (5 x 5L cm^3) and dried in vacuo (48 h) to afford a white free flowing powder.

(ii) Oxidation of the anchored chloride.

This was carried out as described for chlorinated Bio-beads[26] to yield a cream coloured powder which displayed a broad band in the i.r. at about 1 640 cm^{-1} indicative of an aldehyde or

ketone. However, the filtrate was found to contain leached ligand.

(iii) Hydrolysis of (-)-Diop.

This was carried out as described for 1,4-ditosyl- 2,3,-O-isopropylidene-Lg-thietol[10] to yield 1,4-bisdiphenylphosphino-2,3-dihydroxy-Lg-theitol (25 % yield) as a waxy white solid. ^{1}H n.m.r./$CDCl_3$: 7.4 (m, 20 H, Ph), 4.05 (m, 2 H, C-H), 2.4 (m, 3 H, CH_2), hydroxyl protons undetected.

(iv) Condensation of the anchored aldehyde with hydrolysed (-)-Diop.

A mixture of anchored aldehyde (5 g), hydrolysed Diop (1.0 g), p-toluene sulphoric acid (0.1 g) in benzene (150 cm^3) was refluxed for 6 h while the water/benzene azeotrope was continuously removed. After cooling the solid was recovered by filtration, washed (CH_2Cl_2, 6 x 100 cm^3) and dried in vacuo. The i.r. spectrum of a disc of this cream coloured powder besides demonstrating the existence of the phosphine, also shows the presence of phosphine oxide (1 110 cm^{-1}).

(v) Reaction of anchored (-)-Diop with $|Ru_6C(CO)_{17}|$

A sample of the anchored phosphine (100 mg) was stirred overnight in a CH_2Cl_2 solution of cluster (15 mg). The pale red-brown solid was filtered off, washed (3 x 50 cm^3, CH_2Cl_2) and dried in vacuo. The very weak i.r. spectrum of this sample indicated the existence of small quantities of $|Ru_6C(CO)_{15}$Diop$|$ together with " $Ru_6C(CO)_{16}P|$" and other unidentified species.

Route (ii)

(i) Preparation of $(EtO)_3SiH$

Dry EtOH (78 cm^3, 1.3 mole) was added dropwise at 0 - -10 °C to a mixture of Cl_3SiH (33 cm^3, 0.3 mole) and benzene (100 cm^3). After two hours standing and distillation off excess ethanol, there was obtained at 132 - 135 °C (760 mm Hg) $(EtO)_3SiH$ (50 % yield).

(ii) Preparation of $(EtO)_3SiCH_2CH_2C(H)(OEt)_2$.

A mixture of $(EtO)_3SiH$ (30 g), acrolein acetal (20 g, prepared[27]), and $Pt(NH_4)_2Cl_6$ (0.1 g) was stirred for one hour at r.t. and then refluxed overnight (temperature rose from 120 °C to 135 °C as the acetal was consumed). The mixture was distilled from the black-grey platinum residue under reduced pressure (10^{-1} - 1 mm Hg). The major liquid fraction obtained (B.pt. 122 - 130 °C/10^{-1} mm Hg) proved to be the desired product.

^1H n.m.r./$CDCl_3$: 4.4 (t, 1 H, CH), 3.75 (m, 10 H, C-O$\underline{CH_2}$ and SiO$\underline{CH_2}$), 1.5 (quintet(distorted), 2 H, $SiCH_2\underline{CH_2}$), 1.2 (2t, 15 H, $COCH_2\underline{CH_3}$ and $SiOCH_2\underline{CH_3}$) and 0.7 (t, 2 H, $SiCH_2$).

m.s.

measured mass.	% intensity base peak	assignment
294.01	0.1	Parent ion
249.02	2.2	loss of one ethoxide
220.00	1.0	loss of one ethoxide and a ethyl group.
204.02	2.6	loss of two ethoxides
175.00	10.6	loss of two ethoxides and a ethyl group

m.s.(Cont.)

163.01	16.4	$(EtO)_3Si^+$
159.99	1.3	loss of three ethoxides
131.01	7.6	$(EtO)_2C(H)CH_2CH_2^+$
103.00	100.0	loss of one ethoxide and $Si(OEt)_3$ group.

iii) Anchoring of the sylyl acetal.

This was carried out in an identical manner to the anchoring of $(MeO)_3Si(CH_2)_3Cl$ onto γ-Al_2O_3 and SiO_2, (described previously) and gave as products cream coloured free flowing powders, whose i.r. spectra showed a weak band at about 1 640 cm^{-1} assignable to an anchored aldehyde. This can be taken to indicate that partial hydrolysis of the acetal occured on anchoring.

(iv) Condensation of the anchored aldehyde with hydrolysed (-)-Diop.

This was carried out exactly as described for route (i) and the results obtained were identical except that the loading of the phosphine obtained was much higher.

(v) Reaction of anchored (-)-Diop with $[Ru_6C(CO)_{17}]$.

This was also carried out as described for route (i). The results obtained were also identical to those of route (i) except that the loading of the cluster achieved (by i.r. spectroscopy) was much higher.

Route (iii)

Specific anchoring of $[Ru_6C(CO)_{15}\{(-)\text{-Diop}\}]$.

One equivalent of the silyl acetal cluster (50 mg) and

p-Toluene sulphoric acid in freshly distilled tetraglyme were stirred for 7 days under vacuum. G.l.c. analysis of the contents of the cold trap indicated the presence of acetal, acetone and ethanol. The column was found to cause partial hydrolysis of a pure acetal sample . The mixture was neutralised by the addition of two equivalents of anhydrous $NaHCO_3$, then a sample of the oxide (250 mg) was added and the sample stirred under vacuum for a few days, during which ethanol was detected in the cold trap (by g.l.c.). The samples were washed with CH_2Cl_2 (some cluster was removed in both cases, 3 x 50 cm^3) to yield pale red-brown powders.

I.r./Nujol mull: (see Figure 5.15).

$M'O_n$ =

SiO_2, 2 069(m), 2 030(s), 2 019(vs), 1 997(s), 1 965(vbr,m) and 1 841(vbr,w) cm^{-1}.

γ-Al_2O_3, 2 070(s), 2 034(s), 2 020(vs), 1 998(s), 1 965(vbr,m) and 1 835(vbr,w) cm^{-1}.

References to Chapter 5.

1. K.A. Azam, C.C. Yin, and A.J. Deeming,; J.Chem.Soc.,Dalton Trans., (1978), 1201.

2. F. Piacenti, M. Bianchi, P. Frediani, and E. Benedetti; Inorg.Chem., (1971), 10, 2759.

3. A.A. Arduini, A.A. Bahsoun, J.A. Osborn, and C. Voelker; Angew.Chem.,Int.Ed.Engl., (1980), 19, 1024.

4. J.A. Osborn and G.G. Stanley; Angew.Chem.,Int.Ed.Engl., (1980), 19, 1025.

5. J.J. DeBoer, J.A. van Doorn, and C. Masters; J.Chem.Soc., Chem.Commun., (1978), 1005.

6. M.M. Harding, B.S. Nicholls, and A.K. Smith; J.Organomet. Chem., (1982), 226, C17.

7. B.E. Mann, C. Masters, and B.L. Shaw; J.Chem.Soc.(A), (1971), 104, and J.Chem.Soc.,Dalton Trans., (1972), 704.

8. P.E. Carrou; Chem.Rev., (1981), 81, 229.

9. L. Beni, H.C. Clark, J.A. Davies, D. Drexler, C.A. Fyfe, and R. Wasylishen; J.Organomet.Chem., (1982), 224, C5.

10. W. Dumont, J.C. Paulin, T.P. Dang, and H.B. Kagan; J.Am.Chem.Soc., (1973), 95, 8295.

11. H. Goetz and S. Nomin; Ann.Chem., (1967), 704, 1.

12. K. Issleib and D.W. Muller; Chem.Ber., (1959), 92, 3175.

13. W. Henderson, R.A. Shaw, and B.C. Smith; J.Chem.Soc., (1964), 1020.

14. K.B. Mallion and F.G. Mann; J.Chem.Soc., (1964), 5710.

15. K.B. Mallion and F.G. Mann, J.Chem.Soc., (1964), 6121.

16. Monsanto Co., C.A. 1964), 60, 12055c.

17. S.O. Grim, W. McFarlane, and E.F. Davidoff; J.Org.Chem., (1967), 32, 781.

18. F.A. Hart; J.Chem.Soc., (1960), 3324.

19. S.T.D. Gough and S. Trippett; J.Chem.Soc., (1961), 4263.

20. M.M. Rauhut and A.M. Semsel; J.Org.Chem., (1963), 28, 473.

21. S.O. Grim and W. McFarlane; Nature, (1965), 208, 995.

22. J.R. Lyerla, L.S. Vannoni, and C.A. Fyle; Acc.Chem.Res., (1982), 15, 208.

23. V.K. Issleib and H.P. Abicht; J.Praktische Chemie, (1970), 312, 456.

24. M. Cormock and C.J. Kelly; J.Org.Chem., (1968), 33, 2171.

25. P.W. Fèit; J.Med.Chem., (1964), 7, 14.

26. J.M. Frechet and C. Schuerch; J.Am.Chem.Soc., (1971) 93, 492.

27. J.A. Van Allan; Org.Syn.Coll., (1963), 4, 21.

28. M.I. Bruce, G. Shaw, and F.G.A. Stone; J.Chem.Soc.,Dalton Trans., (1972), 2094, and references therein.

29. A. Poe and M.V. Twigg; J.Chem.Soc.,Dalton Trans., (1974), 1860.

30. A. Poe and S.K. Mauk, Inorg.Chem., (1979), 18, 1241.

31. B.F.G. Johnson, J. Lewis, and M.V. Twigg; J.Chem.Soc., Dalton Trans., (1975), 1876.

32. E.J. Forbes, N. Goodhand, D.L. Jones, and T.A. Hamor; J.Organomet.Chem., (1979), 182, 143.

33. G. Raper and W.S. McDonald; J.Chem.Soc.(A), (1971), 3430.

34. R.E. Benfield, B.F.G. Johnson, P.R. Raithby, and G.M. Sheldrick, Acta Crystallogr., (1978), B34, 666.

35. S. Aime and D. Osella, J.Chem.Soc.,Chem.Commun., (1981), 500.

36. G.R. Hays, A.D.H. Clague, R. Hus, and G. van der Velden; App.Sur.Science, (1982), 10, 247.

37. H.D. Kaesz and S.A.R. Knox; J.Am.Chem.Soc., (1971), 93, 4594.

38. R. Bau and R.D. Wilson, J.Am.Chem.Soc., (1976), 98, 4684.

39. K. Sasvari, P. Main, F.H. Cano, M. Martinez-Ripoll, and P. Frediani; Acta Crystallogr.,Sec.B, (1979), B35, 87. also, R.D. Wilson, S.M. Wu, R.A. Love, and R. Bau; Inorg.Chem., (1978), 17, 1271.

40. D.H. Farrar, P.F. Jackson, B.F.G. Johnson, J. Lewis, J.N. Nicholls, and M. McPartlin; J.Chem.Soc.,Chem.Commun., (1981), 415.

41. J. Lewis and B.F.G. Johnson; Pure and Appl.Chem., (1982), 54, 97.

42. S.C. Brown, J. Evans, and M. Webster; J.Chem.Soc.,Dalton Trans., (1981), 2263.

43. B.F.G. Johnson, J. Lewis, K. Wong, and M. McPartlin; J.Organomet.Chem., (1980), 185, C17.

44. W.O. Siegl, S.L. Lapporte, and J.P. Collman; Inorg.Chem., (1973), 12, 674.

45. M.I. Bruce, T.W. Hambley, B.K. Nickolson, and M.R. Snow; J.Organomet.Chem., (1982), 235, 83.

46. F.A. Cotton and B.A. Hanson; Inorg.Chem., (1977), 16, 3369.

47. J. Trotter; J.Chem.Soc.(A), (1971), 1479.

48. "Multiple Bonds Between Metal Atoms", F.A. Cotton and R.A. Walton, Wiley Interscience, Chichester, (1982).

49. J.J. Bonnet and G. Lavigne; Inorg.Chem., (1981), 20, 2713.

50. G. Lavigne, N. Lugan, and J.J. Bonnet; Nouv.J.Chim., (1981), 5, 423.

51. J.R. Shapley, S.I. Richter, M.R. Churchill, and R.A. Lashewycz; J.Am.Chem.Soc., (1977), 99, 7384.

52. M.R. Churchill and R.A. Lashewycz; Inorg.Chem., (1978), 18, 1950.

53. D.F. Foster, B.S. Nicholls, and A.K. Smith, J.Organomet. Chem., (1982), 236, 395.

54. K. Nomiya and H. Suzuki, J.Organomet.Chem., (1979), 168, 115.

55. C.A. Tolman, Chem.Rev., (1977), 77, 313.

56. S.C. Brown, Personal communication.

57. A.G. Jones, Personal communication.

58. G. Lavigne, N. Lugan, and J.J. Bonnet, Acta Crystallogr., (1982), B38, 1911.